

Inês Maria de Carvalho Laíns

Metabolomics, Genetics and Environment: a Novel Integrative Approach to Age-related Macular Degeneration

Tese de Doutoramento do Programa em Ciências da Saúde, Ramo de Medicina,
orientada por Professor Doutor Rufino Silva, Professora Doutora Isabel Carreira,
Professora Doutora Ana Gil e apresentada à Faculdade de Medicina

Março 2018



UNIVERSIDADE DE COIMBRA

Table of Contents

Acknowledgments	2
Abstract	5
Resumo (Abstract in Portuguese)	7
Thesis outline	9
Chapter I: Project Background and Design	10
I.1) Background	10
I.2) Study Design	13
I.3) Included Study Population	16
Chapter II: Metabolomics	19
Manuscript 1 - Human Plasma Metabolomics in Age-related Macular Degeneration (AMD) Using Nuclear Magnetic Resonance Spectroscopy.....	21
Manuscript 2 - Human Plasma Metabolomics Study Across all Stages of Age-related Macular Degeneration Identifies Potential Lipid Biomarkers	39
Manuscript 3 - Metabolomics of Retinal Diseases	49
Chapter III: Phenotype	114
Manuscript 4 - Automated Brightness and Contrast Adjustment of Color Fundus Photographers for the Grading of Age-related Macular Degeneration	117
Manuscript 5 - Choroidal Changes Associated with Subretinal Drusenoid Deposits in Age-related Macular Degeneration Using Swept-source Optical Coherence Tomography	130
Manuscript 6 - Novel Grid Combined with Peripheral Distortion Correction for Ultra-widefield Imaging Grading of Age-related Macular Degeneration	139
Manuscript 7 - Structural Changes Associated with Delayed Dark Adaptation in Age-related Macular Degeneration	147
Manuscript 8 - Health Conditions Linked to Age-related Macular Degeneration Associated with Dark Adaptation.....	160
Chapter IV – Discussion and future directions	171
References	176
Supplements	186

Acknowledgments

Know where you are going, but don't forget where you are coming from.

Unknown

We all have a story, and almost all we do in our life also does. I believe that the story of this project is exceptional, and it was only possible thanks to the tremendous support I had from several people, who I would like to acknowledge.

I would also like to highlight that the concretization of this work was just possible due to the Junior Grant and Career Development Award of the Harvard Medical School (HMS) Portugal Program/ Portuguese Foundation for Science and Technology (FCT). This Grant provided funding to initiate this project, but it also gave me the unique opportunity of starting a research fellowship at the Massachusetts Eye and Ear (MEE), HMS, Boston, United States (US). Therefore, this project was developed through a close collaboration between the involved Portuguese and American institutions, and I was fortunate to have mentors in both places. In Portugal, Rufino Silva, MD, PhD, Isabel Carreira, PhD and Ana Gil, PhD. In Boston, Joan W. Miller, MD and Deeba Husain, MD.

In this context, I would like to especially thank:

. Rufino Silva, MD, PhD for his constant support, and for always allowing me to develop new ideas and new projects, even when they did not seem likely to succeed *a priori*. I would also like to thank you for your relentless efforts to make this project possible in Portugal, even when everything seemed so challenging. Thank you for all the opportunities and support!

. Joan W. Miller, MD, for being the reason why I believe that we can always work to make our biggest dreams come true. You are my inspiration! I learned so much from you, as an investigator and as a person... Thank you for allowing me to be part of your team, and especially to be part of your life! Thank you also for being so present, and always making me feel that I could count on you. Finally, I would like to sincerely thank you for your financial support to this project, which was crucial for our achievements.

. Deeba Husain, MD, for allowing me to fly, but steering me in the right the direction whenever it was needed. Thank you for your daily support, care and loyalty! You were always my "home" in the US, and I cannot thank you enough for your love, and the countless times you listened to me (always with a smile!) and helped me moving forward! Thank you for all you mean to me, and all you represent in my life!

. Joaquim Murta, MD, PhD, my sincere gratitude for the close mentorship and constant care. Thank you for showing me how ophthalmology was definitely the right choice for me, and for all the doors you opened for me, including the one of your house and your family. You were always there, and you were always able to transform my hardest moments in opportunities to grow. Thank you for all you taught me, but especially for your care and friendship.

. Isabel Carreira, PhD for believing in me since I was an 18-year-old medical student, and helping me building this project from the very first moment. Thank you for your support, and for always making things look much simpler and possible!

. Ana Gil, PhD, for all the support during the design of this project and our application for funding, and for all the work to make it become a reality. Thank you for all the hours that you and your team from Aveiro dedicated to this work.

. Eduardo Silva, MD, PhD, for being with me since my very first day as an ophthalmology resident, and for always stimulating me to question things and to fight to understand the “why”. You always made me feel that I could dream, and that I should aim to fly, because the “wings” were with me. Thank you!

. José Cunha-Vaz, MD, PhD for his support, and for allowing me to count with the collaboration of AIBILI, which was crucial for the development of this project.

. Patrícia Barreto, MSc for her constant support to this project in Portugal, but especially for her close friendship. Thank you for your loyalty and for the countless times you were here for me.

. João Figueira, MD, PhD and Maria da Luz Cachulo, MD, PhD for their close friendship and support. You were crucial for me since the very first moment, and I will never be able to thank you for all your love and care, on a personal and professional level.

. John B. Miller, MD for being a close friend and a tremendous support. Thank you also for all the projects we built and developed together, and for giving me so many opportunities.

. Demetrios G. Vavvas, MD, PhD and Ivana K. Kim, MD for being so supportive throughout this journey. Thank you for all your feedback and inputs. I feel that I learned a lot from you, and you helped me become better.

. Tânia Mesquita, BSc, Luísa Ribeiro, MD, PhD, Inês Marques, MD, Isabel Pires, MD, PhD for taking so good care of our Portuguese patients, and giving always their best to make everything work.

. Ana Rita Santos, MSc for all her help and support planning our imaging protocols, and for her friendship.

. To all the Portuguese and American technicians and photographers who helped us with our study protocols.

. João Gil, MD and Pedro Gil, MD, my dearest colleagues and friends, who were crucial to make this project possible, and are also crucial in my life!

. Marco Marques, MD and Joana Providencia, MD for her help with data analysis and collection in Portugal.

. Tiago Reis Marques, MD, PhD for being an inspiration, and for all the guidance to pursue a career as a clinician-scientist. Thank you also for your close and permanent support and friendship.

. To my family and my friends outside the “professional world”, who forgave me for all my absences, and gave me the emotional support required to make all this possible!

. To Patrick, for always making me smile, even in the hardest circumstances. Thank you for your unconditional love, and for always making me believe that “there are no problems, only solutions”.

. A very special acknowledgment to my parents. I owe you everything! Thank you for all the love, stimulus, and unbelievable support... every single day, since I was born. I am who I am thanks to you! Thank you!

Abstract

Age-related macular degeneration (AMD) is the leading cause of blindness in the elderly in developed countries. The presence of macular drusen or pigmentary changes represent the early phases of the disease, with some subjects progressing to its late forms - choroidal neovascularization or geographic atrophy. The diagnosis and management of AMD currently relies on ophthalmic examination and/or imaging by skilled clinicians. As it is often asymptomatic in its early phases, unless a routine exam is done, AMD early/ intermediate stages may remain undetected. Therefore, it is crucial to develop screening tools for AMD diagnosis and to predict its progression.

Several attempts have been made to identify serologic biomarkers of AMD. However, probably due to the complex multifactorial nature of this disease, involving interactions between genetic and environmental risk factors, results have been inconsistent. Thus, there is currently a lack of reliable and accessible AMD biofluid biomarkers. Metabolomics, the study of the small molecules (<1 kDa) comprising a biological system, offers a well-suited tool to address this need. The metabolites are the downstream product of the cumulative effects of the genome and its interaction with environmental exposures. Therefore, the metabolome is thought to closely mirror the phenotype, especially of multifactorial diseases, such as AMD. Metabolomic profiles can be assessed with two main techniques: nuclear magnetic resonance (NMR) spectroscopy and mass spectrometry (MS).

Our group hypothesized that the metabolome is impacted in AMD, with differences according to its severity stages, and that AMD-progressors have a distinct metabolome. To test our hypotheses, we designed a study including subjects with AMD and a control group (> 50 years with normal macula) from two distinct geographic origins (Coimbra, Portugal and Boston, United States). In addition to a complete ophthalmological exam, we obtained medical history and lifestyle profiles. Fasting blood and urine samples were collected on all subjects, and detailed imaging of the retina, including color fundus photographs (CFP) and optical coherence tomography (OCT), was performed. For a subset of patients, functional assessments, such as dark adaptation, were also obtained.

Our initial work focused on the characterization of metabolomic profiles of AMD and its severity stages. Using NMR spectroscopy, we observed a separation of plasma metabolomics profiles between multiple AMD stages for the Boston cohort, and between control and late stages of AMD for the Coimbra cohort. The metabolomic fingerprints of AMD in the two cohorts presented both similarities and differences, thus suggesting the existence of specific signs of the disease and signs of environmental influences, respectively. We are currently finalizing the analysis of urine NMR metabolomic profiles. Compared to blood, urine

composition can present greater variations of endogenous metabolites, therefore it may better reflect changes in disease.

The encouraging results of the NMR study motivated us to pursue work with MS, a complementary technique with higher sensitivity. A pilot analysis of plasma samples of the Boston cohort using MS revealed that 87 metabolites differed significantly between patients with AMD and controls. Most of them were lipids, with glycerophospholipids playing a major role. Of these metabolites, over half also differed significantly across AMD severity stages. We are now analyzing the remaining plasma MS data (n=500), by using our two independent cohorts (Coimbra and Boston) as a training and validation set, to characterize metabolomic signs of the disease.

In our study, AMD classification was based on CFP, the current gold-standard. Due to the variability of CFP on brightness and contrast, we developed software to automatically standardize them. We also did pioneering work in defining structure-functional associations in AMD, namely by studying the relation between OCT features of AMD with visual function, as assessed by dark adaptation. Acknowledging the potential relevance of peripheral changes on AMD, we also defined methodology to assess them using ultra-widefield imaging.

In conclusion, this project demonstrated for the first time that metabolomics enables the identification of plasma profiles associated with AMD, thus supporting the development of metabolomic biomarkers of this blinding disease. Integrated with genetic and lifestyle information, this work also has the potential to increase the current knowledge on the mechanisms of AMD, and thus point to druggable targets for its treatment.

Resumo

A degenerescência macular relacionada com a idade (DMI) é a causa líder de cegueira em idosos nos países desenvolvidos. As fases precoces da doença caracterizam-se pela presença de drusen maculares ou alterações pigmentares; alguns indivíduos progridem para as formas tardias – neovascularização coroideia ou atrofia geográfica. O diagnóstico e seguimento da DMI é atualmente baseado num exame oftalmológico efetuado por clínicos experientes e/ou em exames de imagem. Como frequentemente os doentes com DMI são assintomáticos nas suas fases precoces, exceto se um exame de rotina for efetuado, aqueles com estadios precoces ou intermédios podem permanecer por diagnosticar. Assim, é essencial desenvolver ferramentas para rastreio da DMI e para predizer o seu risco de progressão.

Várias tentativas têm sido efetuadas para identificar biomarcadores serológicos de DMI. No entanto, provavelmente devido à complexa natureza multifatorial da doença, que envolve fatores genéticos e ambientais, os resultados dos diversos estudos têm sido inconsistentes. Deste modo, não existem atualmente biomarcadores de DMI acessíveis e fidedignos. A metabolómica, definida como o estudo das pequenas moléculas (<1KDa) que formam um sistema, representa uma ferramenta apropriada para enfrentar este desafio. Os metabolitos são o produto último do processo de transcrição genética e das suas interações com as exposições ambientais. Assim sendo, pensa-se que o metaboloma é a representação mais próxima do fenótipo, especialmente em doenças multifatoriais, como a DMI. Os perfis metabolómicos podem ser estudados com duas técnicas principais: espectroscopia por ressonância magnética e espetrometria de massa (MS).

O nosso grupo colocou a hipótese de que o metaboloma está alterado na DMI, com diferenças de acordo com os estadios de gravidade da doença, e que os indivíduos que progridem ao longo do tempo (progressores) têm um metaboloma distinto. Para avaliar as nossas hipóteses, desenhamos um estudo que incluiu doentes com DMI e um grupo controlo (>50 anos, mácula normal), de duas origens geográficas distintas (Coimbra, Portugal e Boston, Estados Unidos). Para além de um exame oftalmológico completo, efetuámos a todos os participantes uma história clínica completa e colhemos dados sobre o seu estilo de vida, bem como amostras de sangue e de urina em jejum. Efetuados ainda vários exames de imagem, incluindo retinografias e tomografia de coerência óptica (OCT). Para um subgrupo de doentes, efetuámos também avaliações funcionais, nomeadamente adaptação ao escuro.

O nosso trabalho inicial focou-se na caracterização do perfil metabolómico da DMI e dos seus diversos estadios. Utilizando espectroscopia por ressonância magnética, verificámos a presença de uma separação entre os perfis metabolómicos do plasma de vários estadios de DMI, na coorte de Boston. Na coorte portuguesa, verificámos uma separação entre

doentes com DMI tardia comparativamente com o grupo controlo. Os perfis metabolómicos nas duas coortes demonstraram tanto semelhanças como diferenças, sugerindo deste modo a existência tanto de sinais específicos da doença como ambientais. Estamos atualmente a finalizar a análise dos perfis metabolómicos de urina utilizando a mesma técnica. Comparada com o sangue, a urina pode apresentar maiores variações de metabolitos endógenos, pelo que pode refletir melhor alterações na doença.

Os resultados encorajadores com espectroscopia por ressonância magnética, motivaram-nos a prosseguir o nosso estudo com MS - uma técnica complementar, com maior sensibilidade. Com esta técnica, a nossa análise inicial de amostras de plasma da coorte de Boston demonstrou que 87 metabolitos diferiam significativamente entre doentes com DMI e controlos. A maioria dos metabolitos responsáveis por esta separação eram lípidos, sobretudo glicero-fosfolípidos. Destes metabolitos, mais de metade diferiam também entre os diferentes estadios de DMI. Neste momento, estamos a terminar a análise dos restantes dados obtidos com MS (n= 500), utilizando as nossas duas coortes independentes (Coimbra e Boston) como grupo de teste e de validação, para caracterizar os sinais metabolómicos da DMI.

Neste estudo, a classificação de DMI foi baseada em retinografias, já que estas são atualmente o *gold-standard*. Devido à variabilidade verificada nas mesmas em termos de brilho e contraste, desenvolvemos um programa para as standardizar automaticamente. Efetuámos também trabalho pioneiro na definição de associações estrutura-função na DMI, nomeadamente através do estudo da relação entre as alterações observadas no OCT e a função visual avaliada através da adaptação ao escuro. Devido ao reconhecimento da potencial relevância das alterações da periferia na DMI, definimos também metodologia para as avaliar utilizando imagens com amplo campo de captação.

Em conclusão, este projeto demonstrou pela primeira vez que utilizando metabolómica é possível identificar perfis plasmáticos associados à DMI, suportando assim o desenvolvimento de biomarcadores metabolómicos desta doença. Integrado com o estudo genético e de perfis de vida, este trabalho tem também o potencial de aumentar o atual conhecimento dos mecanismos de DMI e de identificar potenciais novos alvos terapêuticos.

Thesis outline

This Thesis is organized in four chapters plus supplements. It includes seven original manuscripts published in international, peer-reviewed journals; and one review paper, which was written by invitation of an international, peer-reviewed journal, and is currently under review.

Chapter I presents the scientific background that led to the project, our leading hypotheses and aims. We also present the study design of the entire project, including the study procedures performed in our two study sites – Coimbra, Portugal, and Boston, United States. Data on the recruited study population is provided. We include also information on obtained funding for the project, as well as the scientific recognitions that it received over the last four years.

Chapter II presents our two original manuscripts published on the application of metabolomics to the study of age-related macular degeneration (AMD), using two distinct and complementary techniques – nuclear magnetic resonance spectroscopy (NMR) and mass spectrometry (MS). A review manuscript on the application and potential of metabolomics to the study of vitreoretinal diseases is also included.

Chapter III includes five published manuscripts related to AMD phenotyping and structural-function associations. During the design and execution of this project, as it will be detailed, we faced challenges in terms of AMD classification and staging. We felt that this project provided a unique opportunity to improve the current phenotypic assessment of the disease, which is crucial to perform any associations with ‘omics data, such as metabolomics and genomics.

Chapter IV provides an integrative discussion of the work published so far, and it details all the ongoing research we are performing, namely related to metabolomic-genomic-lifestyle associations. Future directions for this project are also discussed, namely the initiation of a follow-up study on this study cohort. An overview of the contribution of this Thesis to AMD assessment and knowledge is also included.

Chapter I: Project Background and Design

I.1) Background

Age-related macular degeneration (AMD) is the leading cause of adult blindness in developed countries. Worldwide, it ranks third, and is expected to affect 288 million people by 2040.¹ Even when it does not cause blindness, AMD often leads to central vision distortions and significant impairment in patients' quality of life.² The natural history of AMD typically comprises "dry" early and intermediate forms, and some subjects can progress to atrophic (geographic atrophy, GA) and/or neovascular lesions (choroidal neovascularization, "wet" AMD), the advanced forms of AMD.^{3,4}

For many years, the scientific community has been trying to understand what causes AMD and its progression. Why some people older than 50 years develop AMD and others don't? And why, among those with AMD, some subjects progress to the late blinding forms of the disease? The current answers are mostly based on the clinical phenotype, namely the size of drusen and the presence of pigmentary changes.⁵ Environmental risk factors were also found to play a role. Age, cigarette smoking, gender, race, diet, and various cardiovascular risk factors were identified as potential modulators.⁶ More recently, several genomic regions have also been shown to be associated with AMD.^{7,8} The most common alleles with high effect seem to be complement system deregulation (CFH), age-related maculopathy susceptibility 2 (ARMS2) and high-temperature requirement factor H (HTRA1); however, genes related to oxidative stress, DNA repair, mitochondrial dysfunction, neovascularization, microglial recruitment and lipid and cholesterol deregulation have also been linked to the disease.^{7,8} Therefore, it is currently well-established that AMD is a multifactorial disease, with a complex interaction between genetic and environmental risk factors.

Clinically, AMD is usually asymptomatic in its early stages and diagnosed only on routine eye exam, thus often remaining undetected until it is more advanced with visual symptoms and loss.⁹ Therefore, it is crucial to develop tools to detect AMD earlier and treatments to slow progression and vision loss. These include easily accessible screening tools for diagnosis and tools to predict progression of disease.

Serological biomarkers have been studied, primarily looking at serum levels of biomarkers related to inflammation¹⁰⁻¹³ or lipid levels,¹⁴ as both appear to play a role in AMD pathogenesis. However, to date results have been inconsistent.¹⁵ Therefore, in our daily clinical practice, we continue to rely on observable characteristics for diagnosis and monitoring of progression, and reliable and accessible biofluid biomarkers are still lacking in AMD.

Our group hypothesized that metabolomics could be an appropriate approach to address this need. Metabolomics, the global profiling of all the small molecules (<1 kDa) in a

biological system,¹⁶ is a novel approach that is increasingly being explored to identify biomarkers.^{3,4,17} Metabolites are the downstream product of the cumulative effects of the genome and its interaction with environmental exposures.¹⁸ Therefore, the metabolome is thought to closely represent the “true functional state” of the biological system and thus current disease phenotype. This is particularly useful for the study of multifactorial diseases, such as AMD.¹⁹

The value of metabolomics as a translational tool for the clinical setting has been demonstrated through several studies in other medical disciplines, including cancer and Alzheimer disease.^{20–24,25–27} Metabolomics studies can be readily performed on easily accessible biological samples, such as blood and urine. Two main techniques are available - mass spectrometry (MS) and nuclear magnetic resonance spectroscopy (NMR).^{28,29} Both approaches have strengths and weaknesses and they are currently considered complementary.³⁰ In AMD, to our knowledge, before our work, only one study had been published,³¹ comparing plasma metabolomic profiles of subjects with neovascular AMD and a control group.

In this project, for the first time, we assess the metabolomic profiles related to AMD and its different stages, with the ultimate goal of identifying potential biomarkers of the disease and its progression. This is based on the hypothesis that the organism’s metabolism is impacted in AMD, with differences according to evolution stages, and that AMD-progressors will have a distinct metabolome.

Importantly, it is currently recognized that a successful diagnosis, therapy and prevention of complex disorders, requires an understanding of the interactions between genetic, environmental and lifestyle factors.³² In AMD, the mechanisms by which genes and environment interact to promote the disease are still poorly understood.³³ Risk prediction could be considerably improved if there was a better understanding of the biological pathways and the specificity of genetic and environmental interactions, which are reflected in the metabolome. Our project represents the first attempt in this direction, by studying metabolomic-genetic-lifestyle associations. The possibility of analyzing a wide range of metabolomic phenotypes in association with genetic variance has been described in the last few years.^{34,35} With the conventional genome-wide association studies (GWAS), the effect sizes of genetic associations are generally small, and information on the underlying biological processes is often lacking. Conversely, single nucleotide polymorphism (SNPs)–metabolite associations point to the underlying biological mechanism, thus have bigger effect sizes and can increase the statistical power of the performed analysis.^{36,37} Therefore, the focus of GWAS is now shifting increasingly away from studying associations with disease end points towards studying associations with intermediate traits, such as metabolomic phenotypes.³² Moreover, pathway based approaches are uniquely suited to metabolomics-GWAS owing to the

abundance of knowledge on proteins involved in metabolite conversion and secretion, as captured in various databases of metabolic pathways and reactions.³²

For any metabolomics or genomics study, an accurate phenotyping is crucial.^{38,39} Indeed, previous studies demonstrated that phenotypic misclassification can dramatically reduce the power to detect associations, or make it impossible to detect a true association.⁴⁰

The current AMD phenotyping and staging are based on color fundus photographs (CFP).^{41,42} Nevertheless, it is currently recognized that fundus appearance is inadequate for a complete understanding of AMD structural alterations – optical coherence tomography (OCT), fundus autofluorescence (FAF) or wide-field imaging provide additional important information.⁴³ Namely, other imaging modalities enable the identification of unique phenotypic features, such as subretinal drusenoid deposits (SDD),⁴⁴ which have been proposed as an independent risk factor for AMD progression;⁴⁵ or peripheral changes, which seem to be present in eyes with AMD more likely than in eyes of subjects with the same age without this disease, and to be associated with AMD risk alleles.^{46,47,48} Indeed, it is increasingly recognized that there is a real need to develop new AMD classification schemes including detailed and refined AMD phenotypes, as assessed by multimodal imaging.^{43,49,50} The current gold-standard (CFP) is certainly incomplete, because it misses important features, and thus has a limited capability to explain AMD, its association with function, or to predict AMD progression.⁵⁰ Bearing this in mind, our study cohort was imaged with infra-red, red-free, FAF, OCT and ultra-widefield imaging. Our goal is to contribute to improve AMD phenotyping, and also to use a detailed phenotypic characterization in our assessment of AMD metabolomic profiles, and metabolomic-genomic-lifestyle associations.

Additionally, one needs to consider that an ideal biomarker that could be used as a surrogate end point in AMD should reflect not only morphological changes, but also alterations in visual function. Therefore, it is essential to study the relationships between them (structural and visual functional changes).⁵¹ Moreover, an improved understanding of structure-function relationships in AMD, particularly in its early phases, can shed the light on underlying biological mechanisms associated with the emergence and progression of the condition. Visual acuity is the most well-established and accepted functional endpoint in ophthalmology.⁵² However, it has a limited ability to serve as a surrogate end point for AMD, as it remains largely unchanged during the early and intermediate stages of the disease.

In this project, we performed structural-functional assessments, namely by using dark adaptation (DA). There is increasing evidence that DA is one of the best functional assessments for the earliest phases of AMD.⁵¹ This is in agreement with reports of patients with early AMD that described vision problems under dim lighting or at night,^{53,54} as well as with histopathologic data showing that rods degenerate earlier and more severely than

cones,^{55,56} and that AMD initially affects the parafoveal region (that has more rods than cones). Fundus- tracked microperimetry is another modality to measure visual function with retina sensitivity. It measures the differential light sensitivity, which is the minimum luminance of a white-spot stimulus superimposed on a white background of uniform luminance needed to perceive the stimulus with eye position correction using the eye-tracking system. In addition, a real-time *en-face* image of the posterior pole is provided, enabling direct comparison between the visual function outcome and the underlying retina pathology.^{57,58}

In summary, our leading research question relates to the application of metabolomics to the study of AMD, namely to identify potential biomarkers of the disease and its progression. We also aim to perform an integration of metabolomics with genomics and lifestyle data. This has the potential to contribute to the current understanding of the mechanisms of AMD, namely by identifying novel pathways that can represent new targets for treatment development. Additionally, we included a detailed phenotypic characterization incorporating complete visual function assessments, which is crucial for our 'omics assessments, but also to improve the current AMD classification schemes, which do not account for the diverse phenotypic presentations that are currently recognized with more advanced imaging modalities.

I.2) Study Design

This is a prospectively designed, cross-sectional study, which was conducted at two study sites: Portugal – Faculty of Medicine, University of Coimbra (FMUC), in collaboration with the Association for Innovation and Biomedical Research on Light and Image (AIBILI) and the Centro Hospitalar e Universitário de Coimbra, Coimbra, Portugal; US – Massachusetts Eye and Ear (MEE), Harvard Medical School, Boston, United States.

The study was approved by the Institutional Review Boards of FMUC, AIBILI, MEE and by the Portuguese National Data Protection Committee (CNPD) – Supplements 1 to 4. All participants provided written informed consent. The study was conducted in accordance with HIPAA (Health Insurance Portability and Accountability Act) requirements and the tenets of the Declaration of Helsinki.

Study population

Over eighteen months (January 2015 to July 2016), we recruited patients with a diagnosis of AMD and a control group of subjects without any evidence of the disease in both eyes, aged 50 years or older. For both, the exclusion criteria included diagnosis of any other

vitreoretinal disease, active uveitis or ocular infection, significant media opacities that precluded the observation of the ocular fundus, refractive error equal or greater than 6 diopters of spherical equivalent, past history of retinal surgery, history of any ocular surgery or intra-ocular procedure (such as laser and intra-ocular injections) within the 90 days prior to enrolment and diagnosis of diabetes mellitus, with or without concomitant diabetic retinopathy (due to the remaining study purposes).

At MEE, participants were consecutively recruited at the Retina Service and the Comprehensive Ophthalmology and Optometry Services, when they were coming for their regular appointments. In Portugal, the study population was derived from a population-based cohort study.^{59,60} All subjects with an established diagnosis of any stage of AMD were invited to participate. Subjects without signs of AMD in the prior evaluation^{59,60} were also invited, and included as controls if they remained without the disease (see below AMD diagnosis). Those who presented AMD at the time of the current evaluation were included in the AMD study group.

Ophthalmological exam, medical history and lifestyle assessment

All participants underwent a comprehensive eye exam, including measurement of best-corrected visual acuity (BCVA), current refraction, intra-ocular pressure, biomicroscopy and dilated fundus exams.

A standardized medical history questionnaire was designed specifically for this study – Supplement 5.

Additionally, all subjects were invited to complete a food frequency questionnaire (FFQ), to assess dietary habits from the preceding year. The Portuguese semi-quantitative FFQ²⁸ is a validated instrument for this population and includes 86 food items. For each of them, participants indicated their average frequency of consumption, by choosing 1 of 9 options, from “never or less than once in a month” to “6 or more per day”. Data processing was performed in collaboration with the Public Health Institute of the University of Porto (PHIUP). For the American population, the Willet FFQ, a semi-quantitative questionnaire designed and validated by the Harvard T.H. Chan School of Public Health (HSPH) was used.²⁹ This questionnaire includes 61 food items and it has one standard portion size indicated for each one of them. Respondents were asked to indicate their estimated frequency of consumption from 9 different response alternatives, ranging from “never or less than once per month” to “6 or more times per day”. For data processing, the obtained questionnaires from the American population were sent to the HSPH.

Due to the absence of a validated and translated questionnaire for both populations at the beginning of this study, physical activity was assessed using 2 different methodologies.

Individuals recruited at MEE were invited to answer the Rapid Assessment of Physical Activity (RAPA) test.⁶¹ This is an easy to read, 9-question (yes/no) test, specifically designed for individuals older than 50 years, being able to discriminate and quantify light, moderate and vigorous activity. Individuals recruited in Portugal were invited to answer a previously validated questionnaire translated to Portuguese - International Physical Activity Questionnaire (IPAQ).⁶² This short, 7-questions' test, provides information about the level of physical activity spent per week, stratified in light, moderate and vigorous activities.⁶³

Imaging exams

For all study participants, non-stereoscopic, 7-field fundus photographs were obtained with one of two types of cameras: Topcon TRC-50DX (Topcon Corporation, Tokyo, Japan), or Zeiss FF-450 Plus (Carl Zeiss Meditec Inc, Dublin, CA). All subjects were also imaged with infra-red, blue-reflectance, fundus autofluorescence, and spectral-domain optical coherence tomography (SD-OCT) using Spectralis®, Heidelberg, Germany –Supplement 6. If the referring retina specialist deemed necessary, fluorescein angiography was performed as part of the regular clinical assessment of patients with CNV.

Additionally, in Portugal all study participants were also imaged with swept-source OCT (SSOCT) (Atlantis, Topcon®). In the US, SSOCT is not yet approved by the Food and Drug Administration (FDA), so this was an optional procedure, for which specific consent was obtained.

In the US, all included participants were also imaged with the Optos® 200 Tx camera (Optos Inc, Marlborough, MA) in three gaze positions: primary gaze, up gaze and down gaze. In this case, both pseudo-color and FAF images were obtained. For Portuguese study participants, ultra-widefield imaging was not available.

Functional exams

For the Boston study population, two functional exams were available: dark adaptation (DA) and microperimetry. Both tests were optional, as our protocol required no prior light exposure, so they had to be performed on a separate day. Therefore, subjects had to come on a separate day, within a maximum time limit of 1 month after enrolling in the study. For DA, we used the AdaptDx® (MacuLogix, PA) extended protocol (20 minutes), and both eyes were tested. Details are described in our papers.^{64,65} For microperimetry, we used the MAIA (Macular Integrity Assessment) microperimetry (CentreVue, Padova, Italy). Patients were tested in both eyes with a supra-threshold protocol, 37 points, centered on the fovea.

Collection of samples

For all participants, fasting blood samples were collected into sodium-heparin tubes, and centrifuged within 30 min (1500 rpm, 10 min, 20°C). Plasma aliquots of 1.5 mL (MEE) and 5 mL (FMUC/AIBILI) were transferred into sterile cryovials and stored at -80°C. In the same day, morning, fasting urine samples were also collected into sterile cups. Within a maximum of 20 minutes, urine aliquots of 1.5 mL (MEE) and 5 mL (FMUC/AIBILI) were transferred into sterile cryovials and stored at -80°C.

1.3) Included Study Population

In Boston, US, we recruited and consented 239 subjects. Of these, 42 (17.5%) withdrew or did not complete the study procedures, so the final study cohort comprises 197 subjects: 47 controls and 150 patients with AMD.

In Coimbra, Portugal, we consented 318 subjects, of which 20 (6.3%) were screening failures, thus the final study cohort includes 298 individuals: 54 controls and 244 subjects with AMD. Table 1 presents the demographics of the final study population.

Coimbra, Portugal					
	Control	Early AMD	Intermediate AMD	Late AMD	p-value
Number of patients, n (%)	54 (18)	58 (19)	132 (44)	54 (18)	NA
Age, mean ± SD	68±5.1	71±6.1	76±7.5	82±6.8	0.0001
BMI, mean ± SD	26.9 ± 4.8	27.2 ± 4.2	27.4 ± 4.4	26.5 ± 4.3	0.65
Gender n, (%)					0.512
Female	36 (67)	35 (60)	91 (69)	32 (59)	
Male	18 (33)	18 (33)	41 (31)	22 (41)	
Smoking n, (%)					0.126
Non-smoker	44 (81)	50 (86)	118 (89)	39 (72)	
Ex-smoker	10 (19)	8 (14)	14 (11)	14 (26)	
Current smoker	0 (0)	0 (0)	0 (0)	1 (2)	
Race n, (%)					0.604
White	54 (100)	58 (100)	130 (98)	53 (98)	
Black	0 (0)	0 (0)	2 (2)	1 (2)	
Asian	0 (0)	0 (0)	0 (0)	0 (0)	
Hispanic	0 (0)	0 (0)	0 (0)	0 (0)	
Boston, United States					
	Control	Early AMD	Intermediate AMD	Late AMD	p-value
Number of patients, n (%)	47 (24)	35 (18)	65 (33)	50 (25)	NA
Age, mean ± SD	67.8 ± 8.5	68.5 ± 7.1	72.5 ± 7.1	76.1 ± 8.2	0.0001*

BMI , mean \pm SD	26.8 \pm 4.3	26.7 \pm 4.3	27.6 \pm 5.6	26.9 \pm 4.5	0.932
Gender n, (%)					0.530
Female	29 (62)	23 (66)	46 (71)	29 (58)	
Male	18 (38)	12 (34)	19 (29)	21 (42)	
Smoking n, (%)					0.097
Non-smoker	24 (52)	21 (60)	28 (43)	17 (35)	
Ex-smoker	20 (43)	14 (40)	34 (52)	31 (66)	
Current smoker	2 (4)	0 (0)	3 (4)	0 (0)	
Race n, (%)					0.632
White	39 (95)	30 (91)	64 (98)	44 (94)	
Black	1 (2)	0 (0)	0 (0)	0 (0)	
Asian	0 (0)	1 (3)	1 (2)	0 (0)	
Hispanic	1 (2)	2 (6)	0 (0)	3 (6)	

Legend: AMD – age-related macular degeneration; n – number; SD – standard deviation; BMI – body mass index; NA – non-applicable. * p-value < 0.05.

I.4) Competing Funding and Grants

- This project was funded by the Portuguese Foundation for Science and Technology (*Fundação para a Ciência e Tecnologia*, FCT) and the Harvard Medical School Portugal Program: Junior Research and Career Development Award (HMSP-ICJ/0006/2013).
- This project was approved by the Residency-PhD Scholarship (*Internos Doutorandos*) from FCT (SFRH/SINTD/93679/2013).
- Two posters derived from this project were awarded with best poster presentation of the MEE Annual Meeting (2016 and 2017), HMS Department of Ophthalmology, Boston, US: *Structural Changes Associated with Delayed Dark Adaptation in Age-Related Macular Degeneration* (2016) and *Human Plasma Metabolomics Study Across all Stages of Age-related Macular Degeneration Identifies Potential Lipid Biomarkers* (2017).
- A manuscript derived from this project was awarded with the most innovative presentation award at the Annual Portuguese Meeting of Ophthalmology 2016, Coimbra, Portugal: *Automated Brightness and Contrast Adjustment of Color Fundus Photographs for the Grading of Age-Related Macular Degeneration*.
- A manuscript derived from this project was awarded with the Dr. Evangelos Gragoudas Award (best paper published in clinical research in vitreoretinal diseases) (2017). MEE,

HMS Department of Ophthalmology, Boston, US: *Structural Changes Associated with Delayed Dark Adaptation in Age-Related Macular Degeneration.*

- A manuscript derived from this project was awarded with the most innovative presentation award at the Annual Portuguese Meeting of Ophthalmology 2017, Vilamoura, Portugal: *Human Plasma Metabolomics Study Across all Stages of Age-related Macular Degeneration Identifies Potential Lipid Biomarkers (2017).*

Chapter II: Metabolomics

This project, for the first time, characterized the plasma metabolomic profiles of AMD and its severity stages. Before our work, the only other available data in the literature referred to a comparison between plasma metabolomics changes of a small cohort of “wet” AMD patients (n=26) and a control group (n=19).³¹

Our results were published in two original manuscripts. Our initial work – Manuscript 1 - was performed using NMR metabolomics, based on the principal that this is an appropriate technique for an initial untargeted approach. NMR offers high reproducibility, simple sample handling and the possibility of sample reuse.^{30,32} At the time of this analysis, we had not finished the recruitment of our study population. Therefore, we included in this study a total of 396 subjects, 61% (n=243) from Coimbra, Portugal and the remaining from Boston, US (n=153). The inclusion of two large cohorts from distinct geographical origins had the advantage of enabling the evaluation of geographical effects on metabolomic profiles. In this manuscript, for the first time, we characterized the plasma metabolomic signatures of patients with AMD at different severity stages (early, intermediate and late AMD stages). We further investigated signature specificity to AMD by evaluating the impact of potential confounders (gender, smoking history, body mass index (BMI) and age) on plasma profiles. The strong age dependence of AMD presented a significant challenge in the search for disease-specific markers. Due to the difficulty in using age-matched groups in this context, we performed an objective evaluation of the impact of age on metabolic profiles and used unmatched cohorts, which better represent actual AMD patients’ population. The potential confounding role of comorbidities was also discussed.

Our results revealed a separation in plasma metabolomic profiles of multiple severity AMD stages for the Boston cohort, and between extreme stages (late AMD vs controls and late AMD vs early AMD) for the Coimbra cohort. Interestingly, the metabolomic fingerprints of AMD in the two cohorts presented both similarities and differences. The observed similarities included variations of histidine, unsaturated fatty acids and protein levels. These might represent a global reflection of the disease, transversal to different cohorts. On the other hand, cohort differences included variations in low-M_w compounds, such as glutamine, alanine, creatine, dimethyl sulfone and pyruvate. Most likely, these represent the potential importance of local nutritional and lifestyle effects on the suggested AMD metabolic fingerprints. Also of note, in both cohorts, we observed differences between controls and subjects with early AMD. These observations relate to two naturally age-matched groups (thus not affected by possible age effects on the metabolome) and may contribute importantly to the future definition of biomarkers for AMD diagnosis.

After this pilot characterization using NMR spectroscopy, we decided to pursue our work using MS metabolomics – [Manuscript 2](#). MS has a higher sensitivity than NMR, enabling the measurement of a broader range of metabolites.^{66,67,68} Additionally, there is a growing acknowledgment of the value of combining NMR and MS.⁶⁹ These are complementary techniques, so combining them is likely to improve the overall quality of a study and enhance the coverage of the metabolome.⁷⁰ This work refers to a preliminary cohort of our Boston study population (n= 120). Using MS, we observed that after controlling confounding factors, 87 metabolites differed significantly between AMD cases and controls. Indeed, a summary score based on these 87 metabolites increased the ability to predict AMD cases, relative to clinical covariates alone. Of these metabolites, over half (48 metabolites) also differed significantly across AMD severity stages. Consistently, both for the comparison between AMD *versus* controls and the different stages of AMD, the vast majority of the identified significant metabolites are involved in lipid metabolism. In particular, we performed pathway analysis for the first time, which revealed a significant enrichment of glycerophospholipid metabolites (i.e. the identified significant metabolites belonged more to glycerophospholipid pathway than what we expected by chance). Additionally, similarly to what we observed using NMR, we also identified significantly different levels of metabolites linked to dipeptides and amino acids in patients with AMD, including a significant role for alanine metabolism.

Our ongoing work on plasma and urine metabolomics is described in Chapter IV, where we also discuss the future directions we aim to pursue.

During the development and execution of this project, we observed that the application of metabolomics to the study of retinal diseases is recent and relatively scarce. Therefore, we set out to compile a comprehensive summary of the tools and knowledge required to perform a metabolomics study, including those specific to retinal diseases, as well as to critically analyze what has been done so far. This work is presented in [Manuscript 3](#), which is currently under submission at *Progress in Retinal and Eye Research*, a peer-reviewed journal where we were invited to publish. Our goal is to improve the current understanding of metabolomics and to help inform future studies, in order to expand the application of metabolomics to the study of retinal diseases in general, and AMD in particular.

The above-mentioned manuscripts can be found in the next pages.

RESEARCH ARTICLE

Human plasma metabolomics in age-related macular degeneration (AMD) using nuclear magnetic resonance spectroscopy

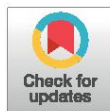
Inês Láins^{1,2,3,4}*, Daniela Duarte⁵*, António S. Barros⁵*, Ana Sofia Martins⁵, João Gil^{2,3,4}, John B. Miller¹, Marco Marques^{2,3,4}, Tânia Mesquita³, Ivana K. Kim¹, Maria da Luz Cachulo^{2,3,4}, Demetrios Vavvas¹, Isabel M. Carreira², Joaquim N. Murta^{2,4}, Rufino Silva^{2,3,4}, Joan W. Miller¹, Deeba Husain^{1,‡}, Ana M. Gil^{5‡*}

1 Department of Ophthalmology, Massachusetts Eye and Ear, Harvard Medical School, Boston, United States, 2 Faculty of Medicine, University of Coimbra (FMUC), Coimbra, Portugal, 3 Association for Innovation and Biomedical Research on Light and Image (AIBILI), Coimbra, Portugal, 4 Department of Ophthalmology, Centro Hospitalar e Universitário de Coimbra (CHUC), Coimbra, Portugal, 5 CICECO-Aveiro Institute of Materials (CICECO/UA), Department of Chemistry, University of Aveiro, Aveiro, Portugal

* These authors contributed equally to this work.

‡ These authors also contributed equally to this work.

* agil@ua.pt


 OPEN ACCESS

Citation: Láins I, Duarte D, Barros AS, Martins AS, Gil J, Miller JB, et al. (2017) Human plasma metabolomics in age-related macular degeneration (AMD) using nuclear magnetic resonance spectroscopy. PLoS ONE 12(5): e0177749. <https://doi.org/10.1371/journal.pone.0177749>

Editor: Simon J. Clark, University of Manchester, UNITED KINGDOM

Received: February 20, 2017

Accepted: May 2, 2017

Published: May 18, 2017

Copyright: This is an open access article, free of all copyright, and may be freely reproduced, distributed, transmitted, modified, built upon, or otherwise used by anyone for any lawful purpose. The work is made available under the [Creative Commons CC0](https://creativecommons.org/licenses/by/4.0/) public domain dedication.

Data Availability Statement: The data obtained in this study was deposited into the NIH Common Fund's Data Repository and Coordinating Center (supported by NIH grant, U01-DK097430) website, <http://www.metabolomicsworkbench.org>, where it has been assigned a Metabolomics Workbench Project ID: PR000431. The data will be directly accessible at <http://www.metabolomicsworkbench.org/data/DRCCMetadata.php?Mode=Project&ProjectID=PR000431>.

Abstract

Purpose

To differentiate the plasma metabolomic profile of patients with age related macular degeneration (AMD) from that of controls, by Nuclear Magnetic Resonance (NMR) spectroscopy.

Methods

Two cohorts (total of 396 subjects) representative of central Portugal and Boston, USA phenotypes were studied. For each cohort, subjects were grouped according to AMD stage (early, intermediate and late). Multivariate analysis of plasma NMR spectra was performed, followed by signal integration and univariate analysis.

Results

Small changes were detected in the levels of some amino acids, organic acids, dimethyl sulfone and specific lipid moieties, thus providing some biochemical information on the disease. The possible confounding effects of gender, smoking history and age were assessed in each cohort and found to be minimal when compared to that of the disease. A similar observation was noted in relation to age-related comorbidities. Furthermore, partially distinct putative AMD metabolite fingerprints were noted for the two cohorts studied, reflecting the importance of nutritional and other lifestyle habits in determining AMD metabolic response and potential biomarker fingerprints. Notably, some of the metabolite changes detected were noted as potentially differentiating controls from patients diagnosed with early AMD.

Funding: This project was funded by the Portuguese Foundation for Science and Technology (HMSP-ICJ/0006/2013), the Miller Retina Research Fund (MEE) and the Miller Champalimaud Award (MEE). This work was also developed within the scope of the project CICECO-Aveiro Institute of Materials, POCI-01-0145-FEDER-007679 (FCT ref. UID /CTM /50011/2013), financed by national funds through the FCT/MEC and when appropriate co-financed by FEDER under the PT2020 Partnership Agreement. We also acknowledge the Portuguese National NMR Network (RNRMN), supported by FCT funds. The funders had no role in study design, data collection and analysis, decision to publish, or preparation of the manuscript.

Competing interests: The authors have declared that no competing interests exist.

Conclusion

For the first time, this study showed metabolite changes in the plasma of patients with AMD as compared to controls, using NMR. Geographical origins were seen to affect AMD patients' metabolic profile and some metabolites were found to be valuable in potentially differentiating controls from early stage AMD patients. Metabolomics has the potential of identifying biomarkers for AMD, and further work in this area is warranted.

Introduction

Age-related Macular Degeneration (AMD) is the leading cause of adult blindness in developed countries and the third most common cause of adult blindness worldwide. It is anticipated that global AMD prevalence will reach 196 million in 2020 and 288 million in 2040. [1] Approximately 90% of patients with AMD have early or intermediate forms, which may progress to advanced disease, in the form of either geographic atrophy and/or neovascular AMD (also known as "wet AMD"). [2], [3] Often asymptomatic in the early stages, in some patients AMD ultimately leads to loss of central vision deterioration and interferes with daily living activities, with profound effects on the quality of life of the elderly. [4] AMD pathogenesis is multifactorial, with complex genetic risk factors interacting with several lifestyle and environmental factors. [2], [3] Serologic biomarkers of AMD incidence and progression have been sought, primarily relating to pathways responsive to inflammation, [5–7] cell stress (particularly oxidative stress) or toxicity. [2], [7], [8] Such studies have, however, provided inconsistent results and, hence, clinical practice still solely relies on the evaluation of phenotypic characteristics, such as fundus appearance. Biofluid markers may be useful to help predict incidence and prevalence of the disease, but reliable markers are still lacking.

Metabolomics, the qualitative and quantitative analysis of metabolites ($M_w < 1$ kDa), [9] may provide an integrated biomarker signal for AMD. Metabolites are the downstream result of genetic transcription processes and, simultaneously, reflect environmental and lifestyle factors as well as individual characteristics related to dietary response and gut microflora. [10], [11] The metabolome should therefore closely reflect the global health state and phenotype of the subject. Two complementary analytical techniques are currently used in metabolomics: mass spectrometry (MS) and nuclear magnetic resonance (NMR) spectroscopy. Briefly, MS provides higher sensitivity, and NMR offers higher reproducibility, simpler sample handling and the possibility of sample reuse. [12], [13] The potential of metabolomics has been established in the search for biofluid (blood and urine) marker profiles for several diseases, including cancer. [14–16] In ophthalmology, recent reviews highlighted its potential applications, [17–19] although results are still scarce and mostly related to animal models. [19] Metabolomic studies of human samples using liquid chromatography (LC)-MS analysis of tears of healthy subjects [20] and patients with keratoconus suggested differences in metabolites related to the urea cycle, Krebs' cycle and oxidative stress. [21] Additionally, NMR studies of vitreous samples from subjects with proliferative vitreoretinopathy and retinal detachment suggested that these diseases might present a specific metabolic signature. [22], [23], [24]. Metabolomics of human plasma has been used to characterize diabetic retinopathy [25], [26], open angle glaucoma [27] and anterior uveitis. [28] In AMD, investigators have used untargeted LC-MS metabolomics to investigate changes in the plasma of "wet" AMD patients ($n = 26$), compared to controls ($n = 19$). [29]

In the current study, we have used NMR metabolomics to characterize the plasma metabolomic signatures of patients with AMD at different severity stages (early, intermediate and late

AMD stages), considering two large cohorts from distinct geographical origins, Southern European (Coimbra, central Portugal) and Northeastern United States (Boston Metropolitan area, US), which allows for evaluation of geographical effects on metabolomic profiles. We further investigated signature specificity to AMD by evaluating the impact of potential confounders (gender, smoking history, body mass index (BMI) and age) on plasma profile. The strong age dependence of AMD presents a significant challenge in the search for disease-specific markers. Due to the difficulty in using age-matched groups in this context, we have performed an objective evaluation of the impact of age on metabolic profile and used unmatched cohorts, which better represent actual AMD patients' population. The potential confounding role of comorbidities is also discussed.

Materials and methods

Study design and subject recruitment

This study is part of a cross-sectional, observational study performed in the Department of Ophthalmology of Massachusetts Eye and Ear (MEE), Harvard Medical School, Boston, United States, and the Faculty of Medicine of the University of Coimbra (FMUC), Coimbra, Portugal, in collaboration with the Association for Innovation and Biomedical Research on Light and Image (AIBILI) and the "Centro Hospitalar e Universitário de Coimbra", Coimbra, Portugal. The clinical protocol was conducted in accordance with HIPAA (Health Insurance Portability and Accountability Act) requirements and the tenets of the Declaration of Helsinki, and was approved by the Institutional Review Boards of MEE, FMUC and AIBILI, and by the Portuguese National Data Protection Committee (CNPD). All subjects enrolled in the study provided written informed consent.

From January 2015 to July 2016, in both sites (Coimbra and Boston), patients diagnosed with AMD were prospectively recruited, as well as control groups of subjects with no evidence of AMD and aged ≥ 50 years. At MEE, participants were consecutively recruited from the Retina Service and the Comprehensive Ophthalmology and Optometry Services, at their regular appointments. For those not fasting at that time, a new appointment was scheduled within a maximum of one month for blood collection under fasting. The Portuguese (FMUC/AIBILI) study population was derived from a population-based cohort study,^[30] where all subjects with an established diagnosis of any stage of AMD were invited to participate. Subjects without signs of AMD in a prior evaluation^[30] were also invited, and included as controls if they remained without the disease in the present evaluation (see criteria below). For both cohorts, the exclusion criteria were: diagnosis of any other vitreoretinal disease, active uveitis or ocular infection, significant media opacities that precluded the observation of the ocular fundus, refractive error equal or greater than 6 diopters of spherical equivalent, past history of retinal surgery, history of any ocular surgery or intra-ocular procedure (such as laser and intra-ocular injections) within the 90 days prior to enrolment, and diagnosis of diabetes mellitus. Other common age-related conditions (hypertension, dyslipidemia, rheumatic disease, renal or liver conditions, and neurological diseases) were not considered for exclusion and their potential effect on the results will be discussed.

Clinical examination

All participants received complete bilateral ophthalmologic examination, including a dilated fundus exam. Recruited subjects were also imaged with 7-field, non-stereoscopic color fundus photographs (CFP) either with a Topcon TRC-50DX (Topcon Corporation, Tokyo, Japan) or a Zeiss FF-450Plus (Carl Zeiss Meditec, Dublin, CA) camera. At the same visit, a complete medical history was obtained, according to a standardized questionnaire specifically built for

the purposes of this study (S1 Appendix), based on the current knowledge of AMD pathogenesis and the input of five Retina specialists. This included self-reported data on smoking habits (smokers were considered those who reported current smoking and ex-smokers those who have ever smoked, regardless of when they stopped), and weight and height (used for BMI calculations). If the study participants did not know their current height and/or weight, these were recorded by a study investigator.

For AMD diagnosis and staging, two of three independent experienced graders analyzed all field 2 CFP, according to the AREDS classification system.[31][32] In case of disagreement, a senior author (RS or DH) established the final categorization. Images taken with Topcon cameras were evaluated with IMAGEnet 2000 software (version 2.56; Topcon Medical Systems), and those obtained with a Zeiss camera were observed using VISUPAC (version 4.5.1; Carl Zeiss Meditec). Images were standardized using software developed by our group. We adopted the most recent AREDS2 definitions,[32] namely that the standard disc diameter equals 1800 μm (rather than 1500 μm), which affects the size of the ETDRS grid and of the standard drusen circles; and that geographic atrophy (GA) is present if the lesion has a diameter equal or superior than 433 μm (AREDS circle I-2) and at least two of the following features are present—absence of RPE pigment, circular shape, or sharp margins (thus meaning that the involvement of the central fovea is not a requirement). Therefore, the following groups were established and used for further assessments[31],[32]: controls—presence of drusen maximum size < circle C0 and total area < C1; early AMD—drusen maximum size \geq C0 but < C1 or presence of AMD characteristic pigment abnormalities in the inner or central subfields; intermediate AMD—presence drusen maximum size \geq C1 or of drusen maximum size \geq C0 if the total area occupied is $>$ 12 for soft indistinct drusen and $>$ O2 for soft distinct drusen; late AMD—presence of GA according to the criteria described above (GA or “dry” late AMD) or evidence of neovascular AMD (choroidal neovascularization, CNV or “wet” AMD). For participants with different stages in the two eyes, the worse of the two was considered as the subjects’ classification.

Plasma collection and NMR analysis

The present cross-sectional study relied on a single plasma collection per individual. For all participants, fasting blood samples were collected into sodium-heparin tubes, and centrifuged within 30 min (1500 rpm, 10 min, 20°C). Plasma aliquots of 1.5 mL (MEE) and 5 mL (FMUC/AIBILI) were transferred into sterile cryovials and stored at -80°C. Plasma samples from MEE were shipped to Portugal for metabolomic profiling in dry ice (through TNT Express, USA, INC). Samples arrived frozen in less than 48 hours and were immediately stored at -80°C until NMR analysis. Prior to analysis, plasma samples were thawed at room temperature and homogenized in a vortex mixer. Then, 400 μl of saline solution (NaCl 0.9% in 10% D₂O) were added to 200 μl of sample. After centrifugation (4500 g, 5min, 25°C), 550 μl of each sample was transferred to a 5 mm NMR tube. NMR spectra were recorded, at 300 K, using a Bruker Avance DRX 500 spectrometer operating at 500.13 MHz for proton, with a 5 mm TXI probe. For each sample, three one-dimensional (1D) ¹H NMR spectra were obtained: a standard spectrum (*noesypr1d*, Bruker library), a Carr–Purcell–Meiboom–Gill (CPMG) spectrum (*cpmgpr*) and a diffusion-edited spectrum (*ledbpgp2s1dpr*). Standard spectra were acquired with a 100 ms mixing time and water suppression during the relaxation delay (RD = 4 s) and mixing time. CPMG spectra were acquired with water presaturation, with 80 loops (n) and a total spin–spin relaxation time (2n τ) of 64 ms (with τ = 400 μs). Diffusion-edited spectra were recorded with a diffusion time of 100 ms, a pulsed-field gradient (G1) of 1 ms, a spoil gradient (G2) of 0.6 ms, an eddy current recovery time (τ) of 5 ms, and 90% of the maximum gradient strength

(48.15 G/cm). All 1D spectra were acquired into 32k complex data points with 10330.58 Hz spectral width. Each free induction decay was zero-filled to 64 k points and multiplied by a 0.3 Hz exponential line-broadening function prior to Fourier transformation. Spectra were manually phased and baseline corrected and chemical shifts referenced internally to the α -glucose H1 resonance (δ 5.23). Peak assignments were carried out using 2D NMR spectra and databases Bruker B-BIOREFCODE and HMDB.[33]

Statistical analysis of metadata and NMR data

Statistical descriptive and inference methods (t-test, Fisher-exact test, Chi-square test and density distribution) were used to describe the clinical and demographic characteristics of the study population. Multivariate analysis was applied to a total of 729 NMR spectra from Coimbra cohort (42 controls and 201 AMD patients) and 459 spectra from Boston cohort (40 controls and 113 AMD patients). For each type of spectrum (standard, CPMG, diffusion-edited), data matrices were built (Amix 3.9.14, Bruker, BioSpin, Rheinstetten, Germany) excluding the water region (δ 4.50–5.15). Spectra were aligned using recursive segment-wise peak (RSPA), [34] normalized to total area, and scaled to unit variance. Initial analysis by Principal Component Analysis (PCA),[35] an unsupervised technique (no consideration of sample class or characteristics) that accommodates all inter-subject variability sources, was followed by supervised assessments (where information on sample class is considered) by Partial Least Squares Discriminant Analysis (PLS-DA),[36] and orthogonal (O)-PLS-DA[37] (SIMCA-P 11.5, Umetrics, Umeå, Sweden). PLS-DA loading weights were back-transformed, multiplying each variable by its standard deviation, and false-colored according to variable importance to the projection (VIP) (Matlab 7.9.0, The MathWorks, Inc, Natick, MA). For PLS-DA models, randomized (Monte Carlo) cross validation (MCCV, in-house developed) was carried out, with recovery of Q^2 values and confusion matrices; simultaneous randomized class-permutation assessed the null hypothesis. Classification rates (CR), specificity (spec.), and sensitivity (sens.) were computed.

In order to filter out random phenotypic effects unrelated to AMD, variable selection was employed (with $VIP > 1$, $VIP/VIP_{cvSE} > 1$ and $|b/bcvSE| > 1$)[38] and PLS-DA reapplied. The models with higher Q^2 values enabled relevant resonances to be identified and subsequently integrated across AMD stages (Amix 3.9.14). Integrals were normalized to total intensity and variations assessed by univariate analysis (Wilcoxon test, R statistical software). Effect size and corresponding confidence intervals were computed using the Hedges' g index.[39] Generalized linear regression was used as a flexible generalization of ordinary multiple linear regression by allowing the magnitude of the variance of each measurement (age, sex, BMI, and AMD status) to be a function of the metabolite semi-quantitative variation.

Results

Study population

We recruited a total of 396 subjects, 61% ($n = 243$) in Coimbra (42 controls and 201 patients with AMD) and the remaining in Boston ($n = 153$) (40 controls and 113 patients with AMD). The study population demographics and AMD staging classification are shown in Table 1. Not surprisingly, there were significant differences in age (p -values 1.3×10^{-2} – 3.2×10^{-5}) and age distributions (S1 Fig, left) between controls and AMD patients in both cohorts and across the stages of AMD, except between controls and early AMD (p -values 0.31 and 0.55, for Coimbra and Boston, respectively). This confirms age as a potentially important confounder in human plasma profiling studies of AMD. Similarly, the possible confounding nature of gender among AMD severity groups (in Coimbra only, p -value 4.2×10^{-2}) and smoking history (expressed as

Table 1. Characterization of the study population. Characterization of the study populations (Coimbra and Boston cohorts), with corresponding number of subjects (n), age (years), female (F)/male (M) ratio, body mass index (BMI) (kg.m⁻²) and smoking history.

	Coimbra cohort (n _{total} = 243)				Boston cohort (n _{total} = 153)			
	Controls	Early AMD	Int. AMD	Late AMD	Controls	Early AMD	Int. AMD	Late AMD
n ^a	42 (17.3)	45 (18.5)	124 (51.0)	32 (13.2) ^b	40 (26.1)	30 (19.6)	45 (29.4)	38 (24.8) ^c
Age (years)	68 (58–77)	70 (61–82)	75 (60–91)	81 (62–92)	70 (51–95)	68 (54–91)	71 (61–85)	75 (56–89)
Gender (F/M)	26/16	29/16	85/39	16/16	24/16	20/10	29/16	24/14
BMI (kg.m ⁻²) ^d	27 (18–38)	27 (18–36)	28 (19–42)	27 (17–36)	26 (19–40)	26 (18–39)	27 (21–53)	26 (20–37)
Smoking history ^e :								
Smokers	0	0	0	1	2	0	2	0
ex-smokers	8	6	14	11	16	11	24	23
non-smokers	34	39	110	20	21	19	19	13

Int. AMD: intermediate AMD.

^a: numbers in brackets correspond to % of cohort

^b: further classified as “wet” (n = 27) and “dry” AMD (n = 5)

^c: further classified as “wet” (n = 31) and “dry” AMD (n = 7)

^d: information unavailable for 2 Coimbra subjects (1 early and 1 intermediate AMD) and 14 Boston subjects (3 controls and 2 early, 4 intermediate and 5 late AMD)

^e: information unavailable for 3 Boston subjects (1 control and 2 late AMD).

<https://doi.org/10.1371/journal.pone.0177749.t001>

ex-smokers/non-smokers ratio, as only residual numbers of smokers were identified) was also considered. No significant BMI differences were observed across groups (*p*-values > 0.2) (Table 1 and S1 Fig, right). Furthermore, the age-related comorbidities observed in our cohorts were well balanced (S2 Table), except for a small number of conditions between intermediate and late AMD groups.

Plasma profile differences

Fig 1 shows representative standard, CPMG and diffusion-edited ¹H NMR spectra of a control plasma sample, reflecting all visible compounds (standard spectrum, Fig 1A), mainly low-M_w compounds (CPMG spectrum, Fig 1B) and high-M_w compounds (diffusion-edited spectrum, Fig 1C), respectively. Editing of spectral information in the latter two spectra (Fig 1B and 1C) reduces spectral overlap and provides specific information on small molecule and macromolecule metabolites, respectively. It should be noted, however, that lipid resonances corresponding to smaller and/or more mobile lipids also contribute to CPMG spectra. Overall, spectral assignment revealed just under 30 low-M_w metabolites, in agreement with previous reports, [40] and several different macromolecule environments arising from proteins (albumin, glycoproteins) and lipoprotein cholesterol, choline, glyceryl and fatty acid moieties (lipids assignment shown in S1 Table).

Initial PCA revealed no separation between controls and AMD patients in either cohort, thus reflecting high inter-individual variability of plasma profiles. Subsequent pairwise PLS-DA analysis of full CPMG and diffusion-edited spectra provided models with no classification power (*Q*² < 0.5) for AMD status in either cohort (S3 Table). The highest pairwise model *Q*² values were observed in the Boston cohort for: intermediate vs. early AMD (CPMG spectra, i.e. low-M_w metabolites domain) (*Q*² = 0.32, 80% sensitivity, 53% specificity); and late vs early AMD (diffusion-edited spectra or high M_w domain) (*Q*² = 0.39, 78% sensitivity, 79% specificity) (S3 Table). This indicates that AMD does not strongly impact the plasma profile when analyzed by NMR (i.e. when metabolites down to sub-millimolar concentrations are considered). Furthermore, no distinction was detected between the small sub-cohorts of late

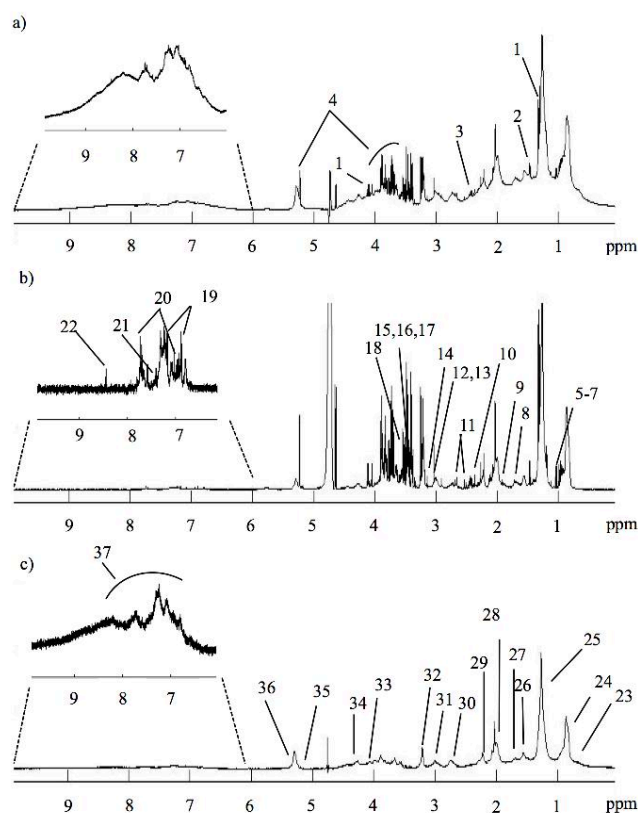


Fig 1. Representative ^1H NMR spectra of control plasma. 500 MHz ^1H NMR spectra of blood plasma from a control subject: a) standard 1D spectrum; b) CPMG spectrum; c) diffusion-edited spectrum. Signal assignment: 1-lactate; 2-alanine; 3-glutamine; 4-glucose; 5-isoleucine; 6-leucine; 7-valine; 8-lysine; 9-acetate; 10-pyruvate; 11-citrate; 12-creatine; 13-creatinine; 14-dimethyl sulfone; 15-TMAO, trimethylamine-*N*-Oxide; 16, proline; 17-methanol; 18-glycine; 19-tyrosine; 20-histidine; 21-phenylalanine; 22-formate; 23-C18H cholesterol; 24- CH_3 lipids; 25- $(\text{CH}_2)_n$ lipids; 26- $\text{CH}_2\text{CH}_2\text{CO}$ lipids; 27- $\text{CH}_2\text{CH}_2\text{C}=\text{C}$ lipids; 28- $\text{CH}_2\text{C}=\text{C}$ lipids; 29- CH_2CO lipids; 30- $\text{C}=\text{CCH}_2\text{CH}=\text{C}$ lipids; 31-albumin lysyl groups; 32- $\text{N}(\text{CH}_3)_3$ choline; 33-glycerol C1,3H; 34-glycerol C1,3H'; 35-glycerol C2H; 36-HC=CH lipids; 37-NH protein region.

<https://doi.org/10.1371/journal.pone.0177749.g001>

AMD subjects with “dry” (geographic atrophy) or “wet” (choroidal neovascularization) AMD (^b and ^c in Table 1).

Variable selection was then performed to filter off random variability unrelated to sample classes. [38] In this study, it led to improved model robustness for some pairwise comparisons, in both cohorts (as shown by higher values of Q^2 , CR, sensitivity and specificity, underlined bold in S3 Table), and some group separation in PLS-DA score plots. Fig 2 shows the PLS-DA score plots obtained when comparing late AMD subjects with controls. In the Coimbra cohort, group separations were mostly seen between extreme stages (late AMD vs controls and late vs early AMD, with $Q^2 = 0.32-0.35$). In Boston, group separations were also noted between

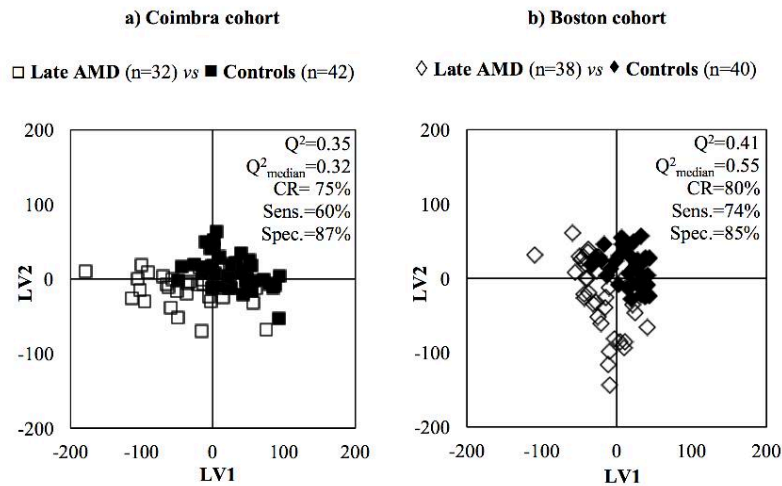


Fig 2. Examples of PLS-DA score plots. PLS-DA scores scatter plots and MCCV quality parameters (pairwise model Q^2 , Q^2_{median} (obtained through MCCV), % CR, % sens. and % spec.) obtained for variable selected CPMG NMR spectra of late AMD patients vs controls, in the a) Coimbra cohort: late AMD patients (\square , $n = 32$), controls (\blacksquare , $n = 42$) and b) Boston cohort: late AMD patients (\diamond , $n = 38$), controls (\blacklozenge , $n = 40$).

<https://doi.org/10.1371/journal.pone.0177749.g002>

multiple AMD stages; for example, for early AMD vs controls, $Q^2 = 0.50\text{--}0.54$ (S3 Table). The best performing models were further studied through analysis of the corresponding loading plots, signal integration and subsequent calculation of effect size (E.S.). The metabolites changing significantly in at least one of the pairwise models in S3 Table were thus identified, and tracked thereafter across the various degrees of AMD severity (Table 2). The graphical representations of E.S. for low- M_w and macromolecule metabolomes (Fig 3 and S2 Fig, respectively) help visualize the most relevant metabolite variations across AMD stages (Table 2), as do the boxplot representations in Figs 4 and 5.

Compared to controls, Coimbra subjects with early AMD exhibited higher circulating levels of creatine, acetate and dimethyl sulfone (Table 2, shaded areas in Fig 3A, top), C18 cholesterol and HDL-choline resonances (S2A Fig, top); and lower levels of unsaturated fatty acids (F.A.) (Table 2, Fig 3A and S2A Fig, top). In this cohort, increasing AMD severity produced small changes in low- M_w metabolites (Table 2, Fig 3A): higher pyruvate for intermediate AMD and lower levels of histidine, acetoacetate, β -hydroxybutyrate and trimethylamine-*N*-oxide (TMAO) for late AMD (the latter not statistically relevant). In the macromolecules domain (S2A Fig), qualitative lower protein levels (expressed by NH resonances) were noted in intermediate AMD and initial low levels of unsaturated F.A. increased at later AMD stages. Boston subjects differed slightly in terms of the low- M_w domain (Table 2, Fig 3B), exhibiting higher levels of glutamine in early AMD and lower levels for intermediate AMD; low histidine levels in intermediate and late AMD (similarly to the Coimbra cohort); and low alanine levels in late AMD. In the macromolecule domain (S2B Fig), results were broadly similar between cohorts, with unsaturated fatty acid levels again increasing from early AMD into more severe stages, and a tendency for low protein levels (including albumin) characterizing intermediate AMD.

Table 2. Variations in plasma metabolites of AMD patients. Main variations in plasma metabolites across AMD evolution through different severity stages, in Coimbra and Boston cohorts.

Coimbra cohort				Boston cohort			
Family	Compound (δ /ppm, multiplicity)	E.S.	p-value ^a	Family	Compound (δ /ppm, multiplicity)	E.S.	p-value ^a
Early AMD vs Controls							
A.A.	Creatine (3.03, s) ^b	0.53 [0.09,0.97]	2.9E-2	A.A.	Glutamine (2.43, m) ^b	0.59 [0.07,1.10]	1.6E-2
Lipids	C18H cholesterol (0.59–0.70) ^c	0.52 [0.08,0.96]	2.1E-2	Lipids	HC = CH F.A. LDL+VLDL (5.28–5.37) ^c	-0.36 [-0.85, 0.13]	2.9E-2
	HC = CH F.A. (5.24–5.37) ^b	-0.55 [-0.99,-0.11]	1.6E-2				
	N(CH ₃) ₃ choline HDL (3.16–3.21) ^c	0.65 [0.21,1.10]	4.9E-3				
	HC = CH F.A. LDL+VLDL (5.28–5.37) ^c	-0.50 [-0.94,-0.06]	2.9E-2				
O.A.	Acetate (1.91, s) ^b	0.50 [0.06,0.94]	1.6E-2				
Other	Dimethyl sulfone (3.15, s) ^{b, d}	0.57 [0.13,1.01]	7.1E-3				
Intermediate vs Early AMD							
O.A.	Pyruvate (2.36, s) ^b	0.43 [0.08, 0.78]	1.8E-2	A.A.	Glutamine (2.43, m) ^b Histidine (7.74, s) ^b	-0.65 [-1.15,-0.15] -0.54 [-1.04,-0.04]	6.4E-3 1.9E-2
				Lipids	CH ₂ CH ₂ COOR F.A. (1.45–1.61) ^c	-0.57 [-1.06, -0.09]	3.6E-2
					CH ₂ CH ₂ C = C F.A. (1.62–1.74) ^c	-0.57 [-1.05,-0.08]	2.3E-3
					HC = CH F.A. (5.24–5.37) ^b	0.63 [0.13,1.13]	6.1E-3
					HC = CH F.A. LDL + VLDL (5.28–5.37) ^c	0.46 [-0.02,0.95]	7.4E-3
				Other	Albumin lysil (2.92–3.02) ^c	-0.56 [-1.04,-0.07]	4.5E-3
Late vs Intermediate AMD							
A.A.	Histidine (7.74, s) ^b	-0.43 [-0.82,-0.03]	4.0E-2	A.A.	Alanine (1.47, d) ^b Histidine (7.74, s) ^b	-0.44 [-0.90,0.03] -0.61 [-1.07,-0.14]	4.2E-2 1.3E-2
O.A.	Acetoacetate (2.27, s) ^b	-0.31 [-0.70, 0.09]	3.7E-2				
	β -hydroxybutyrate (2.39, m) ^b	-0.40 [-0.80,-0.005]	1.0E-3	Lipids	Glycerol C1,3H'(4.20–4.34) ^c	-0.43 [-0.87,0.02]	3.0E-2

E.S.: effect size, values in square brackets correspond to E.S. range; A.A.: amino acids, O.A.: organic acids, d: doublet, s: singlet, m: multiplet, F.A.: fatty acids.

^a: all p-values indicated become > 0.05 upon Bonferroni correction for multiple comparisons.

^b and ^c: integrals measured in CPMG and in diffusion-edited spectra, respectively

^d: metabolite with possible contribution from different subjects' age.

<https://doi.org/10.1371/journal.pone.0177749.t002>

In the boxplot representations for Coimbra (Fig 4) and Boston (Fig 5) cohorts, a number of small metabolite variations (some only qualitative in nature) emerge as potentially differentiating controls from early AMD, namely: 1) acetate, creatine, dimethyl sulfone, cholesterol, HDL-choline and unsaturated fatty acids in Coimbra subjects and 2) glutamine, histidine, unsaturated fatty acids and albumin, in Boston subjects (highlighted metabolite names in Figs 4 and 5). This observation refers to the two naturally age-matched groups of controls and early AMD, thus not being affected by possible age confounding effects, and may potentially lay the ground for future AMD biomarkers. The role of age and other characteristics as possible confounders is discussed in the next section.

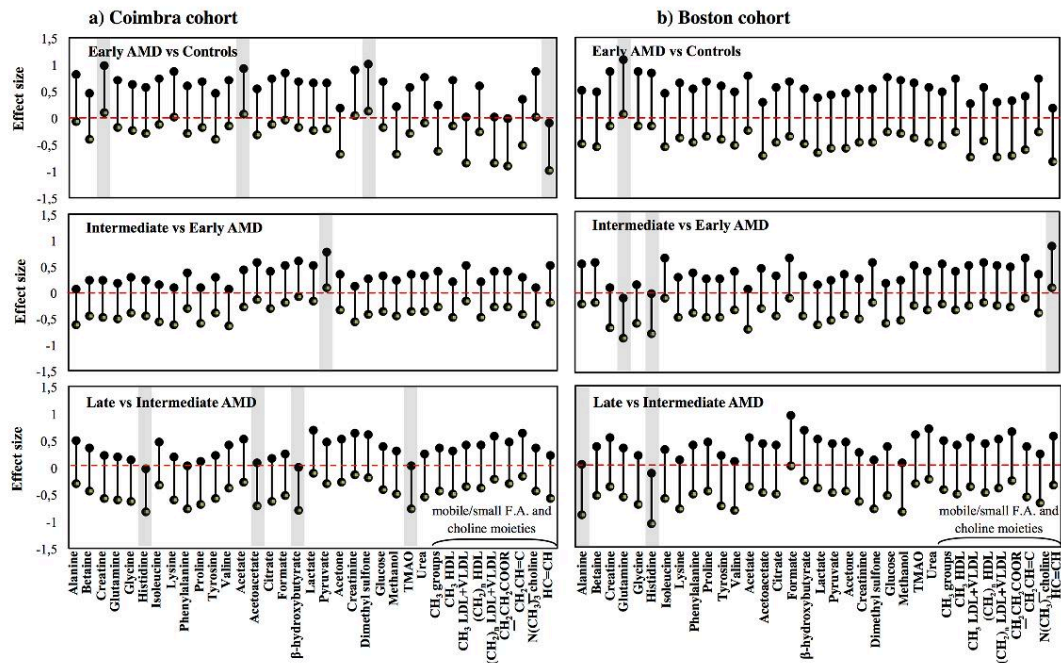


Fig 3. Effect size plots for CPMG spectra integrals. Effect size (E.S.) plots for resonances varying in the CPMG spectra across AMD evolution through different severity stages in the a) Coimbra and b) Boston cohorts. Resonances are listed alphabetically within each compound family (amino acids, organic acids, other low- M_w compounds and lipids). The dashed horizontal line refers to null E.S. and the length of the vertical segments corresponds to E.S. range. E.S. segments not intercepting the null E.S. line are considered as relevant variations (shaded rectangles). F.A.: fatty acids.

<https://doi.org/10.1371/journal.pone.0177749.g003>

Potential confounders

We evaluated the importance of age and other potential confounders, namely gender and smoking history (as mentioned, BMI was not statistically different in these cohorts), on the subjects' plasma metabolic profile and, in particular, on the putative AMD fingerprints shown in Table 2. To investigate this, the larger groups of subjects diagnosed with intermediate AMD (Table 1) were used for multivariate analysis as a function of each parameter, independently of AMD staging. Regarding the gender imbalance between intermediate and late AMD groups in Coimbra (no imbalance was observed in Boston), PLS-DA indicated that Coimbra females had lower circulating levels of isoleucine (p -value = 8.85×10^{-6}), valine (p -value = 2.13×10^{-3}), creatinine (p -value = 4.74×10^{-5}), lactate (p -value = 2.09×10^{-4}) and methanol (p -value = 1.67×10^{-3}). Assuming that such differences are independent of AMD staging, their absence in the putative AMD fingerprint in Table 2 indicates that gender is not a confounder in this cohort. Regarding smoking habits, ex-smokers in Coimbra were found to have slightly higher levels of formate (p -value = 5.65×10^{-3}) than non-smokers; increases in methanol (p -value = 2.96×10^{-2}) and lactate (p -value = 2.57×10^{-2}) were also noted but probably are due to a higher proportion of female ex-smokers in this group. In Boston, ex-smokers showed a slight increase in isoleucine (p -value = 4.35×10^{-2}), compared to non-smokers. Since none of these

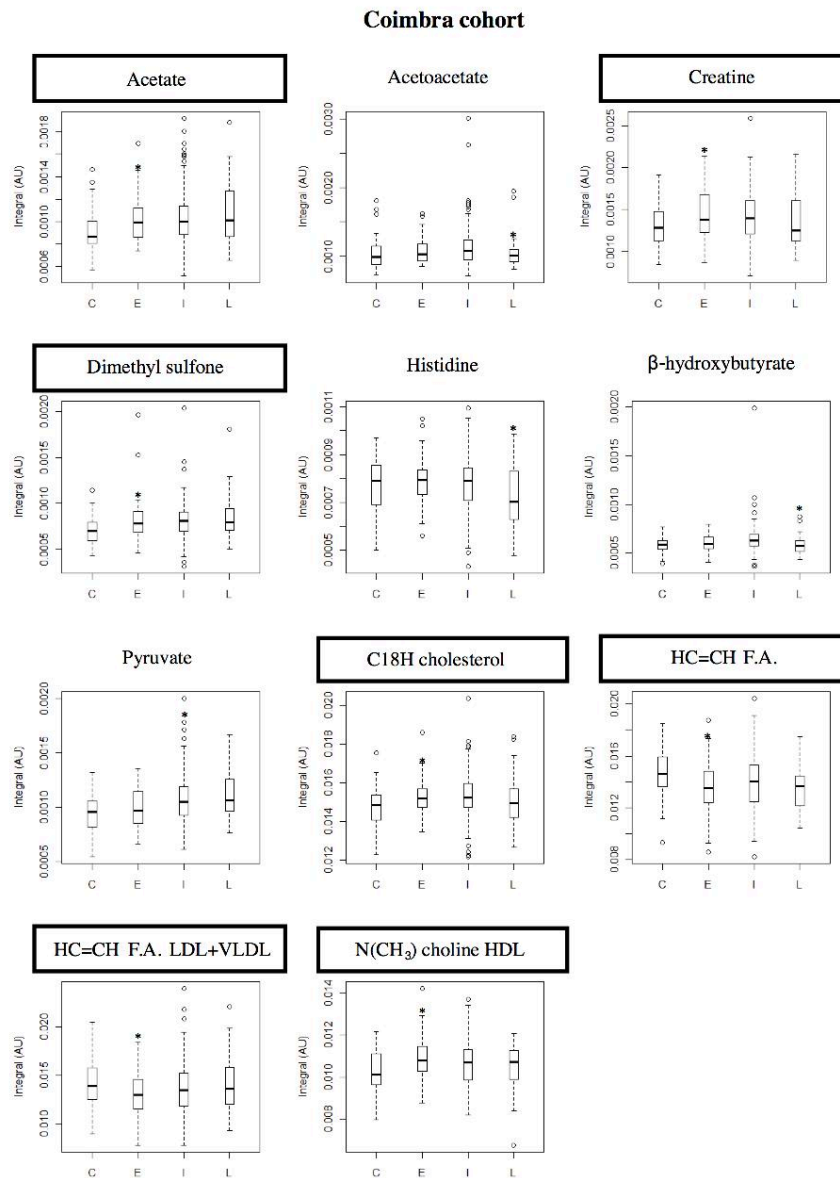


Fig 4. Boxplot graphs for metabolites varying in Coimbra cohort. Coimbra cohort: boxplot representations of the metabolite variations found statistically relevant (* indicates p -value < 0.05) in at least one pairwise PLS-DA model. Compound names in rectangles correspond to compounds differentiating between controls and early AMD patients. C: controls, E: early AMD, I: intermediate AMD, L: late AMD. F.A.: fatty acids.

<https://doi.org/10.1371/journal.pone.0177749.g004>

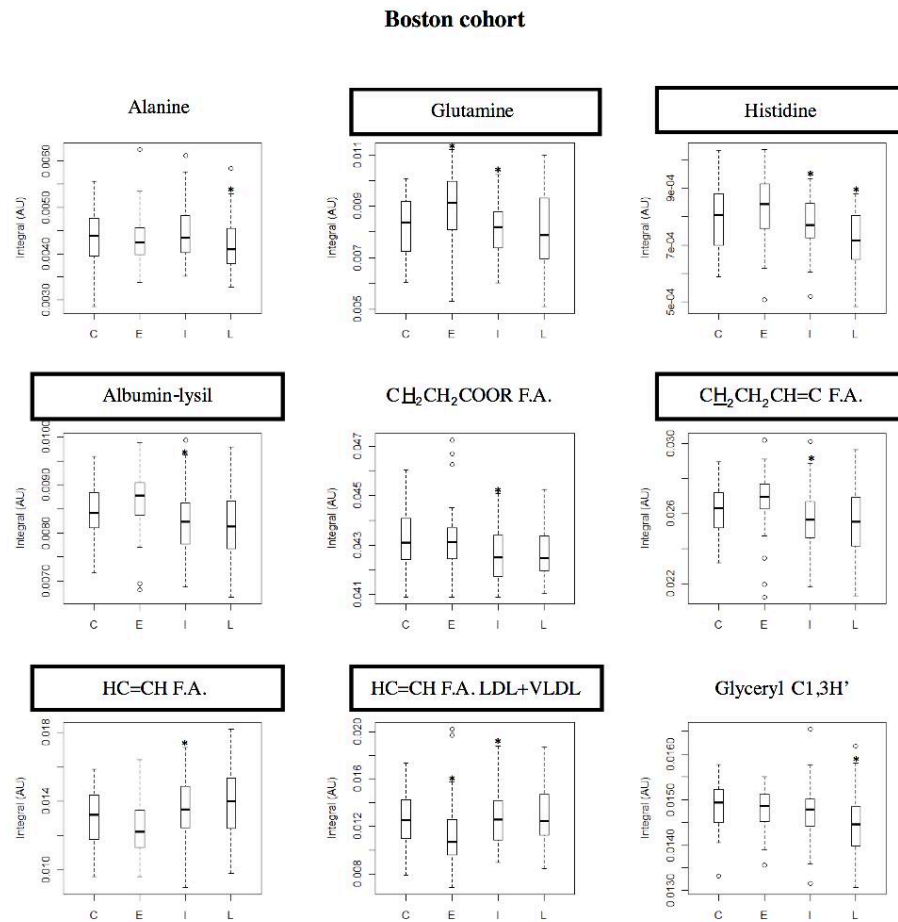


Fig 5. Boxplot graphs for metabolites varying in Boston cohort. Boston cohort: boxplot representations of the metabolite variations found statistically relevant (* indicates p -value < 0.05) in at least one pairwise PLS-DA model. Compound names in rectangles correspond to compounds differentiating between controls and early AMD patients. C: controls, E: early AMD, I: intermediate AMD, L: late AMD. F.A.: fatty acids.

<https://doi.org/10.1371/journal.pone.0177749.g005>

changes coincided with the suggested AMD fingerprints (Table 2), smoking history may also be ruled out as an important metabolic confounder in these cohorts. Finally, PLS-DA models of age of intermediate AMD groups revealed increases in acetoacetate (p -value = 3.8×10^{-2}), citrate (p -value = 1.9×10^{-4}), dimethyl sulfone (p -value = 1.4×10^{-2}) and β -hydroxybutyrate (p -value = 8.6×10^{-3}) in older Coimbra subjects, whereas older Boston subjects exhibited a weak tendency for higher circulating urea levels (p -value = 3.9×10^{-2}). Again, these variations do not compromise the potential fingerprint features, except for dimethyl sulfone († in Table 2, note the opposite variation of β -

Table 3. Generalized linear regression results. Generalized linear regression coefficients obtained through modeling of metabolite variations as a function of gender proportion, smoking history, body-mass index (BMI), age and AMD status. F.A.: Fatty acids. Values in bold illustrate the higher contributions of AMD status for each metabolite variation, compared to confounders. Similar metabolite variations in the two cohorts are denoted by underline.

Compound	Gender proportion	Smoking history	BMI	Age	AMD status
Coimbra cohort					
Acetate	-4.0x10 ⁻⁵	2.1x10 ⁻⁵	-5.3x10 ⁻⁶	1.0x10 ⁻⁶	1.1x10⁻³
Acetoacetate	-3.8x10 ⁻⁵	-3.1x10 ⁻⁵	-3.1x10 ⁻⁶	7.3x10 ⁻⁶	6.9x10⁻⁴
Creatine	1.4x10 ⁻⁴	-1.8x10 ⁻⁵	4.2x10 ⁻⁶	-4.8x10 ⁻⁶	1.6x10⁻³
Dimethyl sulfone	-1.8x10 ⁻⁵	2.8x10 ⁻⁵	-4.8x10 ⁻⁷	7.5x10 ⁻⁶	2.4x10⁻⁴
HC = CH F.A.	7.6x10 ⁻⁴	2.9x10 ⁻⁴	1.2x10 ⁻⁵	-3.3x10 ⁻⁵	1.5x10⁻²
<u>Histidine</u>	1.3x10 ⁻⁷	-6.5x10 ⁻⁶	-1.3x10 ⁻⁶	3.1x10 ⁻⁸	8.1x10⁻⁴
β -hydroxybutyrate	-1.3x10 ⁻⁵	-4.6x10 ⁻⁶	-1.3x10 ⁻⁶	2.5x10 ⁻⁶	4.6x10⁻⁴
Pyruvate	-9.9x10 ⁻⁵	1.5x10 ⁻⁵	3.3x10 ⁻⁶	6.2x10 ⁻⁷	9.3x10⁻⁴
Boston cohort					
Alanine	-8.0x10 ⁻⁵	2.9x10 ⁻⁵	-2.0x10 ⁻⁵	-5.5x10 ⁻⁶	4.2x10⁻³
Glutamine	-4.6x10 ⁻⁴	-1.2x10 ⁻⁴	-8.5x10 ⁻⁵	3.2x10 ⁻⁵	7.1x10⁻³
<u>Histidine</u>	-2.3x10 ⁻⁵	4.0x10 ⁻⁶	-4.0x10 ⁻⁶	3.6x10 ⁻⁶	5.1x10⁻⁴
HC = CH F.A.	3.0x10 ⁻⁴	-1.7x10 ⁻⁴	5.5x10 ⁻⁶	-5.4x10 ⁻⁵	1.4x10⁻²

<https://doi.org/10.1371/journal.pone.0177749.t003>

hydroxybutyrate which rules it out as originating from subjects' older age). Dimethyl sulfone was only seen in the Coimbra cohort, and its variation differentiated groups with similar age (controls and early AMD). Therefore, this variation seems to mostly likely be AMD-related, although bearing a possible contribution from age. Altogether, the above analysis shows that the putative metabolite fingerprints listed in Table 2 are not significantly affected by differences in gender, smoking history or even age across patients' groups, thus establishing that no group restrictions are necessary regarding these characteristics. This was also confirmed by covariance analysis of the main suggested fingerprint metabolites/resonances in Table 2 with gender proportion, smoking history, BMI, age and AMD status (Table 3). The consistently higher contributions of AMD severity (noted in bold) confirmed AMD as the primary origin of the metabolite changes observed. This is also supported by the fact that the role of comorbidities (S2 Table) was found to be negligible, as discussed below.

Discussion

We present a cross-sectional study of two distinct cohorts of subjects with different severity stages of AMD and corresponding control groups. Using NMR metabolomics, we have observed small differences in the levels of some circulating metabolites (some amino acids and organic acids, dimethyl sulfone, lipid and protein moieties) between multiple AMD stages, in both cohorts. The potential confounding effects of gender, smoking history and age on these results were found to be negligible. To our knowledge, this study presents the first characterization of the different stages of AMD using NMR metabolomics, building up on a previous report [29] of MS metabolomics of the plasma of a small cohort of subjects with a single subtype of late AMD ("wet" AMD), compared to controls. The authors reported higher circulating levels of di- and tripeptides and modified amino acids in patients with AMD, along with lower levels of bile acids, histidine-arginine and tryptophan-phenylalanine, and metabolites related to vitamin-D metabolism. Our observation of changes in amino acids and protein levels in AMD patients is in broad agreement with the previously reported changes.

Interestingly, the metabolomic fingerprints of AMD suggested for the two cohorts presented both similarities and differences. The observed similarities in the variations of histidine, unsaturated

fatty acids and protein levels suggest that such variations may be a global reflection of the disease, possibly transversal to different cohorts and, therefore, with potential value in contributing to the current knowledge of the biology of AMD. On the other hand, cohort differences in relation to variations in particular low- M_w compounds (e.g. glutamine, alanine, creatine, dimethyl sulfone, pyruvate) may reflect the potential importance of local nutritional and lifestyle effects on the suggested AMD metabolic fingerprints. Also of note are the differences observed between controls and subjects with early AMD, in both cohorts. These observations relate to two naturally age-matched groups (thus not affected by possible age effects on the metabolome) and may contribute importantly to the future definition of AMD biomarkers.

In any case, even though age was a potential major confounder in this study, differences in this parameter were found to only possibly affect plasmatic dimethyl sulfone levels, leaving the remaining fingerprint unaffected. Apart from other potential confounder contributions (gender and smoking habits), which were also found negligible, the possible effect of comorbidities had to be considered. Indeed, some comorbidities differed in proportion between intermediate and late AMD (S2 Table): heart, liver and rheumatologic diseases, in the Coimbra cohort; and kidney and neurologic diseases in the Boston cohort. However, in most cases only a few % of subjects were affected by these conditions (average 5%), thus rendering significant contributions unlikely. Heart disease in the Coimbra cohort may constitute an exception since about 23% of subjects with intermediate AMD were affected, compared to 6% of subjects with late AMD. It is, thus, possible that the metabolite changes noted from intermediate to late AMD in Coimbra may be at least partially due to heart disease, particularly regarding acetoacetate and β -hydroxybutyrate levels, since histidine variations (common to both cohorts) seem to constitute an AMD-related feature.

Acknowledged limitations of this study include its cross-sectional nature, which precludes the assessment of AMD time progression. Also of note is the self-reporting nature of the questionnaire used to assess demographics and prior medical history, which allows for the possibility of some degree of response bias. Despite representing the first complete analysis of AMD by NMR metabolomics, with the inclusion of more than 30 subjects in all study groups, higher sample sizes would be desirable in future validation studies. In addition, the important assessment of the influence of relevant confounders (assuming that their impact on plasma metabolome is independent of disease) should, in future studies, include the impacts of diet and genetic profiles on AMD metabolomic fingerprints. The study presented here benefits from the fact that it was prospectively designed to follow adequate standard operating procedures at all stages (metadata, samples and data collection), while ensuring that each individual underwent a complete ophthalmologic exam performed by a retina specialist. The latter aspect is particularly important since it circumvents the possible subjectivity of procedures relying on repositories or databases, which may lack in adequate phenotypic information, particularly regarding ophthalmic diseases.

Conclusions

Our results demonstrate for the first time that plasma NMR metabolomics of patients with AMD detects small changes in the levels of selected amino acids and organic acids, as well as particular lipid moieties and protein levels. The changes observed are not very robust, but appear to be associated with the presence of the disease and its severity, rather than age, based on the identification of the particular age-dependent metabolite sets in each cohort. Other potential confounders (gender, smoking history, BMI, comorbidities) were also found not to affect the proposed AMD signatures significantly. Furthermore, the AMD-specific metabolite variations detected were found to partially differ between the two cohorts (Coimbra, Portugal

and Boston, US), thus indicating that nutritional and other lifestyle habits may be determining the metabolic response in AMD in different regions. A particularly important result of this study is that, in each cohort, a subgroup of metabolite changes tended to differentiate the controls from the patients diagnosed with early AMD stage (namely acetate, creatine, dimethyl sulfone, cholesterol, HDL-choline and unsaturated fatty acids for Coimbra subjects, and albumin, histidine, glutamine and also unsaturated fatty acids for Boston subjects). This is an important observation that needs to be further investigated since it may contribute to the future definition of AMD biomarkers.

In summary, our results suggest that even though the overall metabolite changes detected in relation to AMD in both cohorts are of low magnitude and weak statistical relevance, they appear to be AMD-specific and should, therefore, be explored further in expanded cohorts and with methodologies targeting the metabolic domains of the specific compounds identified. This work has the potential to offer novel biomarkers for AMD, as well as to improve the current understanding of the pathogenesis of this blinding disease.

Supporting information

S1 Appendix. Questionnaire used in this study to assess demographics and prior medical history of each individual.

(PDF)

S1 Fig. Age and BMI histograms. Histograms of age and BMI distributions for controls and AMD patients for Coimbra and Boston cohorts: controls (—), early AMD patients (·····), intermediate AMD patients (- - -) and late AMD patients (·····).

(TIFF)

S2 Fig. Effect size plots for diffusion-edited spectra integrals. Plots of effect size (E.S.) for integrals measured in diffusion-edited spectra a) Coimbra and b) Boston cohorts. F.A.: fatty acids. Resonance list: *N*-acetyl-glycoproteins, δ 2.02–2.05; albumin-lysyl groups, δ 2.92–3.02; protein NH region, δ 5.50–10.0; C18H cholesterol, δ 0.59–0.70; F.A. resonances: CH₃ HDL, δ 0.79–0.85; CH₃ LDL + VLDL, δ 0.85–0.91; (CH₂)_n HDL, δ 1.18–1.25; (CH₂)_n LDL+VLDL, δ 1.25–1.37; CH₂CH₂COOR, δ 1.45–1.62; CH₂CH₂CH = CH, δ 1.62–1.74; CH₃CH = C, δ 1.90–2.02; CH₂COOR, δ 2.17–2.26; C = CCH₂C = C, δ 2.65–2.84; N(CH₃)₃ choline HDL, δ 3.19–3.21; N(CH₃)₃ choline LDL+VLDL, δ 3.23–3.26; CH₂-N(CH₃)₃ choline, δ 3.62–3.68; Glycerol C1,3H, δ 4.02–4.10; Glycerol C1,3H', δ 4.21–4.32; Glycerol C2H, δ 5.13–5.21; HC = CH F.A. HDL, δ 5.24–5.28; HC = CH F.A. LDL+VLDL, δ 5.28–5.37. E.S. segments not intercepting the null E.S. line are considered as reflecting relevant variations (shaded rectangles).

(TIFF)

S1 Table. Assignment of lipid NMR resonances. Assignment of lipid NMR resonances and corresponding lipid structures. Chemical shift ranges are indicated, as all resonances are broad and often structured. F.A.: fatty acids. R: alkyl group.

(DOCX)

S2 Table. List of comorbidities found in the different subject groups considered. Comorbidities characterizing each of the subject groups with corresponding percentages and statistical relevance; *p*-values < 0.05 (Fisher Exact Test) are highlighted in bold; NA: non applicable.

(DOCX)

S3 Table. Pairwise PLS-DA quality parameters. Pairwise PLS-DA quality parameters, Q² (predictive power of pairwise model), classification rate (CR), % sensitivity (sens.) and % specificity (spec.), for PLS-DA models obtained with original (full) spectra and variable-selected

spectra, for Coimbra and Boston cohorts and for CPMG and diffusion-edited spectra. Values in bold and underlined refer to best PLS-DA models.
(DOCX)

Acknowledgments

This project was funded by the Fundação para a Ciência e a Tecnologia (FCT) (HMSP-IC/0006/2013), the Miller Retina Research Fund (MEE) and the Miller Champalimaud Award (MEE). This work was also developed within the scope of the project CICECO-Aveiro Institute of Materials, POCI-01-0145-FEDER-007679 (FCT Ref. UID /CTM /50011/2013), financed by national funds through the FCT/MEC and when appropriate co-financed by FEDER under the PT2020 Partnership Agreement. AMG acknowledges the Portuguese National NMR Network (RNRMN), supported by FCT funds.

Author Contributions

Conceptualization: IL IMC JWM RS JNM DH AMG.

Data curation: IL JG JBM MM TM IKK MLC DV RS JWM DH.

Formal analysis: DD ASM ASB IL AMG.

Funding acquisition: IL RS JNM JNM DH AMG.

Investigation: DD ASM ASB IL DH RS AMG.

Methodology: AMG ASB.

Project administration: IL AMG.

Resources: IL TM RS MLC DH JWM JBM IKK DM AMG ASB.

Software: ASB.

Supervision: DH JNM RS AMG.

Validation: IL AMG.

Visualization: DD ASM ASB AMG.

Writing – original draft: IL DD ASB AMG.

Writing – review & editing: IL DH JWM RS IKK DV ASB AMG.

References

1. Wong WL, Su X, Li X, Cheung CMG, Klein R, Cheng C-Y, et al. Global prevalence of age-related macular degeneration and disease burden projection for 2020 and 2040: a systematic review and meta-analysis. *Lancet Glob Heal*. 2014; 2: e106–16.
2. Sobrin L, Seddon JM. Nature and nurture- genes and environment- predict onset and progression of macular degeneration. *Prog Retin Eye Res*. 2013;
3. Yonekawa Y, Miller JW, Kim IK. Age-Related Macular Degeneration: Advances in Management and Diagnosis. *J Clin Med*. 2015; 4: 343–59. <https://doi.org/10.3390/jcm4020343> PMID: 26239130
4. Handa JT. How does the macula protect itself from oxidative stress? *Mol Aspects Med*. 2012; 33: 418–35. <https://doi.org/10.1016/j.mam.2012.03.006> PMID: 22503691
5. Mitta VP, Christen WG, Glynn RJ, Semba RD, Ridker PM, Rimm EB, et al. C-reactive protein and the incidence of macular degeneration: pooled analysis of 5 cohorts. *JAMA Ophthalmol*. 2013; 131: 507–13. <https://doi.org/10.1001/jamaophthalmol.2013.2303> PMID: 23392454

6. Hong T, Tan AG, Mitchell P, Wang JJ. A review and meta-analysis of the association between C-reactive protein and age-related macular degeneration. *Surv Ophthalmol*. 56: 184–94. <https://doi.org/10.1016/j.survophthal.2010.08.007> PMID: 21420705
7. Klein R, Myers CE, Cruickshanks KJ, Gangnon RE, Danforth LG, Sivakumar TA, et al. Markers of inflammation, oxidative stress, and endothelial dysfunction and the 20-year cumulative incidence of early age-related macular degeneration: the Beaver Dam Eye Study. *JAMA Ophthalmol*. 2014; 132: 446–55. <https://doi.org/10.1001/jamaophthalmol.2013.7671> PMID: 24481424
8. Uğurlu N, Aşık MD, Yülek F, Neselioglu S, Cagil N. Oxidative stress and anti-oxidative defence in patients with age-related macular degeneration. *Curr Eye Res*. 2013; 38: 497–502. <https://doi.org/10.3109/02713683.2013.774023> PMID: 23432778
9. Fiehn O. Metabolomics—the link between genotypes and phenotypes. *Plant Mol Biol*. 2002; 48: 155–71. PMID: 11860207
10. Nicholson JK, Holmes E, Kinross JM, Darzi AW, Takats Z, Lindon JC. Metabolic phenotyping in clinical and surgical environments. *Nature*. 2012; 491: 384–92. <https://doi.org/10.1038/nature11708> PMID: 23151581
11. Nicholson J.K., Lindon J.C. HE. “Metabonomics”: understanding the metabolic responses of living systems to pathophysiological stimuli via multivariate statistical analysis of biological NMR spectroscopic data. *Xenobiotica*. 1999; 1181–1189. <https://doi.org/10.1080/004982599238047> PMID: 10598751
12. Psychogios N, Hau DD, Peng J, Guo AC, Mandal R, Bouatra S, et al. The human serum metabolome. *PLoS One*. 2011; 6: e16957. <https://doi.org/10.1371/journal.pone.0016957> PMID: 21359215
13. Suhre K, Gieger C. Genetic variation in metabolic phenotypes: study designs and applications. *Nat Rev Genet*. 2012; 13: 759–69. <https://doi.org/10.1038/nrg3314> PMID: 23032255
14. Duarte IF, Gil AM. Metabolic signatures of cancer unveiled by NMR spectroscopy of human biofluids. *Prog Nucl Magn Reson Spectrosc*. 2012; 62: 51–74. <https://doi.org/10.1016/j.pnmrs.2011.11.002> PMID: 22364616
15. Duarte IF, Rocha CM, Barros AS, Gil AM, Goodfellow BJ, Carreira IM, et al. Can nuclear magnetic resonance (NMR) spectroscopy reveal different metabolic signatures for lung tumours? *Virchows Arch*. 2010; 457: 715–25. <https://doi.org/10.1007/s00428-010-0993-6> PMID: 20941505
16. Rocha CM, Carrola J, Barros AS, Gil AM, Goodfellow BJ, Carreira IM, et al. Metabolic signatures of lung cancer in biofluids: NMR-based metabolomics of blood plasma. *J Proteome Res*. 2011; 10: 4314–24. <https://doi.org/10.1021/pr200550p> PMID: 21744875
17. Young SP, Wallace GR. Metabolomic analysis of human disease and its application to the eye. *J Ocul Biol Dis Infor*. 2009; 2: 235–242. <https://doi.org/10.1007/s12177-009-9038-2> PMID: 20157358
18. Midelfart A. Metabonomics—a new approach in ophthalmology. *Acta Ophthalmol*. 2009; 87: 697–703. <https://doi.org/10.1111/j.1755-3768.2009.01516.x> PMID: 19604162
19. Tan SZ, Begley P, Mullard G, Hollywood KA, Bishop PN. Introduction to metabolomics and its applications in ophthalmology. *Eye (Lond)*. 2016; 30: 773–83.
20. Chen L, Zhou L, Chan ECY, Neo J, Beuerman RW. Characterization of the human tear metabolome by LC-MS/MS. *J Proteome Res*. 2011; 10: 4876–82. <https://doi.org/10.1021/pr2004874> PMID: 21800913
21. Karamichos D, Zieske JD, Sejersen H, Sarker-Nag A, Asara JM, Hjortdal J. Tear metabolite changes in keratoconus. *Exp Eye Res*. 2015; 132: 1–8. <https://doi.org/10.1016/j.exer.2015.01.007> PMID: 25579606
22. Li M, Li H, Jiang P, Liu X, Xu D, Wang F. Investigating the pathological processes of rhegmatogenous retinal detachment and proliferative vitreoretinopathy with metabolomics analysis. *Mol Biosyst*. 2014; 10: 1055–62. <https://doi.org/10.1039/c3mb70386j> PMID: 24556753
23. Barba I, Garcia-Ramírez M, Hernández C, Alonso MA, Masmiquel L, García-Dorado D, et al. Metabolic fingerprints of proliferative diabetic retinopathy: an 1H-NMR-based metabolomic approach using vitreous humor. *Invest Ophthalmol Vis Sci*. 2010; 51: 4416–21. <https://doi.org/10.1167/iov.10-5348> PMID: 20375324
24. Young SP, Nessim M, Falciani F, Trevino V, Banerjee SP, Scott RAH, et al. Metabolomic analysis of human vitreous humor differentiates ocular inflammatory disease. *Mol Vis*. 2009; 15: 1210–7. PMID: 19536306
25. Li X, Luo X, Lu X, Duan J, Xu G. Metabolomics study of diabetic retinopathy using gas chromatography-mass spectrometry: a comparison of stages and subtypes diagnosed by Western and Chinese medicine. *Mol Biosyst*. 2011; 7: 2228–37. <https://doi.org/10.1039/c0mb00341g> PMID: 21559540
26. Chen L, Cheng C-Y, Choi H, Ikram MK, Sabanayagam C, Tan GSW, et al. Plasma Metabonomic Profiling of Diabetic Retinopathy. *Diabetes*. 2016; 65: 1099–108. <https://doi.org/10.2337/db15-0661> PMID: 26822086

27. Burgess LG, Uppal K, Walker DI, Roberson RM, Tran V, Parks MB, et al. Metabolome-Wide Association Study of Primary Open Angle Glaucoma. *Invest Ophthalmol Vis Sci*. 2015; 56: 5020–8. <https://doi.org/10.1167/iovs.15-16702> PMID: 26230767
28. Guo J, Yan T, Bi H, Xie X, Wang X, Guo D, et al. Plasma metabolomics study of the patients with acute anterior uveitis based on ultra-performance liquid chromatography-mass spectrometry. *Graefes Arch Clin Exp Ophthalmol = Albr von Graefes Arch für Klin und Exp Ophthalmol*. 2014; 252: 925–34.
29. Osborn MP, Park Y, Parks MB, Burgess LG, Uppal K, Lee K, et al. Metabolome-wide association study of neovascular age-related macular degeneration. *PLoS One*. 2013; 8: e72737. <https://doi.org/10.1371/journal.pone.0072737> PMID: 24015273
30. Cachulo M da L, Lobo C, Figueira J, Ribeiro L, Láins I, Vieira A, et al. Prevalence of Age-Related Macular Degeneration in Portugal: The Coimbra Eye Study—Report 1. *Ophthalmologica*. 2015; 233: 119–127. <https://doi.org/10.1159/000371584> PMID: 25677077
31. The Age-Related Eye Disease Study system for classifying age-related macular degeneration from stereoscopic color fundus photographs: the Age-Related Eye Disease Study Report Number 6. *Am J Ophthalmol*. 2001; 132: 668–81. PMID: 11704028
32. Danis RP, Domalpally A, Chew EY, Clemons TE, Armstrong J, SanGiovanni JP, et al. Methods and reproducibility of grading optimized digital color fundus photographs in the Age-Related Eye Disease Study 2 (AREDS2 Report Number 2). *Invest Ophthalmol Vis Sci*. 2013; 54: 4548–54. <https://doi.org/10.1167/iovs.13-11804> PMID: 23620429
33. Wishart DS, Tzur D, Knox C, Eisner R, Guo AC, Young N, et al. HMDB: the Human Metabolome Database. *Nucleic Acids Res*. 2007; 35: D521–6. <https://doi.org/10.1093/nar/gkl923> PMID: 17202168
34. Veselkov KA, Lindon JC, Ebbels TMD, Crookford D, Volynkin V V, Holmes E, et al. Recursive segment-wise peak alignment of biological (1)h NMR spectra for improved metabolic biomarker recovery. *Anal Chem*. 2009; 81: 56–66. <https://doi.org/10.1021/ac8011544> PMID: 19049366
35. Wold S, Esbensen K GP. Principal component analysis. *Chemom Intell Lab Syst*. 1987; 2: 37–52.
36. Martens H, Naes T. *Multivariate Calibration*. Chichester: John Wiley & Sons; 1992.
37. Trygg J, Wold S. Orthogonal projections to latent structures (O-PLS). *J Chemom*. 2002; 16: 119–128.
38. Diaz SO, Barros AS, Goodfellow BJ, Duarte IF, Galhano E, Pita C, et al. Second trimester maternal urine for the diagnosis of trisomy 21 and prediction of poor pregnancy outcomes. *J Proteome Res*. 2013; 12: 2946–57. <https://doi.org/10.1021/pr4002355> PMID: 23611123
39. Hedges L. Distribution theory for Glass's estimator of effect size and related estimators. *J Educ Stat*. 1981; 6: 106–128.
40. Pinto J, Domingues MRM, Galhano E, Pita C, Almeida M do C, Carreira IM, et al. Human plasma stability during handling and storage: impact on NMR metabolomics. *Analyst*. 2014; 139: 1168–77. <https://doi.org/10.1039/c3an02188b> PMID: 24443722



AMERICAN ACADEMY
OF OPHTHALMOLOGY

Human Plasma Metabolomics Study across All Stages of Age-Related Macular Degeneration Identifies Potential Lipid Biomarkers

Inês Laíns, MD, MSc,^{1,2,3,4} Rachel S. Kelly, PhD,⁵ John B. Miller, MD,¹ Rufino Silva, MD, PhD,^{2,3,4} Demetrios G. Vavvas, MD, PhD,¹ Ivana K. Kim, MD,¹ Joaquim N. Murta, MD, PhD,^{2,3,4} Jessica Lasky-Su, PhD,⁵ Joan W. Miller, MD,^{1,*} Deeba Husain, MD^{1,*}

Purpose: To characterize the plasma metabolomic profile of patients with age-related macular degeneration (AMD) using mass spectrometry (MS).

Design: Cross-sectional observational study.

Participants: We prospectively recruited participants with a diagnosis of AMD and a control group (>50 years of age) without any vitreoretinal disease.

Methods: All participants underwent color fundus photography, used for AMD diagnosis and staging, according to the Age-Related Eye Disease Study classification scheme. Fasting blood samples were collected and plasma was analyzed by Metabolon, Inc. (Durham, NC), using ultrahigh-performance liquid chromatography (UPLC) and high-resolution MS. Metabolon's hardware and software were used to identify peaks and control quality. Principal component analysis and multivariate regression were performed to assess differences in the metabolomic profiles of AMD patients versus controls, while controlling for potential confounders. For biological interpretation, pathway enrichment analysis of significant metabolites was performed using MetaboAnalyst.

Main Outcome Measures: The primary outcome measures were levels of plasma metabolites in participants with AMD compared with controls and among different AMD severity stages.

Results: We included 90 participants with AMD (30 with early AMD, 30 with intermediate AMD, and 30 with late AMD) and 30 controls. Using UPLC and MS, 878 biochemicals were identified. Multivariate logistic regression identified 87 metabolites with levels that differed significantly between AMD patients and controls. Most of these metabolites (82.8%; $n = 72$), including the most significant metabolites, belonged to the lipid pathways. Analysis of variance revealed that of the 87 metabolites, 48 (55.2%) also were significantly different across the different stages of AMD. A significant enrichment of the glycerophospholipids pathway was identified ($P = 4.7 \times 10^{-9}$) among these metabolites.

Conclusions: Participants with AMD have altered plasma metabolomic profiles compared with controls. Our data suggest that the most significant metabolites map to the glycerophospholipid pathway. These findings have the potential to improve our understanding of AMD pathogenesis, to support the development of plasma-based metabolomics biomarkers of AMD, and to identify novel targets for treatment of this blinding disease. *Ophthalmology* 2017; ■:1–10 © 2017 by the American Academy of Ophthalmology



Supplemental material available at www.aajournal.org.

Age-related macular degeneration (AMD) is the leading cause of adult blindness in developed countries. Worldwide, it ranks third and is expected to affect 288 million people by 2040.¹ Even when it does not cause blindness, AMD often leads to altered central visual function and significant impairment in patient quality of life.² The natural history of AMD typically comprises early and intermediate forms, which can progress to atrophic lesions (i.e., geographic atrophy) or neovascular lesions (i.e., choroidal neovascularization, wet AMD), or both in some.^{3,4}

Age-related macular degeneration usually is asymptomatic in its early stages and is diagnosed only on routine eye

examination; thus, it often remains undetected until it is more advanced and accompanied by loss of vision. It is important to find tools to detect AMD earlier and to develop treatments to slow progression and vision loss. Ideally, a screening test for AMD should be performed easily and should be able to predict disease progression. Serologic biomarkers have been studied, mostly related to biomarkers of inflammation^{5–8} or lipid levels,⁹ because both seem to play a role in AMD pathogenesis. However to date, results have been inconsistent.¹⁰ Therefore, we continue to rely on fundus examination to diagnose and monitor progression, and useful biofluid biomarkers are still

lacking in AMD. Metabolomics, the global profiling of all the small molecules (<1 kDa) constituting a biological system,¹¹ is a new approach that is now recognized for its promising role in identifying biomarkers.^{3,4,12} Metabolites are the downstream products of the cumulative effects of the genome and its interactions with environmental exposures.¹³ Therefore, the metabolome is thought to represent closely the so-called true functional state of the biological system and thus disease phenotype in multifactorial diseases, such as AMD.¹⁴

The vital role of metabolomics as a translational tool for the clinical setting has been demonstrated through several studies in other medical disciplines,¹³ including cancer and prenatal diseases.^{15–19} Metabolomics studies can be performed readily on easily accessible biological samples, such as plasma, serum, and urine. Two main techniques can be used for metabolomic profiling: mass spectrometry (MS) and nuclear magnetic resonance spectroscopy.^{20,21} Both approaches have strengths and weaknesses, and currently they are considered complementary.²² Mass spectrometry presents a high sensitivity and selectivity, which renders it increasingly popular in large-scale metabolomics studies.^{22–24} Recent work also has highlighted the potential and versatility of metabolomics for the study of eye diseases.^{25–27} However, to our knowledge, only 1 study has been published on AMD to date,²⁸ comparing plasma metabolomic profiles of participants with neovascular AMD and those of a control group.

The current study aimed to characterize the plasma metabolomic profiles of patients with AMD and to compare them with those of participants with no AMD, and also to compare the findings across the different stages of AMD (early, intermediate, and late disease) using MS-based metabolomics. Ultimately, we aim to support the development of novel metabolic biomarkers for this blinding disease to aid in diagnosis and prognosis, as well as to understand disease mechanisms better and to identify new druggable targets.

Methods

Study Design

This study was part of a cross-sectional observational study on AMD biomarkers at Massachusetts Eye and Ear, Harvard Medical School, Boston, Massachusetts. The research protocol was conducted in accordance with Health Insurance Portability and Accountability Act requirements and the tenets of the Declaration of Helsinki and was approved by the Massachusetts Eye and Ear Institutional Review Board. All included participants provided written informed consent and were recruited prospectively.

Study Protocol

From January 2015 through July 2016, we recruited participants with a diagnosis of AMD at the time of their regular appointments at the Massachusetts Eye and Ear Retina Service. Exclusion criteria included diagnosis of any other vitreoretinal disease, active uveitis or ocular infection, significant media opacities that precluded the observation of the ocular fundus, refractive error of 6 diopters or more of spherical equivalent, history of retinal surgery, history of any ocular surgery or intraocular procedure (such as laser and

intraocular injections) within the 90 days before enrollment, and diagnosis of diabetes mellitus, with or without concomitant diabetic retinopathy. Additionally, a control group of participants 50 years of age or older without any evidence of AMD in either eye was identified and gave informed consent at the Massachusetts Eye and Ear Comprehensive Ophthalmology and Optometry Services. The same exclusion criteria were applied.

All participants underwent a comprehensive eye examination, including best-corrected visual acuity assessment, current refraction, intraocular pressure measurement, slit-lamp biomicroscopy, and dilated fundus examination. A standardized medical history questionnaire was designed specifically for this study, including, among others, self-reported data on smoking habits (smokers were considered those who reported current smoking and former smokers were considered those who have ever smoked, regardless of when they stopped, but who do not currently smoke), and weight and height, which were used to calculate body mass index (BMI). If the study participants did not know their current height or weight, these were obtained by a study investigator.

Nonstereoscopic 7-field color fundus photographs (Topcon TRC-50DX [Topcon Corporation, Tokyo, Japan] or Zeiss FF-450Plus [Carl Zeiss Meditec, Dublin, CA]) were obtained at the same visit. These were used to diagnose and grade AMD according to the Age-Related Eye Disease Study (AREDS) classification system.^{29,30} Two independent experienced graders analyzed all field 2-color fundus photographs (<https://www.ncbi.nlm.nih.gov/pubmed/28316876>) on IMAGEnet 2000 software (version 2.56; Topcon Medical Systems). In cases of disagreement, a senior author (D.H.) established the final categorization. All graders were masked to the patients' clinical and demographic characteristics during this process.

We adopted the most recent AREDS 2 definitions,³⁰ namely that the standard disc diameter equals 1800 μm (rather than 1500 μm), which affects the size of the Early Treatment Diabetic Retinopathy Study grid and of the standard drusen circles, and that geographic atrophy is present if the lesion has a diameter of 433 μm or more (AREDS circle I-2) and has at least 2 of the following features: absence of retinal pigment epithelium (RPE) pigment, circular shape, or sharp margins (foveal involvement not a requirement). With these criteria, we established the following groups^{29,30}: controls (AREDS stage 1), presence of drusen maximum size less than circle C0 and total area less than C1; early AMD (AREDS stage 2), drusen maximum size C0 or more but less than C1 or presence of AMD characteristic pigment abnormalities in the inner or central subfields; intermediate AMD (AREDS stage 3), presence of drusen maximum size of C1 or more or of drusen maximum size of C0 or more if the total area occupied was more than I-2 for soft indistinct drusen and more than O2 for soft distinct drusen; and late AMD (AREDS stage 4), presence of geographic atrophy according to the criteria described above or evidence of neovascular AMD. For participants with different severity stages in the 2 eyes (for example, early AMD in one eye and intermediate in the other eye), the more advanced stage was assumed.

Sample Collection and Mass Spectrometry Analysis

This study used a single plasma collection per individual. For all participants, after confirmed overnight fasting, blood samples were collected in the morning, into sodium-heparin tubes and centrifuged within 30 minutes (1500 rpm, 10 minutes, 20°C). Plasma aliquots of 1.5 ml were transferred into sterile cryovials and immediately stored at -80°C . When all participants had been recruited, plasma samples were shipped to Metabolon, Inc., in dry ice (through TNT Express, Inc., Melville, NY). Samples arrived

frozen in less than 24 hours and were stored immediately at -80°C until processing, which was performed according to the protocol described in the [Supplemental Material](#) (available at www.aaojournal.org). Nontargeted MS analysis was performed by Metabolon, Inc., using ultrahigh-performance liquid chromatography–tandem MS, according to protocols that have been described previously³¹ and are summarized in the [Supplemental Material](#) (available at www.aaojournal.org).

Statistical and Data Analysis

Traditional descriptive methods were used to describe the clinical and demographic characteristics of the included study population: mean and standard deviation for continuous variables and percentages for dichotomous or categorical variables. The 4 study groups were compared using analysis of variance and chi-square tests.

In this data set, 878 named metabolites were identified, of which 384 (44%) mapped to the lipid pathways. A total of 173 metabolites determined to be exogenous to humans (including medications, food additives, and buffering agents) were excluded from analysis because we were interested in endogenous metabolites that could be driving systemic biological factors. As part of our quality-control procedures, we observed that 1 participant (a man with early AMD) had missing or undetectable levels for more than 30% of metabolites and therefore was excluded. Any missing values for the remaining participants were imputed with half the minimum detected level for that metabolite. To ensure that only the most informative metabolites were included in the analysis, those metabolites with an interquartile range of 0 were excluded. This left 698 metabolites that were Pareto scaled and log-transformed for analysis. [Figure S1](#) (available at www.aaojournal.org) presents the included metabolites and samples.

Owing to the large number of metabolites that can now be measured in the human body, specialized statistical methods are required to analyze high-dimensional metabolomic data sets.³² One of the most commonly used dimensionality reduction techniques is principal component analysis, which we performed in our study.³³ Principal component analysis is an unsupervised clustering approach that assesses how participants cluster based on their metabolome. Basically, it relies on the transformation of metabolites into a set of linearly uncorrelated variables known as *principal components*, which summarize a large number of metabolites with a smaller number of variables. This decomposition method maximizes the variance explained by the first component, whereas the subsequent components explain increasingly reduced amounts of variance.³⁴

To isolate the metabolites significantly associated with AMD compared with normal macular health, a multivariate logistic regression was performed to account for potential confounding factors (age, gender, BMI, and smoking status). The discriminatory ability of the significant metabolites then was assessed using a summary score based on their first principal component and receiver operating characteristic (ROC) curve analyses. The significant metabolites were studied further using an analysis of variance to see whether they differed between early, intermediate, and late AMD cases. Pathway analysis using MetaboAnalyst 3.0 (available at: <http://www.metaboanalyst.ca/faces/home.xhtml>)³⁵ was performed on the significant metabolites to interpret these findings biologically. This combines overrepresentation analysis with topology analysis to identify pathways that are dysregulated in AMD based on (1) the number of metabolites from our significant metabolites that fall within Kyoto Encyclopedia of Genes and Genomes–defined metabolic pathways and (2) the positional importance of our metabolites within these pathways. It generates a pathway impact score and the associated *P* value.

Results

Study Population

We recruited 120 participants, 25% ($n = 30$) with normal macular health (control group) and 75% ($n = 90$) with AMD. As described, 1 patient with AMD (early AMD) was considered an outlier and was excluded from further analyses. [Table 1](#) presents the clinical and demographic characteristics of the study group. Among the potential confounders evaluated, only age showed a statistically significant difference among the different study groups ($P = 0.0005$; [Table 1](#)).

Principal Component Analysis

In our data set, the first 2 principal components (PC1 and PC2) accounted for 20% of the variance in the data ([Fig 1](#)). As shown, there is a suggestion of a shift between the late-stage patients (blue) and the controls (black).

Multivariate Logistic Regression Analysis

To identify the metabolites driving the differences in the metabolome of AMD cases and controls observed in the principal component analysis, we conducted multivariate regression analyses controlling for potential confounders. We considered a dichotomous outcome: normal macular health (controls; $n = 30$) versus AMD ($n = 89$). Our results revealed that, after controlling for age, gender, BMI, and smoking status, 87 metabolites were associated with AMD ([Table 2](#)). Most of these metabolites (82.8%; $n = 72$) belonged to the lipid superpathway, followed by amino acids (5.7%; $n = 5$; including *N*-acetylasparagine, a component of alanine and aspartate metabolism). The remaining metabolites were peptides (4.6%; $n = 4$), cofactors and vitamins (2.3%; $n = 2$), and metabolites involved in purine and pyrimidine metabolism (4.6%; $n = 4$). Of the 7 most significant metabolites ($P < 0.001$; [Table 3](#)), all but 1 (adenosine) were lipids (4 diacylglycerols and 2 phosphatidylcholines). Pathway analysis of these 87 metabolites confirmed the importance of lipid metabolism, specifically glycerophospholipid metabolism, in AMD. Indeed, this pathway was highly enriched among the significant metabolites ($P = 4.7 \times 10^{-9}$; [Fig 2](#)).

Receiver Operating Characteristic Curve Analysis

The significant metabolites identified in the multivariate logistic regression were used to create a predictive model for AMD, which was tested using ROC curve analyses. When a summary score based on the first principal component of these 87 metabolites was included as a model predictor, ROC analysis (area under the ROC curve, 0.80; 95% confidence interval, 0.71–0.90) demonstrated that outperformed ($P = 0.142$) a baseline model including only age, gender, BMI, and smoking status (area under the ROC curve, 0.71; 95% confidence interval, 0.59–0.85; [Fig 3](#)).

Analysis of Variance

We further explored whether the identified significant metabolites ($n = 87$) were able to discriminate between early, intermediate, and late AMD cases. Analysis of variance revealed that, of the 87 metabolites, 48 (55.2%) were significantly different across the different stages of AMD. Consistent with the previous data, all but 1 of the 13 most significant metabolites ($P < 0.01$) belonged to the lipid pathways (diacylglycerol, $n = 4$; phosphatidylcholine, $n = 3$; fatty acid metabolism, $n = 3$; and phosphatidylinositol, $n = 2$). [Figure 4](#) displays the mean peak intensity of these 13 metabolites

Table 1. Clinical and Demographic Characteristics of the Study Population

	Total Population (n = 119)	Control (n = 30)	Early (n = 29)	Intermediate (n = 30)	Late (n = 30)	P Value
Age (yrs), mean (SD)	70 (8)	68 (10)	68 (7)	70 (5)	76 (8)	0.0005*
Gender, no. (%)						
Male	43 (36)	12 (40)	9 (31)	9 (30)	13 (43)	0.640
BMI (kg/m ²), mean (SD)	27 (5)	26 (4)	27 (5)	29 (7)	27 (4)	0.070
Ethnicity, no. (%)						
White	101 (85)	22 (73)	24 (83)	30 (100)	25 (83)	0.176
Black/Hispanic/Asian	7 (6)	2 (7)	3 (10)	0	2 (7)	
Unknown	11 (9)	6 (20)	2 (7)	0	3 (10)	
Smoking, no. (%)						
Nonsmoker	57 (48)	18 (60)	18 (62)	13 (43)	8 (27)	0.057
Former smoker	56 (47)	10 (33)	11 (38)	15 (50)	20 (67)	
Smoker	3 (3)	1 (3)	0	2 (7)	0	
NA	3 (3)	1 (3)	0	0	2 (7)	
Age started smoking (yrs), mean (SD)	19 (7)	20 (7)	16 (4)	22 (10)	17 (4)	0.055
Age stopped smoking (yrs), mean (SD)	39 (13)	37 (11)	34 (16)	42 (12)	42 (13)	0.315
No. of cigarettes per day, mean (SD)	18 (14)	18 (10)	9 (8)	20 (18)	20 (14)	0.244
AMD subtype, no. (%)						
Choroidal neovascularization (wet)	25 (28)	n/a	n/a	n/a	25 (83)	1.8 × 10 ⁻¹⁷
Geographic atrophy (dry)	4 (5)	n/a	n/a	n/a	4 (13)	

AMD = age-related macular degeneration; BMI = body mass index; NA = not available; n/a = not applicable; no. = number; SD = standard deviation.
*Significant differences ($P < 0.05$), analysis of variance for continuous variables and chi-square test for dichotomous variables.

across the 3 AMD groups. Similar to what was observed between AMD and controls, metabolite set enrichment analysis of the 48 metabolites that differed significantly among the 3 AMD groups revealed an enrichment of the glycerophospholipids pathway ($P = 0.01$).

Discussion

Using a broad-based MS platform, we assessed the plasma metabolomic profiles of a cohort of patients with AMD compared with participants with healthy maculae. After controlling for age, gender, BMI, and smoking status, 87

metabolites differed significantly between AMD patients and controls. Indeed, a summary score based on these 87 metabolites increased the ability to predict AMD cases relative to clinical covariates alone. Of these metabolites, more than half (48 metabolites) also differed significantly across AMD severity stages. Most of the significant metabolites are involved in lipid metabolism, in particular glycerophospholipid metabolism. These metabolites include stearoyl-arachidonoyl-glycerol, a diacylglycerol, and 1-stearoyl-2-arachidonoyl-glycerophosphocholine, a phosphatidylcholine.

Our work presents a pioneer assessment of MS plasma metabolomics across all stages of AMD. Osborn et al.²⁸ applied MS plasma metabolomics to the study of this disease, but focused their investigation on a single subtype of advanced AMD (choroidal neovascularization) and described differences primarily related to peptides and modified amino acids. Similarly, we identified significantly increased levels of metabolites linked to dipeptides and amino acids in patients with AMD, including a significant role for alanine and aspartate metabolism. Although lipids were present in the samples from Osborn et al.,²⁸ they could not be distinguished and therefore were not analyzed, rendering a direct comparison with our lipid findings impossible.

The potential role of lipids in the pathophysiologic process of AMD has been proposed by several investigators, but their exact role remains somewhat controversial. Candidate gene and genome-wide association studies also have pointed to the role of lipid pathways in the pathogenesis of AMD.¹² At a histopathologic level, similarities have been described between the aging process of Bruch's membrane and atherosclerosis, with deposition of lipids and lipoproteins and associated para-inflammation.^{36,37}

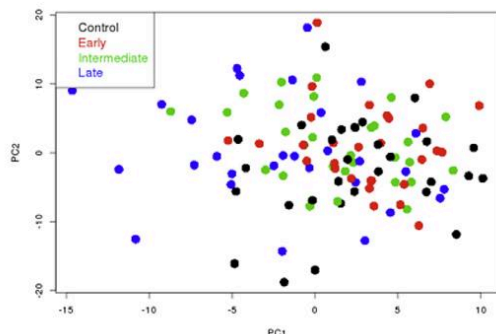


Figure 1. Scatterplot showing principal component 1 (PC1) and principal component 2 (PC2) with controls and age-related macular degeneration (AMD) groups. The x-axis corresponds to PC1 and the y-axis to PC2.

Table 2. Multivariate Logistic Regression Analysis for Age-Related Macular Degeneration Patients versus Controls

Significance Level	Metabolites in AMD Groups Compared with Controls					
	Decreased in AMD Patients (Odds Ratio <1)		Increased in AMD Patients (Odds Ratio >1)		Total	
	No.	%	No.	%	No.	%
$P < 0.05$	59	8.5	28	4.0	87	12.5
$P < 0.01$	24	3.4	9	1.3	33	4.7
$P < 0.001$	6	0.9	1	0.1	7	1.0

AMD = age-related macular degeneration; No = number.

Lipids were identified early as a component of drusen, the visible hallmark of AMD.³⁶ It has been postulated by Curcio and others^{36,37} that these derive from an imbalance of lipoprotein influx and efflux from the RPE,^{36,37} coming from phagocytosis of the lipid-rich outer photoreceptor segments, RPE synthesis, and only a minor contribution from plasma lipoproteins.^{38–41} Indeed, pooled data from large epidemiologic studies have failed to show associations between serum cholesterol levels and AMD incidence and progression.¹⁰ Clearly, a complete understanding of the role of lipids in AMD pathogenesis remains to be elucidated.⁴² Metabolomic profiling may provide novel insights into these relationships.

Our data support the relevance of lipid-related metabolites in AMD and, in particular, a significant dysregulation of the glycerophospholipids pathway. Glycerophospholipids are a major component of cell membranes and are especially enriched in neural membranes, accounting for up to 25% of the dry weight of the adult brain. They provide structural stability and membrane fluidity. They also participate in forming ion channels and receptors, generating second messengers in signal transduction, and regulating neurotransmitter release.^{43,44} Additionally, the metabolites of glycerophospholipids (together with sphingolipids) seem to play an important role in initiating and promulgating oxidative stress in neurologic disorders, as well as a role in neural cell proliferation, differentiation, and apoptosis.⁴⁵

Alterations in glycerophospholipids and their metabolism have been investigated extensively in neurodegeneration and in several chronic neurologic diseases.^{43,46} In particular,

glycerophospholipids have been shown to be reduced in the plasma of participants with Alzheimer disease and to play a central role in the pathogenesis of this condition.^{47,48} Metabolomics currently is considered a promising tool to identify valid biomarkers and new targets in Alzheimer disease.^{49–51} Using MS metabolomics and lipidomics, Mapstone et al⁵² identified a panel of 10 plasma lipids, most of them phosphatidylcholines (a class of glycerophospholipids), that predicted with high accuracy conversion to mild cognitive impairment and to frank Alzheimer disease in elderly participants. Changes in plasmalemmas of Alzheimer-affected brain tissue, alterations in local cellular glycerophospholipid metabolism, and increased free-radical-mediated lipid peroxidation all have been suggested as potential causes for the observed glycerophospholipid depletion in this disease. These findings in Alzheimer disease are interesting in the context of our findings in AMD, because both are neurodegenerative diseases and have been noted to share other features and pathologic mechanisms.^{53–56}

The photoreceptors and the RPE are rich in phospholipids, which are important for the transduction of visual stimuli.^{57,58} As mentioned (Table 3), our study revealed that metabolites linked to the key glycerophospholipids, such as diacylglycerols and phosphatidylcholines, are found at lower levels in participants with AMD, suggesting that impaired cell membrane structure and function may be important components of AMD pathogenesis. The observed depletion of glycerophospholipids in AMD patients could be explained by decreased levels of parent

Table 3. Significantly Different Metabolites ($P < 0.001$) between Patients with Age-Related Macular Degeneration and Controls

Biochemical	Superpathway	Subpathway	Metabolites in AMD Patients vs. Controls		
			Metabolites in AMD Patients vs. Controls	Odds Ratio*	P Value
Linoleoyl-arachidonoyl-glycerol (18:2/20:4) [2]*	Lipid	Diacylglycerol	Decreased	0.0961	0.0008
Stearoyl-arachidonoyl-glycerol (18:0/20:4) [1]*	Lipid	Diacylglycerol	Decreased	0.0411	0.0009
Oleoyl-arachidonoyl-glycerol (18:1/20:4) [2]*	Lipid	Diacylglycerol	Decreased	0.0463	0.0002
Oleoyl-arachidonoyl-glycerol (18:1/20:4) [1]*	Lipid	Diacylglycerol	Decreased	0.111	0.0007
1-Palmitoyl-2-arachidonoyl-GPC (16:0/20:4n6)	Lipid	Phosphatidylcholine	Decreased	0.0004	0.0006
1-Stearoyl-2-arachidonoyl-GPC (18:0/20:4)	Lipid	Phosphatidylcholine	Decreased	0.0002	0.0005
Adenosine	Nucleotide	Purine metabolism, adenine containing	Increased	3.7422	0.0009

AMD = age-related macular degeneration; GPC = glycerol-3-phosphocholine; PC = phosphatidylcholine.

*Reference term for odds ratios is the control group, which means that values of less than 1 represent a decrease in patients with age-related macular degeneration as compared with controls (and the opposite for values of more than 1).

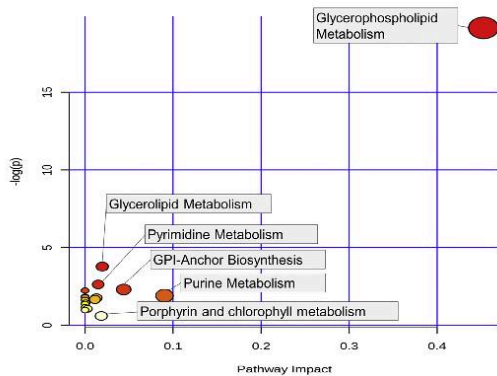


Figure 2. Graph showing pathway analysis based on the 87 metabolites associated significantly with age-related macular degeneration. $-\log(p)$ = minus logarithm of the P value.

molecules or a change in metabolism or lipid peroxidation. Decreased levels of parent molecules could happen locally in the eye or systemically, because fatty acids required for synthesis in the central nervous system are transported from the gastrointestinal tract (coming from the diet or being produced by the liver).⁵⁹ Decreased levels of glycerophospholipids also could be the result of altered catabolism because of a change in phospholipases, the enzymes responsible for the catabolism of glycerophospholipids in the central nervous system and the retina.⁶⁰ Phospholipase C is involved in the regulation of phototransduction and is responsible for the hydrolyzation of phospholipids into inositol 1,4,5-triphosphate and diacylglycerol.⁴³ Phospholipase A2 is another phospholipase that seems to play a role in apoptosis, inflammation, and neurodegeneration.⁴³ One of the catabolic metabolites of phospholipase A2 is glycerol-phosphocholine, a metabolite that was decreased in participants with AMD in our cohort. Interestingly, changes in this metabolite also have been identified in Alzheimer disease,^{50,61,62} once again supporting the hypothesis that there are similarities in the pathogenesis of AMD and Alzheimer disease. Further investigation is needed to understand fully and to validate the role of enzymes and metabolites in AMD.

The current study has a number of limitations, including a relatively small sample size. It was well powered to evaluate the difference between patients with AMD and controls,³³ but its relatively small sample size precluded a thorough analysis of AMD subtypes especially the late AMD subgroup - specifically, geographic atrophy and choroidal neovascularization.⁴⁰ Additionally, our cohort comprised almost solely white participants, which is related in part to the epidemiologic factors of AMD³ and in part to the population served by the enrolling site of our tertiary care hospital. Age differed significantly across the AMD subtypes, which can have an important effect on plasma metabolomic profiles.⁶³ We accounted

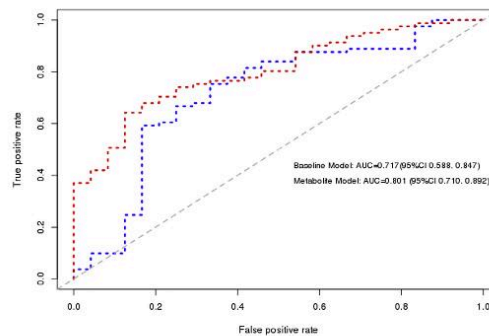


Figure 3. Receiver operating characteristic (ROC) curve analysis of model including the 87 significant metabolites compared with the baseline model. The results of the ROC analysis, including metabolite data, which outperformed (area under the ROC curve [AUC], 0.80; 95% confidence interval [CI], 0.71–0.90) a baseline model including only age, gender, body mass index, and smoking status (AUC, 0.71; 95% CI, 0.59–0.85), appear in red.

for this by performing multivariate analysis, controlling for age and other relevant confounding factors. We did not have access to a validation cohort in this study, and this will be sought out for a future study. Additionally, it would be interesting to analyze how other parameters, namely, dietary patterns, as well as conventional measures of lipid levels (such as serum cholesterol) and other serologic biomarkers, relate to our findings. Data on smoking and BMI were collected through self-reported questionnaires; this means that there is a potential response bias. Another interesting analysis for the future will be to correlate these findings with the genetic risk profiles of patients and controls. Finally, this was a cross-sectional study and provided a snapshot of the metabolome for the participants studied. Yet the metabolome is highly dynamic and susceptible to external factors. Longitudinal studies are needed to confirm our findings and to assess the evolution of the metabolome with the progression of AMD. Future work should address these limitations and explore how the identified plasma metabolomic profiles relate to the genetic risk factors that have been linked with AMD. This likely will provide important insights into the pathogenesis of the disease.

An important advantage of our study is that it was designed prospectively, and all data collection was standardized according to a predefined protocol. In addition, participants underwent a complete ophthalmologic examination performed by a retina specialist, ensuring excellent phenotypic characterization. This is particularly important because many other metabolomic studies rely on established repositories and databases that often lack good phenotypic characterization of ophthalmic disease. Our samples were collected after fasting, were processed within 30 minutes, and were stored immediately for metabolomic profiling, which was performed using a state-of-the-art platform that

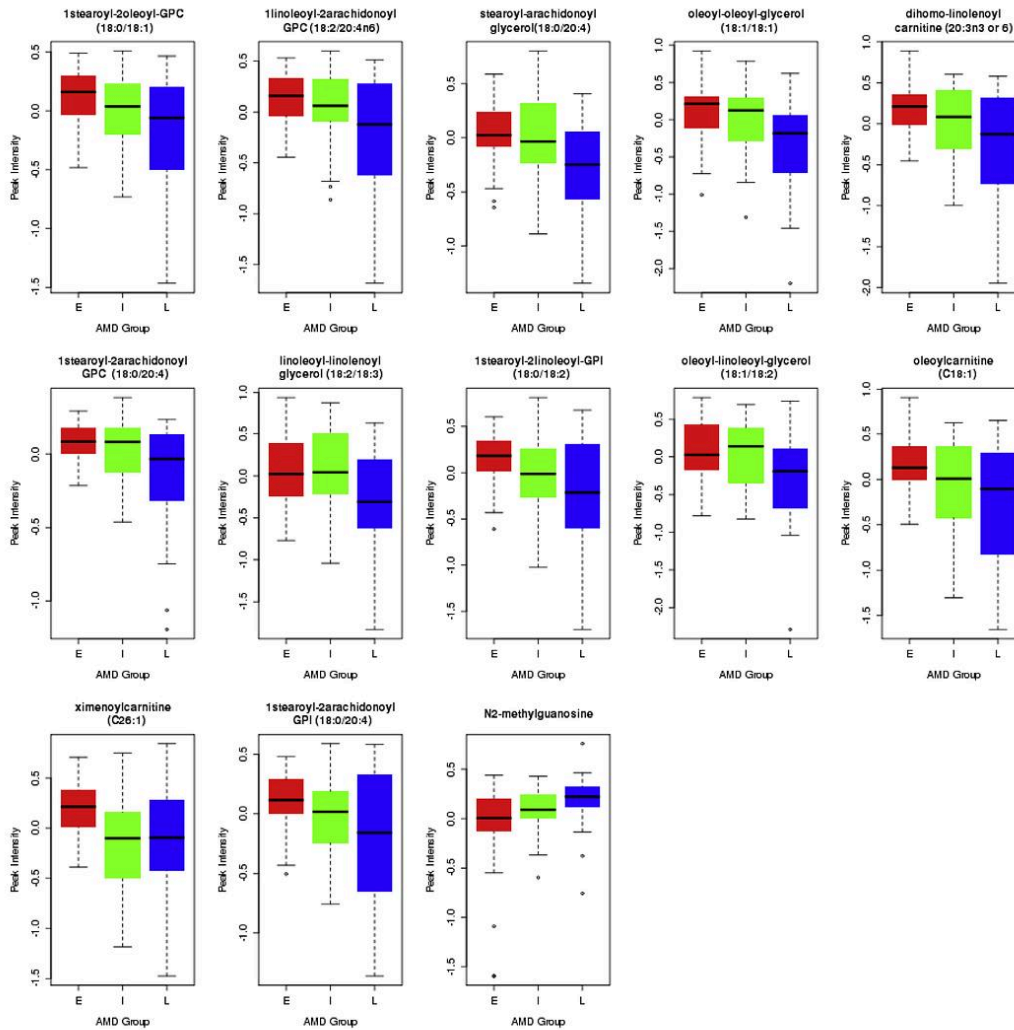


Figure 4. Boxplots of the 13 most significant metabolites ($P < 0.01$) in analysis of variance results comparing severity stages of age-related macular degeneration (AMD). E = early; I = intermediate; L = late.

covers a wide range of the metabolome and identifies metabolites using a chemocentric approach with standards for each identified metabolite.

In conclusion, our data provide for the first time a comprehensive overview of AMD metabolomics and suggest that MS plasma metabolomic profiling is a powerful tool to identify participants with AMD and to distinguish the different stages of disease. Our findings also contribute to the current knowledge of AMD pathophysiology by

highlighting the role of lipid metabolism. In particular, our work points to the relevance of the glycerophospholipid pathway and the need for further research into its role in AMD. These findings offer potential novel targets for early diagnosis and screening, for providing prognostic information and aiding in the monitoring of disease progression, and for identifying druggable targets for treatment of AMD. This work has the potential to lead us into an era of precision medicine in AMD.

References

- Wong WL, Su X, Li X, et al. Global prevalence of age-related macular degeneration and disease burden projection for 2020 and 2040: a systematic review and meta-analysis. *Lancet Glob Heal*. 2014;2(2):e106-e116.
- Handa JT. How does the macula protect itself from oxidative stress? *Mol Aspects Med*. 2012;33(4):418-435.
- Sobrin L, Seddon JM. Nature and nurture—genes and environment—predict onset and progression of macular degeneration. *Prog Retin Eye Res*. 2014;40:1-15.
- Yonekawa Y, Miller JW, Kim IK. Age-related macular degeneration: advances in management and diagnosis. *J Clin Med*. 2015;4(2):343-359.
- Mitta VP, Christen WG, Glynn RJ, et al. C-reactive protein and the incidence of macular degeneration: pooled analysis of 5 cohorts. *JAMA Ophthalmol*. 2013;131(4):507-513.
- Hong T, Tan AG, Mitchell P, Wang JJ. A review and meta-analysis of the association between C-reactive protein and age-related macular degeneration. *Surv Ophthalmol*. 2011;56(3):184-194.
- Klein R, Myers CE, Cruickshanks KJ, et al. Markers of inflammation, oxidative stress, and endothelial dysfunction and the 20-year cumulative incidence of early age-related macular degeneration: the Beaver Dam Eye Study. *JAMA Ophthalmol*. 2014;132(4):446-455.
- Ügurlu N, Aşık MD, Yülek F, et al. Oxidative stress and anti-oxidative defence in patients with age-related macular degeneration. *Curr Eye Res*. 2013;38(4):497-502.
- Chakravarthy U, Wong TY, Fletcher A, et al. Clinical risk factors for age-related macular degeneration: a systematic review and meta-analysis. *BMC Ophthalmol*. 2010;10:31.
- Klein R, Myers CE, Buitendijk GHS, et al. Lipids, lipid genes, and incident age-related macular degeneration: the Three Continent Age-Related Macular Degeneration Consortium. *Am J Ophthalmol*. 2014;158(3):513-524.e3.
- Fiehn O. Metabolomics—the link between genotypes and phenotypes. *Plant Mol Biol*. 2002;48(1-2):155-171.
- Fritsche LG, Igl W, Bailey JNC, et al. A large genome-wide association study of age-related macular degeneration highlights contributions of rare and common variants. *Nat Genet*. 2016;48(2):134-143.
- Nicholson JK, Holmes E, Kinross JM, et al. Metabolic phenotyping in clinical and surgical environments. *Nature*. 2012;491(7424):384-392.
- Nicholson JK, Lindon JC, Holmes E. “Metabonomics”: understanding the metabolic responses of living systems to pathophysiological stimuli via multivariate statistical analysis of biological NMR spectroscopic data. *Xenobiotica*. 1999;11:1181-1189.
- Dessi A, Marincola FC, Fanos V. Metabolomics and the great obstetrical syndromes—GDM, PET, and IUGR. *Best Pract Res Clin Obstet Gynaecol*. 2015;29(2):156-164.
- Kelly RS, Virkud Y, Giorgio R, et al. Metabolomic profiling of lung function in Costa-Rican children with asthma. *Biochim Biophys Acta Mol Basis Dis*. 2017;1863(6):1590-1595.
- Wishart DS. Emerging applications of metabolomics in drug discovery and precision medicine. *Nat Rev Drug Discov*. 2016;15(7):473-484.
- Lima AR, Bastos M de L, Carvalho M, Guedes de Pinho P. Biomarker discovery in human prostate cancer: an update in metabolomics studies. *Transl Oncol*. 2016;9(4):357-370.
- Kalita-de Croft P, Al-Ejeh F, McCart Reed AE, et al. ‘Omics approaches in breast cancer research and clinical practice. *Adv Anat Pathol*. 2016;23(6):356-367.
- Junot C, Fenaille F, Colsch B, Bécher F. High resolution mass spectrometry based techniques at the crossroads of metabolic pathways. *Mass Spectrom Rev*. 2014;33(6):471-500.
- Beckonert O, Keun HC, Ebbels TMD, et al. Metabolic profiling, metabolomic and metabonomic procedures for NMR spectroscopy of urine, plasma, serum and tissue extracts. *Nat Protoc*. 2007;2(11):2692-2703.
- Psychogios N, Hau DD, Peng J, et al. The human serum metabolome. *PLoS One*. 2011;6(2):e16957.
- Suhre K, Gieger C. Genetic variation in metabolic phenotypes: study designs and applications. *Nat Rev Genet*. 2012;13(11):759-769.
- Emwas A-HM. The strengths and weaknesses of NMR spectroscopy and mass spectrometry with particular focus on metabolomics research. In: Bjerrum J, ed. *Metabonomics. Methods in Molecular Biology*. vol 1277. Humana Press, New York, NY: 2015:161-193. Available at: https://link.springer.com/protocol/10.1007%2F978-1-4939-2377-9_13.
- Young SP, Wallace GR. Metabolomic analysis of human disease and its application to the eye. *J Ocul Biol Dis Infor*. 2009;2(4):235-242.
- Midelfart A. Metabonomics—a new approach in ophthalmology. *Acta Ophthalmol*. 2009;87(7):697-703.
- Tan SZ, Begley P, Mullard G, et al. Introduction to metabolomics and its applications in ophthalmology. *Eye (Lond)*. 2016;30(6):773-783.
- Osborn MP, Park Y, Parks MB, et al. Metabolome-wide association study of neovascular age-related macular degeneration. *PLoS One*. 2013;8(8):e72737.
- The Age-Related Eye Disease Study system for classifying age-related macular degeneration from stereoscopic color fundus photographs: the Age-Related Eye Disease Study report number 6. *Am J Ophthalmol*. 2001;132(5):668-681.
- Danis RP, Domalpally A, Chew EY, et al. Methods and reproducibility of grading optimized digital color fundus photographs in the Age-Related Eye Disease Study 2 (AREDS2 report number 2). *Invest Ophthalmol Vis Sci*. 2013;54(7):4548-4554.
- Mazzone PJ, Wang X-F, Beukemann M, et al. Metabolite profiles of the serum of patients with non-small cell carcinoma. *J Thorac Oncol*. 2016;11(1):72-78.
- Chi Y-Y, Gribbin MJ, Johnson JL, Muller KE. Power calculation for overall hypothesis testing with high-dimensional commensurate outcomes. *Stat Med*. 2014;33(5):812-827.
- Barnes S, Benton HP, Casazza K, et al. Training in metabolomics research. II. Processing and statistical analysis of metabolomics data, metabolite identification, pathway analysis, applications of metabolomics and its future. *J Mass Spectrom*. 2016;51(8):535-548.
- Yin P, Peter A, Franken H, et al. Preanalytical aspects and sample quality assessment in metabolomics studies of human blood. *Clin Chem*. 2013;59(5):833-845.
- Xia J, Wishart DS. Using MetaboAnalyst 3.0 for comprehensive metabolomics data analysis. *Curr Protoc Bioinforma*. 2016;55:14.10.1-14.10.91.
- Curcio CA, Millican CL, Bailey T, Kruth HS. Accumulation of cholesterol with age in human Bruch’s membrane. *Invest Ophthalmol Vis Sci*. 2001;42(1):265-274.
- Curcio CA, Johnson M, Rudolf M, Huang J-D. The oil spill in ageing Bruch membrane. *Br J Ophthalmol*. 2011;95(12):1638-1645.
- Fliesler SJ, Bretillon L. The ins and outs of cholesterol in the vertebrate retina. *J Lipid Res*. 2010;51(12):3399-3413.

39. Pikuleva IA, Curcio CA. Cholesterol in the retina: the best is yet to come. *Prog Retin Eye Res.* 2014;41:64-89.
40. Miller JW. Beyond VEGF. The Weisenfeld Lecture. *Invest Ophthalmol Vis Sci.* 2016;57(15):6911-6918.
41. Miller JW. Age-related macular degeneration revisited—piecing the puzzle: the LXIX Edward Jackson Memorial Lecture. *Am J Ophthalmol.* 2013;155(1):1-35.e13.
42. Wang Y, Wang M, Zhang X, et al. The association between the lipids levels in blood and risk of age-related macular degeneration. *Nutrients.* 2016;8(10):E663.
43. Farooqui AA, Horrocks LA, Farooqui T. Glycerophospholipids in brain: their metabolism, incorporation into membranes, functions, and involvement in neurological disorders. *Chem Phys Lipids.* 2000;106(1):1-29.
44. Hopiavuori BR, Agbaga M-P, Brush RS, et al. Regional changes in CNS and retinal glycerophospholipid profiles with age: a molecular blueprint. *J Lipid Res.* 2017;58(4):668-680.
45. Farooqui AA, Horrocks LA, Farooqui T. Interactions between neural membrane glycerophospholipid and sphingolipid mediators: a recipe for neural cell survival or suicide. *J Neurosci Res.* 2007;85(9):1834-1850.
46. Kosciak M, Hecimovic S. Phospholipids and Alzheimer's disease: alterations, mechanisms and potential biomarkers. *Int J Mol Sci.* 2013;14(1):1310-1322.
47. Farooqui AA. Lipid mediators and their metabolism in the nucleus: implications for Alzheimer's disease. *J Alzheimers Dis.* 2012;30(Suppl 2):S163-S178.
48. Frisardi V, Panza F, Seripa D, et al. Glycerophospholipids and glycerophospholipid-derived lipid mediators: a complex meshwork in Alzheimer's disease pathology. *Prog Lipid Res.* 2011;50(4):313-330.
49. Mapstone M, Lin F, Nalls MA, et al. What success can teach us about failure: the plasma metabolome of older adults with superior memory and lessons for Alzheimer's disease. *Neurobiol Aging.* 2017;51:148-155.
50. Whitley L, Sen A, Heaton J, et al. Evidence of altered phosphatidylcholine metabolism in Alzheimer's disease. *Neurobiol Aging.* 2014;35(2):271-278.
51. Proitsi P, Kim M, Whitley L, et al. Association of blood lipids with Alzheimer's disease: a comprehensive lipidomics analysis. *Alzheimers Dement.* 2017;13(2):140-151.
52. Mapstone M, Cheema AK, Fiandaca MS, et al. Plasma phospholipids identify antecedent memory impairment in older adults. *Nat Med.* 2014;20(4):415-418.
53. Kaamiranta K, Salminen A, Haapasalo A, et al. Age-related macular degeneration (AMD): Alzheimer's disease in the eye? *J Alzheimers Dis.* 2011;24(4):615-631.
54. Ohno-Matsui K. Parallel findings in age-related macular degeneration and Alzheimer's disease. *Prog Retin Eye Res.* 2011;30(4):217-238.
55. Sivak JM. The aging eye: common degenerative mechanisms between the Alzheimer's brain and retinal disease. *Invest Ophthalmol Vis Sci.* 2013;54(1):871-880.
56. Ermilov VV, Nesterova AA. β -amyloidopathy in the pathogenesis of age-related macular degeneration in correlation with neurodegenerative diseases. *Adv Exp Med Biol.* 2016;854:119-125.
57. Giusto NM, Pasquare SJ, Salvador GA, Ilincheta de Boscher MG. Lipid second messengers and related enzymes in vertebrate rod outer segments. *J Lipid Res.* 2010;51(4):685-700.
58. Delgado R, Muñoz Y, Peña-Cortés H, et al. Diacylglycerol activates the light-dependent channel TRP in the photosensitive microvilli of *Drosophila melanogaster* photoreceptors. *J Neurosci.* 2014;34(19):6679-6686.
59. Horrocks LA, Yeo YK. Health benefits of docosahexaenoic acid (DHA). *Pharmacol Res.* 1999;40(3):211-225.
60. Frank RN. Potential new medical therapies for diabetic retinopathy: protein kinase C inhibitors. *Am J Ophthalmol.* 2002;133(5):693-698.
61. Klein J. Membrane breakdown in acute and chronic neurodegeneration: focus on choline-containing phospholipids. *J Neural Transm.* 2000;107(8-9):1027-1063.
62. Walter A, Korth U, Hilgert M, et al. Glycerophosphocholine is elevated in cerebrospinal fluid of Alzheimer patients. *Neurobiol Aging.* 2004;25(10):1299-1303.
63. Nicholson JK, Wilson ID. Opinion: understanding "global" systems biology: metabolomics and the continuum of metabolism. *Nat Rev Drug Discov.* 2003;2(8):668-676.

Footnotes and Financial Disclosures

Originally received: May 10, 2017.

Final revision: August 1, 2017.

Accepted: August 7, 2017.

Available online: ■■■■.

Manuscript no. 2017-804.

¹ Retina Service, Massachusetts Eye and Ear, Harvard Ophthalmology AMD Center of Excellence, Department of Ophthalmology, Harvard Medical School, Boston, Massachusetts.

² Faculty of Medicine, University of Coimbra, Coimbra, Portugal.

³ Association for Innovation and Biomedical Research on Light and Image (AIBILI), Coimbra, Portugal.

⁴ Centro Hospitalar e Universitário de Coimbra, Coimbra, Portugal.

⁵ Systems Genetics and Genomics Unit, Channing Division of Network Medicine, Brigham and Women's Hospital and Harvard Medical School, Boston, Massachusetts.

Presented at: Association for Research in Vision and Ophthalmology Annual Meeting, Baltimore, MD, May 2017; Macula Society Annual Meeting, Singapore, June 2017.

*Both authors contributed equally as first authors.

Financial Disclosure(s):

The author(s) have made the following disclosure(s): LL: Patent – Biomarkers for Age-Related Macular Degeneration

R.S.K.: Patent – Biomarkers for Age-Related Macular Degeneration

R.S.: Consultant – Novartis, Bayer, Thea, Allergan, Alcon, aLIMERA

I.K.K.: Financial support – Genentech, Allergan, Ironic Therapeutics

J.N.M.: Financial support – Alcon

J.L.-S.: Consultant – Metabolon; Patent – Biomarkers of AMD pending

J.W.M.: Consultant – Amgen, Inc., KalVista Pharmaceuticals, Ltd., Maculogix, Inc., Biogen Idec, Inc., Alcon Research Council; Financial support – Lowy Medical Research Institute, Ltd.; Patents – Valeant Pharmaceuticals, ONL Therapeutics LLC

D.H.: Patent - Biomarkers for Age-Related Macular Degeneration

Supported by the Miller Retina Research Fund (to Massachusetts Eye and Ear); the Champalimaud Vision Award (to J.W.M.); Research to Prevent Blindness, Inc., New York, New York (unrestricted departmental grant); and the Portuguese Foundation for Science and Technology/Harvard Medical School Portugal Program (grant no.: HMSP-ICJ/006/2013). None of the aforementioned funding organizations had any role in the design or conduct of this research.

Author Contributions:

Conception and design: Laíns, Murta, J.W. Miller, Silva, Husain

Analysis and interpretation: Laíns, Kelly, J.B. Miller, Silva, Vavvas, Kim, Lasky-Su, J.W. Miller, Husain

Data collection: Laíns, J.B. Miller, Silva, Vavvas, Kim, J.W. Miller, Husain

Obtained funding: none

Overall responsibility: Laíns, Kelly, J.B. Miller, Vavvas, Kim, Murta, Lasky-Su, J.W. Miller, Husain

Abbreviations and Acronyms:

AMD = age-related macular degeneration; **AREDS** = Age-Related Eye Disease Study; **BMI** = body mass index; **MS** = mass spectrometry; **ROC** = receiver operating characteristic; **RPE** = retinal pigment epithelium.

Correspondence:

Deeba Husain, MD, Retina Service, Massachusetts Eye and Ear, Harvard Medical School, 243 Charles Street, Boston, MA 02114. E-mail: Deeba_Husain@meei.harvard.edu.

Metabolomics of Retinal Diseases

Inês Láins^{a,b}, Mari Gantner^c, Salome Murinello^c, Jessica A. Lasky-Su^d, Joan W. Miller^a, Martin Friedlander^c, Deeba Husain^a

- a. Retina Service, Massachusetts Eye and Ear, Harvard Medical School, 243 Charles Street, Boston, Massachusetts, 02114, United States.
- b. Faculty of Medicine, University of Coimbra, 3000 Coimbra, Portugal.
- c. The Scripps Research Institute, The Lowy Medical Research Institute, 10550 N Torrey Pines Rd, La Jolla, California, 92037, United States.
- d. Systems Genetics and Genomics Unit, Channing Division of Network Medicine Brigham and Women's Hospital and Harvard Medical School, 75 Francis Street, Boston, Massachusetts, 02115, United States.

Email addresses:

Ines Láins – ines_lains@meei.harvard.edu
Mari Gantner – mgantner@gmail.com
Salome Murinello - smuri@scripps.edu
Jessica A. Lasky-Su – jessica.a.su@gmail.com
Joan W. Miller – joan_miller@meei.harvard.edu
Martin Friedlander - friedlan@scripps.edu

Corresponding Author:

Deeba Husain, MD
Retina Service, Massachusetts Eye and Ear
Harvard Medical School
243 Charles St, Boston, MA, 02114
Deeba_Husain@meei.harvard.edu
Tel: [617-573-4371](tel:617-573-4371)
Fax: [617-573-3698](tel:617-573-3698)

Financial support: This work was financially supported by the Miller Retina Research Fund (Mass. Eye and Ear), the Champalimaud Vision Award (JVM), the unrestricted departmental Grant from Research to Prevent Blindness, Inc. New York, and the Portuguese Foundation for Science and Technology/ Harvard Medical School Portugal Program (HMSP-ICJ/006/2013). None of the aforementioned funding organizations had any role in the design or conduct of this work.

Metabolomics of Retinal Diseases

Abstract

Metabolomics is the qualitative and quantitative assessment of all the metabolites (small molecules < 1.5 KDa) in body fluids. The metabolites represent the downstream product of the cumulative effects of the genome and its interaction with environmental exposures, and therefore closely represents the phenotype, especially in subjects with multifactorial disorders. In the last decade, metabolomics has been increasingly used to identify biomarkers in disease, and it is currently recognized as a very powerful tool with great potential for clinical translation. The metabolome and the associated pathways also helps improve our understanding of the pathophysiology and mechanisms of disease.

While there has been increasing interest and research in metabolomics of the eye, application of metabolomics to retinal diseases has been limited, even though retinal diseases remain a leading cause of blindness. In this manuscript, we perform a comprehensive summary of the tools and knowledge required to perform a metabolomics study, and we highlight essential statistical methods for rigorous study design and data analysis. We review available protocols, summarize the best approaches, and address the current unmet need for information on collection and processing of tissues and biofluids that can be used for metabolomics of retinal diseases. Additionally, we critically analyze recent work in this field, both in animal models and in human clinical disease, including diabetic retinopathy and age-related macular degeneration. Finally, we identify opportunities for future research applying metabolomics to improve our current assessment and understanding of mechanisms of vitreoretinal diseases.

Key-words: Metabolomics, Retina, Vitreous, Biomarkers, Mass Spectrometry, Magnetic Resonance Spectroscopy.

Table of Contents

- 1. Metabolomics: concepts and opportunities**
- 2. Analytical tools for metabolomic profiling**
- 3. Sampling collection and processing**
 - 3.1 General concepts
 - 3.2 Animal tissue
 - 3.3 Human tissue and samples
 - 3.3.1 Serum and plasma
 - 3.3.2 Urine
 - 3.3.3 Other biofluids
 - 3.3.4 Parafin-embedded tissue
 - 3.3.5 Human fresh retinal tissue and vitreous samples
- 4. Role of statistics and data analysis**
 - 4.1 Main statistical approaches
 - 4.2 Sample size and power
 - 4.3 Multiple hypothesis testing
- 5. Metabolomics of vitreoretinal disease**
 - 5.1 Normal retina
 - 5.2 Diabetic retinopathy
 - 5.3 Retinal detachment
 - 5.4 Age-related macular degeneration
 - 5.5 Macular telangiectasia
 - 5.6 Others
- 6. Limitations**
- 7. Future directions**

1. Metabolomics: concept and opportunities

Human biology is diverse and complex. It was initially believed that human genetic makeup remains stable over a lifespan. However, it is currently recognized that genes undergo epigenetic modifications, and that DNA transcription into RNA, and its translation into proteins, is influenced by several environmental exposures.(Crick, 1970; Jafari et al., 2017) Indeed, it is the combination of genetic factors and external influences that leads to many different phenotypes in complex diseases.(Dunn et al., 2011a) The closest and most direct biological representation of the phenotype is thought to be the metabolome. The metabolites, low molecular weight molecules (<1-1.5 kDa), reflect the cumulative effects of the genome, transcription, translation, and metabolism, influenced by environment, diet, age and microbiome, among other factors(Patti et al., 2012) – Figure 1.

Metabolomics (nowadays used interchangeably with metabonomics), is a multidisciplinary field studying the metabolome, which is the global qualitative and quantitative composition of metabolites in a biological system.(Fiehn, 2002) The total number of metabolites varies among different biological specimens, and remains unknown. According to the Human Metabolome Database (<http://www.hmdb.ca/statistics#metabolite-statistics>), the largest metabolite database worldwide, humans have at least 1,141,000 metabolites. These include breakdown products of lipids, nucleotides, amino acids and carbohydrates, among others. Importantly, each body compartment has its own metabolome, but they are connected through the vascular and lymphatic systems, which also have a specific metabolomic profile.(Jeremy K Nicholson et al., 2012b) In contrast to the genotype, which remains relatively stable over a lifespan, the metabotype (metabolomic phenotype) varies with time and every metabolomic characterization of a biosample represents a snapshot of that particular state and time.(Suhre and Gieger, 2012)

Compared to genomics and proteomics, metabolomics is a relatively new field,(Kell and Oliver, 2016) but it is becoming an increasingly important tool in medicine, as it can provide information during normal and pathological conditions. This is because the study of the variations of the metabolome has major advantages, including the possibility of: increasing the understanding of the pathophysiology of a disease at a molecular level and generating new hypotheses for disease mechanisms; identifying biomarkers of disease risk prediction and diagnosis; predicting progression; interpreting the influence of our environment and lifestyle exposures in disease; assessing drug efficacy, toxicity and adverse drug reactions.(Jeremy K Nicholson et al., 2012b),(Jové et al., 2014),(Kohler et al., 2016) Also, metabolomic profiles of individuals can be measured from easily accessible biofluids or tissues that can be sampled readily in the outpatient setting, which represents an additional advantage.(Jeremy K Nicholson et al., 2012b) The strength of association with

disease outcomes also tends to be higher in metabolomics than in genetics. Thus, metabolomic studies require smaller sample sizes than genetic studies.(Manolio et al., 2009)

Metabolomics has an important role to play in personalized and stratified medicine.(Ziegelstein, 2017) Clinical diagnosis, prognosis prediction, and treatment selection are improved by tools that can help classify diseases and their subtypes, as well as define underlying individual variations in patient biology and responses. Metabolomics is one of these tools.(Jeremy K Nicholson et al., 2012b) and also aids our understanding by providing insight into the interactions between genetic, environmental and lifestyle factors.(Suhre and Gieger, 2012) Because of this, metabolomics has been employed in several medical fields,(Trivedi et al., 2017) including in large epidemiological and population-based studies.(Patel et al., 2017; Suhre et al., 2010) Its utility in ophthalmology has recently been explored as well.(S Z Tan et al., 2016),(Midelfart, 2009),(Young and Wallace, 2009)

In this manuscript, we set out to compile a comprehensive summary of the tools and knowledge required to perform a metabolomics study, including those specific to retinal diseases. We have also critically analyzed published work to date, and discuss how a better understanding of metabolomics can help in our understanding of eye diseases, as well as inform future studies.

2. Analytical tools for metabolomic profiling

The study of metabolites has a long history, but in the past targeted specific compounds known *a priori* - targeted metabolomics.(Wilcken et al., 2003) A good example is the study of blood glucose levels for the diagnosis of diabetes, or lipoproteins' levels for the assessment of dyslipidemia. In the last few decades, however, metabolomics has shifted to a non-targeted approach. With this untargeted or global approach, studies measure as many metabolites as possible, and compare them between samples without bias. Such untargeted metabolomics analysis is predicated on the development of "metabolite libraries" that contain well characterized metabolite profiles that may be used as standards against which profiles of specimen metabolites may be compared for identification. This has led to new discoveries, linking cellular pathways to biological mechanisms, and shaping our understanding of physiology and medicine.(Patti et al., 2012)

The global analysis of metabolites can be performed with two main analytical tools: nuclear magnetic resonance (NMR) spectroscopy and mass spectrometry (MS).(Emwas, 2015),(Barnes et al., 2016a) Depending on the instrument or protocol used, typically they are able to identify from 50 to up to 5000 different metabolites at a time, but no tool, metric or platform is able to identify all existing metabolites. The majority of metabolomic studies use a single analytical source. However, there is a growing acknowledgment of the value of

combining NMR and MS.(Marshall and Powers, 2017) They are complementary techniques, so combining them is likely to improve the overall quality of a study and enhance the coverage of the metabolome.(Dunn et al., 2011a)

Regardless of the technical analytical tool chosen, minimum requirements for reporting a metabolite profiling experiment include sample preparation, experimental analysis, quality control, metabolite identification, and data pre-processing.(Khamis et al., 2017) Validation of metabolomic profiles should include at least a description of the calibration model (linearity and range), repeatability and intermediate precision, accuracy and lower limit of quantification.(Scalbert et al., 2009)

2.1 Nuclear magnetic resonance (NMR) spectroscopy metabolomics

NMR spectroscopy measures the behavior of atoms when they are subjected to a magnetic field. When submitted to an external magnetic field, atoms with an odd mass, such as hydrogen (^1H) or carbon (^{13}C), behave as dipoles and align along the axis of the applied magnetic field (excitation). This higher energy level is less stable, so these atoms then undergo relaxation, generating radiofrequency signals, which can be expressed as a frequency spectrum(Tognarelli et al., 2015),(Barnes et al., 2016a) – Figure 2.

Hydrogen is the most abundant atom in living organisms and proton NMR is the most commonly used NMR technique.(Barnes et al., 2016a) In a ^1H spectrum, the position of each peak (chemical shift) represents the hydrogen atoms' environment (i.e., proximity of electronegative groups such as nitrogen, oxygen, double bonds, etc). The size of the peaks, most precisely the area under the curve, provides important information about the number of hydrogen atoms in each environment. Currently, 500 and 600 MHz NMR instruments are the most widely used, but the higher the magnetic field strength, the greater the resolution.(Barnes et al., 2016a)

NMR spectroscopy can be applied to liquid samples, but also to solid, gas phase and tissue samples.(Ernwas, 2015) One of its biggest advantages is the minimal sample preparation required, and the preservation of samples (i.e., even after analysis, samples can still be used for other studies). NMR is also acknowledged to be highly reproducible and less susceptible to instrument variability. Its major disadvantage relates to its sensitivity, which is lower than that of MS. The number of metabolites visible in the proton NMR spectrum ranges from about 50 in serum/plasma samples to roughly 200 in urine.(Kohler et al., 2016) Also, the interpretation of NMR spectra is considered complex and requires substantial training, as signals from different metabolites can overlap.(Markley et al., 2017)

2.2 Mass spectrometry (MS) metabolomics

MS identifies metabolites primarily based on their mass to charge (m/z) ratio.(Crutchfield et al., 2016) A good analogy is to imagine a cannonball and a tennis ball travelling together, which we hope to deflect with a jet of water. The cannonball is so heavy that it will hardly be deflected at all from its original course. Conversely, the tennis ball is light, and will have a large deflection. In this example, the mass of each ball determines the ability to deflect them. The same principle applies to MS. Atoms and molecules can be deflected by magnetic fields. First, they need to be turned into ions (ionization), and then these are accelerated so that they all have the same kinetic energy. The ions are then deflected by a magnetic field according to their masses and their number of positive charges.(Gika et al., 2014; Lind et al., 2016; X. Wang et al., 2011) Several techniques are available for ionization,(Kohler et al., 2016) with electrospray ionization being one of the most commonly used.(Wilm, 2011)

A MS spectrum of a sample can be obtained by direct injection, but it is usually performed in tandem with separation techniques, such as liquid chromatography (LC), gas chromatography (GC) or capillary electrophoresis (CE). Importantly, no separation method (GC, LC or CE) enables the simultaneous separation of all metabolites. In addition, there is no one detector that can measure all metabolites, as some metabolites may not ionize with a certain methods, or because their concentration is too low.(Khamis et al., 2017)

In biosciences, LC, particularly ultra-high-performance liquid chromatography (UPLC), is becoming increasingly popular and is probably the most widely used MS technology.(Patti et al., 2012) This is primarily due to the ability of LC to separate and detect a wide range of metabolites,(Jové et al., 2014),(Jeremy K Nicholson et al., 2012b) and because of the large number of accessible instruments and open-source data processing software available for this technique.(Jové et al., 2014) A disadvantage of LC–MS is ion suppression: ionization of metabolites may depend on the presence of matrix compounds, and on atmospheric pressure chemical ionization. GC has high separation efficiency and reproducible retention times.(Khamis et al., 2017) However, it presents three main pitfalls: possible loss of thermolabile analytes; complex sample preparation; and higher variability compared with LC-based metabolomics.(Dunn et al., 2011b) Also of note, concerns have emerged about degradation of metabolites during GC–MS analysis, due to the required exposure to elevated temperatures.(Fang et al., 2015) CE is rarely used due to its overall lower sensitivity and poor reproducibility.(Kohler et al., 2016)

In general, MS has a much higher sensitivity (detection level of picomoles to femtomoles) than NMR, therefore enabling the measurement of a broader range of metabolites. Additionally, the different MS technologies provide an array of operational principles that can be applied, thus increasing the number of metabolites that can potentially

be detected. This is particularly relevant for biological samples.(Emwas, 2015) Importantly, MS requires the use of multiple internal standards simultaneously (typically at least 3), as well as the use of quality control samples.(Barnes et al., 2016a),(Gika et al., 2014)

2.3 Mass spectrometry imaging metabolomics

Mass spectrometry imaging (MSI) is a method by which molecular information is obtained over two or three spatial dimensions, thus enabling one to determine the distribution of small molecules within a tissue.(Petras et al., 2017a) For each ion in the collected mass to charge (m/z) range, reconstruction of its intensity in every x-y coordinate pair creates an image of its distribution.

Several MSI techniques have been developed, which mostly differ in their spatial resolution, molecular specificity and sensitivity.(Naru et al., 2017) Matrix-assisted laser desorption ionization (MALDI) is currently the most widely applied method, and typically provides a lateral spatial resolution ranging from a few μm to mm. This is dependent on the technique applied and laser diameter.(Petras et al., 2017b) In general, most MALDI studies are performed on linear MALDI time-of-flight (TOF) platforms, which enable a resolution to the level of proteomics. Bowrey et al.(Bowrey et al., 2016) recently reviewed the application of MSI proteomics to the study of the visual system. However, for metabolomics, Fourier-transform ion cyclotron resonance (FTICR) or quadrupole-TOF is recommended, as they both provide higher resolution and mass accuracy.(H.-Y. Wang et al., 2011) MSI metabolomics has been used to study porcine retina tissue.(Sun et al., 2014)

One of the big advantages of MSI is the ability to correlate the metabolite information with histological data. It enables the virtual dissection of tissue based on macular mass signatures.(Sun et al., 2014) Unlike traditional MS, sample preparation methods do not result in the loss of spatial localization, while allowing non-targeted analysis. In a single experiment, it is possible to detect the spatial distribution of thousands of molecules.(Naru et al., 2017) However, this technique still has important limitations in terms of instrumentation, namely resolution, and sample preparation.(Petras et al., 2017a),(Zemski Berry et al., 2014) Importantly, the time required for data acquisition increases following an inverse squared relationship with lateral spatial resolution, and the sensitivity of mass analysis increases with decreased lateral spatial resolution. Additionally, quantitative analysis is worse than with the traditional extraction and analysis by liquid chromatography MS.(Petras et al., 2017b)

3. Sampling collection and processing

3.1 General concepts

Unlike the genetic sequence, metabolomic profiles vary depending on the biofluid being assessed. Appropriate sample collection and processing is an important requirement for successful metabolomic studies.(Khamis et al., 2017) All efforts should be made to ensure that the collected samples are qualitatively and quantitatively representative of their source,(Ammerlaan et al., 2014) and that bias and uncontrolled experimental variances are minimized.(Yu et al., 2011)

Protocols should be developed and reviewed before beginning any collection, as they vary. For example, if metabolomic profiling is going to be performed by a different laboratory/ institution than the one that is obtaining the samples, the entire protocol should be discussed with all the involved parties, and defined *a priori*. Standard operating procedures (including check lists and labeling procedures) are essential to prevent mistakes and increase efficiency. Supply sources should be uniform and the collection and storage conditions should be well defined. In large-scale human metabolomics studies, samples are frequently collected at different sites. It is therefore important to provide written procedures or guidelines to all researchers, clinicians and laboratory staff involved in the project to ensure the highest reproducibility throughout sample collection and handling.(Kohler et al., 2016) Despite the definition of standardized protocols, their strict execution within single- or multi-center clinical studies can be challenging, so monitoring and samples quality assessment is also crucial.(Jobard et al., 2016)

For studies using samples already collected as part of biobanks, it is essential to obtain all possible information about the conditions of sample collection and storage.(Yu et al., 2011) Since a relatively long time may elapse between the collection of the samples and their analysis, multiple parameters must be monitored to lower the risks for degradation and interconversion, including temperature, light, humidity, time span, quenching and number of freeze–thaw cycles.(Kohler et al., 2016) A consensus is still lacking on the effect of freeze–thaw cycles on the metabolome, so multiple freeze–thaw cycles should be avoided as much as possible.(Kohler et al., 2016)

In the following section, we discuss the specific requirements to obtain biofluids and other tissue samples that can be relevant for the study of retinal diseases. Metabolomics workbench (www.metabolomicsworkbench.org) is a website supported by the National Institute of Health that has a large and excellent resource of experimental protocols and general guidelines for sample preparation. In general, for untargeted metabolomics, sample preparation should be as simple as possible to obtain the widest metabolite coverage.(Kohler et al., 2016)

3.2 Animal tissue

It is essential to plan animal tissue collection in advance and consider euthanasia method, tissues desired, post mortem time to quenching/freezing and consumable selection. Compounds commonly used for euthanasia are known to have broad effects on cell function and metabolite levels. Isoflurane affects glucose metabolism in mice, and if metabolites of interest are linked to glucose, their metabolism may also be affected in the tissue being studied.(Federation of American Societies for Experimental Biology. et al., 2010) Ideally, rapid cervical dislocation or a guillotine should be used in mice, but these protocols need to be discussed and approved by the Institutional Animal Care and Use Committee. Response to stress also affects metabolism and balancing the euthanasia approach with minimization of stress to the animal is essential for reliable outcomes with animal models.(Ghosal et al., 2015; Hurst and West, 2010)

Many metabolites have very rapid turnover rates. Therefore, as with other sample collection, it is key to handle tissue samples as quickly as possible to prevent metabolite degradation. Snap freezing samples in liquid nitrogen is commonly considered best practice. However, if and when that is not possible, cooling to 4°C maintains most but not all metabolites in the retina for up to 8 h.(Shi Z. Tan et al., 2016) Collecting the entire eye and snap freezing in liquid nitrogen is the quickest and most reliable method and should be used if the broadest metabolite profile possible is desired.(Paris et al., 2016) Micro-dissection of specific tissues such as the cornea, lens, vitreous, retina and choroid allows for tissue-specific metabolite analysis but increases post mortem processing time and potential changes in metabolite levels. Collection speed must be balanced with sample integrity. If specific tissues are to be dissected it is best to practice ahead of time to increase speed and accuracy.

The consumables used for tissue collection should be selected based on the subsequent extraction and mass spectrophotometer analyses. For broad metabolomics analysis including non-polar and lipid species, glass is the best material to work with. Not all glass products are equivalent and it is advisable to consult with those running the extraction and analysis for their recommendations. If the analyses focus on polar metabolites plastic tubes may be appropriate, but not all plastics are equivalent. The same container type should be used throughout all samples in an experiment and a vessel-alone extraction in parallel can help to distinguish non-tissue derived metabolites.

3.3 Human tissue and samples

3.3.1 Plasma and serum

Blood provides a snapshot of the metabolism that integrates many tissues in the human body, and thus provides a global metabolomic picture.(Chetwynd et al., 2017) Therefore, along with urine, which is also an integrative biofluid, blood is one of the most commonly used biofluids for metabolomics in biomedical sciences.(Dunn et al., 2011a) The influence of the pre-analytics practices for blood samples has been discussed in the literature,(Hebels et al., 2013) and seems to be very relevant.(Kohler et al., 2016)

Either serum or plasma can be obtained from blood, and the preferred fluid remains to be established for metabolomics - plasma seems to be more reproducible, and serum to have higher concentrations of metabolites.(Yu et al., 2011) The main difference between them refers to the presence or absence of clotting factors. For serum, whole blood is collected into tubes and is allowed to clot.(Chetwynd et al., 2017) One must record the clotting time and temperature at which the clotting occurred, and this should be standardized across all samples.(Khamis et al., 2017) Plasma is obtained when whole blood is mixed with an anticoagulant to inhibit clotting. Typical anticoagulants include lithium heparin, EDTA and citrate. In general, the use of lithium heparin is recommended,(Chetwynd et al., 2017)(Yu et al., 2011) especially for NMR, even though heparin may lead to ion suppression.(Barnes et al., 2016a) Citrate and EDTA have molecular masses similar to some metabolites, and citrate is an endogenous metabolite, which therefore requires caution when analyzing the results. EDTA has the advantage of chelating the potential divalent metal cations present in the sample, which otherwise might accelerate the hydrolysis of important energy metabolites. However, EDTA may also lead to ion suppression.(Kohler et al., 2016) Importantly, blood collection tubes can also release materials into the samples and interfere with metabolomic analysis, so the same tubes should be used across a study and this information should be registered. Circadian oscillations can also significantly influence the metabolome, particularly for lipids, therefore it is important to collect samples in the same time of day and document this information.(Kohler et al., 2016)

After collection into the appropriate tubes (without or with anticoagulant), serum or plasma are separated by centrifugation from the blood clot or cell mass, respectively. Samples should be immediately stored as 0.5 or 1.0 mL aliquots at $-80\text{ }^{\circ}\text{C}$ or in liquid nitrogen. NMR studies require larger sample volumes.(Barnes et al., 2016a) A delay in time between aliquoting and storage can affect the quality of the samples.(Yu et al., 2011) Some authors have argued that centrifugation parameters (such as rotation speed and temperature) are not particularly relevant,(Jobard et al., 2016) but this remains controversial.(Ammerlaan et al., 2014)

3.3.2 Urine

Urinary metabolomic profiling has expanded in the last few years.(Slupsky et al., 2007)(Khamis et al., 2017) Urine is easily obtained at a reasonable cost.(Emwas et al., 2016) Moreover, compared to blood, urine is not subject to many homeostatic mechanisms, and greater varieties of endogenous metabolites can be present, so some authors argue that it may better reflect the changes in human metabolism.(Mal, 2016)

Typically three types of urine samples can be collected, and they have important differences among them: first morning void, spot urine and 24-hour urine collection.(Chetwynd et al., 2017),(Slupsky et al., 2007) The last (24 hours collection) is the ideal, as it reduces the impact of any circadian variation and represents a complete circadian cycle. However, it is often not feasible to obtain 24 hours samples for clinical studies,(Kohler et al., 2016) so first morning void is the choice in most cases. This option can reduce the effect of meals or medication, as it is collected following an overnight fast. Spot urine samples refer to those taken at any time point, which makes them highly influenced by the variable daily excretion rate, as well as by other environmental factors.(Slupsky et al., 2007),(Chan et al., 2011; Giskeødegård et al., 2015)

For urine collection, subjects are simply asked to provide a mid-stream urine sample in a sample cup. For immobile subjects it can be collected with a catheter, and for babies urine can be collected with absorbent pads in nappies.(Chetwynd et al., 2017) After collection, the samples should be frozen at -80°C as soon as possible, as prior work has shown that urine modifications can occur in a short period of time,(Gika et al., 2008) especially at room temperature. At -20°C, samples can remain stable for a relatively long time, but -80°C remains the best choice.(Gika et al., 2008) Freeze thaw cycles should be kept to a minimum.(Khamis et al., 2017)

In a healthy individual, urine is sterile, however it can become contaminated during urination, which can modify the urinary metabolites. In addition to storage at -80°C and collection of mid-stream samples, which are both beneficial,(Kohler et al., 2016) antibacterial additives such as sodium azide and sodium fluoride seem to increase the stability of samples.(Chetwynd et al., 2017)

3.3.3 Other biofluids

Recent research in metabolomics has given increasing attention to saliva, a biofluid obtainable non-invasively and with a relatively low cost. Saliva provides an easy access to the metabolites secreted by the human body.(Kelly et al., 2011),(Cuevas-Cordoba and Santiago-Garcia, 2014; Zhang et al., 2012) It can be obtained by stimulation with citric acid,

or without stimulation (resting). Previous studies suggest that almost all metabolites are higher in unstimulated saliva when compared to the stimulated saliva.(Takeda et al., 2009) Therefore, most groups choose to use unstimulated saliva samples, usually following a period of fasting and delayed oral hygiene to prevent contamination.(Chetwynd et al., 2017) Typically, saliva samples are collected, centrifuged to eliminate cellular and food debris, and then immediately stored at -80 °C until analysis.(Álvarez-Sánchez et al., 2012) Storage at -20°C can be performed for up to 3 weeks with no detrimental effects.(Takeda et al., 2009) To our knowledge, saliva metabolomics has not been yet applied to the study of retinal diseases. However, salivary metabolic profiling in conjunction with serum based metabolic profiling was able to provide diagnostic biomarkers of neurodegenerative dementia, such as Alzheimer's disease and frontotemporal lobe dementia.(Mal, 2016)

Another biofluid that can be obtained non-invasively is tears. Recently, human tears have been used to identify potential biomarkers of ocular surface diseases.(Nishtala et al., 2016; Zhou et al., 2006),(Zhou and Beuerman, 2012) However, recent work suggests the potential of this biofluid to the study of diseases of the posterior segment, in particular diabetic retinopathy,(Ting et al., 2016) and also non-ophthalmologic systemic diseases.(Pieragostino et al., 2015) Two main methods for tear collection for metabolomic profiling have been described: the use of Shimer's strips and the use of glass capillary tubes. Shimer's strips are routinely used in ophthalmology and enable a simple procedure. Collection should be performed without anesthesia, and then the strips should be stored at -80°C in glass vials.(Lam et al., 2014) The main disadvantage relates to the risk of cellular contamination with epithelial cells.(Chen et al., 2011) Glass capillary collection has minimal cells contamination risk, but is a more complex procedure. Previous authors described collection from the lower conjunctival sac with glass micropipets, followed by cooling to 4°C and centrifugation to remove possible cellular debris. The resultant supernatant was then stored at -20°C(Rantamäki et al., 2011) or -80°C.(Lam et al., 2014)

3.3.4 Paraffin-embeded tissue

Tissues in available biobanks have often been preserved with formalin fixation followed by paraffin embedding (FFPE). Although fresh frozen samples are the gold standard for metabolomics, available archival FFPE tissue samples may be a viable alternative.(Nirmalan et al., 2008) These tissues have two major challenges: first, fixation in formalin can alter proteins and biomolecules present in the tissue, and secondly, it is hard to subsequently remove the paraffin (water insoluble) without damaging or losing compounds. However, investigators have described successful metabolomics using FFPE tissue, with good correlation with results from fresh-frozen samples.(Cacciatore et al., 2017;

Wojakowska et al., 2015),(Kelly et al., 2011) For example, Wojakowska et al.(Wojakowska et al., 2015) reported the applicability of FFPE kidney specimens for non-targeted GS/MS-based profiling, and mass spectrometry imaging might be particularly well suited for the use of these tissues.(Buck et al., 2016) The possibility of conducting metabolomic studies using FFPE material would open a wide range of tissues for clinical research.

3.3.5 Human fresh retinal tissue and vitreous samples

Human tissues are metabolically active and therefore require rapid metabolic quenching immediately after collection. In general, it is recommended to rapidly wash them after collection (in a phosphate-buffered aqueous solution or in saline), and then proceed as soon as possible with freezing, in order to quench metabolism. Washing of tissues to remove as much blood as possible is also an important step, as the blood metabolome is different from the tissue metabolome, and would confound the results. Storage should be performed at -80°C .

Retinal tissue is not an exception. In the 1980s, Schmidt et al.(Schmidt and Berson, 1980) described that retinas from postmortem human donor eyes can retain their metabolic activity for 4 to 4.5 hours, namely for photoreceptor cell-specific metabolic processes. However, to our knowledge, no studies have been performed proposing a specific protocol for human retinal tissue processing for metabolomics. Based on their findings in rat retina tissue, Tan et al.(Shi Z. Tan et al., 2016) recommended that post-mortem human tissue should be stabilized within 8 h following enucleation.

Regarding the amount of tissue required, for untargeted or targeted metabolomic studies, typically 20–100 mg of tissue is required to provide good coverage of the tissue metabolome.(Ammerlaan et al., 2014) This can be challenging for eye tissue, especially for the study of the retina. For the vitreous, Young et al.(Young et al., 2009) described successful results with undiluted samples of 0.1 to 0.2 mL, but we would advise larger volumes of 0.5 to 1 mL.(Paris et al., 2016) These samples should be transferred to sterile tubes, and frozen immediately until analysis. This is important as time dependent post-mortem biochemical changes have been demonstrated in the vitreous, even though they are relatively slow.(Boulagnon et al., 2011a),(Zilg et al., 2015)

4. Role of biostatistics and data analysis

Overall, the analytical path from data acquisition to biomarker discovery in metabolomics involves numerous steps to produce biologically meaningful data, including

both statistical and bioinformatic approaches.(Barnes et al., 2016a) Investigators should consult with a biostatistician before initiating a metabolomics study in order to develop an appropriate experimental design, incorporate proper data cleaning, and create an analytical plan for the metabolomic data. During the study, it is also essential to record all the steps taken in the design of the experiment, sample collection, storage and processing. It is also important to be aware of the strengths and weaknesses of the analytical platform, the pre-processing of the data and the statistical and pathway tools used to interpret the data.

4.1 Main statistical approaches

As described, untargeted metabolomic studies are characterized by the simultaneous measurement of a large number of metabolites on each sample. This strategy, known as top-down strategy, avoids the need for an “*a priori*” hypothesis on a particular set of metabolites and, instead, considers the global metabolome. Consequently, these studies are characterized by the generation of a diverse array of metabolites with a range of chemical properties.(Alonso et al., 2015) Targeted metabolomic studies are hypothesis- driven experiments and are characterized by the measurement of predefined sets of metabolites, most often in a specific metabolic pathway, with absolute quantification, which results in a high level of precision and accuracy.(Putri et al., 2013)

Alonso et al.(Alonso et al., 2015) described with great detail the typical methodological pipeline of an untargeted metabolomic study. Briefly, the first step is the processing of spectral data to generate metabolomic information (i.e. metabolic features), which is highly dependent on the analytical technique used (for example, NMR or LC-MS). Once the complete set of metabolomic features has been generated and run through a quality control pipeline, univariate and multivariate statistics can be applied to determine how the metabolomic features are related to each other and to the phenotypes of interest. Bioinformatic approaches can then be used to assess the metabolic pathways that are related to the phenotype. In this manuscript, we aim to summarize the main statistical techniques available for data analysis.

After metabolomic data are generated, the distribution of each metabolite is most often largely skewed. Therefore, transformation of the data is necessary in order to perform most statistical analyses, which require the data to be normally distributed. A common approach is to log-scale the data, as it has been observed that metabolite concentrations are more often close to log-normal distributions than to normal distributions. However, other options are available for data pre-processing.(Suhre et al., 2011)

Univariate analysis methods are often performed initially, in order to evaluate the basic relationships between each metabolite and the phenotype of interest.(Barnes et al.,

2016b) However, more complex analyses that consider important covariates and possible interactions are necessary in order to comprehensively analyze the data. The metabolomic data obtained from biological samples is often very complex with the presence of correlations between features from the same metabolite and correlations between metabolites from the same pathway. Also, the effect of potential confounding variables like gender, diet, or body mass index is not taken into account by univariate methods, increasing the probability of obtaining false positive or false negative results.(Alonso et al., 2015)

Another approach is to evaluate the relationship between a group of metabolites, and thus analyze metabolomic features simultaneously. In this case, both unsupervised and supervised techniques are utilized.

Unsupervised techniques do not use any phenotypic classifications that are specific to the dataset, which means that, for example, in a study comparing samples from patients with a certain disease with a control group, with this approach one does not inform the software which samples belong to each group.(Barnes et al., 2016b) This provides an effective way to detect data patterns that are correlated with biological variables.(Alonso et al., 2015) One of the most commonly used unsupervised techniques is principal component analysis (PCA) – Figure 3. PCA is based on the linear transformation of the metabolic features into a set of linearly uncorrelated (i.e., orthogonal) variables known as principal components, which can be used as independent variables. By plotting the scores (the weighted sum of the contribution of each metabolite to a principal component) of these components, it is possible to find if a group of samples is distinct from one another. This decomposition method maximizes the variance explained by the first component, while the subsequent components explain increasingly reduced amounts of variance. The first principal components usually capture most of the variability in the dataset. PCA is also used in metabolomics studies to assess data quality, since it can identify sample outliers or reveal hidden biases in the study.(Yin et al., 2013)

In supervised techniques, the phenotypic information is used in conjunction with the metabolomic data. Using the same example described above, in the study comparing samples from patients with a certain disease with a control group, with this approach one would inform the software which samples belong to each group. One of the most commonly performed techniques is partial least squares (PLS). Unlike PCA, PLS does not maximize the explained dataset variance but rather the covariance between the variable of interest and the metabolomics data. Therefore, the feature coefficients (loadings) of PLS components represent a measure of how much a feature contributes to the discrimination of the different sample groups.(Alonso et al., 2015) The major disadvantage of this approach is that some metabolic features that are not correlated with the variable of interest can actually

influence the results and are missed. Orthogonal PLS is a derivation of PLS and has been developed to deal with this limitation.(Bujak et al., 2016)

Supervised techniques, such as partial PLS-discriminant analysis (PLS-DA, Figure 4), are usually preferred to identify new metabolomic biomarkers. Their usefulness, however, must be evaluated, as a significant difference in the average levels of metabolites between two patient groups does not necessarily mean that the given compound will be a good classifier/biomarker.(Xia et al., 2013) Indeed, PLS-DA has the risk of overestimating group separation, thus its R^2 (degree of fit to the data) and Q^2 (quality assessment) parameters should be assessed. These parameters, however, have limitations and are strongly application dependent. An invalid or irrelevant model can still produce good values, but empirically the acceptable value for Q^2 is $\geq 0.4/0.5$. Highly disparate R^2 and Q^2 values are an indicator of possible model over-fitting.(Szymańska et al., 2012),(Triba et al., 2015) As in most other biomedical fields, receiving operator characteristic (ROC) curve analysis is generally considered a standard method for performance assessment.(Obuchowski et al., 2004) A ROC curve is a non-parametric (i.e. not dependent on data normality) measure of biomarker utility,(Xia et al., 2013) that compares specificity against sensitivity according to a specific decision boundary – Figure 5. They are usually summarized with the area under the curve (AUC), which gives the probability that a classifier will rank a randomly chosen positive sample higher than a randomly chosen negative one. A rough guide for assessing the utility of a biomarker based on its AUC is as follows: 0.9–1.0 = excellent; 0.8–0.9 = good; 0.7–0.8 = fair; 0.6–0.7 = poor; 0.5–0.6 = fail.(Xia et al., 2013) Typically biomarker discovery studies are relatively small ($n < 100$) when compared to the size of the proposed target population (potentially millions of subjects). As such, any performance measure is a sample approximation to the (unmeasurable) performance of the biomarker applied to the target population as a whole. Therefore, confidence intervals (CIs) should always be reported.

It is also imperative that, regardless of the reported predictive indices, the performance of any biomarker is validated. The easiest approach for cross-validation is to split the dataset into two parts, the training set and the validation set. The model optimization should be performed on the training subset, and then model performance is assessed on the validation set. Several rounds should be performed.(Xia et al., 2013) However, the most robust measure of validation is replication in an entirely independent cohort. Following this, targeted metabolomics and studies to assess the biological mechanisms is also recommended.

4.2 Sample size and power

In research, sample size determination is a critical part of study design,(Chi et al.,

2014) and it is determined utilizing statistical power calculations. Power is the probability of rejecting the null hypothesis when one is truly there.(Billoir et al., 2015) In medical studies, researchers often have to balance sufficient statistical with the other costs involved in a project. If a study is underpowered, the risk is that important findings are missed increases, thus resulting in a waste of time and money. Alternatively, if a study is oversized, there overall cost of the study increases.

In metabolomic studies, many factors complicate the sample size determination, thus requiring adapted tools. The metabolome is considered to be more diverse and thus more complex than other ensembles, and metabolic data sets are characterized by strong correlations between variables. Multiple signals can belong to the same metabolites, and metabolic connections can exist along physiological pathways.(Blaise et al., 2010) Metabolites do not operate in isolation but through a complex network of interactions. Most of the conventional methods developed for sample size determination are based on the principle of variable independence, which is obviously not appropriate for metabolomic studies.(Billoir et al., 2015) Finally, like the remaining omics, in metabolomics we also have to face constraints connected to multiple hypothesis testing, as discussed below.

A recent report by the training workshop group on metabolomics, supported by the NIH Common Fund Program in Metabolomics, has highlighted a few general points to consider.(Barnes et al., 2016a) According to these authors, for studies with laboratory animals on controlled diets, a sample size of 6–12 animals may be adequate, although if female animals undergoing estrus cycling are used, they should be studied during the same point in the estrus cycle. Controlled clinical studies where subjects provide multiple samples or where the subjects are carefully matched may be able to be carried out with as few as 10–20 patients, but this will depend on the variance of the disease traits, drug response or that which is introduced by an interventional procedure. These sample numbers ($n = 3–20$) are suitable for generating preliminary and/or pilot data. For epidemiological studies, where the samples are collected from a general population, often over long periods of time, variance is a substantial issue and may require patient numbers in the thousands.(Barnes et al., 2016a) In the last few years, important research has addressed the challenge of merging data from different large scale studies and biobanks.(Chi et al., 2014),(Dane et al., 2014; Dunn et al., 2011a)

Recently, online platforms, such as MetaboAnalyst 3.0(Xia et al., 2015) or metaX,(Wen et al., 2017) developed modules that enable a precise sample size estimation and power analysis for designing metabolomic studies. In both cases, the available software relies on the Bioconductor Package SSPA that was originally developed for genomic data.(van Iterson et al., 2009) This method requires the use of pilot data. Briefly, users first need to upload their pilot metabolomic data and perform the conventional data processing

and normalization steps. Several diagnostic plots are then presented to allow users to check whether the test statistics follow an approximately normal distribution, and whether there are relatively a large number of P values that are close to zero (i.e. the effect indeed exists). When these assumptions are reasonably met, users can proceed to estimate the statistical power with regard to different sample sizes.

Considering that pilot data is often not available, another option is MetSizeR,(Nyamundanda et al., 2013) which is based on the idea that the method for selecting sample size firmly depends on the type of data analysis the researcher intends to employ. In a situation where experimental pilot data are not available, pseudo-metabolomic data can be simulated from a statistical model. The specific statistical model from which the pseudo-metabolomic data are simulated depends on the type of statistical analysis that the metabolomic scientist intends to use (such as, for example, principal component analysis). The main criticism of this approach is that experimental conditions (including sample preparation, storage, data acquisition) should be identical in the simulated data and the planned experiments, which is difficult to account for. Therefore, some authors argue that pilot studies might be inevitable despite their cost, and that inadequate sample size estimations would raise more ethical issues and costs than a properly designed pilot study.(Billoir et al., 2015)

4.3 Multiple hypothesis testing

Like the remaining omics sciences, owing to high throughput, metabolomics deals with multiple hypothesis testing concerns, which increases the risk of false discovery - type I error, false positives. Numerous methods have been developed to control for this in the genomics and transcriptomics fields. The most well established are family-wise error risk (FWER) controls, such as the Bonferroni correction; and false discovery rate (FDR) measurements, such as the Benjamini-type corrections.(Billoir et al., 2015) The FWER estimates the number of variables associated with a true null hypothesis and that are proposed as significant by any given statistical test. The FDR controls the rate at which variables identified as significant by a given test are in fact associated with a true null hypothesis.(Billoir et al., 2015) The FDR correction of the p-value results in a q value.(Barnes et al., 2016b)

In metabolomics, the optimal method is still under debate. However, in general, it is recognized that the FWER corrections are too conservative, and FDR measurements are more suited and thus are becoming widely accepted.(Billoir et al., 2015),(Barnes et al., 2016b),(Alonso et al., 2015) FDR is a less stringent, multiple testing correction that results in fewer features/metabolites as false negatives.(Barnes et al., 2016b)

5. Metabolomics applied to the study of the retina and retinal diseases

Metabolomics has been applied by different groups to the study of normal vitreous and retina, as well as to the study of several pathologic conditions. Due to the versatility of metabolomics, these include: clinical applications aiming to identify biomarkers of retinal diseases; attempts to identify novel mechanisms behind the development of certain conditions, in order to discover new potential targets for future research; and clarification of mechanisms identified by other research techniques.

In this section, we critically review relevant work performed in this field (normal and pathology). Table 1 summarizes data on the study design of selected literature applying metabolomics to the study of retinal diseases.

5.1 Normal retina

Understanding the classes of common metabolites that can be expected in normal retina tissue is important, as it serves as baseline knowledge to recognize and comprehend pathological states. By generating a complete metabolomic profile, we can increase our understanding of the potentially multifaceted roles of the different molecules in regulating and maintaining retinal development, health, and function.

Using GC-MS and LC-MS, Du et al.(Du et al., 2016) assessed the metabolomic profile of normal whole mouse retina tissue. Targeted metabolomics of 171 metabolites was performed, and data were obtained for 114 of them. These included metabolites involved in glucose metabolism (anabolism and catabolism), tricarboxylic acid cycle (TCA) cycle, amino acids, nucleotides and their metabolites, tryptophan cycle metabolites, vitamins, and a small number of sugars and lipids/ fatty acids. Tan et al.(Shi Z. Tan et al., 2016) studied the neurosensory rat retinal metabolome, and compared it with the metabolite composition of the remaining rat ocular tissues (cornea, lens and vitreous). Interestingly, the authors found that the retina displayed the most unique profile of identified metabolites, with 655 detected only in this tissue. In total, 21 metabolites were identified in rat retina tissue with GC-MS and 1942 with UHPLC-MS, belonging to many different classes. Importantly, other groups described that the rat retinal metabolome varies with sex (male vs female), mostly in terms of glycerophospholipids, biogenic amines and amino acids metabolites.(de la Barca et al., 2017) This is important for the design of future studies using animal retina tissue.

Imaging MS (MALDI-FTICR-MS) of retina tissue has also been described.(Sun et al., 2014) Using adult porcine eyes, Sun et al. were able to generate segmentation maps, which

were then used to identify areas in which similar spectra occurred across the tissue samples. Twenty-three different metabolites were identified in situ, including nucleotides, glucose-6-phosphate and other metabolites belonging to the central carbon metabolism pathway, and lipids, among others. This was the first study to utilize FTICR-MS, but prior studies with MALDI-TOF had described distributions of different phospholipids and fatty acids in the different retinal layers.(Ly et al., 2015; Zemski Berry et al., 2014)

In addition to the characterization of the global metabolomic profile of the retina, metabolomics has also contributed to the understanding of retinal physiology. The retina has an extremely complex anatomy and physiology, and its main function is to transduce light stimuli into chemical signals through the process of phototransduction.(Luo et al., 2008) This process requires high amounts of energy.(Wong-Riley, 2010) In the outer retina, where the photoreceptors are located, the consumption of oxygen, as well as of glucose, is higher in the dark than in the light;(Linton et al., 2010) in the inner retina, their consumption seems to be more independent of light exposure.(Lau and Linsenmeier, 2012) This happens because, in response to light stimulation, photoreceptors hyperpolarize, and cease neurotransmitter release, thereby decreasing their metabolic demands.(Wong-Riley, 2010)

Du et al.(Du et al., 2016) compared the levels of metabolites from dark-adapted mouse retinas to retinas from mice exposed to light. Their results revealed that with illumination, among other changes, the levels of cGMP were depleted by 55%, probably due to increased hydrolysis by phosphodiesterases; and that inosine monophosphate (IMP) accumulates, but most other purine and pyrimidine metabolites, which seem to be derived from photoreceptors, are depleted. The authors suggested that the observed increase in nucleotide levels in darkness may be linked to: degradation of RNA; accumulation of products from cGMP degradation (such as 5'-GMP) that inhibit *de novo* purine synthesis; or block of purine synthesis via the salvage pathway. The influence of illumination on nucleotide metabolites was a new observation that may have important implications for the study of retinal diseases, namely for understanding why retinas are uniquely sensitive to certain enzyme deficiencies and not to others.

Imaging MS of adult porcine retina tissue(Sun et al., 2014) also showed a number of notable differences in the distribution profiles of the detected metabolites between light and dark-treated tissue samples, particularly those from the glycolysis pathway. As noted above, the metabolism of the outer retina is higher in the dark and reduced with light,(Wong-Riley, 2010) which seems to be confirmed by this metabolomic technique. With light, the authors described a shift of glycolysis' products, such as fructose 1,6 bisphosphate (F1,6BP; a product of glycolysis) and citrate, to the inner retina, while glucose 6 phosphate (G6P) was detected at high intensities both in the inner and outer retina. This is probably due to a slowing of glycolytic activity in the outer retina. The outer retina is avascular and is nourished

by the choroid, which is not altered by light stimulation. Therefore, while the delivery rate of glucose and glucose phosphorylation remains the same as in dark conditions, decreased glycolytic activity would result in decreased levels of downstream metabolites following exposure to light. In general, there were also relatively higher amounts of all metabolites under dark conditions, which probably reflects the function of photoreceptors and their specialized metabolic requirements.(Sun et al., 2014) Understanding the distribution of metabolites in the retina and their differences in light and dark conditions might be important to understand retinal diseases.

Interestingly, De La Barca et al.(de la Barca et al., 2017) recently studied the effect of light stress in the retina metabolome. This was based on the work showing that the mechanisms of light preconditioning (pre-exposure to moderate light before intense light) remained unknown, even though they seemed to have a protective effect. The authors observed that light stimulation induced changes in lipid and amino acid metabolism, with a likely involvement of nitric oxide-related signaling pathways.

With aging, the metabolomic profile of the retina may also change. Using targeted MS applied to an aging mouse model, Hopiavuori et al.(Hopiavuori et al., 2017) studied the changes in whole retina and brain composition of the three major glycerophospholipid classes: phosphatidylcholine (PC), phosphatidylethanolamine (PE) and phosphatidylserine (PS). The authors described that retinal PC contained detectable levels of very-long chain polyunsaturated fatty acids (PUFA), which were not observed in brain tissue, and remained constant with age. However, like the brain, an age-related reduction of PE and PS, as well as some other PCs, was observed in the retina. The authors hypothesized that these age-related changes may have profound effects on synaptic function and cognitive ability. In the same study, it was also described that the retina is unique because PC, PS and PE contain a greater amount of di-PUFA species than the brain, and that plasmalogens (PE) are present but in lower levels. Plasmalogens are important for membrane biophysical properties and neurotransmission, as well as for protection in response to cellular oxidative stress. Gordon et al. performed a mini-review proposing potential targets for lipidomics studies of retina tissue, namely to better understand the mechanisms of inflammation, neuroprotection and nerve regeneration.(Gordon and Bazan, 2013)

5.2 Normal vitreous

The vitreous is the largest structure of the eye, occupying the posterior segment, between the lens and the retina. Although in forensic science the vitreous has long been considered crucial in identifying certain causes of death and to estimate the time of death,(Zilg et al., 2015)(Boulagnon et al., 2011b) in ophthalmology the vitreous was

considered relatively irrelevant until recently. This has changed dramatically in the last few decades, with the vitreous being recognized as an important factor in ocular health and disease, including in the pathogenesis of retinal detachment and macular hole formation, and of diabetic retinopathy.(Holekamp, 2010) In addition to its role in maintaining a normal interface with the retina, the vitreous is also now thought to be involved in normal oxygen metabolism and consumption. Shui et al.(Shui et al., 2009) suggested that the vitreous might metabolize the oxygen diffused from the retina into ascorbate, thus protecting the lens and trabecular meshwork from oxidative stress. This function seems to deteriorate with vitreous age-related liquefaction. The ability of the vitreous to regulate intra-ocular oxygen tension has also been hypothesized to affect VEGF-mediated diseases. However, the data in terms of clinical relevance remain controversial.(Cuilla et al., 2015; Singh et al., 2017)

Using a ¹H-NMR untargeted approach, Locci et al.(Locci et al., 2014) provided interesting inputs into oxygen vitreous metabolism. The authors used vitreous samples from goat, and studied the vitreous gel as a whole, as well as four distinct areas – cortical, core, and superior and inferior basal vitreous. A unique metabolomic signature was observed for each area. The vitreous base (basal vitreous adjacent to the lens and the trabecular meshwork) was characterized by the presence of branched-chain amino acids (BCAA), betaine, alanine, lysine, myo-inositol and ascorbate. The presence of ascorbate in this area is in agreement with the theory that this molecule has a differential expression in the vitreous, protecting the lens and trabecular meshwork from oxidative stress.(Shui et al., 2009) Betaine and myo-inositol probably serve as osmo-regulators, which is important to maintain retinal structure and function. BCAA may represent an alternative energetic source to glucose, which is critical in areas with higher metabolic demands, such as the cortex.(Locci et al., 2014)

In the cortical area, the discriminating metabolites included glutamine, choline and its derivatives, N-acetyl groups, creatine, and glycerol. However, the most abundant metabolite was lactate.(Locci et al., 2014) This suggests that the cortex is the most metabolically active area, relying on a fast glucose-driven metabolic response and its anaerobic pathway since the lactate is the product of anaerobic glycolysis within the eye, when there is limited availability of oxygen. Rucker et al.(Rucker et al., 2003) also described that lactate was the dominant resonance in the human vitreous spectra, using proton magnetic resonance spectroscopy; the authors suggested that lactate could be used as a molecular marker to evaluate retinal and optic nerve metabolism.

The presence of glutamine points to a role of cortical vitreous in preventing neurotoxicity. Glutamate is the main neurotransmitter in the retina, and its toxicity is avoided by converting it into glutamine.(Zeng et al., 2010) The vitreous core revealed the presence of glucose, acetate and scyllo-inositol;(Locci et al., 2014) this led the authors to hypothesize

that this is due to a passive diffusion of these energetic molecules through the vitreous to make them available for the more active areas near the retina.

Despite the evidence suggesting metabolic interactions between the vitreous and the retina, Tan et al.(Shi Z. Tan et al., 2016) described using a rat model, that of the metabolites identified in the vitreous using MS, only a small percentage (1.6%) were exclusively found in the retina and not in other tissues. The authors suggested that the metabolic exchange/movement between the cornea and aqueous, and the lens with vitreous and aqueous may explain the similarities between the metabolites found in the lens, vitreous and cornea. However, due to the posterior bulk flow of water from the vitreous through the retina,(Zeng et al., 2010) the anterior movement of small molecules from the retina into the vitreous might be inhibited, thus resulting in the vitreous metabolome not reflecting that of the retina. Therefore, even though vitreous has been used as the surrogate for analyzing molecular changes taking place in the retina, this might not always be appropriate, especially in physiological states. In some pathological states, where there is increased permeability of the retinal vessels or retinal pigment epithelium, vitreous analysis may be of value.(Shi Z. Tan et al., 2016) Other authors argue however, that exactly because of the existence of the blood-retinal barrier, the vitreous can reflect the intraocular environment effectively.(Yu et al., 2015)

Importantly, most of the described findings for normal metabolomic vitreous composition refer to animal models and they seem to vary among species. For example, Mains et al.(Mains et al., 2012) observed clear differences in the metabolomic profiles of vitreous samples from sheep, rabbits and pigs. These were primarily related to the content of DNA and RNA-related metabolites, as well as metabolites associated with the diet.

5.3 Diabetic retinopathy

Diabetic retinopathy (DR) affects 93 million individuals world-wide, and of those, 5 million are completely blind.(Stem and Gardner, 2013) Irreversible vision loss occurs in mid-to late-stages of DR as a result of either macular edema (due to disruption of the blood-retina-barrier) or neovascularization (due to ischemia). Current therapies that target vascular complications are only effective in 25-50% of DR patients,(Abcouwer and Gardner, 2014) hence there is a real need for new therapies. Metabolic disturbances are a known component in the pathogenesis of diabetes. Thus, metabolomics analysis of human samples may shed light on the mechanisms of DR and identify potential therapeutic targets.

Two studies have used metabolomics analyses on vitreous humor from DR patients, to identify biomarkers of the disease.(Barba et al., 2010)(Paris et al., 2016) Barba and colleagues(Barba et al., 2010) analyzed vitreous samples from 22 type 1 diabetic patients

and 22 controls with macular hole (MH) using an ¹H-NMR-based approach. Through partial least square-discriminant analysis (PLS-DA) the authors were able to correctly classify patients and controls based on metabolomics patterns with a sensitivity of 86% and a specificity of 81%. Notably, they found that acetate, glucose, sorbitol and mannitol levels were elevated in the vitreous of PDR patients. In contrast, galactitol and ascorbic acid levels were significantly lower in the vitreous of PDR patients when compared to control. Paris et al. (Paris et al., 2016) used global metabolomics to both identify proliferative DR (PDR) biomarkers and to confirm the relevance of the rodent model of oxygen-induced retinopathy (OIR) as a model of PDR. For their PDR vitreous studies, the authors used two cohorts. Firstly, untargeted metabolomics, was done on a cohort of 9 PDR vitreous samples and 11 non-diabetic controls. Results from this analysis were then validated using targeted metabolomics on a second cohort. In their studies, 129 metabolites were found to be dysregulated. These included allantoin, glutamate, lysine, arginine, N-acetylaspartate, iditol, glycerate and N-acetylglutamate. Validation with targeted analysis confirmed that arginine and allantoin levels are elevated in the vitreous of PDR patients. Next, to confirm the relevance of OIR as a model of PDR, global metabolomics was performed on mouse retinas. Among other dysregulated metabolites, arginine was also increased in OIR retinas, when compared to controls, similar to what is observed in PDR samples.

As discussed, factors limiting the usefulness of using vitreous metabolomics, are the surgical procedure to collect vitreous (vitrectomy), which limits choice and availability of control samples, and the relatively small volume (a maximum of 1ml) obtained. In contrast, plasma samples are easily collected and in larger volumes. Li and colleagues (Li et al., 2011) successfully used metabolomics analysis of plasma samples to stage DR disease progression according to both Western and Chinese medicine standards and to identify potential biomarkers. In their studies, 89 type 2 diabetic patients with or without DR and 30 non-diabetic controls were used. Through orthogonal signal correction-partial least-squares discriminant analysis (OSC-PLS-DA), the authors were able to segregate the diabetic samples into three stages: pre-clinical DR, non-proliferative DR and proliferative DR. They were also able to segregate these samples into Yang deficiency and non-Yang deficiency, the two-stages of DR according to Chinese medicine. The authors identified 8 metabolites as potential biomarkers for DR, according to Western medicine. These included, β -hydroxybutyric acid, trans-deic acid, linoleic acid and arachidonic acid. Regarding Chinese medicine, a significant decrease in glycerol levels was found in Yang deficiency when compared do non-Yang deficiency.

5.4 Rhegmatogenous retinal detachment

Rhegmatogenous retinal detachment (RRD) is an important cause of vision loss.(D'Amico, 2008) afflicting up to 17.9 persons per 100,000 a year.(Laatikainen et al., 1985; Mitry et al., 2010; Rowe et al., 1999; Törnquist et al., 1987; Wilkes et al., 1982) Among the potential complications of RRD, the development of proliferative vitreoretinopathy (PVR) is the most common and can lead to irreversible vision loss.(Tseng et al., 2004),(Pastor et al., 2016) PVR is an irregular scarring process, characterized by the growth of membranes on both surfaces of a detached retina, and on the posterior surface of the vitreous.(Ciprian, n.d.) Despite the identification of risk factors for the development of RRD, and the recognized role of cellular proliferation, the pathogenesis of this condition remains largely unknown. Additionally, even though several attempts have been made to develop drugs to halt the progression and development of PVR, they have not been successful in humans, and currently there is no accepted treatment besides surgery.(Pastor et al., 2016) There is clearly an unmet need to better understand the mechanisms of this disease and to identify novel potential treatment targets.(Pastor et al., 2016)

Metabolomics has been used as an approach to better understand these mechanisms. Li et al.(Li et al., 2014) compared the metabolomic profile of human vitreous samples from patients with RRD, with those from patients with recurrent retinal detachment and PVR, along with control specimens from donor eyes. A clear metabolomic separation was observed between the 3 groups, with 31 distinguishing metabolites identified. Eleven metabolites were significantly different between the eyes with RRD and PVR. The findings were interpreted as a dysregulation of pathways related to inflammation, proliferation and energy consumption. Most of the identified metabolites were linked to inflammation, including L-carnitine, which was decreased. Interestingly, the decrease in L-carnitine was significantly more pronounced in eyes with simple RRD than in eyes with PVR. Since L-carnitine inhibits inflammation, this suggests that inflammation is more pronounced in eyes with RRD. Conversely, in eyes with PVR, proliferation-related metabolites seem to be more prominent, including ascorbate and valine, which have been linked to fibroblast proliferation. However, another metabolite associated with proliferation, urea, was decreased in PVR which might represent a downregulation to inhibit proliferation. In the same study, an increase in citrate, succinate and d-glucuronolactone was observed in both RRD and PVR eyes, suggesting abnormalities in energy metabolism, namely in the TCA cycle. This study has important limitations, namely a very small sample size (8 patients with RRD, 7 with PVR and 6 normal) and the lack of a validation cohort. However, it suggests the potential role of metabolomics in delineating the pathophysiology of PVR. The authors did not assess if the inclusion of metabolomics data on clinical predictive models can improve their accuracy, which would be interesting to perform as clinical models alone do not provide sufficient predictive power to identify patients at high risk of PVR.(Pastor et al., 2016)

Another group focused on RRD associated with choroidal detachment, another important cause of retinal detachment repair failure, whose pathogenesis remains to be understood.(Yu et al., 2015) The authors compared the metabolomic profile of human vitreous samples obtained from patients with isolated RRD, with samples from patients with RRD and simultaneous choroidal detachment (RRDCD). In both groups, the mean time from diagnosis was 4 days. Both on PCA and PLS-DA the authors observed a separation between RRD and RRDCD profiles, which included 265 metabolites, but only 24 were identified. The authors acknowledged that the many unidentified metabolites represents a limitation of their work, as it is likely that metabolomic changes and pathways were missed. Interestingly, most of the metabolites and pathways identified in this study were similar to those identified by Li et al.(Li et al., 2014) distinguishing RRD and PVR, with most metabolites related to the urea and TCA cycle. In eyes with RRDCD, there were increased levels of TCA metabolites, suggesting a higher level of energy metabolism, as well as proliferation-related and inflammation-related metabolites (even though both study groups had the same grade of PVR).

5.5 Age-related macular degeneration

Age-related macular degeneration (AMD) is the leading cause of blindness in people older than 50 years in developed countries, and the 3rd worldwide.(Wong et al., 2014) Approximately 90% of patients with AMD have early or intermediate forms (Figure 6), which may progress to advanced disease, in the form of either geographic atrophy and/or neovascular AMD (also known as “wet AMD”).(Sobrin and Seddon, 2013),(Yonekawa et al., 2015) AMD is usually asymptomatic in its early stages and diagnosed only on routine eye examination, thus often remaining undetected until it is more advanced with loss of vision. It is important to find tools to detect AMD earlier, and develop treatments to slow progression and vision loss. Ideally, a screening test for AMD should be easily performed and should be able to predict disease progression. Serological biomarkers have been studied, mostly related to biomarkers of inflammation(Hong et al., n.d.; Klein et al., 2014b; Mitta et al., 2013; Uğurlu et al., 2013) or lipid levels,(Chakravarthy et al., 2010) as both appear to play a role in AMD pathogenesis. However, to date results have been inconsistent,(Klein et al., 2014a) probably reflecting disease heterogeneity or pathophysiological complexity.

Since metabolomics is known to closely resemble complex, multifactorial diseases, our group hypothesized that it could be a novel appropriate approach to identify biomarkers of AMD. Osborn et al(Osborn et al., 2013) pioneered the application of metabolomics to the study of AMD, by comparing the metabolomic profile of plasma samples of patients with neovascular AMD with controls. Using LC-MS, the authors described 94 metabolites

separating the two groups, 86 of them identified as known metabolites. However, they acknowledged that several nucleotides, sugars and lipids, among others were undetectable in their study. Among the 94 metabolites identified, 40 of them were consistently different between patients with neovascular AMD and controls regardless of the statistical approach used. The most significant and relevant metabolites for the separation between the groups were peptides and modified amino acids (increased in patients with neovascular AMD), natural products and environmental agents. Other less prominent features included bile acids (decreased in patients with neovascular AMD) and vitamin D-related metabolites (decreased in patients with neovascular AMD). The authors also performed pathway analysis, and described that the identified metabolites mapped to 17 pathways, mostly related to carbohydrate, amino acid, and coenzyme metabolites required for nitrogen balance and energy metabolism.

Our group was the first to study the metabolomic profile of the different stages of AMD (early, intermediate and late), which we compared to control subjects older than 50 years and with normal macula. Our initial work (Lains et al., 2017a) was performed with NMR metabolomics, based on the principle that this can be an appropriate technique for an initial untargeted approach. As discussed before, NMR offers high reproducibility, simple sample handling and the possibility of sample reuse (Psychogios et al., 2011a), (Suhre and Gieger, 2012). In this study, we included a total of 396 subjects, 61% (n=243) from Coimbra, Portugal (42 controls and 201 patients with AMD) and the remaining from Boston, United States (n=153) (40 controls and 113 patients with AMD). Data from both cohorts were analyzed separately. Using variable selection (a technique that enables to filter off random variability unrelated to sample classes (Diaz et al., 2013)), it was possible to observe a separation between multiple AMD stages for the Boston cohort, and between extreme stages (late AMD vs controls and late AMD vs early AMD) for the Coimbra cohort. This separation was mostly due to amino acids and organic acids, dimethyl sulfone, lipid and protein moieties. The potential confounding effects of gender, smoking history and age on these results were found to be negligible. Interestingly, the metabolomic fingerprints of AMD in the two cohorts presented both similarities and differences. We observed similarities in the variations of histidine, unsaturated fatty acids and protein levels, which suggests that such variations may be a universal reflection of the disease, and, therefore, with potential value in contributing to the current knowledge of the pathogenesis of AMD. On the other hand, cohort differences in relation to variations in particular compounds may reflect the potential importance of local diet and lifestyle effects on the suggested AMD metabolic fingerprints. We also observed a number of small metabolite variations potentially differentiating controls from early AMD. This is particularly relevant as these might represent specific signals to distinguish disease from non-disease status.

As discussed, MS has a much higher sensitivity than NMR, enabling the measurement of a broader range of metabolites. Therefore, we continued our investigations using MS metabolomics. In the Boston cohort, (L. Laíns et al., 2017b) we observed that after controlling for age, gender, BMI and smoking status, 87 metabolites differed significantly between AMD cases and controls. Indeed, a summary score based on these 87 metabolites increased the ability to predict AMD cases, relative to clinical covariates alone. Of these metabolites, over half (48 metabolites) also differed significantly across AMD severity stages. Similar to what was described by Osborn et al., (Osborn et al., 2013) and what we observed using NMR, we identified significantly increased levels of metabolites linked to dipeptides and amino acids in patients with AMD, including a significant role for alanine and aspartate metabolism. However, the majority of the identified significant metabolites were involved in lipid metabolism, in particular glycerophospholipid metabolism – Figure 7. Glycerophospholipids are a major component of cell membranes and are especially enriched in neural membranes. Indeed, changes in glycerophospholipids and their metabolism have been extensively investigated in neurodegeneration and in several chronic neurological diseases, (Farooqui et al., 2000) (Kosicek and Hecimovic, 2013) and metabolomics is currently considered a promising tool to identify valid biomarkers and new targets in Alzheimer disease. (Mapstone et al., 2017; Proitsi et al., 2017; Whiley et al., 2014) This is relevant because AMD is a neurodegenerative disease of the retina and shares important features and pathologic mechanisms with Alzheimer disease. (Ernilov and Nesterova, 2016; Kaarniranta et al., 2011; Ohno-Matsui, 2011; Sivak, 2013) In Alzheimer disease, glycerophospholipids have been shown to be reduced, and to play a central role in its pathogenesis. (Farooqui, 2012), (Frisardi et al., 2011) Using MS metabolomics and lipidomics, Mapstone et al. (Mapstone et al., 2014) identified a panel of ten plasma lipids, most of them phosphatidylcholines (a class of glycerophospholipids), that predicted with high accuracy conversion to mild cognitive impairment and to frank Alzheimer disease in elderly subjects.

Interestingly, Li et al. (Li et al., 2016) also described a significant role of glycerophospholipids' plasma metabolites in patients with polypoidal choroidal vasculopathy (PCV) (a subtype of wet AMD), as compared to controls (n= 21 and 19, respectively). Importantly, the authors focused only on lipid metabolites (lipidomics), assessed with untargeted MS. Their results revealed that the glycerophospholipid pathway was one of the most significant pathways involved in the separation of their study groups. However, the key indicator seemed to be platelet activating factor (PAF), which was significantly higher in patients with PCV. As the authors point out, PAF is an endogenous bioactive phospholipid that plays an important role in the promotion of angiogenesis.

Using a aged-mouse model, Rowan et al.(Rowan et al., 2017) found further evidence of the importance of lipid metabolites. The authors performed an integrative assessment of the metabolome (urine and plasma) with the microbiome, to better understand the effect of high-glycemic (HG) *versus* low-glycemic (LG) diets on AMD features, such as photoreceptor cell damage and RPE abnormalities. Plasma metabolomics was assessed by MS and urine metabolomics by NMR. The authors described the identification of 26 metabolites common to both fluids, although the results should be evaluated with the caveat that the two fluids were assessed using two different techniques. The comparison of the plasma and urinary metabolomic profile of mice fed with HG, LG, and switched from HG to LG diets revealed significant differences. Mice with HG diets presented higher levels of lipids and higher retinal damage scores, while mice from the LG diet group presented higher levels of carbohydrates and amino acids, as well as lower retinal damage scores. Additionally, the authors tried to identify metabolites that could be associated with the presence of AMD features, verifying that eight of them, including a phosphatidylcholine and carnitine, enabled a good separation (high area under the curve) between mice with a high retinal damage score and nonaffected animals. In the microbiome, an association was observed with metabolites modulated by the abundance of microbiota, such as serotonin, whose higher levels were associated with less retinal damage. The microbiome composition was different among the three different dietary groups (HG, LG and switch from HG to LG), but interestingly in the mice that were switched from HG to LG, the microbiome was restored to the LG mice. The microbiome of HG mice was enriched in Clostridia and Firmicutes, and both of these were related to a more advanced retinal damage score. These findings led the authors to emphasize the role of diet on AMD pathogenesis. Finally, using analytical techniques to integrate all data, Rowan et al.(Rowan et al., 2017) assessed diet-metabolome-AMD features interactions. These seemed to be mostly driven by a central hub including three lipids, serotonin and lysophosphatidylethanolamine.

The potential role of lipids in the pathophysiologic process of AMD has been proposed by several investigators, but their exact role remains somewhat controversial. Metabolomics may offer additional insights.

5.6 Macular telangiectasia

Macular telangiectasia type 2 (MacTel) is a rare neurodegenerative disease specifically affecting the macular region of the retina, causing progressive central vision loss. It has a late onset, typically presenting between 40-60 years of age.(Charbel Issa et al., 2013) While there is strong evidence for genetic etiology, no causative gene or genes have been identified.

While the clinical manifestations of the disease are primarily restricted to the macular region of the retina, there have been reported associations between MacTel and systemic abnormalities including diabetes, obesity, hypertension and increased BMI.(Charbel Issa et al., 2013) Metabolomic MS analysis was run by the MacTel consortium on patient serum in the hope of identifying systemic metabolite changes that associate with the disease.(Charbel Issa et al., 2013) Fasting serum was collected for 50 MacTel patients and 50 control subjects (matched for age, ethnicity and diabetes). Interestingly, plasma metabolite differences were detected between the MacTel and control cohort. In particular three amino acids - serine, glycine and threonine - were significantly decreased in plasma from MacTel patients. Concurrently, a genome-wide association analysis of MacTel subjects identified disease-associated genetic loci that link to serine and glycine metabolism. This study highlights the application of patient-derived samples, like serum/plasma and possibly cells, to investigate disease-specific questions, even when the disease is rare and samples are not derived directly from the diseased tissue.

5.7 Others

Young et al.(Young et al., 2009) performed one of the first studies applying metabolomics to the study of eye diseases. The authors obtained vitreous humor samples from 42 patients undergoing PPV for several vitreoretinal disorders, thus including a very heterogeneous cohort. Most of the patients had a diagnosis of chronic non-infectious uveitis (n= 20, including panuveitis, pars planitis and Fuch's heterochromic cyclitis) or lens induced uveitis (n= 9). These two groups presented a distinct vitreous metabolome as assessed by three distinct analytical methods. The authors performed a limited assessment of the metabolites responsible for this separation, but these included glucose, oxaloacetate and urea, which were increased in samples from eyes with lens induced uveitis. This is an acute condition, thus being logical to see increased levels of inflammatory metabolites (such as oxaloacetate and urea) as compared to a more chronic process. Importantly, most of these patients were receiving steroids for treatment, which differed between the two groups (lens induced uveitis with topical steroids, while chronic uveitis with oral steroids). This might have introduced an important bias. The authors also did not account for other potential confounding factors.

Loss or reduction of blood flow and/or induction of hypoxia in the retina are thought to be causative or confounding factors in many retinal disorders, including age-related macular degeneration, diabetic retinopathy and glaucoma.(Kurihara et al., 2016; Osborne et al., 2004) Therefore, animal models of reduced blood flow or retinal hypoxia coupled with

metabdomics tools have been used to provide insights into the metabolic signatures that might associate with these retinal diseases.

D'Alessandro et al.(D'Alessandro et al., 2014) used an *ex vivo* mouse model of retinal ischemia to study the consequences of reduced perfusion to the retina, as well as to test the capacity of different peptide therapeutics to recover some of the damage. In their model, the retina was removed and ischemia was induced *ex vivo* by putting the tissue in an air-tight container and adding sodium azide to block mitochondrial oxygen consumption. Untargeted metabolic profiling was used to look at the changes that occur from these treatments compared to controls, as well as the ability of candidate peptides treatment to recover the effects. Metabolite changes of interest arising for the untargeted approach were validated by multiple reaction monitoring (MRM). The *ex vivo* ischemia model leads to extensive cell apoptosis and, not surprisingly, a rapid alteration in the levels of numerous metabolites. Notably, they found metabolites related to oxidative stress, including glutathione, peroxidized lipids and nitric oxide metabolites were all increased due to ischemia with varying levels or rescue by the peptides. Central carbon metabolism was altered with an accumulation of lactate, decreases in glycolytic intermediates and elevation metabolites of the pentose phosphate pathway. They also observed altered levels of purines metabolites, something seen also in the oxygen-induced retinopathy mouse model (OIR).(Paris et al., 2016)

It is well established that ischemia and the total loss of blood supply to the retina results in metabolic dysfunction and photoreceptor death. Interestingly, recent work by Kurihara et al.(Kurihara et al., 2016) has shown that induction of hypoxia signaling alone specifically in the RPE is sufficient to cause substantial photoreceptor dysfunction and death, mirroring features of AMD. The authors used high-resolution untargeted metabdomics to verify a lipid dysregulation in a mouse model of RPE hypoxia signaling. They observed that numerous acylcarnitines were increased in the mouse RPE/choroid complex and this phenotype could be corrected with the deletion of the HIF genes and the prevention of hypoxia signaling.(Kurihara et al., 2016)

Hibernating animals experience dramatically reduced blood flow to their retinas during hibernation, essentially a non-pathological form of ischemia. Metabolic adaptations are used to deal with the reduced blood flow and result in increased resistance to ischemia. Luan et al.(Luan et al., 2018) studied the retinas of hibernating ground squirrels by coupling transcriptome analysis with metabdomics to reveal the metabolic pathways that are altered in the hibernation state. Winter-awake animals were compared to deep torpor (hibernating) animals (6 per group) and untargeted analysis was performed using both GC/MS and LC/MS platforms. The metabdomics data was integrated with transcriptome data and used in pathway analysis. Analysis revealed a shift from carbohydrate metabolism to lipid

oxidation, similar to other tissues and what is expected in a hibernating or fasting state. However, some amino acid levels (including acetylated amino acids) were increased, which appears unique to hibernating retinal metabolism and different than other hibernating tissues.(Luan et al., 2018),(Nelson et al., 2009) Understanding the metabolic adaptations that allow the retina to withstand low blood flow may be informative to treating retina diseases connected to ischemia and/or hypoxia.

To find a potential biomarker for postnatal hypoxia induced brain injury Solberg et al.(Solberg et al., 2013) used a porcine model of hypoxia and examined the retinas as representative neuronal tissue. Five piglets were used in a control and treatment group, and 8 metabolites were identified that surpassed thorough statistical analysis. CDP-choline was identified and further validated and quantified with targeted mass spectrometry as significantly in the hypoxic retinas. Further work will be needed to determine if CDP-choline has value as a biomarker, including testing the levels in plasma.

6. Limitations

The application of metabolomics to the study of retinal diseases, and the studies that have been published to date, have important limitations. These include both limitations specific to the different study designs, and limitations of metabolomics itself.

Of the studies mentioned in this manuscript, only a few(Shi Z. Tan et al., 2016),(Yu et al., 2015),(Li et al., 2014),(Osborn et al., 2013),(Inês Lains et al., 2017) reported un-annotated metabolites (i.e. with no identification available on databases such as HMDB). Un-annotated metabolites are important because if they are associated with disease or normal health, their omission can introduce bias into the reported results. Therefore, they should be described and taken into account in all metabolomic studies. Un-annotated metabolites remain an important problem in metabolomics, since to date no complete characterization of any organismal metabolome has been reported, dramatically contrasting with the genome.(Viant et al., 2017) This is due to several issues, including: the vast heterogeneity of metabolites; their wide variation in concentration and size (for example, of approximately 4000 metabolites in human serum, concentrations range over 11 orders of magnitude with the most abundant metabolites measured at millimolar concentrations, and low abundance metabolites measured at picomolar concentrations(Psychogios et al., 2011b)); and their large number and distinct psychochemical properties (for example, differences in polarity among groups or families of metabolites demand different extraction procedures). Because of the higher sensitivity of MS, this is particularly evident in studies using this analytical approach.(Petras et al., 2017b) Un-annotated metabolites have been

the focus of recent attention, and an international task group is in place to help coordinate metabolome annotation.(Viant et al., 2017) Currently, among the most commonly used public available metabolomic databases are the Human Metabolome Database (<http://www.hmdb.ca/>) and METLIN (<http://metlin.scripps.edu/>), and these are certainly crucial tools to address the challenge of metabolomic annotation.(Kell and Oliver, 2016)

Most studies included in this manuscript provide a detailed description of their methods for sample collection and processing,(Kohler et al., 2016) however, several studies lack quality control samples. This is particularly relevant when large series of samples are analyzed, to control for the analytical systems performance and identify eventual drifts.(Scalbert et al., 2009) Quality control samples are commonly obtained by sample pooling (a pooled sample to represent all the samples to be analyzed),(Barnes et al., 2016a) as performed for example by Li et al.(Li et al., 2014) and Yu et al.,(Yu et al., 2015) or can be achieved by using internal standards from different laboratories.(Hopiavuori et al., 2017) In any case, a laboratory should analyze and report the variation that occurs for repeated analysis of the same sample, for multiple extractions of the same sample on one day, and for multiple extractions of the same sample over a period of time.(Barnes et al., 2016a) Before data analysis, data quality control procedures should also take place, namely to identify and assess the number of metabolites with missing data or undetected levels, to identify outliers, and to analyze the normality of the data.(Kumar et al., 2017) Several techniques are available to deal with these distinct data analysis challenges, and it is crucial to report them.(Di Guida et al., 2016) Unfortunately, in the field of metabolomics applied to retinal diseases very few papers(Sun et al., 2014),(Shi Z. Tan et al., 2016),(Inês Lains et al., 2017) presented their approach to deal with these aspects.

In terms of data analysis, as described in the respective section of this manuscript, it is also important in metabolomics studies, to account for the fact that multiple hypothesis are tested(Hopiavuori et al., 2017),(Shi Z. Tan et al., 2016),(Li et al., 2014),(Yu et al., 2015),(Osborn et al., 2013),(I. Lains et al., 2017a),(de la Barca et al., 2017),(Rowan et al., 2017). Another important concept relates to the requirement of validating metabolomics results, especially if they refer to the identification of potential biomarkers. The ideal approach is to assess an independent cohort,(Monteiro et al., 2013) which despite being sought,(Inês Lains et al., 2017) has not been implemented so far in any of the published studies in the field of retinal diseases. Also, only three studies(Li et al., 2016),(Inês Lains et al., 2017),(Rowan et al., 2017) assessed the performance of their potential metabolomic biomarkers using ROC analysis, which, as mentioned, is the standard method for assessment of biomarkers performance; and only six groups commented on other approaches to validate their results, namely concerning PLS-DA analysis.(Li et al., 2014),(Yu et al., 2015),(Osborn et al., 2013),(I. Lains et al., 2017a),(Locci et al.,

2014),(Young et al., 2009) Importantly, these are mostly cross-sectional association studies, so no causality can be inferred. The observed changes in the metabolomic profiles might be related to causal mechanisms, but may also represent the downstream effect of the metabolomic derangements in the distinct vitreoretinal diseases. To understand the causal roles of metabolites, one should ideally develop prospective studies that allow for future disease risks to be evaluated on the basis of both genetic and metabolic information. This was performed by Rowan et al (Rowan et al., 2017) studying AMD using an animal model. These authors were also the only cited group who assessed the influence of diet in the evaluated metabolomic profiles. In the remaining studies, no assessments have been performed in terms of the potential influence that dietary patterns and genetic profiles may have in the described metabolomic profiles. As stated, all these factors contribute to the overall metabolomic profile and can obscure or enhance differences, thus representing a potential source of bias.(Monteiro et al., 2013)

The inclusion of insufficient sample sizes is also a very important limitation, and is problematic in the application of metabolomics across most medical fields. As described, there is currently no standard method for the determination of sample size when designing a metabolomic experiment,(Blaise et al., 2016; Nyamundanda et al., 2013) but several tools are available for its estimation, and minimum numbers for animal and human studies have been reported.(Barnes et al., 2016a) Our group has published on AMD plasma metabolomics following these recommendations ($n \geq 30$ for each study group),(I. Laíns et al., 2017a)(Inês Laíns et al., 2017) but this is not the case of most of the remaining literature. Indeed, for studies with animal tissue, sample sizes vary between one(Hopiavuori et al., 2017) to seven(S Z Tan et al., 2016) samples per group; and studies with human vitreous samples included as low as eight samples per group.(Li et al., 2014) Collaborative studies, including several institutions from the same country or different countries, are probably the best strategy to overcome this problem, especially for human clinical studies.

In summary, although the potential of the metabolic phenotyping strategy appears obvious, so far, its application to the field of retinal diseases is limited by a lack of well-designed and appropriately powered studies, as well as the lack of validation cohorts.(Holmes et al., 2015) The clinical applicability of metabolomics strongly relies on the quality and accuracy of the acquired data. Study design should be planned in advance, including all crucial steps to ensure the highest data quality and lowest analytical variability. This includes subject/ sample selection, sample collection, sample size, sample handling and storage conditions, preparation and data analysis. Also, new methods should always be evaluated in comparison with the current clinical standards, to ensure that they represent an actual benefit.

7. Future directions

In the last few decades, the field of metabolomics has experienced an exponential growth, and holds great promise to significantly improve diagnosis, provide prognostic information and identify additional therapeutic targets. The potential of this approach for translation to the clinical environment is great. However, as described in this manuscript, the application of metabolomics to the study of vitreoretinal diseases is very limited, and not comparable to what has happened in other medical fields.(Kohler et al., 2016) Clearly, we are still very far from clinical translation. Most studies were hindered by small sample sizes and data analysis constrains. However, we believe that there is a great opportunity for a wider use of metabolomics to further understand the mechanisms of several vitreoretinal diseases, as well as for developing diagnostic and prognostic biomarkers. Indeed, for certain conditions studied, such as AMD, the available results are encouraging, considering the reported biologically plausible metabolites and metabolomic pathways.

One of the new concepts of modern medicine is "precision medicine" or "personalized medicine". According to the Precision Medicine Initiative, it takes into account individual variability in genes, environment and lifestyle for treatment and prevention. This means that differences between individuals are considered, instead of "one-size fits all approach". The goal is that ultimately clinicians can prescribe the right medicine to the right patient at the right time, with maximum efficacy and minimal toxicity, as well as predicting the susceptibility to disease onset among populations.(Sun and Hu, 2016) Metabolomics is one of the most widely applicable areas for the development of precision medicine, as it mirrors genes, environment and lifestyle. For example, metabolomics can help identify disease subtypes and stratify patients with certain conditions. This would be useful for AMD, which is a complex disease with a spectrum of phenotypes and pathways of progression.

Another example, which has also not been explored in vitreoretinal diseases, is pharmacometabolomics/ pharmacometabonomics. Metabolomics is expected to have the ability to identify markers of drug toxicity and efficacy that can accelerate drug discovery and assist to delineate appropriate clinical plans.(Cuperlovic-Culf and Culf, 2016; Tolstikov, 2016) For example, pharmacometabolomics has been used to assess toxicity induced by acetaminophen,(Winnike et al., 2010) as well as to predict efficacy and adverse events of other drugs, such as oral antidiabetics or statins.(Sun and Hu, 2016),(Wishart, 2016; Zhang et al., 2015) This is particularly important considering the global aging of the population. Typically, older patients have more comorbidities and polypharmacy, thus representing a bigger challenge due to the unknown interactions between drugs. Pharmacometabolomics can potentially provide a gateway to stratified medicine, by acting as a screening tool for selecting individuals according to their suitability for treatment with particular drugs.(Jeremy

K Nicholson et al., 2012a) This could be an interesting approach, for example, to study the differences in response to anti-angiogenic treatments, namely why some patients do not respond as opposed to others, and the differences among the different agents; or to study the efficacy of vitamin supplements to halt AMD progression. Metabolomics is used to probe the real-world nature of biochemical functionality and is sensitive to both gene and environmental influences; therefore, it is likely to be more practical than gene-based measurements of response to therapy.(Jeremy K. Nicholson et al., 2012)

One can also speculate that there will be great power in combining data from multiple "omics", (Inouye et al., 2010), (Sun and Hu, 2016) which lead to greater insight and better characterization of complex diseases. To truly understand disease mechanisms, we need to adopt a systems biology approach combining multiple bio-organizational layers, such as the genome, proteome and metabolome. (Holmes et al., 2015) Indeed, with the currently available platforms and options for data analysis, it is possible to analyze wide-ranging metabolomic phenotypes in association with genetic variance, disease-relevant phenotypes and lifestyle and environmental parameters, allowing dissection of the relative influences of these factors. (Suhre and Gieger, 2012) This strategy can allow the visualization of a biological system on a global level. Namely, the so-called metabolome-genome wide association (GWAS) studies are becoming increasingly popular. (Wang et al., 2017) The conventional GWAS studies focus on the association between single nucleotide polymorphisms (SNPs) and disease phenotypes (for example, disease versus non-disease). These require large sample sizes and often do not provide any information on the underlying biological processes. Conversely, metabolome-GWAS studies are more highly powered and, by using metabolomic profiles as intermediate traits, they provide information on the biology of the disease association. This has been demonstrated in several medical fields, including cancer. (Wang et al., 2017) However, these analyses remain in their early stages and clinical utility has yet to be demonstrated. Machine-learning approaches can be a powerful tool to support these and other metabolomics data analysis. (Zhou et al., 2017) Indeed, improvements in technology and computational solutions are still required.

In the future, imaging metabolomics (as described, enabling the study of the distribution of metabolites within a tissue) will also likely play an increasingly important role. (Sun et al., 2014) The retina is a highly specialized tissue, with a complex anatomy. Each layer has a different morphology and function. The ability to assess and obtain qualitative and quantitative metabolomics data *in situ*, preserving this complex anatomy native environments, is of extreme value and can provide new insights into the biological processes at systems biology level, and facilitate the understanding of disease processes and finding of novel biomarkers. This is particularly true if one can integrate these data with

the metabolomic phenotype of easily accessible biofluids, bearing in mind that these represent distinct biological environments, thus the detected biomarkers might differ.

Importantly, to make the most out of metabolomics potential and open new avenues in research and patient care, it is crucial to establish multidisciplinary teams, where clinicians, biostatisticians, bioinformatics, geneticists, and others, work synergistically and capitalize their knowledge in the different required fields. Cross-disciplinary efforts, as well as translational collaborations between academic institutions, pharmaceutical agencies and diagnostic companies are crucial to move forwards.(Kohler et al., 2016)

In conclusion, at present metabolomics is research laboratory-based, and needs to become more practical to be easily implemented in the clinic.(Trivedi et al., 2017) This represents a great challenge for the field of metabolomics in general, and much work lies ahead. For this to happen, one of the most crucial requirements is to standardize and harmonize metabolomic phenotyping and biomarker modeling procedures, and to improve the current publically available databases and promote data sharing.(Holmes et al., 2015)

We envision that metabolomics, and its integration with other omics approaches, will be increasingly applied in the coming years to the study of vitreoretinal diseases. This will lead to increased knowledge on their mechanisms and pathophysiology, the identification of diagnostic and risk-prediction biomarkers, and the assessment of efficacy and toxicity of several drugs. We live in the era of precision medicine, and we are now in a position to develop global systems-biology care for conditions that are characterized by gene–environment interactions. The field of vitreoretinal diseases will certainly benefit from this approach. In this manuscript, we provided tools for a better understanding of metabolomics and its potential in clinical translational research and management of retinal diseases.

References

- Abcouwer, S.F., Gardner, T.W., 2014. Diabetic retinopathy: loss of neuroretinal adaptation to the diabetic metabolic environment. *Ann. N. Y. Acad. Sci.* 1311, 174–190.
<https://doi.org/10.1111/nyas.12412>
- Alonso, A., Marsal, S., Julià, A., 2015. Analytical methods in untargeted metabolomics: state of the art in 2015. *Front. Bioeng. Biotechnol.* 3, 23.
<https://doi.org/10.3389/fbioe.2015.00023>
- Álvarez-Sánchez, B., Priego-Capote, F., Luque de Castro, M.D., 2012. Study of sample preparation for metabolomic profiling of human saliva by liquid chromatography-time of

- flight/mass spectrometry. *J. Chromatogr. A* 1248, 178–81.
<https://doi.org/10.1016/j.chroma.2012.05.029>
- Ammerlaan, W., Trezzi, J.-P., Lescuyer, P., Mathay, C., Hiller, K., Betsou, F., 2014. Method validation for preparing serum and plasma samples from human blood for downstream proteomic, metabolomic, and circulating nucleic acid-based applications. *Biopreserv. Biobank*. 12, 269–80. <https://doi.org/10.1089/bio.2014.0003>
- Barba, I., Garcia-Ramírez, M., Hernández, C., Alonso, M.A., Masmiquel, L., Garcia-Dorado, D., Simó, R., 2010. Metabolic Fingerprints of Proliferative Diabetic Retinopathy: An ¹H-NMR–Based Metabonomic Approach Using Vitreous Humor. *Investig. Ophthalmology Vis. Sci.* 51, 4416. <https://doi.org/10.1167/iops.10-5348>
- Barnes, S., Benton, H.P., Casazza, K., Cooper, S.J., Cui, X., Du, X., Engler, J., Kabarowski, J.H., Li, S., Pathmasiri, W., Prasain, J.K., Renfrow, M.B., Tiwari, H.K., 2016a. Training in metabolomics research. I. Designing the experiment, collecting and extracting samples and generating metabolomics data. *J. Mass Spectrom.* 51, 461–475.
<https://doi.org/10.1002/jms.3782>
- Barnes, S., Benton, H.P., Casazza, K., Cooper, S.J., Cui, X., Du, X., Engler, J., Kabarowski, J.H., Li, S., Pathmasiri, W., Prasain, J.K., Renfrow, M.B., Tiwari, H.K., 2016b. Training in metabolomics research. II. Processing and statistical analysis of metabolomics data, metabolite identification, pathway analysis, applications of metabolomics and its future. *J. Mass Spectrom.* 51, 535–548. <https://doi.org/10.1002/jms.3780>
- Billoir, E., Navratil, V., Blaise, B.J., 2015. Sample size calculation in metabolic phenotyping studies. *Brief. Bioinform.* 16, 813–9. <https://doi.org/10.1093/bib/bbu052>
- Blaise, B.J., Correia, G., Tin, A., Young, J.H., Vergnaud, A.-C., Lewis, M., Pearce, J.T.M., Elliott, P., Nicholson, J.K., Holmes, E., Ebbels, T.M.D., 2016. Power Analysis and Sample Size Determination in Metabolic Phenotyping. *Anal. Chem.* 88, 5179–5188.
<https://doi.org/10.1021/acs.analchem.6b00188>
- Blaise, B.J., Navratil, V., Domange, C., Shintu, L., Dumas, M.-E., Elena-Herrmann, B., Emsley, L., Toulhoat, P., 2010. Two-dimensional statistical recoupling for the identification of perturbed metabolic networks from NMR spectroscopy. *J. Proteome Res.* 9, 4513–20. <https://doi.org/10.1021/pr1002615>
- Boulagnon, C., Garnotel, R., Fomes, P., Gillery, P., 2011a. Post-mortem biochemistry of vitreous humor and glucose metabolism: an update. *Clin. Chem. Lab. Med.* 49, 1265–70. <https://doi.org/10.1515/CCLM.2011.638>
- Boulagnon, C., Garnotel, R., Fomes, P., Gillery, P., 2011b. Post-mortem biochemistry of vitreous humor and glucose metabolism: an update. *Clin. Chem. Lab. Med.* 49, 1265–70. <https://doi.org/10.1515/CCLM.2011.638>
- Bowrey, H.E., Anderson, D.M., Pallitto, P., Gutierrez, D.B., Fan, J., Crouch, R.K., Schey,

- K.L., Ablonczy, Z., 2016. Imaging mass spectrometry of the visual system: Advancing the molecular understanding of retina degenerations. *PROTEOMICS - Clin. Appl.* 10, 391–402. <https://doi.org/10.1002/prca.201500103>
- Buck, A., Balluff, B., Voss, A., Langer, R., Zitzelsberger, H., Aichler, M., Walch, A., 2016. How Suitable is Matrix-Assisted Laser Desorption/Ionization-Time-of-Flight for Metabolite Imaging from Clinical Formalin-Fixed and Paraffin-Embedded Tissue Samples in Comparison to Matrix-Assisted Laser Desorption/Ionization-Fourier Transform Ion Cyclotron Resonance Mass Spectrometry? *Anal. Chem.* 88, 5281–5289. <https://doi.org/10.1021/acs.analchem.6b00460>
- Bujak, R., Dagher-Wojtkowiak, E., Kaliszan, R., Markuszewski, M.J., 2016. PLS-Based and Regularization-Based Methods for the Selection of Relevant Variables in Non-targeted Metabolomics Data. *Front. Mol. Biosci.* 3, 35. <https://doi.org/10.3389/fmolb.2016.00035>
- Cacciatore, S., Zadra, G., Bango, C., Penney, K.L., Tyekucheva, S., Yanes, O., Loda, M., 2017. Metabolic Profiling in Formalin-Fixed and Paraffin-Embedded Prostate Cancer Tissues. *Mol. Cancer Res.* 15, 439–447. <https://doi.org/10.1158/1541-7786.MCR-16-0262>
- Chakravarthy, U., Wong, T.Y., Fletcher, A., Pialt, E., Evans, C., Zlateva, G., Buggage, R., Pleil, A., Mitchell, P., 2010. Clinical risk factors for age-related macular degeneration: a systematic review and meta-analysis. *BMC Ophthalmol.* 10, 31.
- Chan, E.C.Y., Pasikanti, K.K., Nicholson, J.K., 2011. Global urinary metabolic profiling procedures using gas chromatography/mass spectrometry. *Nat. Protoc.* 6, 1483–1499. <https://doi.org/10.1038/nprot.2011.375>
- Charbel Issa, P., Gillies, M.C., Chew, E.Y., Bird, A.C., Heeren, T.F.C., Peto, T., Holz, F.G., Scholl, H.P.N., 2013. Macular telangiectasia type 2. *Prog. Retin. Eye Res.* 34, 49–77. <https://doi.org/10.1016/J.PRETEYERES.2012.11.002>
- Chen, L., Zhou, L., Chan, E.C.Y., Neo, J., Beuerman, R.W., 2011. Characterization of the human tear metabolome by LC-MS/MS. *J. Proteome Res.* 10, 4876–82. <https://doi.org/10.1021/pr2004874>
- Chetwynd, A.J., Dunn, W.B., Rodriguez-Blanco, G., 2017. Collection and Preparation of Clinical Samples for Metabolomics, in: *Advances in Experimental Medicine and Biology*. pp. 19–44. https://doi.org/10.1007/978-3-319-47656-8_2
- Chi, Y.-Y., Gribbin, M.J., Johnson, J.L., Muller, K.E., 2014. Power calculation for overall hypothesis testing with high-dimensional commensurate outcomes. *Stat. Med.* 33, 812–27. <https://doi.org/10.1002/sim.5986>
- Ciprian, D., n.d. THE PATHOGENY OF PROLIFERATIVE VITREORETINOPATHY. *Rom. J. Ophthalmol.* 59, 88–92.
- Crick, F., 1970. Central dogma of molecular biology. *Nature* 227, 561–3.

- Crutchfield, C.A., Thomas, S.N., Sokoll, L.J., Chan, D.W., 2016. Advances in mass spectrometry-based clinical biomarker discovery. *Clin. Proteomics* 13, 1. <https://doi.org/10.1186/s12014-015-9102-9>
- Cuevas-C?rdoba, B., Santiago-Garc?a, J., 2014. Saliva: A Fluid of Study for OMICS. *Omi. A J. Integr. Biol.* 18, 87–97. <https://doi.org/10.1089/omi.2013.0064>
- Cuilla, T.A., Ying, G., Maguire, M.G., Martin, D.F., Jaffe, G.J., Grunwald, J.E., Daniel, E., Toth, C.A., Toth, C.A., Comparison of Age-Related Macular Degeneration Treatments Trials Research Group, 2015. Influence of the Vitreomacular Interface on Treatment Outcomes in the Comparison of Age-Related Macular Degeneration Treatments Trials. *Ophthalmology* 122, 1203–1211. <https://doi.org/10.1016/j.ophtha.2015.02.031>
- Cuperlovic-Culf, M., Culf, A.S., 2016. Applied metabolomics in drug discovery. *Expert Opin. Drug Discov.* 11, 759–770. <https://doi.org/10.1080/17460441.2016.1195365>
- D'Alessandro, A., Cervia, D., Catalani, E., Gevi, F., Zolla, L., Casini, G., 2014. Protective effects of the neuropeptides PACAP, substance P and the somatostatin analogue octreotide in retinal ischemia: a metabolomic analysis. *Mol. Biosyst.* 10, 1290. <https://doi.org/10.1039/c3mb70362b>
- D'Amico, D.J., 2008. Primary Retinal Detachment. *N. Engl. J. Med.* 359, 2346–2354. <https://doi.org/10.1056/NEJMcp0804591>
- Dane, A.D., Hendriks, M.M.W.B., Reijmers, T.H., Harms, A.C., Troost, J., Vreeken, R.J., Boomsma, D.I., van Duijn, C.M., Slagboom, E.P., Hankemeier, T., 2014. Integrating metabolomics profiling measurements across multiple biobanks. *Anal. Chem.* 86, 4110–4. <https://doi.org/10.1021/ac404191a>
- de la Barca, J.M.C., Huang, N.-T., Jiao, H., Tessier, L., Gadras, C., Simard, G., Natoli, R., Tcherkez, G., Reynier, P., Valter, K., 2017. Retinal metabolic events in preconditioning light stress as revealed by wide-spectrum targeted metabolomics. *Metabolomics* 13, 22. <https://doi.org/10.1007/s11306-016-1156-9>
- Di Guida, R., Engel, J., Allwood, J.W., Weber, R.J.M., Jones, M.R., Sommer, U., Viant, M.R., Dunn, W.B., 2016. Non-targeted UHPLC-MS metabolomic data processing methods: a comparative investigation of normalisation, missing value imputation, transformation and scaling. *Metabolomics* 12, 93. <https://doi.org/10.1007/s11306-016-1030-9>
- Diaz, S.O., Barros, A.S., Goodfellow, B.J., Duarte, I.F., Galhano, E., Pita, C., Almeida, M. do C., Carreira, I.M., Gil, A.M., 2013. Second trimester maternal urine for the diagnosis of trisomy 21 and prediction of poor pregnancy outcomes. *J. Proteome Res.* 12, 2946–57. <https://doi.org/10.1021/pr4002355>
- Du, J., Rountree, A., Cleghorn, W.M., Contreras, L., Lindsay, K.J., Sadilek, M., Gu, H., Djukovic, D., Raftery, D., Satrústegui, J., Kanow, M., Chan, L., Tsang, S.H., Sweet, I.R.,

- Hurley, J.B., 2016. Phototransduction Influences Metabolic Flux and Nucleotide Metabolism in Mouse Retina. *J. Biol. Chem.* 291, 4698–4710.
<https://doi.org/10.1074/jbc.M115.698985>
- Dunn, W.B., Broadhurst, D., Begley, P., Zelena, E., Francis-McIntyre, S., Anderson, N., Brown, M., Knowles, J.D., Halsall, A., Haselden, J.N., Nicholls, A.W., Wilson, I.D., Kell, D.B., Goodacre, R., 2011a. Procedures for large-scale metabolic profiling of serum and plasma using gas chromatography and liquid chromatography coupled to mass spectrometry. *Nat. Protoc.* 6, 1060–1083. <https://doi.org/10.1038/nprot.2011.335>
- Dunn, W.B., Broadhurst, D., Begley, P., Zelena, E., Francis-McIntyre, S., Anderson, N., Brown, M., Knowles, J.D., Halsall, A., Haselden, J.N., Nicholls, A.W., Wilson, I.D., Kell, D.B., Goodacre, R., Human Serum Metabolome (HUSERMET) Consortium, 2011b. Procedures for large-scale metabolic profiling of serum and plasma using gas chromatography and liquid chromatography coupled to mass spectrometry. *Nat. Protoc.* 6, 1060–83. <https://doi.org/10.1038/nprot.2011.335>
- Emwas, A.-H., Roy, R., McKay, R.T., Ryan, D., Brennan, L., Tenori, L., Luchinat, C., Gao, X., Zeri, A.C., Gowda, G.A.N., Raftery, D., Steinbeck, C., Salek, R.M., Wishart, D.S., 2016. Recommendations and Standardization of Biomarker Quantification Using NMR-Based Metabolomics with Particular Focus on Urinary Analysis. *J. Proteome Res.* 15, 360–373. <https://doi.org/10.1021/acs.jproteome.5b00885>
- Emwas, A.-H.M., 2015. The Strengths and Weaknesses of NMR Spectroscopy and Mass Spectrometry with Particular Focus on Metabolomics Research, in: *Methods in Molecular Biology* (Clifton, N.J.). pp. 161–193. https://doi.org/10.1007/978-1-4939-2377-9_13
- Ermilov, V. V., Nesterova, A.A., 2016. β -amyloidopathy in the Pathogenesis of Age-Related Macular Degeneration in Correlation with Neurodegenerative Diseases, in: *Advances in Experimental Medicine and Biology*. pp. 119–125. https://doi.org/10.1007/978-3-319-17121-0_17
- Fang, M., Ivanisevic, J., Benton, H.P., Johnson, C.H., Patti, G.J., Hoang, L.T., Uritboonthai, W., Kurczyk, M.E., Siuzdak, G., 2015. Thermal Degradation of Small Molecules: A Global Metabolomic Investigation. *Anal. Chem.* 87, 10935–41.
<https://doi.org/10.1021/acs.analchem.5b03003>
- Farooqui, A.A., 2012. Lipid mediators and their metabolism in the nucleus: implications for Alzheimer's disease. *J. Alzheimers. Dis.* 30 Suppl 2, S163-78.
<https://doi.org/10.3233/JAD-2011-111085>
- Farooqui, A.A., Horrocks, L.A., Farooqui, T., 2000. Glycerophospholipids in brain: their metabolism, incorporation into membranes, functions, and involvement in neurological disorders. *Chem. Phys. Lipids* 106, 1–29.

- Federation of American Societies for Experimental Biology., C., Mean, R., Janssen, B.J., Hedlund, L.W., 2010. Federation proceedings., The FASEB Journal. Federation of American Societies for Experimental Biology.
- Fiehn, O., 2002. Metabolomics--the link between genotypes and phenotypes. *Plant Mol. Biol.* 48, 155–71.
- Frisardi, V., Panza, F., Seripa, D., Farooqui, T., Farooqui, A.A., 2011. Glycerophospholipids and glycerophospholipid-derived lipid mediators: A complex meshwork in Alzheimer's disease pathology. *Prog. Lipid Res.* 50, 313–330. <https://doi.org/10.1016/j.plipres.2011.06.001>
- Ghosal, S., Nunley, A., Mahbod, P., Lewis, A.G., Smith, E.P., Tong, J., D'Alessio, D.A., Herman, J.P., 2015. Mouse handling limits the impact of stress on metabolic endpoints. *Physiol. Behav.* 150, 31–37. <https://doi.org/10.1016/J.PHYSBEH.2015.06.021>
- Gika, H.G., Theodoridis, G.A., Plumb, R.S., Wilson, I.D., 2014. Current practice of liquid chromatography-mass spectrometry in metabolomics and metabonomics. *J. Pharm. Biomed. Anal.* 87, 12–25. <https://doi.org/10.1016/j.jpba.2013.06.032>
- Gika, H.G., Theodoridis, G.A., Wilson, I.D., 2008. Liquid chromatography and ultra-performance liquid chromatography-mass spectrometry fingerprinting of human urine: sample stability under different handling and storage conditions for metabonomics studies. *J. Chromatogr. A* 1189, 314–22. <https://doi.org/10.1016/j.chroma.2007.10.066>
- Giskeødegård, G.F., Davies, S.K., Revell, V.L., Keun, H., Skene, D.J., 2015. Diurnal rhythms in the human urine metabolome during sleep and total sleep deprivation. *Sci. Rep.* 5, 14843. <https://doi.org/10.1038/srep14843>
- Gordon, W.C., Bazan, N.G., 2013. Mediator Lipidomics in Ophthalmology: Targets for Modulation in Inflammation, Neuroprotection and Nerve Regeneration. *Curr. Eye Res.* 38, 995–1005. <https://doi.org/10.3109/02713683.2013.827211>
- Hebels, D.G.A.J., Georgiadis, P., Keun, H.C., Athersuch, T.J., Vineis, P., Vermeulen, R., Portengen, L., Bergdahl, I.A., Hallmans, G., Palli, D., Bendinelli, B., Krogh, V., Tumino, R., Sacerdote, C., Panico, S., Kleinjans, J.C., de Kok, T.M., Smith, M.T., Kyrtopoulos, S.A., EnviroGenomarkers Project Consortium, 2013. Performance in Omics Analyses of Blood Samples in Long-Term Storage: Opportunities for the Exploitation of Existing Biobanks in Environmental Health Research. *Environ. Health Perspect.* 121, 480–7. <https://doi.org/10.1289/ehp.1205657>
- Holekamp, N.M., 2010. The Vitreous Gel: More than Meets the Eye. *Am. J. Ophthalmol.* 149, 32–36.e1. <https://doi.org/10.1016/j.ajo.2009.07.036>
- Holmes, E., Wijeyesekera, A., Taylor-Robinson, S.D., Nicholson, J.K., 2015. The promise of metabolic phenotyping in gastroenterology and hepatology. *Nat. Rev. Gastroenterol. Hepatol.* 12, 458–71. <https://doi.org/10.1038/nrgastro.2015.114>

- Hong, T., Tan, A.G., Mitchell, P., Wang, J.J., n.d. A review and meta-analysis of the association between C-reactive protein and age-related macular degeneration. *Surv. Ophthalmol.* 56, 184–94.
- Hopiavuori, B.R., Agbaga, M.-P., Brush, R.S., Sullivan, M.T., Sonntag, W.E., Anderson, R.E., 2017. Regional changes in CNS and retinal glycerophospholipid profiles with age: a molecular blueprint. *J. Lipid Res.* 58, 668–680. <https://doi.org/10.1194/jlr.M070714>
- Hurst, J.L., West, R.S., 2010. Taming anxiety in laboratory mice. *Nat. Methods* 7, 825–826. <https://doi.org/10.1038/nmeth.1500>
- Inouye, M., Kettunen, J., Soininen, P., Silander, K., Ripatti, S., Kumpula, L.S., Hämäläinen, E., Jousilahti, P., Kangas, A.J., Männistö, S., Savolainen, M.J., Jula, A., Leiviskä, J., Palotie, A., Salomaa, V., Perola, M., Ala-Korpela, M., Peltonen, L., 2010. Metabonomic, transcriptomic, and genomic variation of a population cohort. *Mol. Syst. Biol.* 6, 441. <https://doi.org/10.1038/msb.2010.93>
- Jafari, M., Ansari-Pour, N., Azimzadeh, S., Mirzaie, M., 2017. A logic-based dynamic modeling approach to explicate the evolution of the central dogma of molecular biology. *PLoS One* 12, e0189922. <https://doi.org/10.1371/journal.pone.0189922>
- Jobard, E., Trédan, O., Postoly, D., André, F., Martin, A.-L., Elena-Herrmann, B., Boyault, S., 2016. A Systematic Evaluation of Blood Serum and Plasma Pre-Analytics for Metabolomics Cohort Studies. *Int. J. Mol. Sci.* 17, 2035. <https://doi.org/10.3390/ijms17122035>
- Jové, M., Portero-Otín, M., Naudí, A., Ferrer, I., Pamplona, R., 2014. Metabolomics of human brain aging and age-related neurodegenerative diseases. *J. Neuropathol. Exp. Neurol.* 73, 640–57. <https://doi.org/10.1097/NEN.0000000000000091>
- Kaarniranta, K., Salminen, A., Haapasalo, A., Soininen, H., Hiltunen, M., 2011. Age-related macular degeneration (AMD): Alzheimer's disease in the eye? *J. Alzheimers. Dis.* 24, 615–31. <https://doi.org/10.3233/JAD-2011-101908>
- Kell, D.B., Oliver, S.G., 2016. The metabolome 18 years on: a concept comes of age. *Metabolomics* 12, 148. <https://doi.org/10.1007/s11306-016-1108-4>
- Kelly, A.D., Breitkopf, S.B., Yuan, M., Goldsmith, J., Spentzos, D., Asara, J.M., 2011. Metabolomic Profiling from Formalin-Fixed, Paraffin-Embedded Tumor Tissue Using Targeted LC/MS/MS: Application in Sarcoma. *PLoS One* 6, e25357. <https://doi.org/10.1371/journal.pone.0025357>
- Khamis, M.M., Adamko, D.J., El-Aneed, A., 2017. Mass spectrometric based approaches in urine metabolomics and biomarker discovery. *Mass Spectrom. Rev.* 36, 115–134. <https://doi.org/10.1002/mas.21455>
- Klein, R., Myers, C.E., Buitendijk, G.H.S., Rochtchina, E., Gao, X., de Jong, P.T.V.M., Sivakumaran, T.A., Burlutsky, G., McKean-Cowdin, R., Hofman, A., Iyengar, S.K., Lee,

- K.E., Stricker, B.H., Vingerling, J.R., Mitchell, P., Klein, B.E.K., Klaver, C.C.W., Wang, J.J., 2014a. Lipids, Lipid Genes, and Incident Age-Related Macular Degeneration: The Three Continent Age-Related Macular Degeneration Consortium. *Am. J. Ophthalmol.* 158, 513–524.e3. <https://doi.org/10.1016/j.ajo.2014.05.027>
- Klein, R., Myers, C.E., Cruickshanks, K.J., Gangnon, R.E., Danforth, L.G., Sivakumaran, T.A., Iyengar, S.K., Tsai, M.Y., Klein, B.E.K., 2014b. Markers of inflammation, oxidative stress, and endothelial dysfunction and the 20-year cumulative incidence of early age-related macular degeneration: the Beaver Dam Eye Study. *JAMA Ophthalmol.* 132, 446–55. <https://doi.org/10.1001/jamaophthalmol.2013.7671>
- Kohler, I., Verhoeven, A., Derks, R.J., Giera, M., 2016. Analytical pitfalls and challenges in clinical metabolomics. *Bioanalysis* 8, 1509–1532. <https://doi.org/10.4155/bio-2016-0090>
- Kosicek, M., Hecimovic, S., 2013. Phospholipids and Alzheimer's Disease: Alterations, Mechanisms and Potential Biomarkers. *Int. J. Mol. Sci.* 14, 1310–1322. <https://doi.org/10.3390/ijms14011310>
- Kumar, N., Hoque, M.A., Shahjaman, M., Islam, S.M.S., Mollah, M.N.H., 2017. Metabolomic Biomarker Identification in Presence of Outliers and Missing Values. *Biomed Res. Int.* 2017, 1–11. <https://doi.org/10.1155/2017/2437608>
- Kurihara, T., Westenskow, P.D., Gantner, M.L., Usui, Y., Schultz, A., Bravo, S., Aguilar, E., Wittgrove, C., Friedlander, M.S., Paris, L.P., Chew, E., Siuzdak, G., Friedlander, M., 2016. Hypoxia-induced metabolic stress in retinal pigment epithelial cells is sufficient to induce photoreceptor degeneration. *Elife* 5. <https://doi.org/10.7554/eLife.14319>
- Laatikainen, L., Tolppanen, E.M., Harju, H., 1985. Epidemiology of rhegmatogenous retinal detachment in a Finnish population. *Acta Ophthalmol.* 63, 59–64.
- Laíns, I., Duarte, D., Barros, A.S., Martins, A.S., Gil, J., Miller, J.B., Marques, M., Mesquita, T., Kim, I.K., Da Luz Cachulo, M., Vavvas, D., Carreira, I.M., Murta, J.N., Silva, R., Miller, J.W., Husain, D., Gil, A.M., 2017a. Human plasma metabolomics in age-related macular degeneration (AMD) using nuclear magnetic resonance spectroscopy. *PLoS One* 12. <https://doi.org/10.1371/journal.pone.0177749>
- Laíns, I., Kelly, R.S., Miller, J.B., Silva, R., Vavvas, D.G., Kim, I.K., Murta, J.N., Lasky-Su, J., Miller, J.W., Husain, D., 2017b. Human Plasma Metabolomics Study across All Stages of Age-Related Macular Degeneration Identifies Potential Lipid Biomarkers. *Ophthalmology.* <https://doi.org/10.1016/j.ophtha.2017.08.008>
- Laíns, I., Kelly, R.S., Miller, J.B., Silva, R., Vavvas, D.G., Kim, I.K., Murta, J.N., Lasky-Su, J., Miller, J.W., Husain, D., 2017. Human Plasma Metabolomics Study across All Stages of Age-Related Macular Degeneration Identifies Potential Lipid Biomarkers. *Ophthalmology.* <https://doi.org/10.1016/j.ophtha.2017.08.008>
- Lam, S.M., Tong, L., Duan, X., Petznick, A., Wenk, M.R., Shui, G., 2014. Extensive

- characterization of human tear fluid collected using different techniques unravels the presence of novel lipid amphiphiles. *J. Lipid Res.* 55, 289–298.
<https://doi.org/10.1194/jlr.M044826>
- Lau, J.C.M., Linsenmeier, R.A., 2012. Oxygen consumption and distribution in the Long-Evans rat retina. *Exp. Eye Res.* 102, 50–8. <https://doi.org/10.1016/j.exer.2012.07.004>
- Li, M., Li, H., Jiang, P., Liu, X., Xu, D., Wang, F., 2014. Investigating the pathological processes of rhegmatogenous retinal detachment and proliferative vitreoretinopathy with metabolomics analysis. *Mol. Biosyst.* 10, 1055. <https://doi.org/10.1039/c3mb70386j>
- Li, M., Zhang, X., Liao, N., Ye, B., Peng, Y., Ji, Y., Wen, F., 2016. Analysis of the Serum Lipid Profile in Polypoidal Choroidal Vasculopathy. *Sci. Rep.* 6, 38342.
<https://doi.org/10.1038/srep38342>
- Li, X., Luo, X., Lu, X., Duan, J., Xu, G., 2011. Metabolomics study of diabetic retinopathy using gas chromatography–mass spectrometry: a comparison of stages and subtypes diagnosed by Western and Chinese medicine. *Mol. Biosyst.* 7, 2228.
<https://doi.org/10.1039/c0mb00341g>
- Lind, M. V., Savolainen, O.I., Ross, A.B., 2016. The use of mass spectrometry for analysing metabolite biomarkers in epidemiology: methodological and statistical considerations for application to large numbers of biological samples. *Eur. J. Epidemiol.* 31, 717–733.
<https://doi.org/10.1007/s10654-016-0166-2>
- Linton, J.D., Holzhausen, L.C., Babai, N., Song, H., Miyagishima, K.J., Stearns, G.W., Lindsay, K., Wei, J., Chertov, A.O., Peters, T.A., Caffè, R., Pluk, H., Seeliger, M.W., Tanimoto, N., Fong, K., Bolton, L., Kuok, D.L.T., Sweet, I.R., Bartoletti, T.M., Radu, R.A., Travis, G.H., Zagotta, W.N., Townes-Anderson, E., Parker, E., Van der Zee, C.E.E.M., Sampath, A.P., Sokolov, M., Thoreson, W.B., Hurley, J.B., 2010. Flow of energy in the outer retina in darkness and in light. *Proc. Natl. Acad. Sci. U. S. A.* 107, 8599–604. <https://doi.org/10.1073/pnas.1002471107>
- Locci, E., Scano, P., Rosa, M.F., Nioi, M., Noto, A., Atzori, L., Demontis, R., De-Giorgio, F., d'Aloja, E., 2014. A Metabolomic Approach to Animal Vitreous Humor Topographical Composition: A Pilot Study. *PLoS One* 9, e97773.
<https://doi.org/10.1371/journal.pone.0097773>
- Luan, Y., Ou, J., Kunze, V.P., Qiao, F., Wang, Y., Wei, L., Li, W., Xie, Z., 2018. Integrated transcriptomic and metabolomic analysis reveals adaptive changes of hibernating retinas. *J. Cell. Physiol.* 233, 1434–1445. <https://doi.org/10.1002/jcp.26030>
- Luo, D.-G., Xue, T., Yau, K.-W., 2008. How vision begins: An odyssey. *doi.org* 105, 9855–9862. <https://doi.org/10.1073/pnas.0708405105>
- Ly, A., Schöne, C., Becker, M., Rattke, J., Meding, S., Aichler, M., Suckau, D., Walch, A., Hauck, S.M., Ueffing, M., 2015. High-resolution MALDI mass spectrometric imaging of

- lipids in the mammalian retina. *Histochem. Cell Biol.* 143, 453–462.
<https://doi.org/10.1007/s00418-014-1303-1>
- Mains, J., Tan, L.E., Zhang, T., Young, L., Shi, R., Wilson, C., 2012. Species variation in small molecule components of animal vitreous. *Invest. Ophthalmol. Vis. Sci.* 53, 4778–86. <https://doi.org/10.1167/iov.12-9998>
- Mal, M., 2016. Noninvasive metabolic profiling for painless diagnosis of human diseases and disorders. *Futur. Sci. OA* 2, fsoa-2015-0014. <https://doi.org/10.4155/fsoa-2015-0014>
- Manolio, T.A., Collins, F.S., Cox, N.J., Goldstein, D.B., Hindorf, L.A., Hunter, D.J., McCarthy, M.I., Ramos, E.M., Cardon, L.R., Chakravarti, A., Cho, J.H., Guttmacher, A.E., Kong, A., Kruglyak, L., Mardis, E., Rotimi, C.N., Slatkin, M., Valle, D., Whittemore, A.S., Boehnke, M., Clark, A.G., Eichler, E.E., Gibson, G., Haines, J.L., Mackay, T.F.C., McCarroll, S.A., Visscher, P.M., 2009. Finding the missing heritability of complex diseases. *Nature* 461, 747–753. <https://doi.org/10.1038/nature08494>
- Mapstone, M., Cheema, A.K., Fiandaca, M.S., Zhong, X., Mhyre, T.R., MacArthur, L.H., Hall, W.J., Fisher, S.G., Peterson, D.R., Haley, J.M., Nazar, M.D., Rich, S.A., Berlau, D.J., Peltz, C.B., Tan, M.T., Kawas, C.H., Federoff, H.J., 2014. Plasma phospholipids identify antecedent memory impairment in older adults. *Nat. Med.* 20, 415–418. <https://doi.org/10.1038/nm.3466>
- Mapstone, M., Lin, F., Nalls, M.A., Cheema, A.K., Singleton, A.B., Fiandaca, M.S., Federoff, H.J., 2017. What success can teach us about failure: the plasma metabolome of older adults with superior memory and lessons for Alzheimer’s disease. *Neurobiol. Aging* 51, 148–155. <https://doi.org/10.1016/j.neurobiolaging.2016.11.007>
- Markley, J.L., Brüschweiler, R., Edison, A.S., Eghbalnia, H.R., Powers, R., Raftery, D., Wishart, D.S., 2017. The future of NMR-based metabolomics. *Curr. Opin. Biotechnol.* 43, 34–40. <https://doi.org/10.1016/j.copbio.2016.08.001>
- Marshall, D.D., Powers, R., 2017. Beyond the paradigm: Combining mass spectrometry and nuclear magnetic resonance for metabolomics. *Prog. Nucl. Magn. Reson. Spectrosc.* 100, 1–16. <https://doi.org/10.1016/j.pnmrs.2017.01.001>
- Midelfart, A., 2009. Metabonomics—a new approach in ophthalmology. *Acta Ophthalmol.* 87, 697–703.
- Mitry, D., Charteris, D.G., Yorston, D., Siddiqui, M.A.R., Campbell, H., Murphy, A.-L., Fleck, B.W., Wright, A.F., Singh, J., Scottish RD Study Group, 2010. The Epidemiology and Socioeconomic Associations of Retinal Detachment in Scotland: A Two-Year Prospective Population-Based Study. *Investig. Ophthalmology Vis. Sci.* 51, 4963. <https://doi.org/10.1167/iov.10-5400>
- Mitta, V.P., Christen, W.G., Glynn, R.J., Semba, R.D., Ridker, P.M., Rimm, E.B., Hankinson, S.E., Schaumberg, D.A., 2013. C-reactive protein and the incidence of macular

- degeneration: pooled analysis of 5 cohorts. *JAMA Ophthalmol.* 131, 507–13.
- Monteiro, M.S., Carvalho, M., Bastos, M.L., Guedes de Pinho, P., 2013. Metabolomics analysis for biomarker discovery: advances and challenges. *Curr. Med. Chem.* 20, 257–71.
- Naru, J., Aggarwal, R., Mohanty, A.K., Singh, U., Bansal, D., Kakkar, N., Agnihotri, N., 2017. Identification of differentially expressed proteins in retinoblastoma tumors using mass spectrometry-based comparative proteomic approach. *J. Proteomics* 159, 77–91. <https://doi.org/10.1016/j.jprot.2017.02.006>
- Nelson, C.J., Otis, J.P., Martin, S.L., Carey, H. V, 2009. Analysis of the hibernation cycle using LC-MS-based metabolomics in ground squirrel liver. *Physiol. Genomics* 37, 43–51. <https://doi.org/10.1152/physiolgenomics.90323.2008>
- Nicholson, J.K., Everett, J.R., Lindon, J.C., 2012a. Longitudinal pharmacometabonomics for predicting patient responses to therapy: drug metabolism, toxicity and efficacy. *Expert Opin. Drug Metab. Toxicol.* 8, 135–9. <https://doi.org/10.1517/17425255.2012.646987>
- Nicholson, J.K., Holmes, E., Kinross, J.M., Darzi, A.W., Takats, Z., Lindon, J.C., 2012b. Metabolic phenotyping in clinical and surgical environments. *Nature* 491, 384–92.
- Nicholson, J.K., Holmes, E., Kinross, J.M., Darzi, A.W., Takats, Z., Lindon, J.C., 2012. Metabolic phenotyping in clinical and surgical environments. *Nature* 491, 384–392. <https://doi.org/10.1038/nature11708>
- Nirmalan, N.J., Harnden, P., Selby, P.J., Banks, R.E., 2008. Mining the archival formalin-fixed paraffin-embedded tissue proteome: opportunities and challenges. *Mol. Biosyst.* 4, 712–20. <https://doi.org/10.1039/b800098k>
- Nishtala, K., Pahuja, N., Shetty, R., Nuijts, R.M.M.A., Ghosh, A., 2016. Tear biomarkers for keratoconus. *Eye Vis.* 3, 19. <https://doi.org/10.1186/s40662-016-0051-9>
- Nyamundanda, G., Gormley, I.C., Fan, Y., Gallagher, W.M., Brennan, L., 2013. MetSizeR: selecting the optimal sample size for metabolomic studies using an analysis based approach. *BMC Bioinformatics* 14, 338. <https://doi.org/10.1186/1471-2105-14-338>
- Obuchowski, N.A., Lieber, M.L., Wians, F.H., 2004. ROC curves in clinical chemistry: uses, misuses, and possible solutions. *Clin. Chem.* 50, 1118–25. <https://doi.org/10.1373/clinchem.2004.031823>
- Ohno-Matsui, K., 2011. Parallel findings in age-related macular degeneration and Alzheimer's disease. *Prog. Retin. Eye Res.* 30, 217–238. <https://doi.org/10.1016/j.preteyeres.2011.02.004>
- Osborn, M.P., Park, Y., Parks, M.B., Burgess, L.G., Uppal, K., Lee, K., Jones, D.P., Brantley, M.A., 2013. Metabolome-wide association study of neovascular age-related macular degeneration. *PLoS One* 8, e72737.
- Osborne, N.N., Casson, R.J., Wood, J.P., Chidlow, G., Graham, M., Melena, J., 2004.

- Retinal ischemia: mechanisms of damage and potential therapeutic strategies. *Prog. Retin. Eye Res.* 23, 91–147. <https://doi.org/10.1016/J.PRETEYERES.2003.12.001>
- Paris, L.P., Johnson, C.H., Aguilar, E., Usui, Y., Cho, K., Hoang, L.T., Feitelberg, D., Benton, H.P., Westenskow, P.D., Kurihara, T., Trombley, J., Tsubota, K., Ueda, S., Wakabayashi, Y., Patti, G.J., Ivanisevic, J., Siuzdak, G., Friedlander, M., 2016. Global metabolomics reveals metabolic dysregulation in ischemic retinopathy. *Metabolomics* 12, 15. <https://doi.org/10.1007/s11306-015-0877-5>
- Pastor, J.C., Rojas, J., Pastor-Idoate, S., Di Lauro, S., Gonzalez-Buendia, L., Delgado-Tirado, S., 2016. Proliferative vitreoretinopathy: A new concept of disease pathogenesis and practical consequences. *Prog. Retin. Eye Res.* 51, 125–155. <https://doi.org/10.1016/j.preteyeres.2015.07.005>
- Patel, C.J., Kerr, J., Thomas, D.C., Mukherjee, B., Ritz, B., Chatterjee, N., Jankowska, M., Madan, J., Karagas, M.R., McAllister, K.A., Mechanic, L.E., Fallin, M.D., Ladd-Acosta, C., Blair, I.A., Teitelbaum, S.L., Amos, C.I., 2017. Opportunities and Challenges for Environmental Exposure Assessment in Population-Based Studies. *Cancer Epidemiol. Biomarkers Prev.* 26, 1370–1380. <https://doi.org/10.1158/1055-9965.EPI-17-0459>
- Patti, G.J., Yanes, O., Siuzdak, G., 2012. Innovation: Metabolomics: the apogee of the omics trilogy. *Nat. Rev. Mol. Cell Biol.* 13, 263–9. <https://doi.org/10.1038/nrm3314>
- Petras, D., Jarmusch, A.K., Dorrestein, P.C., 2017a. From single cells to our planet—recent advances in using mass spectrometry for spatially resolved metabolomics. *Curr. Opin. Chem. Biol.* 36, 24–31. <https://doi.org/10.1016/j.cbpa.2016.12.018>
- Petras, D., Jarmusch, A.K., Dorrestein, P.C., 2017b. From single cells to our planet—recent advances in using mass spectrometry for spatially resolved metabolomics. *Curr. Opin. Chem. Biol.* 36, 24–31. <https://doi.org/10.1016/j.cbpa.2016.12.018>
- Pieragostino, D., D'Alessandro, M., di Iorio, M., Di Ilio, C., Sacchetta, P., Del Boccio, P., 2015. Unraveling the molecular repertoire of tears as a source of biomarkers: beyond ocular diseases. *Proteomics. Clin. Appl.* 9, 169–86. <https://doi.org/10.1002/prca.201400084>
- Proitsi, P., Kim, M., Whaley, L., Simmons, A., Sattlecker, M., Velayudhan, L., Lupton, M.K., Soininen, H., Kloszewska, I., Mecocci, P., Tsolaki, M., Vellas, B., Lovestone, S., Powell, J.F., Dobson, R.J.B., Legido-Quigley, C., 2017. Association of blood lipids with Alzheimer's disease: A comprehensive lipidomics analysis. *Alzheimer's Dement.* 13, 140–151. <https://doi.org/10.1016/j.jalz.2016.08.003>
- Psychogios, N., Hau, D.D., Peng, J., Guo, A.C., Mandal, R., Bouatra, S., Sinelnikov, I., Krishnamurthy, R., Eisner, R., Gautam, B., Young, N., Xia, J., Knox, C., Dong, E., Huang, P., Hollander, Z., Pedersen, T.L., Smith, S.R., Bamforth, F., Greiner, R., McManus, B., Newman, J.W., Goodfriend, T., Wishart, D.S., 2011a. The human serum

- metabolome. *PLoS One* 6, e16957. <https://doi.org/10.1371/journal.pone.0016957>
- Psychogios, N., Hau, D.D., Peng, J., Guo, A.C., Mandal, R., Bouatra, S., Sinelnikov, I., Krishnamurthy, R., Eisner, R., Gautam, B., Young, N., Xia, J., Knox, C., Dong, E., Huang, P., Hollander, Z., Pedersen, T.L., Smith, S.R., Bamforth, F., Greiner, R., McManus, B., Newman, J.W., Goodfriend, T., Wishart, D.S., 2011b. The Human Serum Metabolome. *PLoS One* 6, e16957. <https://doi.org/10.1371/journal.pone.0016957>
- Putri, S.P., Yamamoto, S., Tsugawa, H., Fukusaki, E., 2013. Current metabolomics: technological advances. *J. Biosci. Bioeng.* 116, 9–16. <https://doi.org/10.1016/j.jbiosc.2013.01.004>
- Rantamäki, A.H., Seppänen-Laakso, T., Oresic, M., Jauhiainen, M., Holopainen, J.M., 2011. Human tear fluid lipidome: from composition to function. *PLoS One* 6, e19553. <https://doi.org/10.1371/journal.pone.0019553>
- Rowan, S., Jiang, S., Korem, T., Szymanski, J., Chang, M.-L., Szelog, J., Cassalman, C., Dasuri, K., McGuire, C., Nagai, R., Du, X.-L., Brownlee, M., Rabbani, N., Thornalley, P.J., Baleja, J.D., Deik, A.A., Pierce, K.A., Scott, J.M., Clish, C.B., Smith, D.E., Weinberger, A., Avnit-Sagi, T., Lotan-Pompan, M., Segal, E., Taylor, A., 2017. Involvement of a gut–retina axis in protection against dietary glycemia-induced age-related macular degeneration. *Proc. Natl. Acad. Sci.* 114, E4472–E4481. <https://doi.org/10.1073/pnas.1702302114>
- Rowe, J.A., Erie, J.C., Baratz, K.H., Hodge, D.O., Gray, D.T., Butterfield, L., Robertson, D.M., 1999. Retinal detachment in Olmsted County, Minnesota, 1976 through 1995. *Ophthalmology* 106, 154–159. [https://doi.org/10.1016/S0161-6420\(99\)90018-0](https://doi.org/10.1016/S0161-6420(99)90018-0)
- Rucker, J.C., Biousse, V., Mao, H., Sandbach, J., Constantinidis, I., Newman, N.J., 2003. Detection of lactate in the human vitreous body using proton magnetic resonance spectroscopy. *Arch. Ophthalmol. (Chicago, Ill. 1960)* 121, 909–11. <https://doi.org/10.1001/archopht.121.6.909>
- Scalbert, A., Brennan, L., Fiehn, O., Hankemeier, T., Kristal, B.S., van Ommen, B., Pujos-Guillot, E., Verheij, E., Wishart, D., Wopereis, S., 2009. Mass-spectrometry-based metabolomics: limitations and recommendations for future progress with particular focus on nutrition research. *Metabolomics* 5, 435–458. <https://doi.org/10.1007/s11306-009-0168-0>
- Schmidt, S.Y., Berson, E.L., 1980. Postmortem metabolic capacity of photoreceptor cells in human and rat retinas. *Invest. Ophthalmol. Vis. Sci.* 19, 1274–80.
- Shui, Y.-B., Holekamp, N.M., Kramer, B.C., Crowley, J.R., Wilkins, M.A., Chu, F., Malone, P.E., Mangers, S.J., Hou, J.H., Siegfried, C.J., Beebe, D.C., 2009. The gel state of the vitreous and ascorbate-dependent oxygen consumption: relationship to the etiology of nuclear cataracts. *Arch. Ophthalmol. (Chicago, Ill. 1960)* 127, 475–82.

- <https://doi.org/10.1001/archophthalmol.2008.621>
- Singh, R.P., Habbu, K.A., Bedi, R., Silva, F.Q., Ehlers, J.P., Schachat, A.P., Sears, J.E., Srivastava, S.K., Kaiser, P.K., Yuan, A., 2017. A retrospective study of the influence of the vitreomacular interface on macular oedema secondary to retinal vein occlusion. *Br. J. Ophthalmol.* 101, 1340–1345. <https://doi.org/10.1136/bjophthalmol-2016-309747>
- Sivak, J.M., 2013. The Aging Eye: Common Degenerative Mechanisms Between the Alzheimer's Brain and Retinal Disease. *Investig. Ophthalmology Vis. Sci.* 54, 871. <https://doi.org/10.1167/iov.12-10827>
- Slupsky, C.M., Rankin, K.N., Wagner, J., Fu, H., Chang, D., Weljie, A.M., Saude, E.J., Lix, B., Adamko, D.J., Shah, S., Greiner, R., Sykes, B.D., Marrie, T.J., 2007. Investigations of the effects of gender, diurnal variation, and age in human urinary metabolomic profiles. *Anal. Chem.* 79, 6995–7004. <https://doi.org/10.1021/ac0708588>
- Sobrin, L., Seddon, J.M., 2013. Nature and nurture- genes and environment- predict onset and progression of macular degeneration. *Prog. Retin. Eye Res.* <https://doi.org/10.1016/j.preteyeres.2013.12.004>
- Solberg, R., Escobar, J., Arduini, A., Torres-Cuevas, I., Lahoz, A., Sastre, J., Saugstad, O.D., Vento, M., Kuligowski, J., Quintás, G., 2013. Metabolomic Analysis of the Effect of Postnatal Hypoxia on the Retina in a Newly Born Piglet Model. *PLoS One* 8, e66540. <https://doi.org/10.1371/journal.pone.0066540>
- Stem, M.S., Gardner, T.W., 2013. Neurodegeneration in the pathogenesis of diabetic retinopathy: molecular mechanisms and therapeutic implications. *Curr. Med. Chem.* 20, 3241–50.
- Suhre, K., Gieger, C., 2012. Genetic variation in metabolic phenotypes: study designs and applications. *Nat. Rev. Genet.* 13, 759–69.
- Suhre, K., Meisinger, C., Döring, A., Altmaier, E., Belcredi, P., Gieger, C., Chang, D., Milburn, M. V, Gall, W.E., Weinberger, K.M., Mewes, H.-W., Hrabé de Angelis, M., Wichmann, H.-E., Kronenberg, F., Adamski, J., Illig, T., 2010. Metabolic footprint of diabetes: a multiplatform metabolomics study in an epidemiological setting. *PLoS One* 5, e13953. <https://doi.org/10.1371/journal.pone.0013953>
- Suhre, K., Shin, S.-Y., Petersen, A.-K., Mohnney, R.P., Meredith, D., Wägele, B., Altmaier, E., CARDIoGRAM, Deloukas, P., Erdmann, J., Grundberg, E., Hammond, C.J., de Angelis, M.H., Kastenmüller, G., Köttgen, A., Kronenberg, F., Mangino, M., Meisinger, C., Meitinger, T., Mewes, H.-W., Milburn, M. V, Prehn, C., Raffler, J., Ried, J.S., Römisch-Margl, W., Samani, N.J., Small, K.S., Wichmann, H.-E., Zhai, G., Illig, T., Spector, T.D., Adamski, J., Soranzo, N., Gieger, C., 2011. Human metabolic individuality in biomedical and pharmaceutical research. *Nature* 477, 54–60. <https://doi.org/10.1038/nature10354>
- Sun, N., Ly, A., Meding, S., Witting, M., Hauck, S.M., Ueffing, M., Schmitt-Kopplin, P.,

- Aichler, M., Walch, A., 2014. High-resolution metabolite imaging of light and dark treated retina using MALDI-FTICR mass spectrometry. *Proteomics* 14, 913–923. <https://doi.org/10.1002/pmic.201300407>
- Sun, Y. V., Hu, Y.-J., 2016. Integrative Analysis of Multi-omics Data for Discovery and Functional Studies of Complex Human Diseases, in: *Advances in Genetics*. pp. 147–190. <https://doi.org/10.1016/bs.adgen.2015.11.004>
- Szymańska, E., Saccenti, E., Smilde, A.K., Westerhuis, J.A., 2012. Double-check: validation of diagnostic statistics for PLS-DA models in metabolomics studies. *Metabolomics* 8, 3–16. <https://doi.org/10.1007/s11306-011-0330-3>
- Takeda, I., Stretch, C., Barnaby, P., Bhatnager, K., Rankin, K., Fu, H., Weljie, A., Jha, N., Slupsky, C., 2009. Understanding the human salivary metabolome. *NMR Biomed.* 22, 577–84. <https://doi.org/10.1002/nbm.1369>
- Tan, S.Z., Begley, P., Mullard, G., Hollywood, K.A., Bishop, P.N., 2016. Introduction to metabolomics and its applications in ophthalmology. *Eye* 30, 773–783. <https://doi.org/10.1038/eye.2016.37>
- Tan, S.Z., Mullard, G., Hollywood, K.A., Dunn, W.B., Bishop, P.N., 2016. Characterisation of the metabolome of ocular tissues and post-mortem changes in the rat retina. *Exp. Eye Res.* 149, 8–15. <https://doi.org/10.1016/j.exer.2016.05.019>
- Ting, D.S.W., Tan, K.-A., Phua, V., Tan, G.S.W., Wong, C.W., Wong, T.Y., 2016. Biomarkers of Diabetic Retinopathy. *Curr. Diab. Rep.* 16, 125. <https://doi.org/10.1007/s11892-016-0812-9>
- Tognarelli, J.M., Dawood, M., Shariff, M.I.F., Grover, V.P.B., Crossey, M.M.E., Cox, I.J., Taylor-Robinson, S.D., McPhail, M.J.W., 2015. Magnetic Resonance Spectroscopy: Principles and Techniques: Lessons for Clinicians. *J. Clin. Exp. Hepatol.* 5, 320–328. <https://doi.org/10.1016/j.jceh.2015.10.006>
- Tolstikov, V., 2016. Metabolomics: Bridging the Gap between Pharmaceutical Development and Population Health. *Metabolites* 6, 20. <https://doi.org/10.3390/metabo6030020>
- Törnquist, R., Stenkula, S., Törnquist, P., 1987. Retinal detachment. A study of a population-based patient material in Sweden 1971-1981. I. *Epidemiology. Acta Ophthalmol.* 65, 213–22.
- Triba, M.N., Le Moyec, L., Amathieu, R., Goossens, C., Bouchemal, N., Nahon, P., Rutledge, D.N., Savarin, P., 2015. PLS/OPLS models in metabolomics: the impact of permutation of dataset rows on the K-fold cross-validation quality parameters. *Mol. Biosyst.* 11, 13–9. <https://doi.org/10.1039/c4mb00414k>
- Trivedi, D.K., Hollywood, K.A., Goodacre, R., 2017. Metabolomics for the masses: The future of metabolomics in a personalized world. *New Horizons Transl. Med.* 3, 294–305. <https://doi.org/10.1016/j.nhtm.2017.06.001>

- Tseng, W., Cortez, R.T., Ramirez, G., Stinnett, S., Jaffe, G.J., 2004. Prevalence and risk factors for proliferative vitreoretinopathy in eyes with rhegmatogenous retinal detachment but no previous vitreoretinal surgery. *Am. J. Ophthalmol.* 137, 1105–1115. <https://doi.org/10.1016/j.ajo.2004.02.008>
- Uğurlu, N., Aşık, M.D., Yülek, F., Neselioglu, S., Cagil, N., 2013. Oxidative stress and anti-oxidative defence in patients with age-related macular degeneration. *Curr. Eye Res.* 38, 497–502.
- van Iterson, M., 't Hoen, P.A.C., Pedotti, P., Hoiveld, G.J.E.J., den Dunnen, J.T., van Ommen, G.J.B., Boer, J.M., Menezes, R.X., 2009. Relative power and sample size analysis on gene expression profiling data. *BMC Genomics* 10, 439. <https://doi.org/10.1186/1471-2164-10-439>
- Viant, M.R., Kurland, I.J., Jones, M.R., Dunn, W.B., 2017. How close are we to complete annotation of metabolomes? *Curr. Opin. Chem. Biol.* 36, 64–69. <https://doi.org/10.1016/J.CBPA.2017.01.001>
- Wang, C., Qin, N., Zhu, M., Chen, M., Xie, K., Cheng, Y., Dai, J., Liu, J., Xia, Y., Ma, H., Jin, G., Amos, C.I., Hu, Z., Lin, D., Shen, H., 2017. Metabolome-wide association study identified the association between a circulating polyunsaturated fatty acids variant rs174548 and lung cancer. *Carcinogenesis* 38, 1147–1154. <https://doi.org/10.1093/carcin/bgx084>
- Wang, H.-Y., Chu, X., Zhao, Z.-X., He, X.-S., Guo, Y.-L., 2011. Analysis of low molecular weight compounds by MALDI-FTICR-MS. *J. Chromatogr. B* 879, 1166–1179. <https://doi.org/10.1016/j.jchromb.2011.03.037>
- Wang, X., Sun, H., Zhang, A., Wang, P., Han, Y., 2011. Ultra-performance liquid chromatography coupled to mass spectrometry as a sensitive and powerful technology for metabolomic studies. *J. Sep. Sci.* 34, 3451–3459. <https://doi.org/10.1002/jssc.201100333>
- Wen, B., Mei, Z., Zeng, C., Liu, S., 2017. metaX: a flexible and comprehensive software for processing metabolomics data. *BMC Bioinformatics* 18, 183. <https://doi.org/10.1186/s12859-017-1579-y>
- Whiley, L., Sen, A., Heaton, J., Proitsi, P., García-Gómez, D., Leung, R., Smith, N., Thambisetty, M., Kloszewska, I., Mecocci, P., Soininen, H., Tsolaki, M., Vellas, B., Lovestone, S., Legido-Quigley, C., AddNeuroMed Consortium, 2014. Evidence of altered phosphatidylcholine metabolism in Alzheimer's disease. *Neurobiol. Aging* 35, 271–278. <https://doi.org/10.1016/j.neurobiolaging.2013.08.001>
- Wilcken, B., Wiley, V., Hammond, J., Carpenter, K., 2003. Screening newborns for inborn errors of metabolism by tandem mass spectrometry. *N. Engl. J. Med.* 348, 2304–12. <https://doi.org/10.1056/NEJMoa025225>

- Wilkes, S.R., Beard, C.M., Kurland, L.T., Robertson, D.M., O'Fallon, W.M., 1982. The incidence of retinal detachment in Rochester, Minnesota, 1970-1978. *Am. J. Ophthalmol.* 94, 670-3.
- Wilm, M., 2011. Principles of Electrospray Ionization. *Mol. Cell. Proteomics* 10, M111.009407. <https://doi.org/10.1074/mcp.M111.009407>
- Winnike, J.H., Li, Z., Wright, F.A., Macdonald, J.M., O'Connell, T.M., Watkins, P.B., 2010. Use of Pharmacometabonomics for Early Prediction of Acetaminophen-Induced Hepatotoxicity in Humans. *Clin. Pharmacol. Ther.* 88, 45-51. <https://doi.org/10.1038/clpt.2009.240>
- Wishart, D.S., 2016. Emerging applications of metabolomics in drug discovery and precision medicine. *Nat. Rev. Drug Discov.* 15, 473-484. <https://doi.org/10.1038/nrd.2016.32>
- Wojakowska, A., Marczak, Ł., Jelonek, K., Polanski, K., Widlak, P., Pietrowska, M., 2015. An Optimized Method of Metabolite Extraction from Formalin-Fixed Paraffin-Embedded Tissue for GC/MS Analysis. *PLoS One* 10, e0136902. <https://doi.org/10.1371/journal.pone.0136902>
- Wong-Riley, M., 2010. Energy metabolism of the visual system. *Eye Brain* 2, 99. <https://doi.org/10.2147/EB.S9078>
- Wong, W.L., Su, X., Li, X., Cheung, C.M.G., Klein, R., Cheng, C.-Y., Wong, T.Y., 2014. Global prevalence of age-related macular degeneration and disease burden projection for 2020 and 2040: a systematic review and meta-analysis. *Lancet. Glob. Heal.* 2, e106-16. [https://doi.org/10.1016/S2214-109X\(13\)70145-1](https://doi.org/10.1016/S2214-109X(13)70145-1)
- Xia, J., Broadhurst, D.I., Wilson, M., Wishart, D.S., 2013. Translational biomarker discovery in clinical metabolomics: an introductory tutorial. *Metabolomics* 9, 280-299. <https://doi.org/10.1007/s11306-012-0482-9>
- Xia, J., Sinelnikov, I. V., Han, B., Wishart, D.S., 2015. MetaboAnalyst 3.0?making metabolomics more meaningful. *Nucleic Acids Res.* 43, W251-W257. <https://doi.org/10.1093/nar/gkv380>
- Yin, P., Peter, A., Franken, H., Zhao, X., Neukamm, S.S., Rosenbaum, L., Lucio, M., Zell, A., Häring, H.-U., Xu, G., Lehmann, R., 2013. Preanalytical aspects and sample quality assessment in metabolomics studies of human blood. *Clin. Chem.* 59, 833-45. <https://doi.org/10.1373/clinchem.2012.199257>
- Yonekawa, Y., Miller, J.W., Kim, I.K., 2015. Age-Related Macular Degeneration: Advances in Management and Diagnosis. *J. Clin. Med.* 4, 343-59.
- Young, S.P., Nessim, M., Falciani, F., Trevino, V., Banerjee, S.P., Scott, R.A.H., Murray, P.I., Wallace, G.R., 2009. Metabolomic analysis of human vitreous humor differentiates ocular inflammatory disease. *Mol. Vis.* 15, 1210-7.
- Young, S.P., Wallace, G.R., 2009. Metabolomic analysis of human disease and its

- application to the eye. *J. Ocul. Biol. Dis. Infor.* 2, 235–242.
- Yu, M., Wu, Z., Zhang, Z., Huang, X., Zhang, Q., 2015. Metabolomic Analysis of Human Vitreous in Rhegmatogenous Retinal Detachment Associated With Choroidal Detachment. *Investig. Ophthalmology Vis. Sci.* 56, 5706. <https://doi.org/10.1167/iov.14-16338>
- Yu, Z., Kastenmüller, G., He, Y., Belcredi, P., Möller, G., Prehn, C., Mendes, J., Wahl, S., Roemisch-Margl, W., Ceglarek, U., Polonikov, A., Dahmen, N., Prokisch, H., Xie, L., Li, Y., Wichmann, H.-E., Peters, A., Kronenberg, F., Suhre, K., Adamski, J., Illig, T., Wang-Sattler, R., 2011. Differences between human plasma and serum metabolite profiles. *PLoS One* 6, e21230. <https://doi.org/10.1371/journal.pone.0021230>
- Zemski Berry, K.A., Gordon, W.C., Murphy, R.C., Bazan, N.G., 2014. Spatial organization of lipids in the human retina and optic nerve by MALDI imaging mass spectrometry. *J. Lipid Res.* 55, 504–515. <https://doi.org/10.1194/jlr.M044990>
- Zeng, K., Xu, H., Chen, K., Zhu, J., Zhou, Y., Zhang, Q., Mantian, M., 2010. Effects of taurine on glutamate uptake and degradation in Müller cells under diabetic conditions via antioxidant mechanism. *Mol. Cell. Neurosci.* 45, 192–9. <https://doi.org/10.1016/j.mcn.2010.06.010>
- Zhang, A., Sun, H., Wang, X., 2012. Saliva metabolomics opens door to biomarker discovery, disease diagnosis, and treatment. *Appl. Biochem. Biotechnol.* 168, 1718–27. <https://doi.org/10.1007/s12010-012-9891-5>
- Zhang, C., Hong, H., Mendrick, D.L., Tang, Y., Cheng, F., 2015. Biomarker-based drug safety assessment in the age of systems pharmacology: from foundational to regulatory science. *Biomark. Med.* 9, 1241–1252. <https://doi.org/10.2217/bmm.15.81>
- Zhou, L., Beuerman, R.W., 2012. Tear analysis in ocular surface diseases. *Prog. Retin. Eye Res.* 31, 527–550. <https://doi.org/10.1016/j.preteyeres.2012.06.002>
- Zhou, L., Beuerman, R.W., Foo, Y., Liu, S., Ang, L.P.K., Tan, D.T.H., 2006. Characterisation of human tear proteins using high-resolution mass spectrometry. *Ann. Acad. Med. Singapore* 35, 400–7.
- Zhou, Z., Tu, J., Zhu, Z.-J., 2017. Advancing the large-scale CCS database for metabolomics and lipidomics at the machine-learning era. *Curr. Opin. Chem. Biol.* 42, 34–41. <https://doi.org/10.1016/j.cbpa.2017.10.033>
- Ziegelstein, R., 2017. Personomics: The Missing Link in the Evolution from Precision Medicine to Personalized Medicine. *J. Pers. Med.* 7, 11. <https://doi.org/10.3390/jpm7040011>
- Ziig, B., Bernard, S., Alkass, K., Berg, S., Druid, H., 2015. A new model for the estimation of time of death from vitreous potassium levels corrected for age and temperature. *Forensic Sci. Int.* 254, 158–166. <https://doi.org/10.1016/j.forsciint.2015.07.020>

Figure captions

Figure 1. Schematic representation of metabolomics' concept, characterizing the downstream of the genetic transcription process, also influenced by environmental exposures, and thus being the closest representation of the phenotype.

Figure 2. Example of ¹H plasma nuclear magnetic resonance spectroscopy (NMR) spectra of a normal subject. a) standard 1D spectrum; b) CPMG spectrum; c) diffusion-edited spectrum. Signal assignment: 1-lactate; 2-alanine; 3 -glutamine; 4- glucose; 5-isoleucine; 6-leucine; 7-valine; 8-lysine; 9-acetate; 10-pyruvate; 11-citrate; 12-creatine; 13-creatinine; 14-dimethyl sulfone; 15-TMAO, trimethylamine-*N*-Oxide; 16,proline; 17-methanol; 18-glycine; 19-tyrosine; 20-histidine; 21- phenylalanine; 22-formate; 23-C18H cholesterol; 24-CH₃ lipids; 25-(CH₂)_n lipids; 26-CH₂CH₂CO lipids; 27-CH₂CH₂C=C lipids; 28-CH₂C=C lipids; 29-CH₂CO lipids; 30-C=CCH₂CH=C lipids; 31-albumin lysil groups; 32-N(CH₃)₃ choline; 33-glycerol C1,3H; 34-glycerol C1,3H'; 35-glycerol C2H; 36-HC=CH lipids; 37-NH protein region.

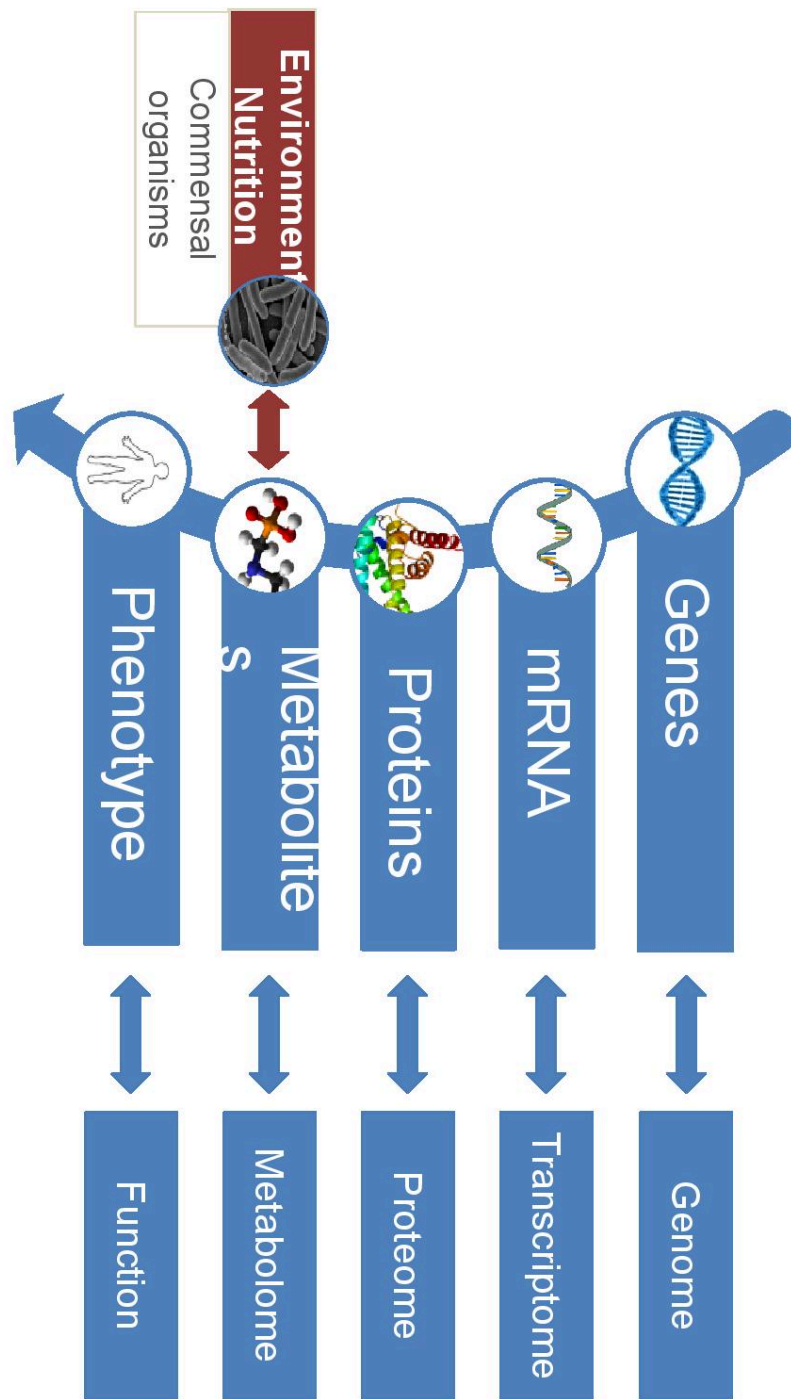
Figure 3. Example of principal component analysis (PCA) scatter plot. PC – principal component. In the graph, the x-axis corresponds to PC1 and the y axis to PC2.

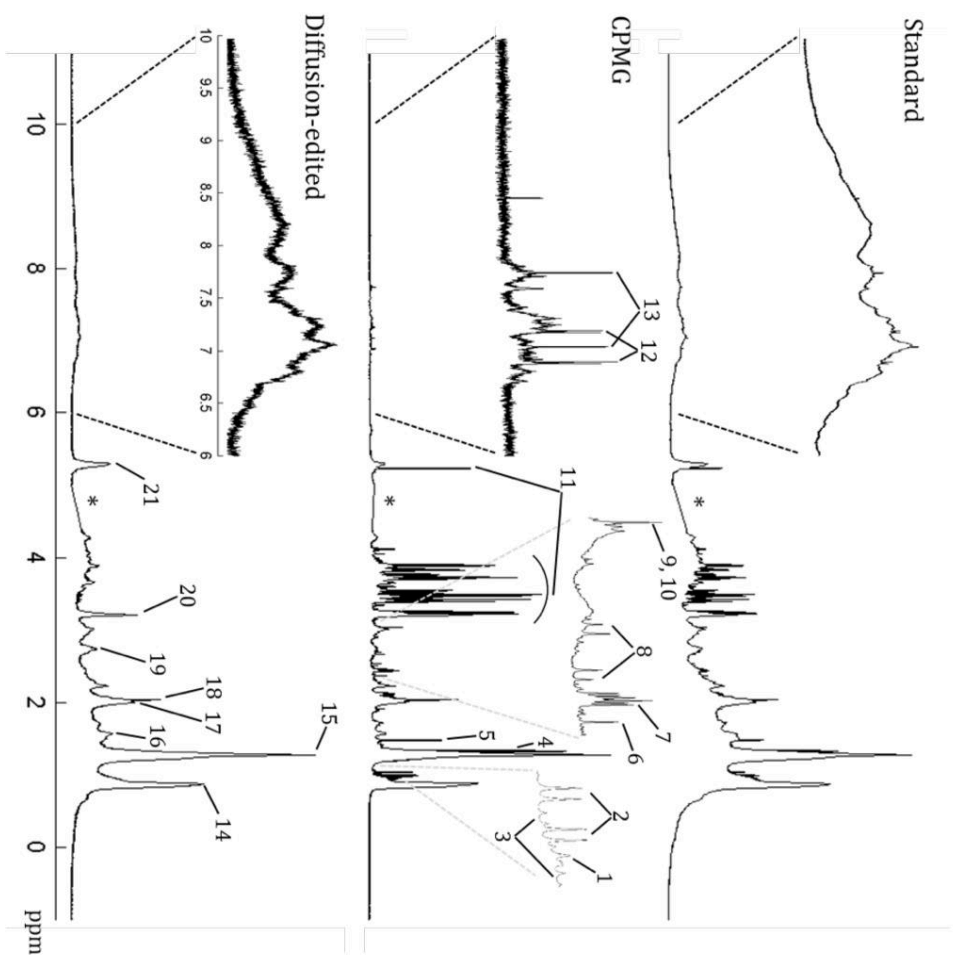
Figure 4. Example of partial least square discriminant analysis (PLS-DA) scores plot. In the graph, the x-axis corresponds to component 1 and the y axis to component 2.

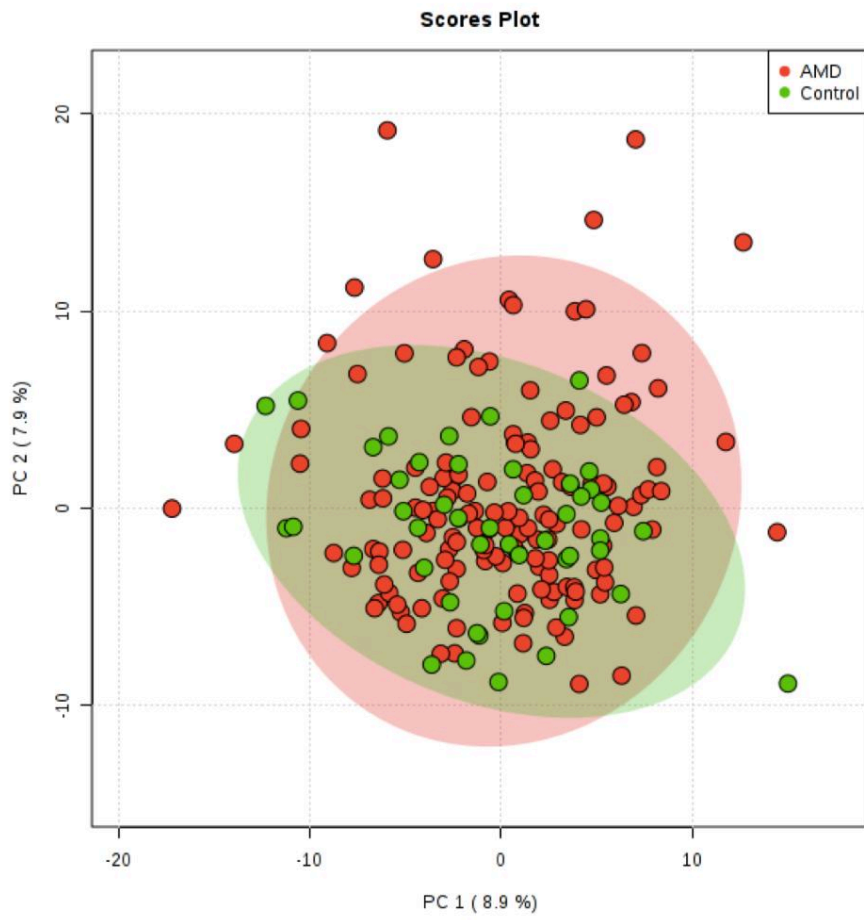
Figure 5. Example of receiver operator curve (ROC) analysis comparing two models (baseline model vs model including also metabolomics' information). AUC – area under the curve; CI – confidence interval.

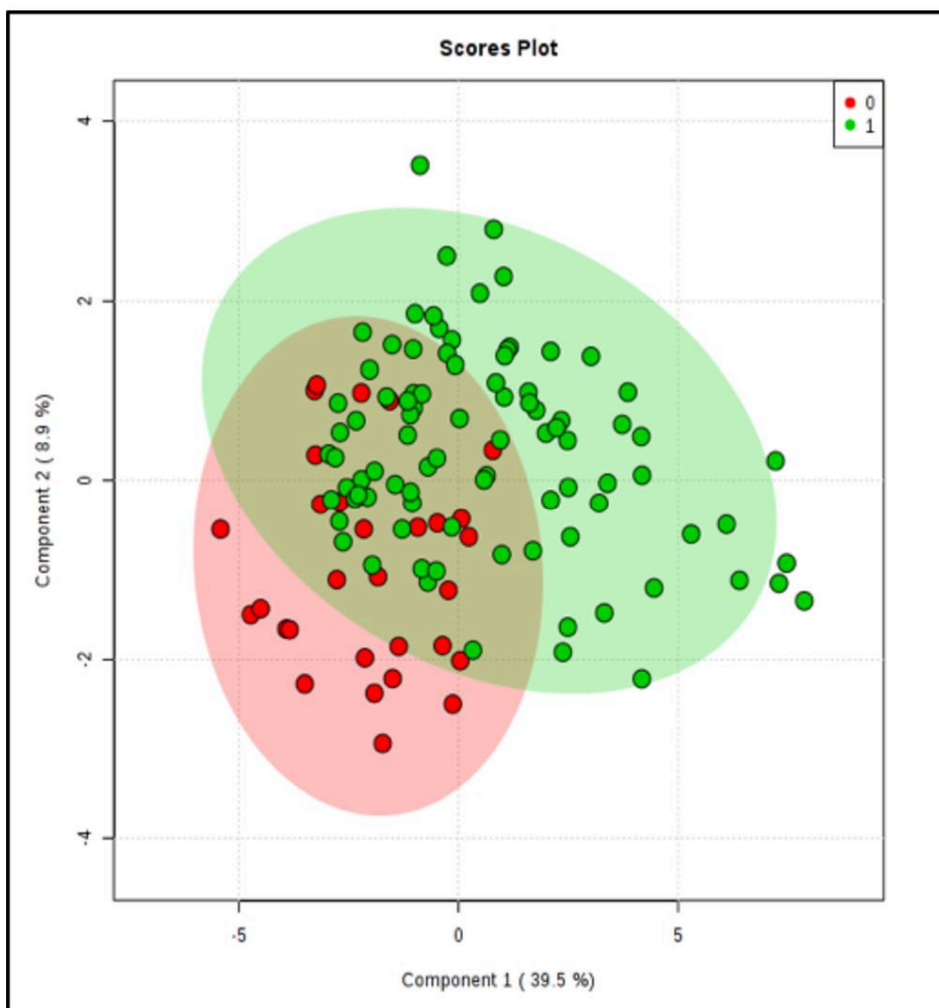
Figure 6. Color fundus photograph of a left eye with intermediate age-related macular degeneration. In the macula, the presence of intermediate and large confluent drusen can be appreciated.

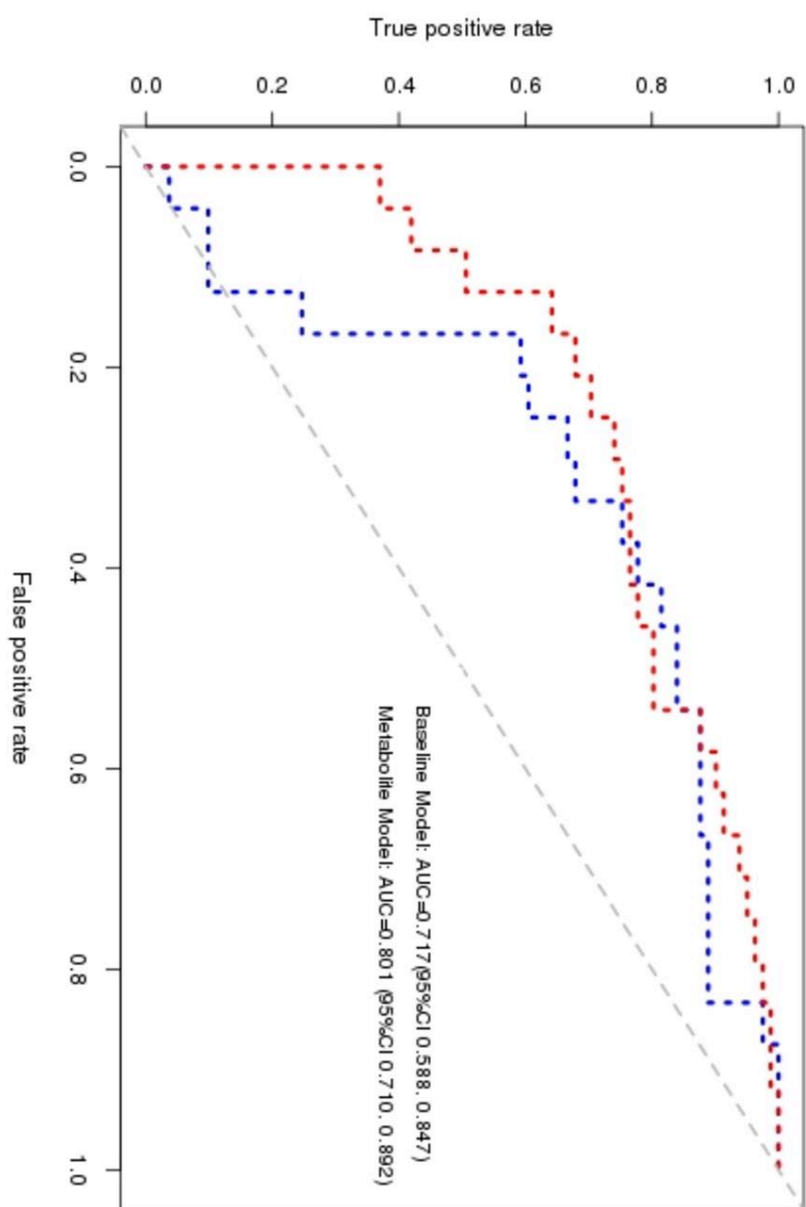
Figure 7. Pathway analysis from a study performed by our group (reference 142) comparing plasma metabolomic profiles of subjects with AMD and a control group. As shown, there is a significant enrichment of the glycerophospholipids' pathway. -log(p) – minus logarithm of the p-value.













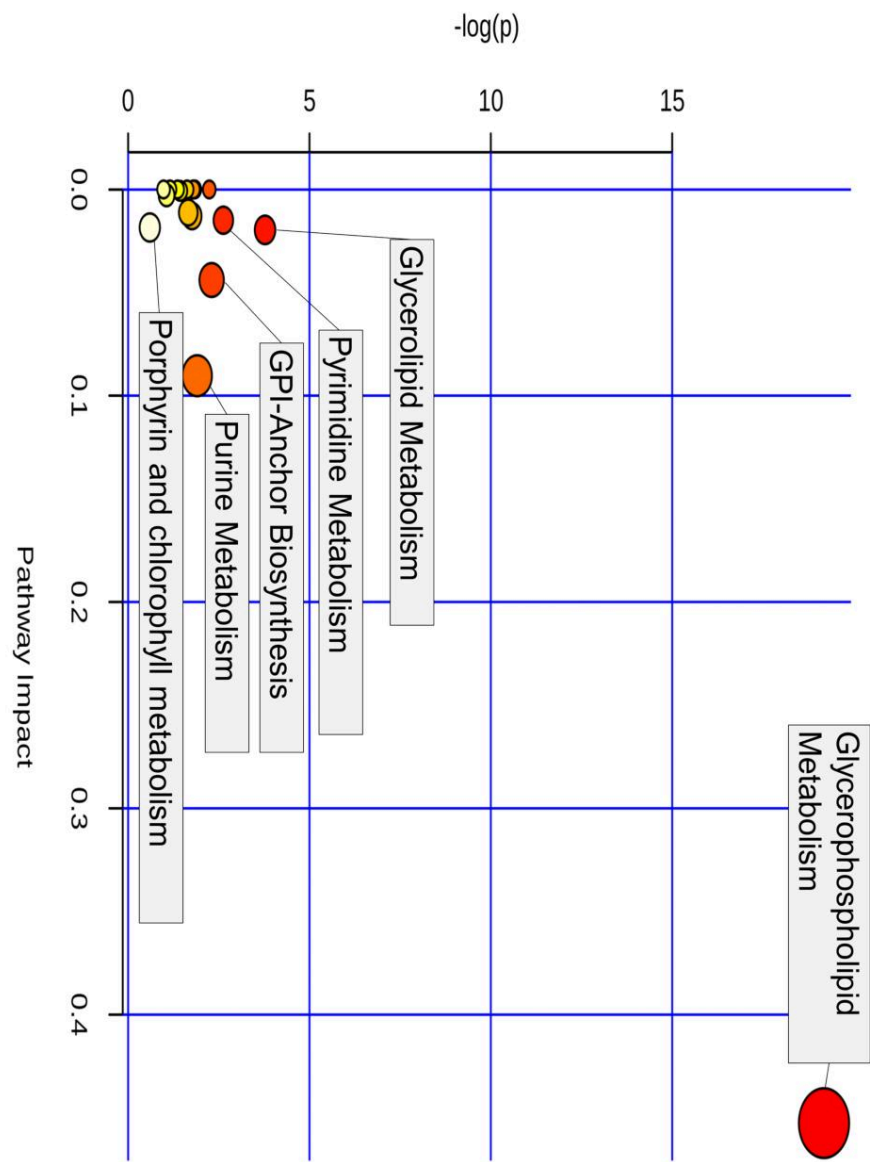


Table 1. Selected literature on the application of metabolomics to the study of retinal diseases

Condition	Authors	Year	Specific focus	Type of samples analyzed	Analytical tool	Sample size
Diabetic retinopathy	Barba et al.	2010	PDR	human vitreous	¹ H-NMR	22 per group
	Paris et al.	2016	PDR	human vitreous and oxidant-induced retinopathy mouse model (whole eye)	LC-MS	9 to 20 per group
Retinal detachment	Li et al.	2011	DR Western and Chinese medicine	human plasma	GC-MS	25 to 50 per group
	Li et al.	2014	RRD and PVR	human vitreous	LC-MS	6 to 9 per group
	Yu et al.	2015	RRD and choroidal detachment	human vitreous	LC-MS	14 to 15 per group
AMD	Osborn et al.	2013	Choroidal neovascularization	human plasma	LC-MS	19 to 26 per group
	Lains et al.	2017	AMD and AMD severity stages	human plasma	¹ H-NMR	30 to 45 per group
	Lains et al.	2017	AMD and AMD severity stages	human plasma	LC-MS	30 per group
	Li et al.	2016	Polypoidal choroidal vasculopathy	human plasma	LC-MS	19 to 21 per group
	Rowan et al.	2017	AMD, diet influence and microbiome	plasma, urine and feces of aged-mouse model	LC-MS plasma and ¹ H-NMR urine	4 to 11 per group
Macular telangiectasia	Scerri et al.	2017	MacTel type 2	human serum	LC-MS	50 per group
	Young et al.	2009	Vitreoretinal disorders (mostly uveitis)	human vitreous	¹ H-NMR	2 to 20 per group
Others	D'Alessandro et al.	2014	Retinal ischemia and effect of neuroprotectors	ex vivo mouse retinas (whole retina) deprived oxygen	LC-MS	5 per group
	Kurihara et al.	2016	Hypoxia induced stress in RPE	mice choroid/RPE complex (non-retinal)	LC-MS	4-6 per genotype
	Luan et al.	2018	Hibernating retina	hibernating squirrels	GC and LC-MS	6 per condition
	Solberg et al.	2013	Postnatal hypoxia	piglet retina after hypoxia	LC-MS	5 per condition

Chapter III: Phenotype

The diagnosis of AMD is based on the presence of the characteristic fundus abnormalities of this condition: drusen and focal pigmentation changes in its early/intermediate stages, which may progress to retinal atrophy and choroidal neovascularization in the advanced forms of the disease.^{71,72} Currently, despite all the advances in imaging, the gold-standard for AMD classification, both for clinical and research purposes, remains the detection of these features on film color photographs and high-resolution digital color images of the macula.^{41,42,72,73} In this project, we realized that the properties of the digital color fundus photographs (CFP) that we obtained were extremely variable, both when comparing our two study sites, and within the same study site. Our research revealed that previous studies on AMD that had assessed digital photographic quality and implemented approaches to improve it relied on manual procedures applied to individual photographs.⁷⁴ Therefore, we developed and tested software to automatically standardize the brightness, contrast and color balance of digital CFP. This work is described in Manuscript 4, where we demonstrated that this software enables a rapid and accurate standardization of CFP for AMD grading.

After standardization, the obtained CFP were used for AMD classification and staging, as this remains the gold-standard, as described. However, as discussed, we included other imaging modalities to improve our phenotypic characterization of this cohort,⁴³ and to contribute to the understanding of the wide-spectrum of presentations that AMD can assume, especially in the so-called “intermediate stages”.⁵⁰ This is particularly relevant bearing in mind that a precise phenotype is crucial for any ‘omics study.

One of the features that is not included in AMD classification schemes and seems particularly relevant are subretinal drusenoid deposits (SDD). These are commonly present in eyes with AMD, with or without concomitant classic drusen, and seem to have a prognostic value.⁴⁹ The pathogenesis of SDD remains only partially understood, but choroidal vasculature might play a role.^{75,76,77} Prior studies described a reduced subfoveal choroidal thickness (CT) in the presence of these subretinal lesions, using the enhanced depth imaging (EDI) protocol for spectral-domain OCT (SD-OCT).^{76,78} Using the advantages of SS-OCT we examined the association between the presence of SDD and macular choroidal thickness (CT). Our results revealed that the presence of these lesions was associated with a significant decrease in mean CT. Eyes with SDD also showed a statistically significant reduction in macular choroidal vessel volume as compared to eyes without SDD. This work is described in Manuscript 5, and its results are in agreement with recent reports by other groups highlighting that disease expression of non-exudative AMD seems to vary with choroidal thickness.⁴⁹ Altogether, this suggests that distinct drusen phenotypes (including SDD) and choroidal characteristics

probably need to be considered in future AMD classification schemes and studies that need a thorough phenotypic characterization, as it is our case.

Patients with AMD also seem to have a higher prevalence of peripheral changes than people of the same age without AMD.^{46,47,48} This has been noted by clinicians, and described since the early 1970s,^{79,80,81} but it has become particularly evident with the recent development of imaging techniques, including ultra-widefield (UWF) imaging,⁸² which has allowed the systematic study of peripheral changes.⁸³ Additionally, some studies have linked peripheral changes with genetic polymorphisms associated with AMD,^{84,85,86} thus further suggesting that this blinding disease may not be limited to the macula. In this context, we assessed UWF images of the patients of our cohort. We realized that, despite previous work on refinement of grids that can be used for grading of peripheral abnormalities on AMD, these presented important limitations, including the fact that these images are distorted in the periphery and hence do not reflect the actual dimensions of the retina. Therefore, we developed a UWF imaging-based grid grading system that incorporates correction for peripheral image distortion and defines regions of the periphery – Manuscript 6. This approach is now being used to assess our pseudocolor and autofluorescence UWF for other manuscripts, which are currently in preparation.

With the characterization of refined AMD phenotypes and the understating of their relevance for the assessment of the disease and its progression, it is also crucial to understand the visual consequences of each type of AMD feature.⁸⁷ Work in this field has been limited, and mostly focused on visual acuity (VA), the standard measurement to evaluate vision. VA is used around the world and serves as a legal standard for disability assessment. However, VA loss typically occurs late in AMD course,⁵¹ making it a less useful measure of retinal function in early and intermediate AMD.⁸⁸

Time to dark-adapt has been recently suggested as one of the most promising functional metrics for AMD.^{89,90} Dark adaptation (DA) seems to differentiate AMD from healthy eyes, as well as detecting the different stages of the disease.^{51,56,91,92} Most of the published literature about DA in AMD characterized the disease using color fundus photographs.^{51,91,92} Yet, as described, OCT offers several important advantages in the assessment of AMD pathology.^{93,94,95} Little had been published about the relationship between time to dark-adapt and structural OCT changes in AMD.^{96,97,98} Therefore, we set out to better define this structure function relationship of OCT and DA in AMD – Manuscript 7. In this study, we used SD-OCT to assess macular morphology in a cohort of AMD and healthy eyes, and evaluated the time to dark-adapt, measuring as rod intercept time (RIT). Unlike previous work, we evaluated OCT abnormalities in the DA testing area (DA testing spot), in addition to the entire macula. Our results revealed that, even accounting for age and AMD stage, the presence of any

abnormalities on OCT within the DA testing spot and in the macula overall, were significantly associated with impairments in DA. Interestingly, in eyes with no structural changes within the DA testing spot, the presence of abnormalities on OCT in the remaining macula was also associated with delayed RITs. This finding supports that DA is a good test for detecting abnormalities in the entire macula and not just within the DA testing spot. When looking at the specific structural lesions, multivariable analyses revealed that the presence of subretinal drusenoid deposits and ellipsoid disruption, whether within the DA testing spot or the macula overall, were consistent predictors of impaired DA.

Despite acceptance of the association of AMD with a prolonged time to dark-adapt, the interaction with other health parameters that are known to affect AMD incidence and progression remains only partially understood. Prior groups⁹⁹ had studied the association between DA time and several health parameters known to increase AMD risk, such as smoking and body mass index (BMI), on older adults with normal maculae. Their main focus was on how these conditions might lead to a transition from normal aging to disease; however, these same parameters also affect AMD severity and progression. Before adopting DA as a useful measure of retinal dysfunction in AMD, the effect of other conditions on the time to dark-adapt should be studied.¹⁰⁰ In this context, we evaluated the influence of various health conditions, as well as known AMD risk factors, on DA in a clinic-based sample of patients with AMD in different stages of disease and our control group – Manuscript 8. In this study, we observed that after controlling for age and AMD stage, known to impact DA, a higher BMI and a family history of AMD were also significantly associated with a prolonged time to dark-adapt. Similar results were observed when abnormal DA (≥ 6.5 minutes) was considered as the outcome. Even after controlling for age and AMD stage, a higher daily alcohol intake was also significantly associated with increased odds of presenting abnormal DA.

The above-mentioned manuscripts can be found in the next pages.

Automated Brightness and Contrast Adjustment of Color Fundus Photographs for the Grading of Age-Related Macular Degeneration

Edem Tsikata^{1,2*}, Inês Laíns^{1,3,4,5,6*}, João Gil^{3,4,5}, Marco Marques^{3,5}, Kelsey Brown¹, Tânia Mesquita⁵, Pedro Melo⁵, Maria da Luz Cachulo^{3,4,5}, Ivana K. Kim^{1,6}, Demetrios Vavvas^{1,6}, Joaquim N. Murta^{3,4}, John B. Miller^{1,6}, Rufino Silva^{3,4,5}, Joan W. Miller^{1,6}, Teresa C. Chen^{1,2}, and Deeba Husain^{1,6}

¹ Massachusetts Eye and Ear, Department of Ophthalmology, Harvard Medical School, Boston, MA, USA

² Glaucoma Service of Massachusetts Eye and Ear, Harvard Medical School, Boston, MA, USA

³ University of Coimbra, Faculty of Medicine, University of Coimbra, Coimbra, Portugal

⁴ Centro Hospitalar e Universitário de Coimbra, Coimbra, Portugal

⁵ Association for Biomedical Research and Innovation on Light and Image, Coimbra, Portugal

⁶ Retina Service of Massachusetts Eye and Ear, Harvard Medical School, Boston, MA, USA

Correspondence: Deeba Husain, Massachusetts Eye and Ear, Harvard Medical School, 243 Charles Street, 12th Floor, Boston, MA, USA. e-mail: Deeba_Husain@meei.harvard.edu

Received: 25 November 2016

Accepted: 22 January 2017

Published: 13 March 2017

Keywords: image analysis; age-related macular degeneration; automated optimization

Citation: Tsikata E, Laíns I, Gil J, Marques M, Brown K, Mesquita T, Melo P, da Luz Cachulo M, Kim IK, Vavvas D, Murta JN, Miller JB, Silva R, Miller JW, Chen TC, Husain D. Automated brightness and contrast adjustment of color fundus photographs for the grading of age-related macular degeneration. *Trans Vis Sci Tech.* 2017;6(2):3. doi:10.1167/tvst.6.2.3
Copyright 2017 The Authors

Purpose: The purpose of this study was to develop an algorithm to automatically standardize the brightness, contrast, and color balance of digital color fundus photographs used to grade AMD and to validate this algorithm by determining the effects of the standardization on image quality and disease grading.

Methods: Seven-field color photographs of patients (>50 years) with any stage of AMD and a control group were acquired at two study sites, with either the Topcon TRC-50DX or Zeiss FF-450 Plus cameras. Field 2 photographs were analyzed. Pixel brightness values in the red, green, and blue (RGB) color channels were adjusted in custom-built software to make the mean brightness and contrast of the images equal to optimal values determined by the Age-Related Eye Disease Study (AREDS) 2 group.

Results: Color photographs of 370 eyes were analyzed. We found a wide range of brightness and contrast values in the images at baseline, even for those taken with the same camera. After processing, image brightness variability (brightest image–dimmest image in a color channel) was reduced 69-fold, 62-fold, and 96-fold for the RGB channels. Contrast variability was reduced 6-fold, 8-fold, and 13-fold, respectively, after adjustment. Of the 23% images considered nongradable before adjustment, only 5.7% remained nongradable.

Conclusions: This automated software enables rapid and accurate standardization of color photographs for AMD grading.

Translational Relevance: This work offers the potential to be the future of assessing and grading AMD from photos for clinical research and teleimaging.

Introduction

Age-related macular degeneration is the leading cause of adult blindness in developed countries and the third leading cause worldwide.^{1,2} Diagnosis of AMD is based on the presence of the characteristic fundus abnormalities of this condition: drusen and focal pigmentation changes in its early stages, which

may progress to retinal atrophy and choroidal neovascularization in the advanced forms of the disease.^{3,4} At this time the gold standard for classification of AMD for clinical research purposes is detection of these features on film color photographs and high-resolution digital color images of the macula.^{4–8} Despite advances in imaging, including the widespread use of optical coherence tomography (OCT), all currently validated AMD grading systems



are based on fundus color photography. Therefore, there is a great need to standardize the color images used for clinical studies.

Fundus images with optimal exposure and color balance are essential for accurate evaluation of retinal features.⁹⁻¹¹ Suboptimal images can lead to inaccurate categorization of drusen and pigment abnormalities,^{12,13} which may impede the diagnosis or correct staging of AMD. Fundus photograph quality has several contributing factors, including patient factors (media opacities and pupil size),⁹ camera properties (sensor resolution and chromatic response), image-processing software, and photographer techniques (exposure settings and focus). Cameras with the same optics and sensors can produce varying output depending on the color profiles specified by the camera manufacturer or photographers. With so many pitfalls, substandard images have been reported to be as high as 20% in clinical studies.^{11,14} Even with best practice, acquisition of consistently high-quality images cannot be guaranteed at the time of capture. Post hoc standardization¹⁵ is therefore necessary for AMD grading.¹⁶

Previous AMD studies^{6,16} assessed digital photographic quality and implemented approaches to improve color balance, brightness, and contrast. Specifically, Hubbard et al. in the Age-Related Eye Disease Study (AREDS) 2 trial, developed an enhancement procedure based on adjustment of the three-color luminance histograms.¹⁶ Though this approach improved the contrast and brightness of the fundus images, it relied on manual procedures applied to individual photographs.

The aim of this study was to develop and test software to automatically standardize the brightness, contrast, and color balance of digital fundus photographs. The effects of the standardization procedure on image quality and the staging of AMD were also investigated. Using the optimal image parameters established by the AREDS 2 group,¹⁶ digital images from two types of cameras were batch-processed to standardize their color characteristics prior to AMD grading.

Methods

This work is part of a prospective, multicenter study on AMD biomarkers. The software was developed at the Massachusetts Eye and Ear (MEE) (Boston, USA). The program was clinically tested at MEE (designated site A) and at the Faculty of Medicine of the University of Coimbra (FMUC) in

collaboration with the Association for Innovation and Biomedical Research on Light and Image (AIBILI) and the Coimbra University Hospital (designated site B).

The study was approved by the institutional review boards of MEE, FMUC, and AIBILI and by the Portuguese National Data Protection Committee. All participants provided written informed consent. The study was conducted in accordance with the Health Insurance Portability and Accountability Act requirements and the tenets of the Declaration of Helsinki.

Study Population and Procedures

From January 2015 to July 2016, we recruited patients with a diagnosis of AMD and a control group of subjects without any evidence of the disease in both eyes, aged 50 years or older. For both, the exclusion criteria included diagnosis of any other vitreoretinal disease, active uveitis or ocular infection, significant media opacities that precluded the observation of the ocular fundus, refractive error equal to or greater than 6 diopters of spherical equivalent, past history of retinal surgery, history of any ocular surgery or intraocular procedure (such as laser and intraocular injections) within the 90 days prior to enrollment, and diagnosis of diabetes mellitus, with or without concomitant diabetic retinopathy (due to the remaining study purposes). At site A, participants were consecutively recruited at the Retina Service and the Comprehensive Ophthalmology and Optometry Services when they came for their regular appointments. The study population in site B was derived from a population-based cohort study.¹⁷ All subjects with an established diagnosis of any stage of AMD were invited to participate. Subjects without signs of AMD in the prior evaluation¹⁷ were also invited and were included as controls if they remained without the disease (see AMD Diagnosis and Staging). Those who presented with AMD at the time of the current evaluation were also considered but included in the AMD study group.

All participants underwent a comprehensive eye exam, including measurement of best-corrected visual acuity, current refraction, intraocular pressure, biomicroscopy, and dilated fundus exams. Nonstereoscopic, seven-field fundus photographs were obtained with one of two types of cameras: Topcon TRC-50DX (Topcon Corporation, Tokyo, Japan), with a 35-degree field of view, or Zeiss FF-450 Plus (Carl Zeiss Meditec Inc., Dublin, CA) with a 30-degree field of view. These cameras used charge coupled device (CCD) sensors: Topcon cameras—Pike 11MP CCD

(site A) and Nikon D2H (site B); Zeiss camera—Escalon E5 (site A).

AMD Diagnosis and Staging

For AMD diagnosis and staging, two independent experienced graders analyzed all field 2 CFP (IL, JG), according to the AREDS classification system.^{18,19} In cases of disagreement, a senior author (RS or DH) established the final categorization. Images taken with Topcon cameras were evaluated with IMAGENet 2000 software (version 2.56; Topcon Medical Systems), and those obtained with a Zeiss camera were observed using VISUPAC (version 4.5.1; Carl Zeiss Meditec). We adopted the most recent AREDS 2 definitions,¹⁹ namely that the standard disc diameter equals 1800 μm , which affects the size of the Early Treatment Diabetic Retinopathy Study grid and of the standard drusen circles, and that geographic atrophy (GA) is present if the lesion has a diameter equal or superior to 433 μm (AREDS circle I-2) and at least two of the following features are present: absence of RPE pigment, circular shape, or sharp margins (thus meaning that the involvement of the central fovea is not a requirement). Therefore, briefly, we established the following groups^{18,19}: controls—presence of drusen of maximum size < circle C0 and total area < C1; early AMD—drusen of maximum size \geq C0 but < C1 or presence of AMD characteristic pigment abnormalities in the inner or central subfields; intermediate AMD—presence of drusen maximum size \geq C1 or of drusen maximum size \geq C0 if the total area occupied is > I2 for soft indistinct drusen and > O2 for soft distinct drusen; and late AMD—presence of GA according to the criteria described above or evidence of neovascular AMD.

Image Processing

In this study, image brightness is based on the pixel intensities for each color channel. Contrast quantifies the variation in the pixel intensities and is measured as four times the standard deviation of the pixel intensity values in each color channel. Color balance is calculated as the ratio of the green and blue channel brightness values to the brightness of the red channel (the brightest channel).

The software program was written in the C++ language, and the Open Computer Vision library (OpenCV version 2.4.3; Willow Garage, Menlo Park, CA) was used for image processing. The graphical

user interface was constructed in the Qt application development framework (Qt 4.8; The QT Company, Oslo, Norway). To analyze each digital photograph, the retinal image was automatically extracted and the brightness and contrast in the red, green, and blue (RGB) color channels measured. In this report, image contrast is synonymous with the standard deviation of the brightness, and the span of a color curve is defined as four times the standard deviation. This definition of the span encompasses 95.5% of the brightness values in the distribution (2 SD above and below the mean). Topcon images had a pure black border, which could readily be distinguished from the retinal picture. For Zeiss images, which had a border that was not completely black, a circular mask of radius 1226 pixels was used to extract the retinal picture. Within the region identified as the retinal image, the pixel values were read by the software, and the mean and standard deviation of the brightness of the RGB channels were calculated.

To enhance image contrast, contrast ratios were calculated by dividing the ideal curve spans by the measured spans. Pixel brightness values were then multiplied by the appropriate contrast ratios to achieve the target image contrast in each color channel. To achieve the target brightness values, constant terms were added to the scaled pixel values to make the overall image brightness equal to the targets.

A mathematical description of these concepts is presented below.

$$\alpha = \Delta_{\text{ideal}}/4\sigma,$$

where α is the contrast ratio, Δ_{ideal} is the ideal brightness span, and σ is the standard deviation of the color channel.

Capitalized symbols refer to global image properties. Lowercase symbols denote pixel values.

$$x_{\text{final}} = \alpha x_{\text{initial}} + (X_{\text{ideal}} - \alpha X_{\text{mean}}),$$

where X_{ideal} is the ideal image brightness, X_{mean} is the mean brightness of the original image, x_{initial} is an initial pixel brightness, and x_{final} is the transformed pixel brightness.

Statistical Analysis of Data

We collected and managed study data using REDCap electronic data capture tools hosted at MEE.²⁰ Mean, standard deviation, and ranges were

Table 1. Demographic Characteristics of the Study Population, Organized by Study Site and Camera Used

Study Site Camera (sensor)	Site A		Site B	Total, <i>n</i> = 370
	Topcon TRC-50DX (Pike 11 MP CCD), <i>n</i> = 114	Zeiss FF-450 (Escalon E5 CCD), <i>n</i> = 33	Topcon TRC-50DX (Nikon D2H CCD), <i>n</i> = 223	
Image format and number (%)				
TIFF	102 (89.5)	0 (0)	0 (0)	102 (27.6)
JPEG	11 (9.6)	0 (0)	223 (100)	234 (63.2)
PNG	1 (0.9)	33 (100)	0 (0)	34 (9.2)
Age, <i>y</i> , mean ± SD	71.4 ± 7.8	76.9 ± 6.5	73.1 ± 8.1	72.9 ± 8.0
Gender, number (%)				
Female	71 (62.3)	23 (69.7)	151 (67.7)	245 (66.2)
Male	43 (37.7)	10 (30.3)	72 (32.3)	136 (33.8)
Race and number (%)				
White	102 (89.5)	32 (97.0)	221 (99.1)	355 (96.0)
Black	0 (0)	0 (0)	2 (0.9)	2 (0.5)
Other	2 (1.7)	0 (0)	0 (0)	2 (0.5)
Unknown	10 (8.8)	1 (3.0)	0 (0)	11 (3.0)
Laterality, number (%)				
OD	57 (50.0)	19 (5.1)	114 (30.8)	190 (51.4)
OS	57 (50.0)	14 (3.8)	109 (29.5)	180 (48.6)
Lens and number (%)				
Phakic	92 (25.0)	22 (57.6)	197 (88.3)	311 (84.1)
Pseudophakic	22 (5.9)	11 (32.4)	26 (11.7)	59 (15.9)
AMD stage and number (%)				
Control	26 (22.8)	0 (0.0)	60 (26.9)	86 (23.2)
Early AMD	14 (12.3)	4 (12.1)	47 (21.1)	65 (17.6)
Intermediate AMD	51 (44.7)	12 (36.4)	89 (39.9)	152 (41.1)
Late AMD	20 (17.5)	15 (45.5)	11 (4.9)	46 (12.4)
Not gradable*	3 (2.6)	2 (6.1)	16 (7.2)	21 (5.7)

Unknown data for race refers to included participants who decided not to provide this information. TIFF, Tagged Image File Format; JPEG, Joint Photographic Experts Group; PNG, Portable Network Graphics; SD, standard deviation; OD, right eye; OS, left eye; AMD, Age-related Macular Degeneration.

* Images not gradable even after adjustment with the developed software.

used to summarize image data, and the characteristics of different types of images and cameras were compared with *t*-tests. Two independent experienced graders masked to the diagnosis (IL and JG) evaluated all images before adjustment and classified them as gradable (if the grader felt able to stage AMD with confidence) or nongradable (if this was not the case). After software processing, the process was repeated for the originally nongradable images. All statistical analysis was performed using Stata (version 12.1; StataCorp LP, College Station, TX) and *P* values < 0.05 were considered statistically significant.

Results

Imaging Properties of the Entire Sample Set before and after Adjustment

We included field 2 color fundus photographs of 370 eyes of 370 subjects with a mean age of 72.9 ± 8.0 years old. The laterality of the eyes was randomly selected using the RAND function in Microsoft Excel (Microsoft Corporation, Redmond, WA). Sixty-six percent of the subjects (*n* = 245) were female. [Table 1](#) presents the demographic characteristics of the

Table 2. Brightness, Standard Deviation of Brightness and Color Balance Ratios for the Analyzed 370 Images before and after Automated Image Enhancement

	Before	After
Brightness parameters		
Red brightness		
Mean \pm SD	155.0 \pm 40.5	191.7 \pm 0.4
Range	52.5–231.1	190.0–192.6
Green brightness		
Green mean \pm SD	72.3 \pm 22.1	96.1 \pm 0.2
Range	15.7–115.5	95.2–96.8
Blue brightness		
Mean \pm SD	25.5 \pm 12.2	32.0 \pm 0.1
Range	0.07–76.8	31.6–32.4
Contrast parameters		
SD red brightness		
Mean \pm SD	25.4 \pm 6.9	30.7 \pm 1.2
Range	11.4–54.5	24.8–32.6
SD green brightness		
Mean \pm SD	16.3 \pm 5.2	31.1 \pm 0.9
Range	4.6–42.8	27.1–32.1
SD blue brightness		
Mean \pm SD	7.5 \pm 3.3	8.0 \pm 0.1
Range	0.9–20.7	6.8–8.3
YCrCb colorspace parameters		
Intensity Y		
Mean \pm SD	91.7 \pm 24.9	117.3 \pm 0.2
Range	28.3–135.8	116.6–118.0
Chrominance red difference (Cr)		
Mean \pm SD	173.1 \pm 13.2	181.0 \pm 0.2
Range	138.2–202.8	180.2–181.3
Chrominance blue difference (Cb)		
Mean \pm SD	90.6 \pm 11.7	79.9 \pm 0.1
Range	64.7–116.3	79.5–80.3
Color balance parameters		
Green/Red ratio		
Mean \pm SD	0.466 \pm 0.084	0.501 \pm 0.001
Range	0.209–0.788	0.498–0.505
Blue/red ratio		
Mean \pm SD	0.167 \pm 0.082	0.167 \pm 0.0005
Range	0.000–0.549	0.165–0.169

included eyes, as well as their AMD staging, organized by study site and camera type.

Table 2 summarizes the image properties before and after software processing. The brightness and contrast values in each channel were larger after adjustment than before, and they were closer to the target values, the ideal AREDS 2 (red brightness =

192, green brightness = 96, blue brightness = 32; red span = 128, green span = 128, blue span = 32), after processing. The range of brightness values (brightest image to dimmest image) decreased 69-fold, 62-fold, and 96-fold for the RGB channels, respectively. The contrast ranges also decreased 6-fold, 8-fold, and 13-fold for the RGB channels, respectively. The range of green/red color balance values decreased 83-fold after adjustment, and the range of blue/red color balance values decreased 137-fold.

Though brightness and contrast were standardized in the RGB color space, the image parameters in the YCrCb color space also exhibited reduced variance after adjustment (Table 2). The YCrCb space describes the pixel properties using an intensity or luma coordinate (Y) and two chrominance coordinates: Cr, for the red difference, and Cb, for the blue difference.²¹ YCrCb parameters are derived from the RGB values using linear equations specified in the International Telecommunication Union–Radiocommunication standard ITU-R 601.7.²¹ The range of values decreased 77-fold, 59-fold, and 65-fold for the intensity, red difference chrominance, and blue difference chrominance, respectively.

Variations among Cameras and within the Same Camera

Baseline images from the three cameras were underexposed relative to the ideal AREDS 2 settings (Fig. 1, top panel). Automated enhancement increased the overall brightness of the images (Fig. 1, middle panel). The histograms confirmed underexposure, and the effect of the software enhancement, which was stretching of the brightness curves to improve the contrast and displacing them to the right to correct underexposure (Fig. 1 bottom panel).

Quantitative analysis confirmed initial underexposure relative to the AREDS 2 ideal values (red brightness = 192, green brightness = 96, blue brightness = 32; red span = 128, green span = 128, blue span = 32) for images from all three cameras (Table 3). Additionally, images acquired with the Topcon camera at site A (Pike 11MP sensor) were significantly underexposed compared to Topcon camera images from site B (Nikon D2H) (red: 115.2 vs. 175.8; green: 48.9 vs. 83.8; blue: 21.6 vs. 28.8; $P < 0.001$ for all). At the same site (A), Topcon camera images were also significantly underexposed relative to those taken with the Zeiss camera in the red and green channels but had comparable exposure in the blue channel (red: 115.2 vs. 132.7, $P = 0.013$; green: 48.9 vs. 70.2, $P < 0.001$; blue: 21.6 vs. 20.4,

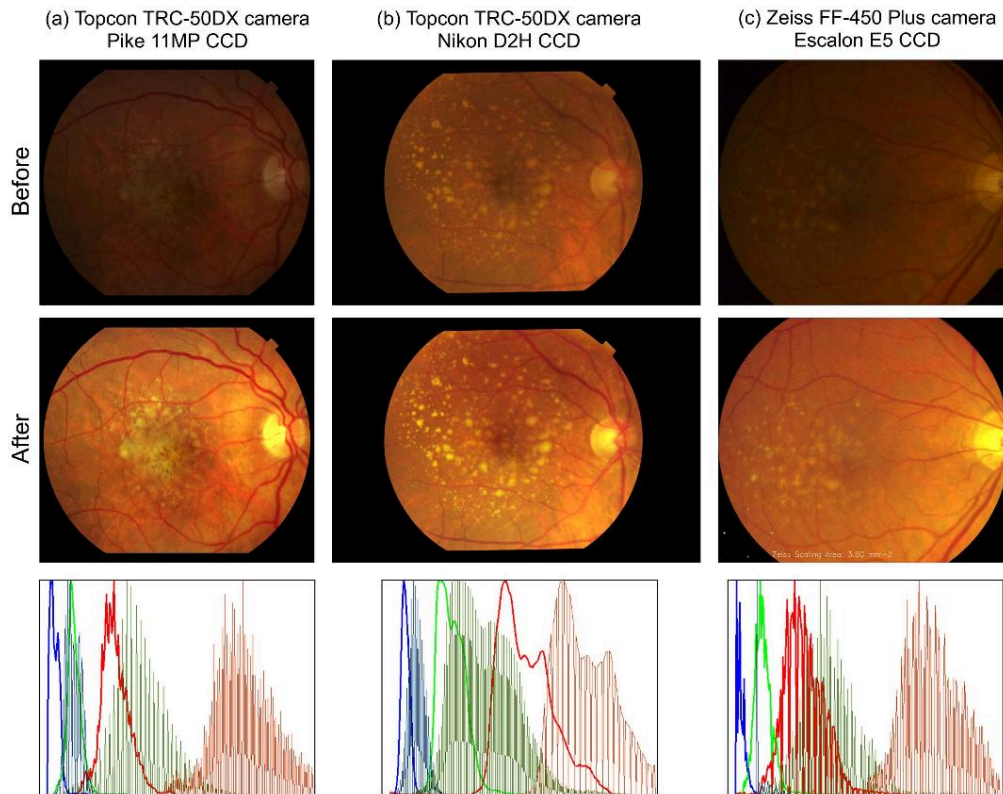


Figure 1. Figure 1a and b (*top panel*) are unmodified fundus photographs acquired with Topcon cameras. Figure 1a was acquired with a Topcon TRC-50DX camera with a Pike 11MP CCD sensor and Figure 1b with a Topcon TRC-50DX camera with a Nikon D2H CCD sensor. Figure 1c was obtained with a Zeiss FF-450 Plus camera with an Escalon E5 CCD sensor. Images in the *middle panel* were produced by processing with the automated enhancement software. In the *bottom row*, the bright *solid lines* represent the color histograms of the original images and the *thinner lines* the histograms of the standardized images.

$P = 0.697$). Before processing, the green to red color balance ratios were also significantly different among the three types of cameras ($P < 0.01$). After adjustment, the green to red color balance ratios for all three cameras were equal to 0.501 ± 0.001 . Despite the similarity in the measured values after adjustment, the differences were statistically significant ($P < 0.001$ for all comparisons). The blue to red color balance ratios were significantly different only for the Topcon Pike versus Topcon Nikon D2H sensors before adjustment (0.181 vs. 0.167 , $P = 0.024$). After adjustment, the blue to red color balance ratios of images from the two Topcon cameras were similar ($P = 0.424$).

Before processing, the brightness and contrast of the photos from the same camera exhibited variability. **Figure 2** illustrates the variation in the brightness of images from a Topcon camera (Topcon TRC-50DX, Nikon D2H sensor, site B, $n = 223$ images). The brightness values were generally below the AREDS 2 target values: 175.8 ± 21.1 versus 192, 83.9 ± 11.0 versus 96 and 28.8 ± 8.0 versus 32 for the RGB channels. After adjustment, the brightness values were consistent with the optimal AREDS 2 values: 191.7 ± 0.3 versus 192, 96.1 ± 0.2 versus 96 and 32.0 ± 0.1 versus 32 for the RGB channels, respectively.

Table 3. Mean Brightness and Color Balance Ratios for Three Types of CCD Sensors Used in This Study

Camera (sensor type) [number of images]	Before Adjustment		
	Topcon (Pike 11MP) [n = 114]	Topcon (Nikon D2H) [n = 223]	Zeiss (Escalon E5 CCD) [n = 33]
Red brightness			
Mean ± SD	115.2 ± 32.7	175.8 ± 21.1	132.7 ± 42.0
Minimum–maximum	52.5–190.8	108.2–231.1	53.6–195.1
Green brightness			
Mean ± SD	48.9 ± 18.2	83.8 ± 11.0	70.2 ± 22.2
Minimum–maximum	15.7–102.1	54.9–115.5	28.9–110.1
Blue brightness			
Mean ± SD	21.6 ± 14.5	28.8 ± 8.0	20.4 ± 18.2
Minimum–maximum	0.3–64.0	10.6–55.6	0.1–76.8
Green/red ratio			
Mean ± SD	0.424 ± 0.098	0.480 ± 0.057	0.539 ± 0.095
Minimum–maximum	0.209–0.706	0.323–0.716	0.384–0.788
Blue/red ratio			
Mean ± SD	0.181 ± 0.101	0.167 ± 0.053	0.163 ± 0.136
Minimum–maximum	0.004–0.433	0.050–0.434	0.000–0.549

Phakic and Pseudophakic Eyes

For all images obtained with a Topcon camera ($n = 337$), the average brightness in the red channel was significantly higher for subjects with natural lenses ($n = 289$) than for those with intraocular lenses ($n = 48$) (159.2 vs. 145.3 , $P = 0.034$), but comparable in the green channel (73.3 vs. 67.8 , $P = 0.130$). The average

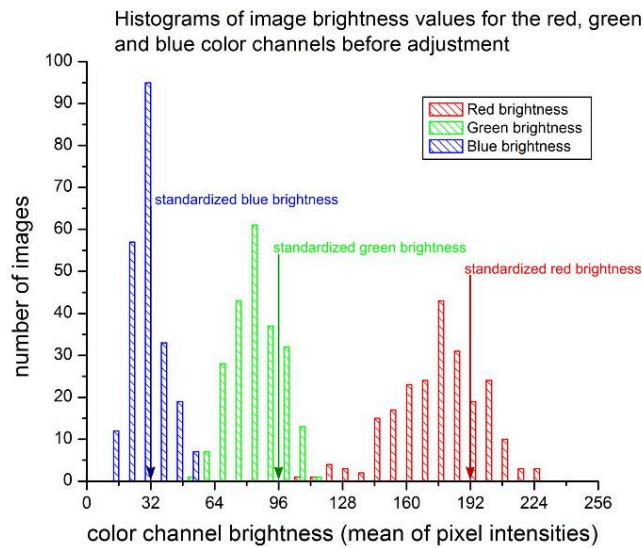


Figure 2. Comparison of the mean brightness of Topcon color photographs in the RGB channels before and after adjustment (223 images, Topcon TRC-50DX, D2H sensor). The target brightness values for the RGB channels were 192, 96, and 32.

Table 3. Extended

Camera (sensor type) [number of images]	After Adjustment		
	Topcon (Pike 11MP) [n = 114]	Topcon (Nikon D2H) [n = 223]	Zeiss (Escalon E5 CCD) [n = 33]
Red brightness			
Mean \pm SD	191.5 \pm 0.4	191.7 \pm 0.4	191.6 \pm 0.3
Minimum–maximum	190.0–192.0	190.6–192.6	190.5–192.2
Green brightness			
Mean \pm SD	95.9 \pm 0.1	96.1 \pm 0.2	96.0 \pm 0.1
Minimum–maximum	95.2–96.1	95.7–96.8	95.8–96.4
Blue brightness			
Mean \pm SD	32.0 \pm 0.1	32.0 \pm 0.1	32.0 \pm 0.1
Minimum–maximum	31.6–32.2	31.7–32.4	31.6–32.3
Green/red ratio			
Mean \pm SD	0.501 \pm 0.001	0.501 \pm 0.001	0.501 \pm 0.001
Minimum–maximum	0.498–0.505	0.499–0.504	0.499–0.504
Blue/red ratio			
Mean \pm SD	0.167 \pm 0.001	0.167 \pm 0.0004	0.167 \pm 0.001
Minimum–maximum	0.165–0.169	0.165–0.169	0.165–0.168

brightness in the blue channel was significantly lower for phakic than for pseudophakic eyes (24.6 vs. 34.0, $P < 0.001$). After adjustment, no significant differences were observed in any color channel ($P \geq 0.188$) (Table 4). As detailed in the same table, before adjustment, the green to red ratios were comparable between phakic and pseudophakic eyes (0.458 vs. 0.461, $P = 0.341$), but pseudophakic eyes showed significantly increased blue to red color balance ratios compared to phakic eyes (0.231 vs. 0.157, $P < 0.001$). The blue to red color balance ratios were not significantly different after software adjustment (0.167 vs. 0.167, $P = 0.136$).

Figure 3 presents an example of an eye with a natural lens (Fig. 3a) and an eye with an intraocular lens (Fig. 3b). In Figure 3a (top panel), the green to red ratio was 0.418, and the blue to red ratio was 0.173. In Figure 3b (top panel), the green to red ratio was 0.501 and the blue to red ratio was 0.343. The tonal differences in the images principally arose from the higher proportion of blue in Figure 3b. After adjustment, the green to red ratio in Figure 3a (middle panel) was 0.500 and the blue to red ratio was 0.168. The green to red ratio in Figure 3b (middle panel) was 0.500, and the blue to red ratio was 0.167. The visibility of the hyperpigmented zone, Figure 3b (inset), is enhanced in the adjusted image.

Processing Time and Grading Discrepancies

The mean processing time per image was 9.47 ± 2.12 seconds (range: 5.2–15.2 seconds) on a computer with a 2.50-GHz Intel i7 processor and 16 gigabytes of memory. In this time, the adjusted images were generated as new files, and the numerical results and histograms were also automatically created by the software. Of the 370 images evaluated, 85 (23.0%) were considered nongradable before software adjustment. After adjustment, 21 images (5.7%) remained nongradable (Table 1). Poor focusing prevented grading in 20 images. In one image, artifacts created by the correction of extreme underexposure precluded grading. Following image adjustment, 11 subjects initially considered controls were classified as having early AMD after adjustment, and seven patients went from early to intermediate AMD. Figure 4 presents an example. Since these color photos were from patients enrolled by us as part of a bigger cross-sectional study on AMD biomarkers, we have detailed clinical exam and OCT imaging on all. All patients that had discrepancy in grading between preadjustment and postadjustment images were evaluated in detail to confirm that the postadjustment grading was consistent with both the clinical exam and the OCT imaging. This was done to verify that the change was real and not a mere artifact.

Table 4. Brightness Values for the RGB Channels of 48 Subjects with Intraocular Lenses and 289 Phakic Subjects

	Before	After
IOL eye red brightness		
Mean \pm SD	145.3 \pm 40.9	191.7 \pm 0.3
Range	52.5–204.5	190.8–192.2
IOL eye green brightness		
Mean \pm SD	67.8 \pm 23.2	96.1 \pm 0.2
Range	18.8–107.0	95.7–96.5
IOL eye blue brightness		
Mean \pm SD	34.0 \pm 14.7	32.0 \pm 0.1
Range	3.57–60.1	31.7–32.2
IOL eye green/red ratio		
Mean \pm SD	0.461 \pm 0.081	0.501 \pm 0.001
Range	0.298–0.716	0.500–0.503
IOL eye blue/red ratio		
Mean \pm SD	0.231 \pm 0.087	0.167 \pm 0.001
Range	0.068–0.434	0.165–0.169
Phakic eye red brightness		
Mean \pm SD	159.2 \pm 39.2	191.7 \pm 0.4
Range	53.7–231.1	190.0–192.6
Phakic eye green brightness		
Mean \pm SD	73.3 \pm 21.8	96.1 \pm 0.2
Range	15.7–115.5	95.2–96.8
Phakic eye blue brightness		
Mean \pm SD	24.6 \pm 10.1	32.0 \pm 0.1
Range	0.3–64.0	31.6–32.4
Phakic eye green/red ratio		
Mean \pm SD	0.458 \pm 0.080	0.501 \pm 0.001
Range	0.209–0.706	0.498–0.505
Phakic eye blue/red ratio		
Mean \pm SD	0.157 \pm 0.067	0.167 \pm 0.0004
Range	0.005–0.433	0.165–0.169

Discussion

The current gold standard for AMD detection and grading for clinical research and teleimaging is color fundus photography. There is considerable variability in quality of images based on patient factors and camera characteristics. Uniform quality of images is essential to accurate detection and grading of AMD. Therefore, we designed this study, where we present a cross-sectional analysis of 370 color fundus photographs and demonstrate that their brightness, contrast, and color balance can be automatically standardized to conform to a color model optimized

for AMD grading.¹⁶ Using image parameters determined by the AREDS 2 group,¹⁶ a software program modified the brightness values of individual image pixels to make the global image parameters match the ideal values. This software was tested on fundus photographs obtained with three types of camera systems. All cameras presented a wide range of luminance characteristics, but after adjustment, variability in brightness, contrast, and color balance was reduced.

Variation in image brightness decreased more than 50-fold for each color channel after processing, and the means of the brightness were within 0.5 units of the defined targets. The observed enhancements in contrast uniformity were less dramatic, and after processing, the means of the contrast measurements were as much as 1.3 units below their targets. Pixel brightness values are constrained to be integers between 0 and 255, and rounding errors (from the integer representation of the numbers) after enhancement led to the observed deviations from perfection. Furthermore, if the adjustments created pixel values larger than 255, these values saturated at 255.

Regardless of the camera system used, measurements in the RGB or YCrCb color spaces indicated that the photos were consistently underexposed relative to the optimal AREDS 2 values. This was corrected by the program. Images acquired with the Topcon camera at study site B were shown to be closer to the ideal targets before adjustment than images acquired with either the Topcon or Zeiss cameras in site A. The appearance of images is influenced by the CCD sensor used to acquire them, the camera image-processing software, and the color calibration settings specified by the manufacturer or operator. Though the IMAGEnet processing software of the Topcon systems was the same, the cameras in the two sites had different sensors: a Nikon D2H sensor was used in site B, while a Pike sensor was used in the site A Topcon camera. The observed differences might therefore be explained by variations in the color balance of sensors (significantly different for the green to red ratios, P value $<$ 0.001, and blue to red ratios, P value = 0.024), but might also reflect the preferences of the photographers.

Color balance ratios determine the tonal characteristics of images. Zeiss images subjectively appeared to be overly yellow, and quantitative analysis confirmed the elevated green to red color balance ratio relative to the Topcon camera before adjustment (Zeiss = 0.539 vs. Topcon site A = 0.424, P value $<$ 0.001, and Topcon site B = 0.480, P value $<$ 0.001).

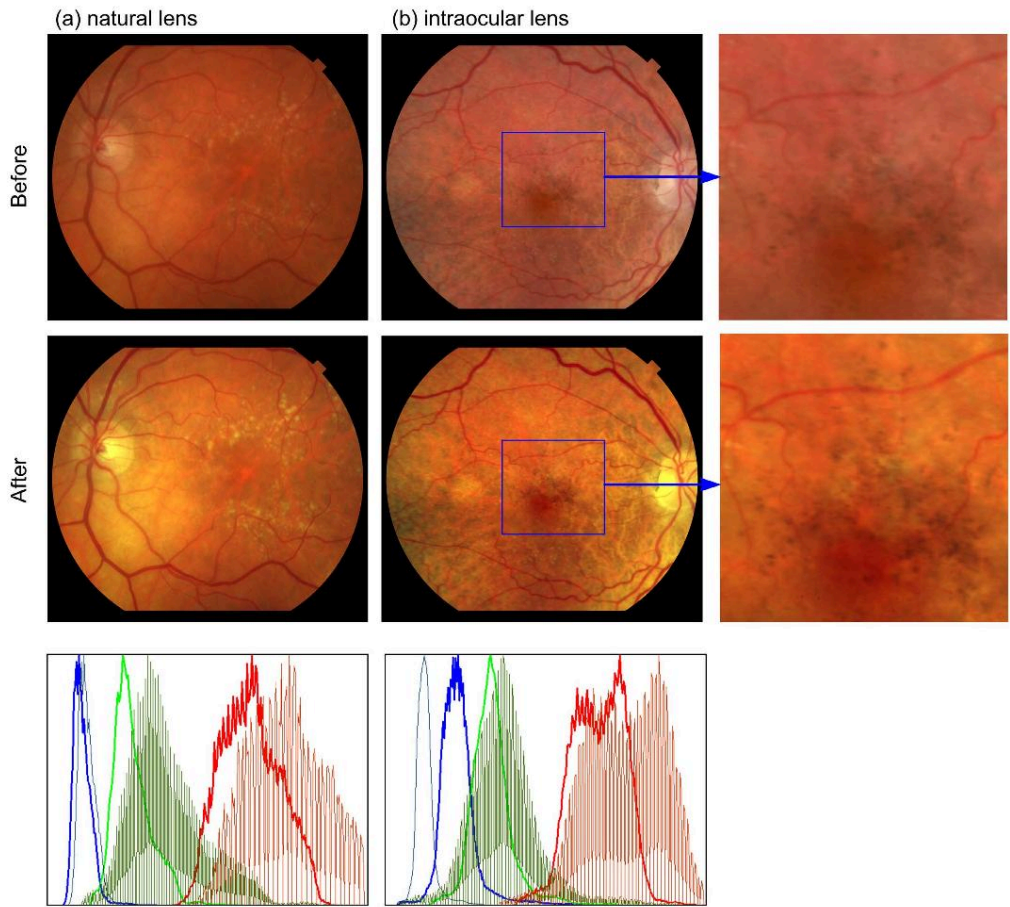


Figure 3. Comparison of the tonal properties of a phakic eye and a pseudophakic eye. Figure 3a (*top panel*) is an unmodified photograph from a subject with a natural lens and Figure 3b (*top panel*) is a photograph from a subject with an intraocular lens. The inset in Figure 3b shows a region of hyperpigmentation. The *middle panels* show the effect of the software enhancement. The histograms on the *bottom* reveal that there is increased transmission of blue light in the eye with the intraocular lens.

After adjustment, the green to red ratios for all cameras were 0.501, and the tonal characteristics of the images were indistinguishable (Fig. 1).

Patient factors, such as lens properties, are known to affect the properties of color fundus photographs. We found that pseudophakic eyes had significantly higher blue to red color balance ratios than phakic eyes (0.231 vs. 0.157, P value < 0.001). This was most likely due to increased transmission of blue light through the intraocular lenses compared to natural

lenses.²²⁻²⁴ To our knowledge, detection of excess blue light in photographs of eyes with intraocular lenses has not been previously reported. The green to red color balance ratios for phakic and pseudophakic eyes measured in this study were statistically similar (0.461 vs. 0.458, P value = 0.341), even though increased green transmission through intraocular lenses has been reported.²³ The effect of an increased blue component in the photos is unclear. The yellowish appearance of drusen is captured well in



Figure 4. Grading of AMD with color fundus photograph enhancement. Before adjustment, this photo was graded as early AMD, and after adjustment, it was changed to intermediate AMD.

the green channel, while the variation in RPE pigment density (hypopigmentation in atrophy and hyperpigmentation in clumping) is captured well in the red channel. The blue channel is a minor component, with a strength three times weaker than the green and six times weaker than the red channels in the ideal AREDS2 color model (32 units in blue vs. 96 in green and 192 in red).¹⁶ However, an increased blue to red color balance ratio in eyes with intraocular lenses may reduce the contrast of hyperpigmentation features (Fig. 3b), leading to inconsistency in grading. The standardization algorithm corrected the high blue to red ratio in the pseudophakic eyes.

The software program can optimize the brightness, contrast, and color balance of substandard images but cannot salvage images where information is lost through poor focus or extremes of under- or overexposure. The fraction of nongradable images recorded in this study before adjustment was 23.0%, which is consistent with previous reports.^{11,14} After adjustment, 5.7% of the images remained nongradable. This demonstrates that enhancement of the color characteristics alone can make the majority of substandard images acceptable for AMD grading. Furthermore, adjustment of the images resulted in diagnosis of early AMD in 11 control subjects and change in grading from early to intermediate in seven patients, indicating the usefulness of the software program in diagnosis and grading of AMD.

This study has several limitations. We assessed our data according to the type of sensor of the different cameras used, but we were not able to account for potential variations due to manufacturers and photographers' preferences, which might have affected

our results. Additionally, adjusting image parameters to conform to a color model may not be appropriate in all circumstances. Based on images showing all stages of AMD, the AREDS 2 color model is most useful in early to intermediate stage AMD to highlight the appearance of yellow drusen against the retinal background. As mentioned by Hubbard et al.,¹⁶ such adjustment may also distort the appearance of eyes with heavily pigmented choroids. The brightness and contrast parameters adopted in this study were chosen to enhance the visibility of characteristic AMD abnormalities, specifically drusen, hyperpigmentation, and depigmentation. Different settings will be necessary to improve the visibility of abnormalities typical of other pathologies. In all circumstances, it will be crucial to examine the images before and after adjustment to ensure that artifacts do not lead to false-positive detection of disease.

Due to the large proportion of Caucasian subjects (with low amounts of choroidal pigment) in this study, the effect of the AREDS 2 color model on eyes with varying amounts of pigmentation could not be explored. Age-related macular degeneration affects people of Caucasian descent at roughly 9 to 10 times the rate of people of African descent.^{2,17,25} The small number of non-Caucasian subjects reflects the disease prevalence in clinical population. While we observed significantly higher blue to red color balance ratios in the 48 pseudophakic eyes, the types of intraocular lenses (blue-blocking or not) were not documented. A further caveat is that the images analyzed in this study had 30- or 35-degree fields of view and exhibited no perceptible vignetting. More sophisticated procedures may be necessary to adjust images with uneven

illumination. A final criticism of this approach is that the image enhancement is meant to be used in conjunction with manual grading of the color photos. Many research groups are pursuing automated drusen detection in color photos,²⁶ and OCT may provide even more information about AMD in three dimensions.^{27–29} However, all currently validated grading systems rely on human evaluation of photographs, and the algorithm developed in this study automates the time-consuming and difficult task of post hoc standardization.

This algorithm was developed to fully automate the standardization of color fundus photographs for AMD classification, thus eliminate problems of manual adjustments, such as subjective variability. Brightness, contrast, and color balance differences due to natural or artificial intraocular lenses or camera type can be rapidly and accurately corrected to give consistent output. Furthermore, the automated enhancement algorithm may improve the visualization of disease features, including drusen and pigmentary changes, and is helpful in the diagnosis, grading, and thus management of AMD. Automated standardization is particularly important when studying biomarkers for AMD progression or the effect of intervention in clinical trials.

Acknowledgments

The authors would like to thank all US and Portuguese ophthalmologists, photographers, technicians, and nurses who performed the required study procedures.

This project was financially supported by the Miller Retina Research Fund (MEE), the Miller Champalimaud Award (MEE), the Portuguese Foundation for Science and Technology/Harvard Medical School Portugal Program (HMSP-ICJ/006/2013), the Fidelity Charitable Fund (Harvard University), the Massachusetts Lions Eye Research Fund, an American Glaucoma Society Mid-Career Award, and a National Institutes of Health award (UL 1 RR025758).

* Edem Tsikata and Inês Laíns equally contributed to this work.

Disclosure: **E. Tsikata**, None; **I. Laíns**, Grant from the Portuguese Foundation of Science and Technology, Harvard Medical School Portugal Program (S); **J. Gil**, None; **M. Marques**, None; **K. Brown**, None; **T.**

Mesquita, None; **P. Melo**, None; **M. da Luz Cachulo**, None; **I.K. Kim**, Genentech (C), Allergan (C), Icon Therapeutics (C); **D. Vavvas**, None; **J. Murta**, Alcon (C); **J.B. Miller**, Allergan (C); **R. Silva**, Allergan (C), Novartis (C), Thea (C), Alimera (C), Alcon (C); **J.W. Miller**, Alcon Research Institute (C), Amgen (C), KalVista Pharmaceuticals (C), Maculogix (C), Valeant Pharmaceuticals via Massachusetts Eye and Ear (P, R), ONL Therapeutics (C, P); **T.C. Chen**, None; **D. Husain**, None

References

1. Wong WL, Su X, Li X, et al. Global prevalence of age-related macular degeneration and disease burden projection for 2020 and 2040: a systematic review and meta-analysis. *Lancet Glob Heal*. 2014;2:e106–e116.
2. Lim LS, Mitchell P, Seddon JM, Holz FG, Wong TY. Age-related macular degeneration. *Lancet*. 2012;379:1728–38.
3. Age-Related Eye Disease Study Research Group. A randomized, placebo-controlled, clinical trial of high-dose supplementation with vitamins C and E, beta carotene, and zinc for age-related macular degeneration and vision loss: AREDS report no 8. *Arch Ophthalmol*. 2001;119:1417–1436.
4. Seddon JM, Sharma S, Adelman RA. Evaluation of the clinical age-related maculopathy staging system. *Ophthalmology*. 2006;113:260–266.
5. Klein R, Davis MD, Magli YL, Segal P, Klein BE, Hubbard L. The Wisconsin age-related maculopathy grading system. *Ophthalmology*. 1991;98:1128–1134.
6. van Leeuwen R, Chakravarthy U, Vingerling JR, et al. Grading of age-related maculopathy for epidemiological studies: is digital imaging as good as 35-mm film? *Ophthalmology*. 2003;110:1540–1544.
7. Somani R, Tennant M, Rudnisky C, et al. Comparison of stereoscopic digital imaging and slide film photography in the identification of macular degeneration. *Can J Ophthalmol*. 2005;40:293–302.
8. Klein R, Meuer SM, Moss SE, Klein BE, Neider MW, Reinke J. Detection of age-related macular degeneration using a nonmydriatic digital camera and a standard film fundus camera. *Arch Ophthalmol*. 2004;122:1642–1646.

9. Rasta SH, Partovi ME, Seyedarabi H, Javadzadeh A. A comparative study on preprocessing techniques in diabetic retinopathy retinal images: illumination correction and contrast enhancement. *J Med Signals Sens.* 5:40–48.
10. Teng T, Lefley M, Claremont D. Progress towards automated diabetic ocular screening: a review of image analysis and intelligent systems for diabetic retinopathy. *Med Biol Eng Comput.* 2002;40:2–13.
11. Fleming AD, Philip S, Goatman KA, Olson JA, Sharp PF. Automated assessment of diabetic retinal image quality based on clarity and field definition. *Invest Ophthalmol Vis Sci.* 2006;47:1120–1125.
12. Neelam K, Muldrew A, Hogg R, Stack J, Chakravarthy U, Beatty S. Grading of age-related maculopathy: slit-lamp biomicroscopy versus an accredited grading center. *Retina.* 2009;29:192–198.
13. Ishiko S, Akiba J, Horikawa Y, Yoshida A. Detection of drusen in the fellow eye of Japanese patients with age-related macular degeneration using scanning laser ophthalmoscopy. *Ophthalmology.* 2002;109:2165–2169.
14. Bartling H, Wanger P, Martin L. Automated quality evaluation of digital fundus photographs. *Acta Ophthalmol.* 2009;87:643–647.
15. Patton N, Aslam TM, MacGillivray T, et al. Retinal image analysis: concepts, applications and potential. *Prog Retin Eye Res.* 2006;25:99–127.
16. Hubbard LD, Danis RP, Neider MW, et al. Brightness, contrast, and color balance of digital versus film retinal images in the age-related eye disease study 2. *Invest Ophthalmol Vis Sci.* 2008;49:3269–3282.
17. Cachulo M da L, Lobo C, Figueira J, et al. Prevalence of age-related macular degeneration in Portugal: The Coimbra Eye Study—report 1. *Ophthalmologica.* 2015;233:119–127.
18. Age-Related Eye Disease Study Research Group. The Age-Related Eye Disease Study system for classifying age-related macular degeneration from stereoscopic color fundus photographs: the Age-Related Eye Disease Study report number 6. *Am J Ophthalmol.* 2001;132:668–681.
19. Danis RP, Domalpally A, Chew EY, et al. Methods and reproducibility of grading optimized digital color fundus photographs in the Age-Related Eye Disease Study 2 (AREDS2 report number 2). *Invest Ophthalmol Vis Sci.* 2013;54:4548–4554.
20. Harris PA, Taylor R, Thielke R, Payne J, Gonzalez N, Conde JG. Research electronic data capture (REDCap)—a metadata-driven methodology and workflow process for providing translational research informatics support. *J Biomed Inform.* 2009;42:377–381.
21. ITU. International Telecommunication Union—Radiocommunication (ITU-R) BT.601 standard. Geneva, Switzerland. 1982.
22. Said FS, Weale RA. The variation with age of the spectral transmissivity of the living human crystalline lens. *Gerontologia.* 1959;3:213–231.
23. Boettner EA, Wolter JR. Transmission of the ocular media. *Invest Ophthalmol Vis Sci.* 1962;1:776–783.
24. Tanito M, Okuno T, Ishiba Y, Ohira A. Transmission spectrums and retinal blue-light irradiance values of untinted and yellow-tinted intraocular lenses. *J Cataract Refract Surg.* 2010;36:299–307.
25. Friedman DS, Katz J, Bressler NM, Rahmani B, Tielsch JM. Racial differences in the prevalence of age-related macular degeneration: the Baltimore Eye Survey. *Ophthalmology.* 1999;106:1049–1055.
26. Mora AD, Vieira PM, Manivannan A, Fonseca JM. Automated drusen detection in retinal images using analytical modelling algorithms. *Biomed Eng Online.* 2011;10:59.
27. Folgar FA, Chow JH, Farsiu S, et al. Spatial correlation between hyperpigmentary changes on color fundus photography and hyperreflective foci on SDOCT in intermediate AMD. *Invest Ophthalmol Vis Sci.* 2012;53:4626–4633.
28. Yi K, Mujat M, Park BH, Sun W, Miller JW, Seddon JM, Young LH, de Boer JF, Chen TC. Spectral domain optical coherence tomography for quantitative evaluation of drusen and associated structural changes in non-neovascular age-related macular degeneration. *Br J Ophthalmol.* 2009;93:176–181.
29. Chiu SJ, Izatt JA, O'Connell RV, Winter KP, Toth CA, Farsiu S. Validated automatic segmentation of AMD pathology including drusen and geographic atrophy in SD-OCT images. *Invest Ophthalmol Vis Sci.* 2012;53:53–61.

Choroidal Changes Associated With Subretinal Drusenoid Deposits in Age-related Macular Degeneration Using Swept-source Optical Coherence Tomography



INÊS LAÍNS, JAY WANG, JOANA PROVIDÊNCIA, STEVEN MACH, PEDRO GIL, JOÃO GIL, MARCO MARQUES, GRAYSON ARMSTRONG, SHADY GARAS, PATRÍCIA BARRETO, IVANA K. KIM, DEMETRIOS G. VAVVAS, JOAN W. MILLER, DEEBA HUSAIN, RUFINO SILVA, AND JOHN B. MILLER

• **PURPOSE:** To compare choroidal vascular features of eyes with and without subretinal drusenoid deposits (SDD), using swept-source optical coherence tomography (SS OCT).

• **DESIGN:** Multicenter, cross-sectional study.

• **METHODS:** We prospectively recruited patients with intermediate age-related macular degeneration (AMD), without other vitreoretinal pathology. All participants underwent complete ophthalmic examination, color fundus photography (used for AMD staging), and spectral-domain OCT (to evaluate the presence of SDD). SS OCT was used to obtain automatic macular choroidal thickness (CT) maps, according to the Early Treatment Diabetic Retinopathy Study (ETDRS) sectors. For data analysis, we considered mean choroidal thickness as the arithmetic mean value of the 9 ETDRS sectors. SS OCT en face images of choroidal vasculature were also captured and converted to binary images. Choroidal vascular density (CVD) was calculated as a percent area occupied by choroidal vessels in a 6-mm-diameter submacular circular. Choroidal vessel volume was calculated by multiplying the average CVD by macular area and CT. Multilevel mixed linear models (to account for the inclusion of 2 eyes of same subject) were performed for analysis.

• **RESULTS:** We included 186 eyes ($n = 118$ subjects), 94 (50.5%) presenting SDD. Multiple regression analysis revealed that, controlling for age, eyes with SDD presented a statistically thinner mean CT ($B = -21.9$, $P = .006$) and CT in all the individual ETDRS fields

($B \leq -18.79$, $P \leq .026$). Mean choroidal vessel volume was also significantly reduced in eyes with SDD ($B = -0.003$, $P = .007$). No significant associations were observed with mean CVD.

• **CONCLUSION:** In subjects with intermediate AMD, choroidal thickness and vessel volume are reduced in the presence of subretinal drusenoid deposits. (Am J Ophthalmol 2017;180:55–63. © 2017 Elsevier Inc. All rights reserved.)

AGE-RELATED MACULAR DEGENERATION (AMD) IS the most common cause of irreversible vision loss in the elderly in developed countries.¹ Classic drusen, histologically described as extracellular deposits located below the retinal pigment epithelium (RPE), are the hallmark in the pathogenesis and progression of the disease.² In recent years, enhanced retinal imaging techniques, particularly high-resolution optical coherence tomography (OCT), have raised interest in subretinal drusenoid deposits (SDD). Despite the lack of agreement on their nomenclature,³ SDD have been described as a unique phenotypic feature⁴ and proposed as an independent risk factor for AMD progression.⁵

The pathogenesis of SDD remains only partially understood, but choroidal vasculature might play a role.^{6–8} Prior studies described a reduced subfoveal choroidal thickness (CT) in the presence of these subretinal lesions, using the enhanced-depth imaging (EDI) protocol for spectral-domain OCT (SD OCT).^{7,9} Though the reports with EDI are generally consistent,^{7,9} it is important to recognize that there are several relevant limitations to this protocol. EDI requires multiple scan averaging to achieve high contrast and low speckle noise, and the SD OCT wavelength is not large enough in some cases to detect the choroidal-scleral boundary. Additionally, for the commercial devices currently available with EDI, CT evaluation requires manual segmentation, thus limiting thickness measurements to a specific number of pinpoint locations.¹⁰

Recent studies have shown that swept-source OCT (SS OCT) has the potential to overcome some of these limitations.¹¹ It uses a different light source

Supplemental Material available at [AJO.com](http://ajoc.com).

Accepted for publication May 25, 2017.

From the Retina Service, Massachusetts Eye and Ear, Department of Ophthalmology, Harvard Medical School, Boston, Massachusetts (I.L., J.W., S.M., G.A., S.G., I.K.K., D.G.V., J.W.M., D.H., J.B.M.); Faculty of Medicine, University of Coimbra, Coimbra, Portugal (I.L., P.G., J.G., R.S.); Centro Hospitalar e Universitário de Coimbra, Coimbra, Portugal (I.L., J.P., P.G., J.G., M.M., R.S.); and Association for Innovation and Biomedical Research on Light, Coimbra, Portugal (I.L., J.P., P.G., J.G., M.M., P.B., R.S.).

Inquiries to John B. Miller, Harvard Medical School, Mass. Eye and Ear, Retina Service, 243 Charles St, Boston, MA 02114; e-mail: john_miller@meei.harvard.edu

0002-9394/\$36.00
<http://dx.doi.org/10.1016/j.ajo.2017.05.021>

© 2017 ELSEVIER INC. ALL RIGHTS RESERVED.

55

(wavelength-tunable laser) and detection method (dual balanced photodetector), and has improved adaptability to longer imaging wavelengths.¹² For example, the Atlantis/Topcon SS OCT (Topcon Medical Systems, Inc, Oakland, New Jersey, USA) has a wavelength of 1050 nm, providing deeper tissue penetration and less scattering at the RPE.¹³ Combined with faster imaging speeds for dense scanning and subsequent 3-dimensional image reconstruction,¹⁴ these features offer potential advantages in assessing the choroid, including highly reproducible measurements of CT.¹³ Furthermore, the Topcon SS OCT can generate automatic choroidal thickness maps,¹⁵ which have been used to examine the choroid in various diseases.¹⁶⁻²¹ Scarce data have been published exploring the potential of SS OCT to analyze choroidal vasculature in the presence of SDD. In addition to having small sample size, prior studies^{16,21} looked at CT but did not account for the effect of AMD in CT.

This study aimed to further explore the relationship between SDD and macular CT, assessed by SS OCT. To exclude the known effect of AMD stage on CT,²² we only included eyes with the intermediate stage of disease. To build upon traditional choroidal thickness measurements, we applied imaging analysis software to measure choroidal vessel density and volume.

METHODS

THIS STUDY IS PART OF A MULTICENTER, PROSPECTIVE, observational study on AMD biomarkers performed by the Massachusetts Eye and Ear (MEE), Harvard Medical School, Boston, Massachusetts, USA; and the Faculty of Medicine of the University of Coimbra (FMUC), Coimbra, Portugal, in collaboration with the Ophthalmology Department of Centro Hospitalar e Universitário de Coimbra and the Association for Innovation and Biomedical Research on Light and Image (AIBILI), Coimbra, Portugal.

This research protocol was conducted in accordance with Health Insurance Portability and Accountability Act requirements and the tenets of the Declaration of Helsinki. The Institutional Review Board of MEE, FMUC, and AIBILI, as well as the Portuguese National Committee of Data Protection, approved this study. Written informed consent was obtained from all participants.

• **STUDY POPULATION:** From January 2015 to July 2016, we prospectively recruited and consented patients with a diagnosis of intermediate AMD (procedures for grading detailed below). At MEE, potential participants were recruited from the Retina, Comprehensive Ophthalmology, and Optometry Services during routine clinic visits. The Portuguese study population was derived from a population-based cohort study.²³

For both cohorts, exclusion criteria included diagnosis of any other vitreoretinal disease, active uveitis or ocular infection, significant media opacities that precluded the observation of the ocular fundus, refractive error equal to or greater than 6 diopters of spherical equivalent, past history of retinal surgery, history of any ocular surgery or intraocular procedure (such as laser or intraocular injections) within 90 days prior to enrollment, and diagnosis of diabetes mellitus, with or without concomitant diabetic retinopathy.

• **STUDY PROTOCOL:** All participants underwent a comprehensive eye examination, including best-corrected visual acuity, current refraction, intraocular pressure, slit-lamp biomicroscopy, and dilated fundus examination. A standardized questionnaire was designed for a larger AMD biomarker study (including data on demographics, past medical history, and current medication) and applied to all study participants, as described in a previous publication.²⁴

In the same visit, all subjects were imaged with nonsteroscopic, 7-field, color fundus photographs (Topcon TRC-50DX; Topcon Medical Systems, Inc) for AMD diagnosis and grading (detailed below), and EDI SD OCT (Spectralis, Heidelberg, Germany). All patients underwent a high-resolution volume scan centered on the fovea with EDI SD OCT; first with 61 lines, 30 × 25 degrees, 30 frames automatic real time (ART), and later changed to 97 lines, 20 × 20 degrees, 15 frames ART owing to concerns with image acquisition times. During the same study visit, SS OCT (Atlantis; Topcon Medical Systems, Inc) imaging was also performed with a 3-dimensional horizontal volume and a raster scan protocol of 512 × 256 covering an area of 12.0 × 9.0 mm centered on the fovea.

• **EVALUATION OF COLOR PHOTOGRAPHS AND OPTICAL COHERENCE TOMOGRAPHY IMAGES:** Using IMAGeNet 2000 software (version 2.56; Topcon Medical Systems, Inc), 2 of 4 independent, experienced, and masked graders (I.L., P.G., J.G., M.M.) determined the AMD stage of every included eye using the Field 2 color fundus photograph. In cases of disagreement, a senior grader (D.H. or R.S.) established the final categorization. The Age-Related Eye Disease Study (AREDS) classification system was used,^{25,26} and, as detailed, only eyes with intermediate AMD were included.

SD OCT images were analyzed by 2 of 4 independent graders (I.L., P.G., J.G., M.M.), masked to any other data, and were classified for the presence of classic drusen (defined as sub-RPE deposits; presence of ≥1 druse was graded as “yes”) and SDD³ (presence of ≥1 was graded as “yes”).

• **THICKNESS MAPS:** Macular retinal and choroidal thicknesses were obtained with the automatic software of the SS OCT device (Topcon FastMap, version 9.12.003.04; Topcon Medical Systems, Inc). User-independent

thickness maps were created according to the conventional Early Treatment Diabetic Retinopathy Study (ETDRS) grid (comprised of inner and outer rings –1 to 3 mm and 3–6 mm in diameter, respectively, divided into 4 quadrants: superior, inferior, temporal, and nasal), with 9 independent sectors (inner and outer temporal, inner and outer superior, inner and outer inferior, inner and outer nasal, and central).

For all subjects, an experienced investigator (I.L., J.P., P.G., or J.J.) confirmed the position of the grid. If the automatic location was not properly centered in the fovea, manual reposition was performed with the function “Grid, Reposition,” using the corresponding B-scan image as reference. Similarly, the same investigators, masked to any other imaging examinations, also confirmed retinal and choroidal automatic segmentations for all the obtained volume scans. Automatic retina segmentation was reviewed using the function “Retina,” which delineates the inner limiting membrane (ILM) and the RPE. Choroidal segmentation was viewed using the “CSI” function that delineates the inner and outer limits of this vascular layer–Bruch membrane (BM) and choroidal-scleral interface (CSI), respectively. When the investigators considered that these limits were not properly delineated, they manually corrected them using the functions “ILM > Modify,” “RPE > Modify,” “BM > Modify,” and “CSI > Modify.” Appropriate boundaries were drawn according to the International Nomenclature for Optical Coherence Tomography.²⁷

Finally, the obtained retinal thickness and CT values in the 9 different ETDRS fields were registered. For analysis, mean retinal thickness and mean CT were calculated as the arithmetic mean of retinal and choroidal thickness in all the ETDRS grid fields, respectively.

• **CHOROIDAL VASCULAR DENSITY AND VOLUME:** SS OCT en face images of choroidal vasculature were obtained and flattened with the Bruch membrane as reference, using the en face tool included in the Topcon OCT visualization software. The en face images were exported in 2.6- μ m sections from BM to CSI, and subsequently imported to ImageJ (National Institutes of Health, Bethesda, Maryland, USA) as an image stack. The image stack was then converted to binary images using the auto-thresholding function of the software (ImageJ command: “Image > Adjust > Threshold > Apply”) in order to distinguish the choroidal vasculature from the stroma. The binarization of the en face images was done using the Otsu method,²⁸ which is an automatic threshold selecting algorithm using gray-level histograms. Noise in the resulting binary images was then removed (ImageJ command “Process > Noise > Remove Outliers”). The signal from the optic disc, retinal blood vessels, and any minor artifact was accounted for by creating a mask from the image slice at the level of BM, and then applying that mask to all subsequent images, thereby eliminating any signal from those lo-

cations throughout the entire image stack (ImageJ command “Process > Image Calculator > Multiply”). A 6-mm-diameter circular submacular region centered on the fovea was cropped from the wide-field image to resemble the ETDRS grid. Finally, the area occupied by choroidal vessels was analyzed (ImageJ command “Analyze > Measure”), and the choroidal vascular density was calculated as a percent area occupied by the choroidal vessels for each slice (within this 6-mm-diameter circle).

As described, CT was automatically obtained. Midpoint choroidal vascular density was recorded as the choroidal vascular density in the image slices at the depth corresponding to halfway between the BM and the average CT. The average of the choroidal vascular densities of all image slices between the BM and the corresponding maximal CT was recorded, and is designated from now on as average choroidal vascular density. The submacular choroidal vascular volume was calculated by multiplying the average choroidal vascular density by macular area and maximal CT.

• **STATISTICAL ANALYSIS:** The study population demographics were summarized with traditional descriptive measures (ie, means and standard deviations for continuous variables, and percentages for binomial/categorical variables). Given the inclusion of both eyes of the same subject, we used multilevel mixed-effect linear models. By definition, these models are appropriate for research designs in which data for participants are organized at more than 1 level (ie, nested data). In this study, the units of analysis were considered the eyes (at a lower level), which are nested within patients that represent the contextual/aggregate units (at a higher level).²⁹

Using these models, our outcomes were as follows: the mean CT within the ETDRS grid and the CT values within the individual ETDRS fields. Univariable analyses were initially performed for all the potential confounders (eg, sex and age) and all variables with a *P* value $\leq .250$ were included in the initial multiple model. A backwards elimination procedure was then performed to achieve the multivariable models presented. For all multilevel assessments we report *P* values and beta coefficients. The beta coefficients represent the change in the outcome variable for 1 unit of change in the predictor variable (while holding other predictors in the model constant, in the case of multivariable analyses).³⁰ This means, for example, given a continuous variable such as age, beta coefficients represent the change in choroidal thickness per year increase in age. For binomial variables, such as presence of SDD, their absence was considered the reference term, so beta coefficients refer to the change in their presence.

A similar statistical approach was followed for the analysis of the 2 outcomes obtained by processing of en face images: choroidal vessel density and choroidal vessel volumes within the central 6 mm.

TABLE 1. Demographic and Clinical Characteristics of the Included Study Eyes

	Eyes With SDD	Eyes Without SDD	Total
Demographics and clinical characteristics			
Included eyes, n (%)			
Total study eyes	94 (51)	92 (49)	186 (100)
Total OD	40 (43)	42 (47)	82 (44)
Total OS	54 (58)	50 (54)	104 (56)
Age, mean ± SD	73.2 ± 6.9	76.3 ± 8.5	74.4 ± 7.8
Sex, n (%)			
Male	32 (34)	41 (45)	73 (39)
Female	62 (66)	51 (55)	113 (61)
Country, n (%)			
United States	46 (49)	14 (15)	60 (32)
Portugal	48 (51)	78 (85)	126 (68)
Eye examination			
Spherical equivalent, diopters, mean ± SD (range)	0.36 ± 1.40 (−3.25; 4.50)	0.26 ± 1.3 (−3.00; 3.50)	0.3 ± 1.4 (−3.25; 4.50)
Pseudophakic, n (%)	16 (9)	17 (9)	33 (18)

SDD = subretinal drusenoid deposits.

All statistics were performed using Stata version 14.1 (StataCorp LP, College Station, Texas, USA) and *P* values < .05 were considered statistically significant.

RESULTS

• **STUDY POPULATION:** We included 186 eyes (*n* = 118 subjects) with intermediate AMD according to AREDS classification (based on color fundus photographs). Of the included eyes, 47.3% (*n* = 88) presented classic drusen only, 5.4% (*n* = 10) SDD only, 45.2% (*n* = 84) both, and 2.1% (*n* = 4) had no classic drusen and no SDD on OCT. Despite being classified as intermediate AMD on color fundus photographs, 14 eyes (5.9%) did not present visible classic drusen on OCT. All but 14 eyes were scanned with the 97-line SD OCT protocol. **Table 1** presents the clinical and demographic characteristics of the included study population. In all eyes, SS OCT images allowed a clear identification of the CSI. The **Figure** presents an example of an eye with SDD and the choroidal boundaries obtained with SS OCT. **Table 2** details the obtained CT parameters.

• **MEAN CHOROIDAL THICKNESS WITHIN THE ETDRS GRID:** **Table 3** presents the results of the univariable analysis considering mean CT of the entire ETDRS grid as the outcome. As shown, in this assessment presence of SDD was not a significant predictor of mean CT, probably owing to the influence of confounding factors. Of the remaining evaluated covariates, age presented a statistically significant association with reduced mean CT ($\beta = -3.1$, $P < .001$)—per 1 year of increased age there was a reduction of 3.1 μm in mean CT within the ETDRS grid.

Multivariable analysis revealed that, controlling for age, the presence of SDD was associated with a statistically significant reduction in mean CT ($\beta = -21.9$, $P = .006$). Eyes with SDD had a thinner mean CT (21.9 μm lower) than eyes without these lesions when holding age constant. The addition of other parameters to the model, including the presence of classic drusen, did not change these results.

• **CHOROIDAL THICKNESS IN THE DISTINCT ETDRS FIELDS:** Similar analyses were performed for central CT and the remaining sectors of the ETDRS grid. For central thickness, univariable analysis revealed that only age presented a statistically significant association with this outcome ($\beta = -3.2$, $P < .001$). On multivariable assessments we observed that, controlling for age, the presence of SDD was associated with decreased central CT ($\beta = -25.6$, $P = .006$). Further analyses, including additional parameters such as classic drusen, did not show any statistically significant results.

Table 4 presents the results of the remaining sectors of the ETDRS grid evaluated. As noted in bold, the presence of SDD was significantly associated with a reduced CT in all sectors, after accounting for age.

• **CHOROIDAL VESSEL DENSITY AND VOLUME:** For analysis of choroidal vessel density and volume, we excluded 1 eye owing to poor image quality. We started this analysis considering mean choroidal vessel density within the central 6-mm defined circle as the outcome (as outlined in the methods section). Univariable assessments indicated that mean choroidal vessel density was only significantly associated with increased age ($\beta = -0.003$, $P = .001$). After controlling for age and other covariates, SDD showed a reduction in the

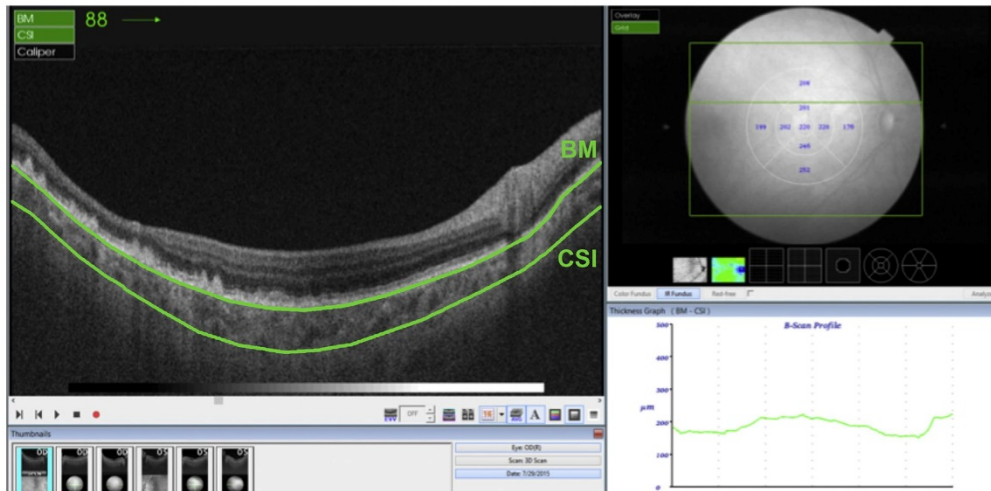


FIGURE. Example of choroidal thickness delineated by swept-source optical coherence tomography (SS OCT). (Left) B-scan of a right eye imaged with SS OCT, where subretinal drusenoid deposits are evident, some of them disrupting the ellipsoid junction. The green superior line corresponds to the Bruch membrane (BM), as automatically delineated by the software; the green inferior line corresponds to the choroidal-scleral interface (CSI), also automatically defined by the available software and manually corrected by an experienced grader in required cases. (Right) Choroidal thickness map centered on the fovea, according to the Early Treatment Diabetic Retinopathy Study (ETDRS) grid. This map is automatically generated by the commercially available software; if required, it can be repositioned to be properly centered on the fovea. Each value represents the thickness (in micrometers) of the corresponding ETDRS subfield.

choroidal vessel density, but it did not quite reach statistical significance ($P = .063$).

Regarding choroidal vessel volume, we observed a statistically significant association between increased age and decreased volume ($\beta = -0.0004, P < .001$). When controlling for age, the presence of SDD was significantly associated with reduced macular choroidal vessel volume ($\beta = -0.003, P = .007$).

DISCUSSION

WE PRESENT A CROSS-SECTIONAL STUDY OF 186 EYES DIAGNOSED WITH INTERMEDIATE AMD, IN WHICH WE USED SS OCT TO EXAMINE THE EFFECT OF SUBRETINAL DRUSENOID DEPOSITS ON MACULAR CHOROIDAL THICKNESS. OUR RESULTS REVEALED THAT, AFTER ACCOUNTING FOR AGE, THE PRESENCE OF THESE LESIONS WAS ASSOCIATED WITH A SIGNIFICANT DECREASE IN MEAN CT, AS WELL AS CT IN ALL SECTORS OF THE ETDRS GRID. EYES WITH SDD ALSO SHOWED A STATISTICALLY SIGNIFICANT REDUCTION IN MACULAR CHOROIDAL VESSEL VOLUME AS COMPARED WITH EYES WITHOUT SDD.

The observed association between the presence of SDD and decreased CT is in agreement with previously published literature, most of which used the EDI protocol for SD OCT.^{6,7,9,31,32} Haas and associates³³ used an SD

OCT device with a longer wavelength (1060 nm) and also detected choroidal thinning in eyes with wet AMD and SDD, as compared with eyes with the same stage of AMD but without subretinal deposits. To our knowledge, scarce data are available on the assessment of the relationship between SDD and CT using SS OCT.^{16,21} Ueda-Arakawa and associates²¹ compared 38 eyes with SDD to 14 macular healthy controls, and observed a significantly reduced macular CT and volume in each sector of the ETDRS grid. Besides having a relatively small sample size, the authors did not account for the effect of AMD on CT per se. Capuano and associates¹⁶ described a thinner choroid in eyes with nonexudative AMD with SDD ($n = 19$) compared with controls and compared with eyes with nonexudative AMD with at least 1 soft druse and no SDD.

Recently, another group³⁴ used a prototype SS OCT and developed a segmentation algorithm to generate CT maps, verifying also a reduced CT in eyes with SDD. The authors included eyes with nonexudative AMD. However, they provide no information about the stage of AMD, which means that a very broad sample might have been included. Interestingly, these authors also developed software to calculate vessel density from en face slabs and verified a significant reduction in this parameter in eyes with SDD. In our study, we followed a similar approach but did not observe significant changes in choroidal vessel density.

TABLE 2. Choroidal Thickness Parameters Assessed, According to Presence or Absence of Subretinal Drusenoid Deposits

	Eyes Without SDD (Mean ± SD)	Eyes With SDD (Mean ± SD)	Total (Mean ± SD)
Choroidal thickness (μm) within the ETDRS grid			
Mean of all sectors	192.5 ± 65.3	171.5 ± 61.8	181.9 ± 64.3
Central	201.3 ± 72.7	177.3 ± 66.8	189.1 ± 70.6
Inner temporal	208.2 ± 67.9	181.3 ± 60.2	194.6 ± 65.4
Inner superior	210.7 ± 73.8	184.6 ± 69.59	197.5 ± 72.7
Inner nasal	191.9 ± 75.1	168.1 ± 70.9	179.8 ± 73.8
Inner inferior	194.1 ± 74.6	176.4 ± 68.5	185.1 ± 71.9
Outer temporal	192.6 ± 57.3	175.9 ± 54.0	184.2 ± 56.2
Outer superior	205.5 ± 68.3	184.6 ± 71.3	194.9 ± 70.5
Outer nasal	151.2 ± 65.9	133.5 ± 66.3	142.3 ± 66.6
Outer inferior	177.6 ± 70.2	162.0 ± 62.1	169.7 ± 66.5
Choroidal vessel density (%) and volume (μm ³) (6 mm centered on the fovea)			
Macular vessel density	0.279 ± 0.074	0.265 ± 0.071	0.272 ± 0.072
Macular vessel volume	0.019 ± 0.009	0.017 ± 0.009	0.018 ± 0.009

ETDRS = Early Treatment Diabetic Retinopathy Study; SDD = subretinal drusenoid deposits.

TABLE 3. Univariable Multilevel Mixed Linear Regression Analysis Considering Mean Choroidal Thickness as the Outcome

Variable	B Coefficient	95% CI	P Value
Age	-3.11	-4.43; -1.78	<.001*
Eye	-1.19	-9.43; 7.05	.778
Sex ^a	15.25	-7.96; 38.46	.198
SDD ^b	-14.97	-31.21; 1.26	.071
Classic drusen ^c	-15.13	-42.96; 12.71	.287
Mean retinal thickness	0.09	-0.41; 0.59	.206

CI = confidence interval; SDD = subretinal drusenoid deposits.

P values < .05 are noted by an asterisk.

^aMale sex considered the reference term.

^bReference term considered as the absence of these lesions.

However, we did find that the submacular choroidal vessel volume was significantly reduced in eyes with SDD. This is probably linked to the nature of our study design, only including eyes with the same stage of AMD (intermediate), and suggests that CT might be the most relevant parameter in the assessment of choroidal vasculature in these eyes. Ueda-Arakawa and associates²¹ also described a reduced volume in eyes with SDD, but compared with normal healthy eyes. Although prior studies of eyes affected by SDD described decreased vessel density in the choriocapillaris³⁵ and Sattler layer,^{33,36} we did not examine distinct choroidal vascular layers because it is fairly accepted that current imaging devices have too many important limitations.³⁷

Although choroidal thinning or reduced choroidal vessel volumes do not necessarily imply choroidal ischemia, altogether our results suggest that atrophy of the choroid, or a choroidopathy, may be involved in the pathogenesis of SDD. The Moorfields AMD consortium³⁸ recently reviewed the current available literature on SDD. The authors highlighted that, despite conflicting results, there is evidence supporting the choroidopathy hypothesis. Indeed, prior authors⁹ suggested that choroidal hypoxia, as assessed by indocyanine green angiography, may have a role in the occurrence or development of SDD. Specifically, SDD seems to be located at sites of choroidal watershed zones.⁹ The characteristic reticular pattern may actually be linked to impaired choroidal filling and choroidal insufficiency, which results in a derangement of the RPE. Histologic reports also showed decreased choroidal vasculature in eyes with SDD.^{21,39,40}

As described in our study, SS OCT enabled a clear identification of the CSI in all of the evaluated B-scans. SS OCT appears to provide significant advantages for the analysis of CT, compared with SD OCT.¹⁰ Data from studies using the EDI protocol suggests that the ability to identify the external limit of the choroid might range between 65% and 93% in normal eyes,⁴¹ and is inferior to 73% in eyes with AMD.⁴² Furthermore, Copete and associates⁴¹ suggested that SD OCT images might present a hyperreflective region that does not represent the real external limit of the choroid, but is located superficially to it, thus underestimating the values of CT. This might justify the reported differences between measurements performed in the same eyes with SS OCT and SD OCT.^{43,44} Moreover, the current software commercially available for SD OCT only enables measuring CT in manually chosen points, which tends to be influenced by

TABLE 4. Univariable and Multivariable Assessments of Choroidal Thickness Within the Distinct ETDRS Grid Sectors

ETDRS Grid Sector	Univariable Analysis			Multivariable Analysis (Controlling for Age)		
	β coefficient	95% CI	P Value	β coefficient	95% CI	P Value
Mean of all sectors	-14.97	-31.21; 1.26	.071	-21.90	-37.54; -6.27	.006*
Central	-17.92	-36.74; 0.91	.062	-25.59	-43.73; -7.46	.006*
Inner temporal	-21.18	-39.26; -3.10	.022*	-28.87	-46.27; -11.46	.001*
Inner superior	-20.42	-39.75; -1.09	.380	-28.99	-47.47; -10.51	.002*
Inner nasal	-20.27	-39.01; -1.53	.034*	-26.99	-45.15; -8.84	.004*
Inner inferior	-15.14	-35.32; 5.04	.142	-22.99	-42.42; -3.57	.020*
Outer temporal	-11.88	-27.84; 4.07	.144	-18.79	-34.15; -3.42	.017*
Outer superior	-18.27	-36.81; 0.27	.053	-26.28	-43.97; -8.61	.004*
Outer nasal	-14.56	-31.78; 2.66	.098	-20.64	-37.36; -3.93	.015*
Outer inferior	-12.45	-31.27; 6.36	.195	-20.49	-38.47; -2.51	.026*

CI = confidence interval.
P values < .05 are noted by an asterisk.

focal irregularities of the choroidal-scleral interface and are observer-dependent.¹³ As described, the Atlantis SS OCT provides automatic CT maps based on the ETDRS grid, which is clinically comprehensive.

Despite representing the largest assessment of the relationship between SDD and CT, this study has some limitations. The cross-sectional design does not allow us to clarify if a reduced CT is a cause or a consequence of the presence of SDD. Additionally, despite only including eyes with a spherical equivalent less than 6 diopters, we did not collect data on axial length, which might have affected our results. As detailed, we followed a statistical approach that enabled us to account for the inclusion of 2 eyes of the same patient.³⁰ However, an alternative approach could be considering solely 1 eye per subject. Also of note, we based our assessment of the presence of SDD solely on high-resolution SD OCT. Although there is no established gold standard to detect these lesions, a multimodal approach might offer some advantages.⁴⁵⁻⁴⁷ Despite this, previous authors⁴⁰ described that SD OCT alone has the highest sensitivity (94.6%) and specificity (98.4%) among

all imaging modalities to detect SDD. Finally, as described in our Methods section, we modified our SD OCT imaging protocol from 30 × 25 degrees to 20 × 20 degrees. This means that, for the eyes imaged with the latter, the scanning range did not cover the width of the entire macular area (ie, some SDD might have been missed). On the other hand, this 97-line protocol provides a distance between scans of only 6 μm, thus allowing the identification of small individual SDD.

In conclusion, SS OCT identified decreased choroidal thickness values in eyes with SDD and intermediate AMD, both on average and across all sectors of the ETDRS grid individually. Choroidal vessel volume was also decreased in the presence of SDD. Importantly, the design of our study (ie, including only eyes with intermediate AMD) suggests that macular choroidal thinning and reduced choroidal vessel volume are related to SDD itself. Understanding choroidal abnormalities can improve our knowledge of the natural history of SDD, which seem to be an important clinical feature of AMD, and may provide insight into the pathogenesis of AMD.

FUNDING/SUPPORT: THE MILLER RETINA RESEARCH FUND (MASS. EYE AND EAR) AND THE MILLER CHAMPALIMAUD VISION Award (Mass. Eye and Ear) (to J.W.M.); Portuguese Foundation for Science and Technology/Harvard Medical School Portugal Program (HMSP-ICJ/006/2013) (to I.L.). Financial Disclosures: Inês Láins: Travel expenses from Allergan. Ivana K. Kim: Consultant to Allergan, Alcon, Genentech, and Iconic Therapeutics. Rufino Silva: Member of advisory board for Alcon, Alimera, Allergan, Bayer, Novartis, Thea. Travel expenses from Novartis, Thea, Bayer, Alcon, Angelini. Personal fees for lectures from Bayer, Novartis. Joan W. Miller: Consultant to Alcon Research Institute, KalVista Pharmaceuticals, Ltd, Maculogix, Inc; Patent with ONL Therapeutics, LLC Royalties from Valeant Pharmaceuticals. John B. Miller: Consultant to Allergan. The following authors have no financial disclosures: Jay Wang, Joana Providência, Steven Mach, Pedro Gil, João Gil, Marco Marques, Grayson Armstrong, Shady Garas, Patrícia Barreto, Demetrios G. Vavvas, and Deeba Husain. All authors attest that they meet the current ICMJE criteria for authorship.

REFERENCES

1. Wong WL, Su X, Li X, et al. Global prevalence of age-related macular degeneration and disease burden projection for 2020 and 2040: a systematic review and meta-analysis. *Lancet Glob Health* 2014;2(2):e106-e116.
2. Patel V, Oetting TA, Manzanaro G, et al. Drusen characterization with multimodal imaging. *Retina* 2011;30(9):1441-1454.
3. Spaide RF, Curcio CA. Anatomical correlates to the bands seen in the outer retina by optical coherence tomography: literature review and model. *Retina* 2011;31(8):1609-1619.

4. Cohen SY, Dubois L, Tadayoni R, Delahaye-Mazza C, Debibie C, Quentel G. Prevalence of reticular pseudodrusen in age-related macular degeneration with newly diagnosed choroidal neovascularisation. *Br J Ophthalmol* 2007;91(3):354-359.
5. Marsiglia M, Boddu S, Bearely S, et al. Association between geographic atrophy progression and reticular pseudodrusen in eyes with dry age-related macular degeneration. *Invest Ophthalmol Vis Sci* 2013;54(12):7362-7369.
6. Yun C, Oh J, Ahn S-E, Hwang S-Y, Kim S-W, Huh K. Peripapillary choroidal thickness in patients with early age-related macular degeneration and reticular pseudodrusen. *Graefes Arch Clin Exp Ophthalmol* 2016;254(3):427-435.
7. Garg A, Oll M, Yzer S, et al. Reticular pseudodrusen in early age-related macular degeneration are associated with choroidal thinning. *Invest Ophthalmol Vis Sci* 2013;54(10):7075-7081.
8. Hogg RE, Silva R, Staurenghi G, et al. Clinical characteristics of reticular pseudodrusen in the fellow eye of patients with unilateral neovascular age-related macular degeneration. *Ophthalmology* 2014;121(9):1748-1755.
9. Alten F, Clemens CR, Heiduschka P, Eter N. Localized reticular pseudodrusen and their topographic relation to choroidal watershed zones and changes in choroidal volumes. *Invest Ophthalmol Vis Sci* 2013;54(5):3250-3257.
10. Michalewski J, Michalewska Z, Nawrocka Z, Bednarski M, Nawrocki J. Correlation of choroidal thickness and volume measurements with axial length and age using swept source optical coherence tomography and optical low-coherence reflectometry. *Biomed Res Int* 2014;2014:639160.
11. Laíns I, Talcott KE, Santos AR, et al. Choroidal thickness in diabetic retinopathy assessed with swept-source optical coherence tomography. *Retina* 2017; <http://dx.doi.org/10.1097/IAE.0000000000001516>.
12. Ferrara D, Mohler KJ, Waheed N, et al. En face enhanced-depth swept-source optical coherence tomography features of chronic central serous chorioretinopathy. *Ophthalmology* 2014;121(3):719-726.
13. Hirata M, Tsujikawa A, Matsumoto A, et al. Macular choroidal thickness and volume in normal subjects measured by swept-source optical coherence tomography. *Invest Ophthalmol Vis Sci* 2011;52(8):4971-4978.
14. Motaghianezam R, Schwartz DM, Fraser SE. In vivo human choroidal vascular pattern visualization using high-speed swept-source optical coherence tomography at 1060 nm. *Invest Ophthalmol Vis Sci* 2012;53(4):2337-2348.
15. Alonso-Caneiro D, Read SA, Collins MJ. Automatic segmentation of choroidal thickness in optical coherence tomography. *Biomed Opt Express* 2013;4(12):2795-2812.
16. Capuano V, Souied EH, Miere A, Jung C, Costanzo E, Querques G. Choroidal maps in non-exudative age-related macular degeneration. *Br J Ophthalmol* 2016;100(5):677-682.
17. Jirarattanasopa P, Ooto S, Tsujikawa A, et al. Assessment of macular choroidal thickness by optical coherence tomography and angiographic changes in central serous chorioretinopathy. *Ophthalmology* 2012;119(8):1666-1678.
18. Ellabban AA, Tsujikawa A, Matsumoto A, et al. Macular choroidal thickness and volume in eyes with angioid streaks measured by swept source optical coherence tomography. *Am J Ophthalmol* 2012;153(6):1133-1143.
19. Park HY, Shin HY, Park CK. Imaging the posterior segment of the eye using swept-source optical coherence tomography in myopic glaucoma eyes: comparison with enhanced-depth imaging. *Am J Ophthalmol* 2014;157(3):550-557.
20. Tan CS, Ngo WK, Cheong KX. Comparison of choroidal thicknesses using swept source and spectral domain optical coherence tomography in diseased and normal eyes. *Br J Ophthalmol* 2015;99(3):354-358.
21. Ueda-Arakawa N, Ooto S, Ellabban AA, et al. Macular choroidal thickness and volume of eyes with reticular pseudodrusen using swept-source optical coherence tomography. *Am J Ophthalmol* 2014;157(5):994-1004.
22. Manjunath V, Goren J, Fujimoto JG, Duker JS. Analysis of choroidal thickness in age-related macular degeneration using spectral-domain optical coherence tomography. *Am J Ophthalmol* 2011;152(4):663-668.
23. Cachulo MdL, Lobo C, Figueira J, et al. Prevalence of age-related macular degeneration in Portugal: The Coimbra Eye Study - Report 1. *Ophthalmologica* 2015;233(3-4):119-127.
24. Laíns I, Miller JB, Mukai R, et al. Health conditions linked to age-related macular degeneration associated with dark adaptation. *Retina* 2017; <http://dx.doi.org/10.1097/IAE.0000000000001659>.
25. The Age-Related Eye Disease Study system for classifying age-related macular degeneration from stereoscopic color fundus photographs: the Age-Related Eye Disease Study Report Number 6. *Am J Ophthalmol* 2001;132(5):668-681.
26. Danis RP, Domalpally A, Chew EY, et al. Methods and reproducibility of grading optimized digital color fundus photographs in the Age-Related Eye Disease Study 2 (AREDS2 Report Number 2). *Invest Ophthalmol Vis Sci* 2013;54(7):4548-4554.
27. Staurenghi G, Sadda S, Chakravarthy U, Spaide RF. Proposed lexicon for anatomic landmarks in normal posterior segment spectral-domain optical coherence tomography: the INOCT consensus. *Ophthalmology* 2014;121(8):1572-1578.
28. Otsu N. A threshold selection method for gray-level histograms. *IEEE Trans Syst Man Cybern* 1979;9:62-66.
29. Burton P, Gurrin L, Sly P. Extending the simple linear regression model to account for correlated responses: an introduction to generalized estimating equations and multi-level mixed modelling. *Stat Med* 1998;17(11):1261-1291.
30. Fitzmaurice GM, Laird NM, Ware JH. Linear mixed effect models. In: Wiley, ed. *Applied Longitudinal Analysis*. 2nd ed. Hoboken, New Jersey: John Wiley and Sons Inc; 2011:189-240.
31. Querques G, Querques L, Forte R, Massamba N, Coscas F, Souied EH. Choroidal changes associated with reticular pseudodrusen. *Invest Ophthalmol Vis Sci* 2012;53(3):1258-1263.
32. Cheng H, Kaszubski PA, Hao H, et al. The relationship between reticular macular disease and choroidal thickness. *Curr Eye Res* 2016;41(11):1492-1497.
33. Haas P, Esmaelpour M, Ansari-Shahrezaei S, Drexler W, Binder S. Choroidal thickness in patients with reticular pseudodrusen using 3D 1060-nm OCT maps. *Invest Ophthalmol Vis Sci* 2014;55(4):2674-2681.
34. Zheng F, Gregori G, Schaal K, et al. Choroidal thickness and choroidal vessel density in nonexudative age-related macular degeneration using swept-source optical coherence tomography imaging. *Invest Ophthalmol Vis Sci* 2016;57(14):6256-6264.

35. Alten F, Heiduschka P, Clemens CR, Eter N. Exploring choriocapillaris under reticular pseudodrusen using OCT-angiography. *Graefes Arch Clin Exp Ophthalmol* 2016; 254(11):2165–2173.
36. Sarks J, Arnold J, Ho I-V, Sarks S, Killingsworth M. Evolution of reticular pseudodrusen. *Br J Ophthalmol* 2011;95(7): 979–985.
37. Ferrara D, Waheed NK, Duker JS. Investigating the choriocapillaris and choroidal vasculature with new optical coherence tomography technologies. *Prog Retin Eye Res* 2015;52: 130–155.
38. Sivaprasad S, Bird A, Nitiapapand R, Nicholson L, Hykin P, Chatziralli I. Perspectives on reticular pseudodrusen in age-related macular degeneration. *Surv Ophthalmol* 2016;61(5): 521–537.
39. Alten F, Clemens CR, Milojcic C, Eter N. Subretinal drusenoid deposits associated with pigment epithelium detachment in age-related macular degeneration. *Retina* 2012; 32(9):1727–1732.
40. Ueda-Arakawa N, Ooto S, Tsujikawa A, Yamashiro K, Oishi A, Yoshimura N. Sensitivity and specificity of detecting reticular pseudodrusen in multimodal imaging in Japanese patients. *Retina* 2013;33(3):490–497.
41. Copete S, Flores-Moreno I, Montero JA, Duker JS, Ruiz-Moreno JM. Direct comparison of spectral-domain and swept-source OCT in the measurement of choroidal thickness in normal eyes. *Br J Ophthalmol* 2014;98(3):334–338.
42. Kim JH, Kang SW, Kim J, Chang YS. Influence of image compression on the interpretation of spectral-domain optical coherence tomography in exudative age-related macular degeneration. *Eye (Lond)* 2014;28(7):825–831.
43. Matsuo Y, Sakamoto T, Yamashita T, Tomita M, Shirasawa M, Terasaki H. Comparisons of choroidal thickness of normal eyes obtained by two different spectral-domain OCT instruments and one swept-source OCT instrument. *Invest Ophthalmol Vis Sci* 2013;54(12):7630–7636.
44. Philip A-M, Gerendas BS, Zhang L, et al. Choroidal thickness maps from spectral domain and swept source optical coherence tomography: algorithmic versus ground truth annotation. *Br J Ophthalmol* 2016; <http://dx.doi.org/10.1136/bjophthalmol-2015-307985>.
45. Sohrab MA, Smith RT, Salehi-Had H, Sadda SR, Fawzi AA. Image registration and multimodal imaging of reticular pseudodrusen. *Invest Ophthalmol Vis Sci* 2011;52(8):5743–5748.
46. Smith RT, Sohrab MA, Busuioc M, Barile G. Reticular macular disease. *Am J Ophthalmol* 2009;148(5):733–743.e2.
47. Gil JQ, Marques JP, Hogg R, et al. Clinical features and long-term progression of reticular pseudodrusen in age-related macular degeneration: findings from a multicenter cohort. *Eye* 2017;31(3):364–371.

Novel grid combined with peripheral distortion correction for ultra-widefield image grading of age-related macular degeneration

Patrick Oellers^{1,*}

Inês Laíns^{1,2,*}

Steven Mach¹

Shady Garas¹

Ivana K Kim¹

Demetrios G Vavvas¹

Joan W Miller¹

Deeba Husain¹

John B Miller¹

¹Retina Service, Department of Ophthalmology, Massachusetts Eye and Ear, Harvard Medical School, Boston, MA, USA; ²Faculty of Medicine, University of Coimbra, Coimbra, Portugal

*These authors contributed equally to this work

Purpose: Eyes with age-related macular degeneration (AMD) often harbor pathological changes in the retinal periphery and perimacular region. These extramacular changes have not been well classified, but may be phenotypically and functionally relevant. The purpose of this study was to demonstrate a novel grid to systematically study peripheral retinal abnormalities in AMD using geometric distortion-corrected ultra-widefield (UWF) imaging.

Methods: This is a cross-sectional observational case series. Consecutive patients with AMD without any other coexisting vitreoretinal disease and control patients over age 50 without AMD or any other vitreoretinal disease were imaged using Optos 200 Tx. Captured 200° UWF images were corrected for peripheral geometric distortion using Optos transformation software. A newly developed grid to study perimacular and peripheral abnormalities in AMD was then projected onto the images.

Results: Peripheral and perimacular changes such as drusen, retinal pigment epithelium changes and atrophy were found in patients with AMD. The presented grid in conjunction with geometric distortion-corrected UWF images allowed for systematic study of these peripheral changes in AMD.

Conclusion: We present a novel grid to study peripheral and posterior pole changes in AMD. The grid is unique in that it adds a perimacular zone, which may be important in characterizing certain phenotypes in AMD. Our UWF images were corrected for geometric peripheral distortion to accurately reflect the anatomical dimensions of the retina. This grid offers a reliable and reproducible foundation for the exploration of peripheral retinal pathology associated with AMD.

Keywords: ultra-widefield, autofluorescence, macular degeneration, grid, periphery, drusen, retinal pigment epithelium changes

Introduction

Age-related macular degeneration (AMD) is a leading cause of blindness in developed countries. Systematic study and grading of AMD has been limited to the posterior pole until recently.^{1,2} However, it is well recognized that pathological changes, such as drusen and retinal pigment epithelium (RPE) changes, also exist in the peripheral fundus in patients with AMD.³⁻⁸ In contrast to the progress that has been made on macular-derived findings of this disease, the impact on function and disease progression of peripheral retinal changes remains not well understood. While regular fundus photography, as well as optical coherence tomography, can be used to objectively document and study macular changes, systematic investigation of the peripheral fundus has been more challenging.^{1,9}

Correspondence: John B Miller
Department of Ophthalmology, Retina Service, Massachusetts Eye and Ear, Harvard Medical School, 243 Charles Street, Boston, MA 02114, USA
Tel +1 617 573 3750
Fax +1 617 573 3698
Email john_miller@meei.harvard.edu

submit your manuscript | www.dovepress.com

Dovepress    
<http://dx.doi.org/10.2147/OPTH.S143246>

Clinical Ophthalmology 2017:11 | 1967-1974

1967



© 2017 Oellers et al. This work is published and licensed by Dove Medical Press Limited. The full terms of this license are available at <https://www.dovepress.com/terms.php> and incorporate the Creative Commons Attribution – Non Commercial (unported, 3.0) License (<http://creativecommons.org/licenses/by-nc/3.0/>). By accessing the work you hereby accept the Terms. Non-commercial uses of the work are permitted without any further permission from Dove Medical Press Limited, provided the work is properly attributed. For permission for commercial use of this work, please see paragraphs 4.2 and 5 of our Terms (<https://www.dovepress.com/terms.php>).

Recently, ultra-widefield (UWF) fundus imaging has been established to create high-resolution images of the peripheral and central retina, which can be used for grading of peripheral retinal diseases. This has been widely performed for diabetic retinopathy and more recently for AMD.^{10,11} In fact, UWF imaging has already demonstrated that peripheral abnormalities seen on pseudocolor and autofluorescence imaging are more prevalent in AMD than healthy patients.^{3,12}

These peripheral abnormalities in AMD may be genetically and phenotypically distinct and hence need to be studied. For example, one recent study that used clinical examination alone without standardized imaging suggests that peripheral drusen and reticular pigment changes are associated with AMD severity. Further, peripheral drusen were associated with CFHY402H genotype and reticular pigment changes were associated with CFHrs1410996 genotype.⁶ Peripheral disease may also impact function in AMD. Impairment in dark adaptation, a rod-driven process and hence topographically mapped to the peripheral retina, has been found to be affected in early-stage macular degeneration as well as to be correlated with AMD disease severity.^{13,14} To this end, systematic UWF imaging grid grading systems are needed to methodically study peripheral abnormalities in AMD.

While different groups work on refinement of grids that can be used for grading of peripheral abnormalities, one of the difficulties encountered in the systematic grading of UWF images has been that these images are distorted in the periphery and hence do not reflect the actual dimensions of the retina.¹⁵

We present a novel UWF imaging-based grid grading system that incorporates correction for peripheral image distortion and defines regions of the periphery, providing a foundation for ongoing cohort studies of patients with AMD.

Methods

This study is part of a prospective, cross-sectional, observational project on AMD biomarkers. It was conducted in accordance with HIPAA (Health Insurance Portability and Accountability Act) requirements and the tenets of the Declaration of Helsinki, and was approved by the Massachusetts Eye and Ear (MEE) Institutional Review Board. All included participants provided written informed consent.

Inclusion and exclusion criteria

We recruited and consented consecutive patients with a diagnosis of AMD when they visited the Retina Service of MEE during their regular appointments. We excluded subjects with any other vitreoretinal disease, active uveitis or ocular

infection, significant media opacities that precluded the observation of the ocular fundus, refractive error equal to or greater than 6 D of spherical equivalent, past history of retinal surgery, history of any ocular surgery or intraocular procedure (such as laser and intraocular injections) within the last 90 days prior to enrollment and diagnosis of diabetes mellitus, with or without concomitant diabetic retinopathy. Additionally, a control group of subjects aged 50 years or older, without any evidence of AMD in both eyes, was included, and the same exclusion criteria were applied.

Image acquisition

All participants were imaged using the Optos 200 Tx camera in three gaze positions (Optos Inc, Dunfermline, UK), both with pseudocolor and autofluorescence. The central image taken in primary gaze missed some aspects of the retinal periphery. The two additional images taken in upgaze and downgaze covered these additional areas, as shown in Figure 1.

Image processing

Following acquisition, images underwent transformation using Optos stereographic projection software (ProView), which takes into account the optical imaging system and the ocular geometry to map each pixel to a consistent, spherical geometry. This preserves angular features and enables accurate representation of retinal features throughout the entire image. This software is incorporated into the newer Optos California device and available as an upgrade for both Optos Advance and V2 Advantage software for use with Optos 200 Tx.

The resulting images are 33.86×33.86 cm in size with a resolution of 300 dots per inch. Thereafter, a novel fundus grid, specifically created to help grade central and peripheral AMD, was applied onto each of the six created images. No image montage was created. The grid consists of three concentric circles and crosshairs centered on the fovea.

The first circle surrounds the macula within the vascular arcades, with a radius of 29 mm. This circle is based on the Early Treatment of Diabetic Retinopathy Study (ETDRS) grid used by the Age-related Eye Disease Study (AREDS).¹ The ETDRS grid was first developed to aid in localization of diabetic macular edema and the assessment of diabetic retinopathy,¹⁶ but it also provides a reliable means for the assessment of central drusen burden in AMD.

The second circle encompasses the perimacular area, including both temporal arcades, with a radius of 65 mm. Through clinical experience, we have found that many

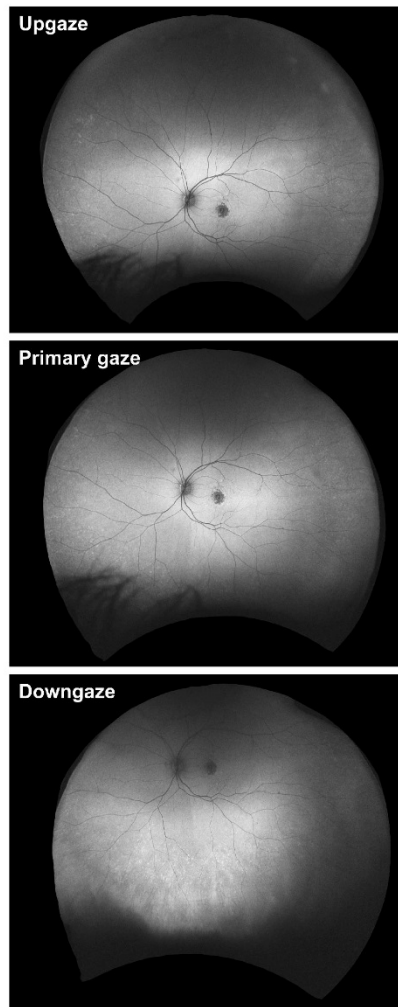


Figure 1 Gaze positions to optimally capture entire fundus in ultra-widefield imaging. Images were routinely captured in primary gaze, upgaze and downgaze. While primary gaze images reflect the temporal and nasal periphery reasonably well, it is necessary to capture images in upgaze and downgaze to better show the superior and inferior periphery as demonstrated in this ultra-widefield autofluorescence image sequence of a left eye.

patients have a high proportion of pathology in this posterior location, yet one that is outside the macula. By including this pericentral location and not just the mid- and far periphery outside the macula, we hope to better categorize these clinical subtypes.

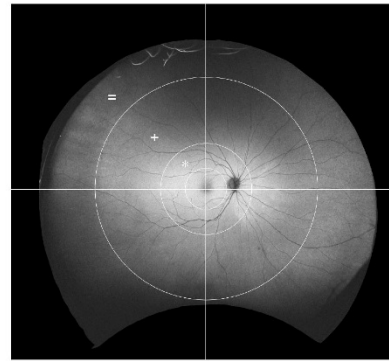


Figure 2 Novel grid to systematically grade peripheral abnormalities in age-related macular degeneration. The grid consists of three concentric circles and two lines. The central circle surrounds the macula area. The middle circle surrounds the perimacular area (*). The largest circle separates the mid periphery (+) from the far periphery (-). A vertical line through the fovea separates temporal from nasal quadrants. A horizontal line through the fovea separates superior from inferior quadrants.

The last and most peripheral circle separates the mid-peripheral area from the far periphery. This circle is drawn with a radius of 160 mm, which was chosen based on the location of the vortex veins. With this grid, the extramacular retina can be divided into 12 zones with the perimacular area, mid periphery and far periphery in each of the four quadrants: superotemporal, superonasal, inferonasal and inferotemporal (Figure 2).

The circles and the crosshairs were all centered on the fovea as opposed to the optic nerve. By centering on the fovea, the perimacular area can be properly positioned with a fixed radius. It also allows the nasal mid periphery to be more analogous to the temporal mid periphery than if the zones were centered on the optic nerve, in which case the macula would be included in the temporal mid-peripheral zones.

Most importantly, the grid corrects for the peripheral distortion inherent to the image acquisition of this UWF imaging device. This allows for an accurate measurement throughout the periphery.

As a result of the image processing, the optic disk measures about 10 mm in these images, whereas it is approximately 1.5 mm in the average human fundus. In this way, images project to about 6.7 times the size of the actual fundus. Images were then stored digitally and used for analysis of macular and peripheral pathology.

Results

Case presentations

To demonstrate feasibility of fundus grading with our novel grid projected onto distortion-corrected UWF imaging we

detail findings of two patients with AMD and one control patient without AMD.

Case 1

A 69-year-old male presented with AMD in both eyes. Best-corrected visual acuity (BCVA) was 20/40 in the right eye and 20/25 in the left eye. In the right eye (Figure 3), there were central RPE changes and macular drusen (Figure 3A–C). There was some RPE atrophy demonstrated by perifoveal hypoautofluorescence (Figure 3D–F). The perimacular zone demonstrated extensive drusen, most prominent inferotemporally and more moderate superotemporally and superonasally (Figure 3A and C), with very few drusen present inferonasally (Figure 3C and F). These drusen extended into the mid periphery and were best seen in upgaze (Figure 3A and D). A few loose drusen were also present in mid periphery inferonasally and inferotemporally, best seen in downgaze (Figure 3C and F). The nasal far periphery also harbored drusen, best seen in upgaze for the superonasal quadrant (Figure 3A and E) and in downgaze for the inferonasal quadrant (Figure 3C and F). There were isolated drusen in the far periphery superotemporally (Figure 3A), but no pathological abnormalities were seen inferotemporally (Figure 3C and F).

Case 2

A 62-year-old female presented with geographic atrophy and drusen in both eyes. BCVA was 20/50 in the right eye and 20/125 in the left eye. The right eye (Figure 4) demonstrated juxtafoveal geographic atrophy as well as several drusen (Figure 4A–C). Few drusen extended into the temporal perimacular area (Figure 4). There was a cluster of nasal and superonasal drusen in the far periphery (Figure 4A, B, D and E). Few drusen were present in the superotemporal and inferotemporal mid- and far periphery, best seen on autofluorescence images (Figure 4D–F). The inferior fundus had several drusen, mostly along the border of the mid- and far periphery (Figure 4C–F). In addition, there were relatively focal hyperautofluorescent and hypoautofluorescent changes in the mid-peripheral nasal to the optic disk, representing RPE atrophy with adjacent increased RPE metabolism. The patchy color changes in the temporal far periphery on pseudocolor images (Figure 4A and B) were artifacts and had no correlation on respective autofluorescence images (Figure 4D and E).

Case 3

A 60-year-old female presented with recurrent corneal abrasions, without signs of AMD or any other vitreoretinal disease.

BCVA was 20/25 in the right eye and 20/20 in the left eye. In the right eye, the macula appeared normal without any drusen or RPE atrophy (Figure 5). There was focal RPE atrophy in the superonasal quadrant of the mid periphery (Figure 5A and D). There were nonspecific patchy hyperautofluorescent changes in the inferotemporal quadrant of the mid- and far periphery (Figure 5F). Speckled dots in the superior fundus were seen on pseudocolor images (Figure 5A) representing artifacts instead of drusen, and there was no correlation on autofluorescence imaging (Figure 5D).

Discussion

We here present a novel UWF imaging grid grading system that can be used for systematic studies of perimacular and peripheral lesions in AMD. Our grading technique has several advantages over other previously described systems, by offering distortion correction to UWF imaging as well as a more refined grid that adds a perimacular zone next to central, mid-peripheral and far-peripheral zones.

Since its inception, UWF imaging has been used to study peripheral findings in AMD. Csutak et al reported a high rate of agreement between regular 45° central fundus photography and UWF imaging for grading of abnormalities in the macula. The authors demonstrated that the level of detail and resolution of UWF imaging should be sufficient to grade findings in the macular region as well, likely allowing comparison of UWF imaging studies with studies that were based on conventional fundus photography.¹⁷

In 2015, Lengyel et al introduced the first grading system for peripheral lesions in AMD based on UWF imaging. The grid suggested by these authors consists of three concentric rings representing the fovea, perifovea and macular zones analogous with the ETDRS grid, in addition to a fourth zone for the mid periphery and fifth zone for the far periphery. While zones 1–3 were chosen based on prespecified parameters of the International AMD Classification Study and hence allow comparison with prior studies, peripheral zones 4 and 5 were chosen arbitrarily. The study demonstrated feasibility of grading peripheral lesions (namely RPE changes, drusen, mixed lesion and atrophy) as well as macular abnormalities in patients with AMD using autofluorescence and pseudocolor UWF imaging with high intergrader agreement.¹⁰ While this study certainly added to our understanding of peripheral AMD findings, it is limited by not correcting for the distortion of images in the periphery.

Our novel method offers several theoretical advantages by reducing distortion of the images of the retinal periphery and adding an additional perimacular zone for grading. Optos

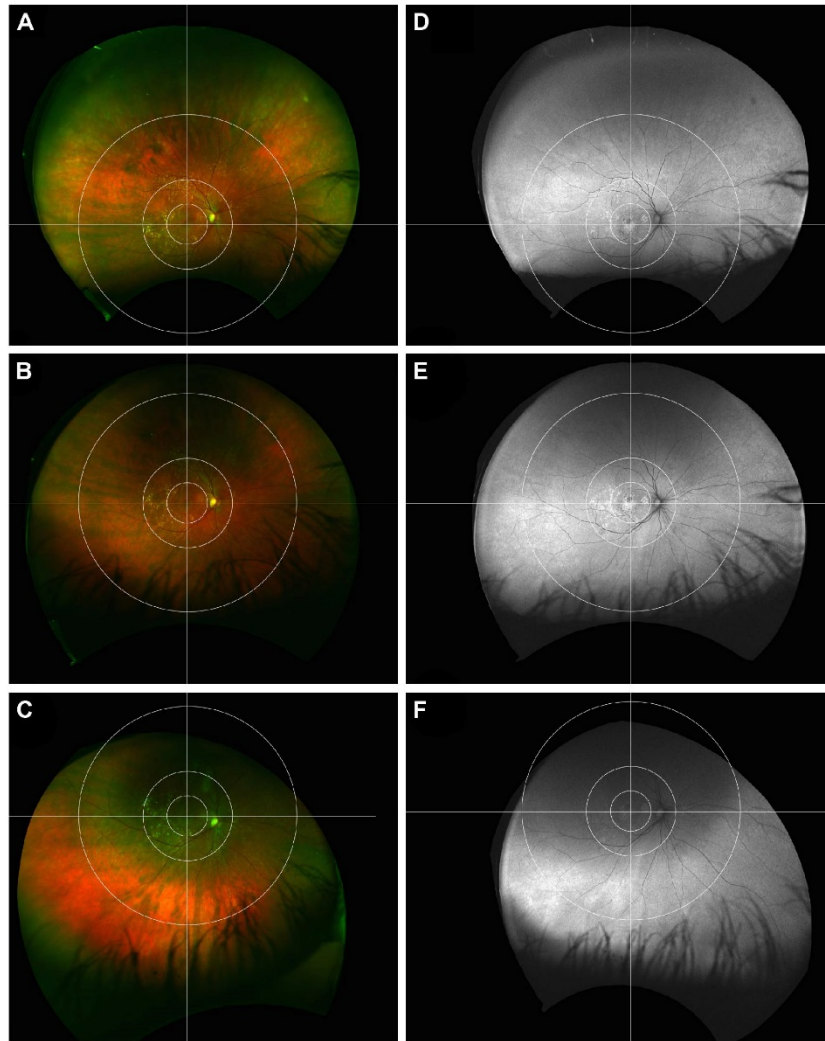


Figure 3 Patient with age-related macular degeneration and widespread perimacular and peripheral abnormalities. Ultra-widefield pseudocolor images of the right eye demonstrate foveal retinal pigment epithelium (RPE) changes along with macular drusen in all quadrants. There are extensive drusenoid changes in the perimacular area in the temporal quadrants, as well as mid-peripheral and far-peripheral drusen and RPE changes (A–C). Analogous to this, ultra-widefield autofluorescence shows mixed hyper/hypoautofluorescence in the macula and hyperautofluorescence in the perimacula. The mid- and far periphery show partially mottled hyperautofluorescence (D–F). Upgaze (A and D); primary gaze (B and E), downgaze (C and F).

captures images of the far-peripheral temporal and nasal retina by utilizing an ellipsoid mirror, which leads to significant distortion of the peripheral image. When analyzing these distorted images, grading may be prone to artifacts as well as over- or underestimation of observed abnormalities.

In addition, unless the degree of image distortion would be stable in future imaging machines, image analysis may not be reproducible.

To reflect this, we used a novel image transformation software developed by Optos that preserves the spherical

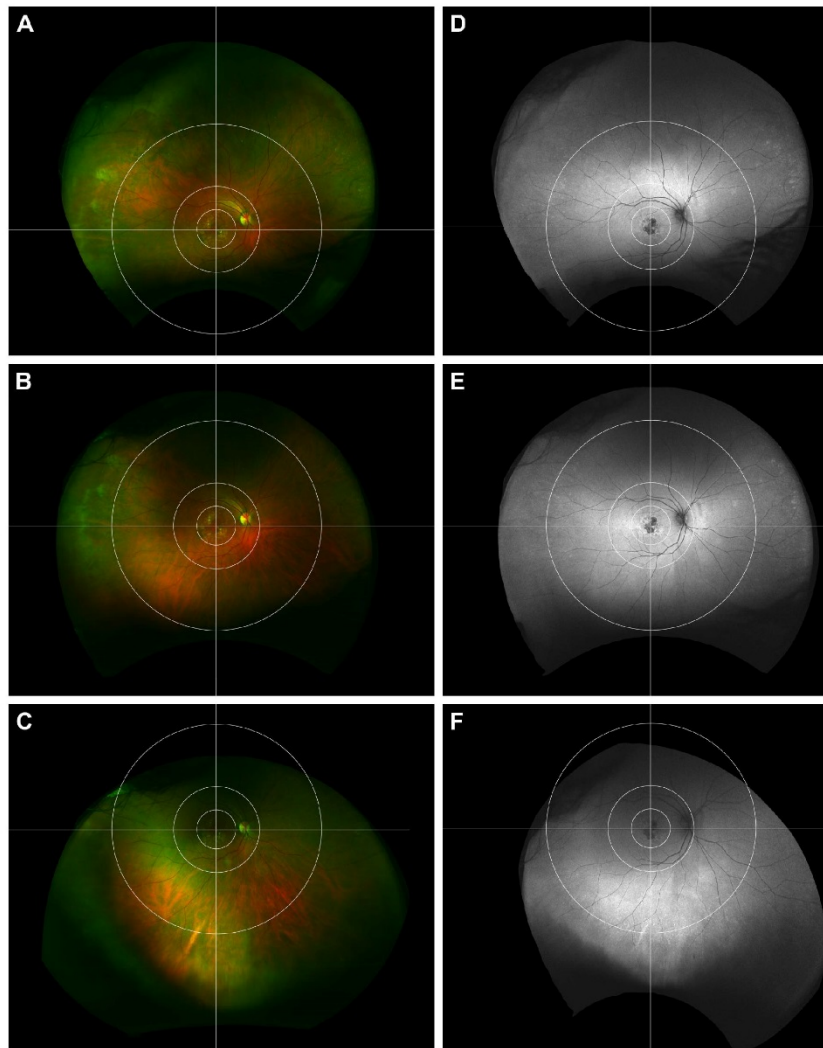


Figure 4 Patient with age-related macular degeneration and peripheral abnormalities. Ultra-widefield pseudocolor images of the left eye demonstrate juxtafoveal geographic atrophy and macular drusen, partially extending into the perimacular region. There are a few drusen, mostly in the nasal far periphery, but also inferior along the border of mid- and far periphery (A–C). Corresponding autofluorescence images demonstrate brisk hypofluorescence juxtafoveally with adjacent hyperautofluorescence. There is hyperautofluorescence, which extends into the temporal perimacular as well as speckled hyperautofluorescence, mostly nasally and inferiorly (D–F). Upgaze (A and D); primary gaze (B and E), downgaze (C and F).

geometry of the peripheral retina in UWF imaging, which hopefully should pave the way for adequate, reliable and reproducible investigation of peripheral abnormalities, especially future quantitative analyses. Furthermore, image distortion correction is now commercially available and

integrated into newer-generation devices. Also, the grid suggested by Lengyel et al as well as the AREDS group separates the peripheral retina into the far- and mid-peripheral zone, whereas we have chosen an additional zone for the perimacular area just outside the vascular arcades. We

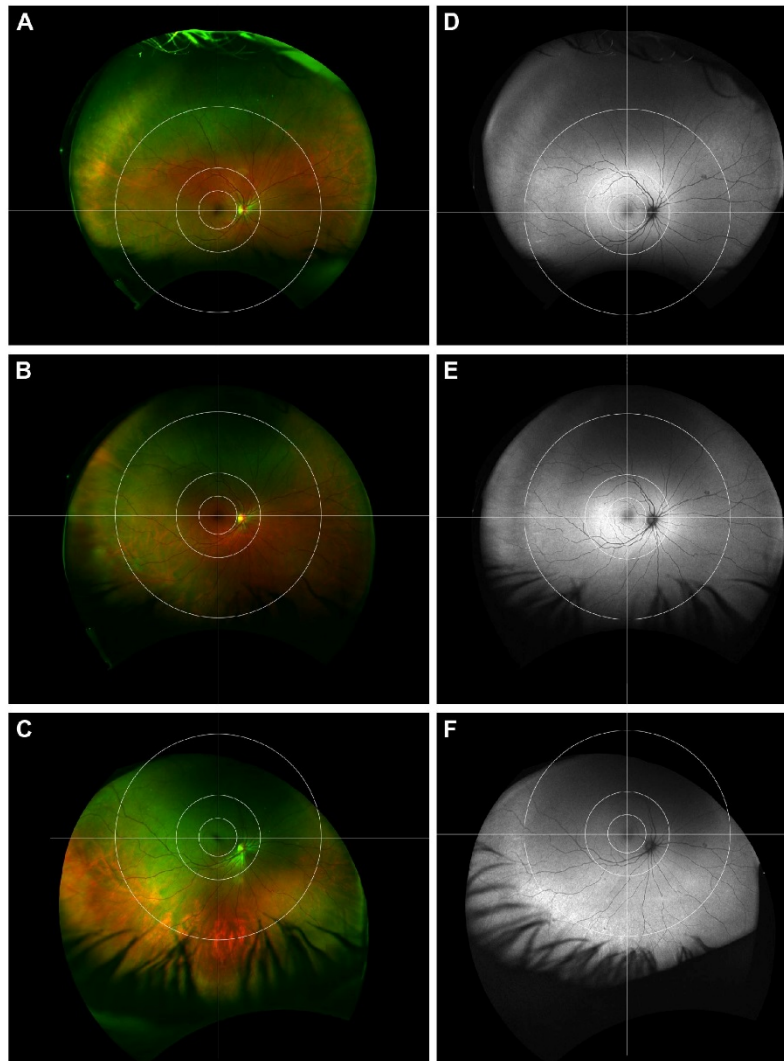


Figure 5 Patient without age-related macular degeneration and nonspecific peripheral retinal changes. Ultra-widefield pseudocolor images of the right eye demonstrate normal macula and a few nonspecific changes in the peripheral retina (A–C). Autofluorescence imaging demonstrates focal retinal pigment epithelium atrophy in the superonasal mid periphery as well as patchy hyperautofluorescence inferotemporally along the border of mid- and far periphery (D–F). Upgaze (A and D); primary gaze (B and E), downgaze (C and F).

feel that the perimacular zone may be important in future classification of peripheral AMD. In our clinical experience, there are many patients with peripheral drusen and RPE abnormalities solely in the perimacular area without findings in the far-peripheral retina, which is exemplified by patient

1 in this series. Hypothesizing that this may be a specific phenotype, we believe there is value by adding a specific zone for grading the perimacular area.

Our new method has some limitations for grading of peripheral pathology. Optos creates pseudocolor images by

way of laser scanning ophthalmoscopy, which in theory is prone to artifacts or misinterpretation of findings. Most retina specialists accept this limitation because conventional fundus photography is more time intensive and limited to the mid periphery. Ultra-widefield autofluorescence imaging can provide useful information, but should be interpreted in conjunction with pseudocolor images to avoid misinterpretation of potential artifacts. Our grid is limited to patients with up to -6 D refractive error due to the enlarged fundus dimensions associated with myopia. While the here-described methodology system is relatively new, we suggest that with further research, UWF imaging in conjunction with image grading methodologies such as described here has potential to assist in teleophthalmology system networks in the future.¹⁸

In summary, we present a novel grid applied to peripheral geometric distortion correction UWF imaging. The grid allows analysis of the peripheral retinal fundus divided into 12 reproducible zones. This systematic assessment will be used in future clinical studies to unravel the peripheral phenotypes and associations of AMD.

Acknowledgment

The authors would like to thank Optos (Optos Inc, Dunfermline, UK) for technical assistance and help with the manuscript.

Disclosure

The authors report no conflicts of interest in this work.

References

- Age-Related Eye Disease Study Research Group. The Age-Related Eye Disease Study system for classifying age-related macular degeneration from stereoscopic color fundus photographs: the Age-Related Eye Disease Study Report Number 6. *Am J Ophthalmol*. 2001;132(5):668–681.
- Bird AC, Bressler NM, Bressler SB, et al. An international classification and grading system for age-related maculopathy and age-related macular degeneration. The International ARM Epidemiological Study Group. *Surv Ophthalmol*. 1995;39(5):367–374.
- Heussen FM, Tan CS, Sadda SR. Prevalence of peripheral abnormalities on ultra-widefield greenlight (532 nm) autofluorescence imaging at a tertiary care center. *Invest Ophthalmol Vis Sci*. 2012;53(10):6526–6531.
- Reznicek L, Wasfy T, Stumpf C, et al. Peripheral fundus autofluorescence is increased in age-related macular degeneration. *Invest Ophthalmol Vis Sci*. 2012;53(4):2193–2198.
- Rudolf M, Clark ME, Chimento MF, Li CM, Medeiros NE, Curcio CA. Prevalence and morphology of druse types in the macula and periphery of eyes with age-related maculopathy. *Invest Ophthalmol Vis Sci*. 2008;49(3):1200–1209.
- Seddon JM, Reynolds R, Rosner B. Peripheral retinal drusen and reticular pigment: association with CFHY402H and CFHrs1410996 genotypes in family and twin studies. *Invest Ophthalmol Vis Sci*. 2009;50(2):586–591.
- Tan CS, Heussen F, Sadda SR. Peripheral autofluorescence and clinical findings in neovascular and non-neovascular age-related macular degeneration. *Ophthalmology*. 2013;120(6):1271–1277.
- Witmer MT, Kozbial A, Daniel S, Kiss S. Peripheral autofluorescence findings in age-related macular degeneration. *Acta Ophthalmol*. 2012;90(6):e428–e433.
- Kanagasam Y, Bhuiyan A, Abramoff MD, Smith RT, Goldschmidt L, Wong TY. Progress on retinal image analysis for age related macular degeneration. *Prog Retin Eye Res*. 2014;38:20–42.
- Lengyel I, Csutak A, Florea D, et al. A population-based ultra-widefield digital image grading study for age-related macular degeneration-like lesions at the peripheral retina. *Ophthalmology*. 2015;122(7):1340–1347.
- Soliman AZ, Silva PS, Aiello LP, Sun JK. Ultra-wide field retinal imaging in detection, classification, and management of diabetic retinopathy. *Semin Ophthalmol*. 2012;27(5–6):221–227.
- Writing Committee for the OPTOS PEripheral RetinA (OPERA) study (Ancillary Study of Age-Related Eye Disease Study 2), Domalpally A, Clemons TE, Danis RP, et al. Peripheral retinal changes associated with age-related macular degeneration in the Age-Related Eye Disease Study 2: Age-Related Eye Disease Study 2 report number 12 by the Age-Related Eye Disease Study 2 Optos PEripheral RetinA (OPERA) Study Research Group. *Ophthalmology*. 2017;124(4):479–487.
- Flamendorf J, Agrón E, Wong WT, et al. Impairments in dark adaptation are associated with age-related macular degeneration severity and reticular pseudodrusen. *Ophthalmology*. 2015;122(10):2053–2062.
- Owsley C, McGwin G Jr, Clark ME, et al. Delayed rod-mediated dark adaptation is a functional biomarker for incident early age-related macular degeneration. *Ophthalmology*. 2016;123(2):344–351.
- Sagong M, van Hemert J, Olmos de Koo LC, Barnett C, Sadda SR. Assessment of accuracy and precision of quantification of ultra-widefield images. *Ophthalmology*. 2015;122(4):864–866.
- Grading diabetic retinopathy from stereoscopic color fundus photographs – an extension of the modified Airlie House classification. ETDRS report number 10. Early Treatment Diabetic Retinopathy Study Research Group. *Ophthalmology*. 1991;98(5 Suppl):786–806.
- Csutak A, Lengyel I, Jonasson F, et al. Agreement between image grading of conventional (45°) and ultra wide-angle (200°) digital images in the macula in the Reykjavik eye study. *Eye (Lond)*. 2010;24(10):1568–1575.
- Azzolini C, Torreggiani A, Eandi C, et al. A teleconsultation network improves the efficacy of anti-VEGF therapy in retinal diseases. *J Telemed Telecare*. 2013;19(8):437–442.

Clinical Ophthalmology

Publish your work in this journal

Clinical Ophthalmology is an international, peer-reviewed journal covering all subspecialties within ophthalmology. Key topics include: Optometry; Visual science; Pharmacology and drug therapy in eye diseases; Basic Sciences; Primary and Secondary eye care; Patient Safety and Quality of Care Improvements. This journal is indexed on

Submit your manuscript here: <http://www.dovepress.com/clinical-ophthalmology-journal>

Dovepress

PubMed Central and CAS, and is the official journal of The Society of Clinical Ophthalmology (SCO). The manuscript management system is completely online and includes a very quick and fair peer-review system, which is all easy to use. Visit <http://www.dovepress.com/testimonials.php> to read real quotes from published authors.



AMERICAN ACADEMY
OF OPHTHALMOLOGY



Structural Changes Associated with Delayed Dark Adaptation in Age-Related Macular Degeneration

Inês Laíns, MD, MSc,^{1,2,3,4} John B. Miller, MD,¹ Dong H. Park, MD, PhD,^{1,5} Edem Tsikata, PhD,⁶ Samaneh Davoudi, MD,¹ Safa Rahmani, MD,¹ Jonathan Pierce, BSc,¹ Rufino Silva, MD, PhD,^{2,3,4} Teresa C. Chen, MD,⁶ Ivana K. Kim, MD,¹ Demetrios Vavvas, MD, PhD,¹ Joan W. Miller, MD,¹ Deeba Husain, MD¹

Purpose: To examine the relationship between dark adaptation (DA) and optical coherence tomography (OCT)-based macular morphology in age-related macular degeneration (AMD).

Design: Prospective, cross-sectional study.

Participants: Patients with AMD and a comparison group (>50 years) without any vitreoretinal disease.

Methods: All participants were imaged with spectral-domain OCT and color fundus photographs, and then staged for AMD (Age-related Eye Disease Study system). Both eyes were tested with the AdaptDx (MacuLogix, Middletown, PA) DA extended protocol (20 minutes). A software program was developed to map the DA testing spot (2° circle, 5° superior to the fovea) to the OCT B-scans. Two independent graders evaluated the B-scans within this testing spot, as well as the entire macula, recording the presence of several AMD-associated abnormalities. Multilevel mixed-effects models (accounting for correlated outcomes between 2 eyes) were used for analyses.

Main Outcome Measures: The primary outcome was rod-intercept time (RIT), defined in minutes, as a continuous variable. For subjects unable to reach RIT within the 20 minutes of testing, the value of 20 was assigned.

Results: We included 137 eyes (n = 77 subjects), 72.3% (n = 99 eyes) with AMD and the remainder belonging to the comparison group. Multivariable analysis revealed that even after adjusting for age and AMD stage, the presence of any abnormalities within the DA testing spot ($\beta = 4.8$, $P < 0.001$), as well as any abnormalities in the macula ($\beta = 2.4$, $P = 0.047$), were significantly associated with delayed RITs and therefore impaired DA. In eyes with no structural changes within the DA testing spot (n = 76, 55.5%), the presence of any abnormalities in the remaining macula was still associated with delayed RITs ($\beta = 2.00$, $P = 0.046$). Presence of subretinal drusenoid deposits and ellipsoid zone disruption were a consistent predictor of RIT, whether located within the DA testing spot ($P = 0.001$ for both) or anywhere in the macula ($P < 0.001$ for both). Within the testing spot, the presence of classic drusen or serous pigment epithelium detachment was also significantly associated with impairments in DA ($P \leq 0.018$).

Conclusions: Our results suggest a significant association between macular morphology evaluated by OCT and time to dark-adapt. Subretinal drusenoid deposits and ellipsoid zone changes seem to be strongly associated with impaired dark adaptation. *Ophthalmology* 2017;124:1340-1352 © 2017 by the American Academy of Ophthalmology

Age-related macular degeneration (AMD) is a multifactorial disease,¹ currently the leading cause of severe vision loss in subjects older than 50 years in developed countries and the third-leading cause worldwide.² AMD prevalence is predicted to increase because of the anticipated aging of the global population, so that by 2040, 288 million people are expected to have this disease.² Patients present with drusen and pigment changes in the macula in early and intermediate AMD, which may progress to advanced disease manifesting as geographic atrophy (GA) or choroidal neovascularization (CNV) in some cases.^{3,4} Visual acuity (VA) loss typically occurs late in the disease course,⁵ making VA a less useful measure of retinal function

in early and intermediate AMD. Despite its well-recognized limitations in characterizing visual impairment of AMD,⁶ VA remains the most widely accepted functional outcome measure for this disease.

Several researchers have tried to establish other functional outcome measurements in AMD, including contrast sensitivity,⁷ low-luminance VA, photopic or scotopic light sensitivity,^{8,9} and dark adaptation (DA).⁵ Patients with AMD often report difficulties performing activities at night, with prior work showing that higher levels of self-reported problems in night vision are associated with an increased risk of vision loss.¹⁰ Moreover, recent studies have shown that DA can differentiate AMD from healthy

eyes, as well as detecting the different stages of the disease.^{5,11,12} Building off this prior work, there is now a commercially available device—the AdaptDx (MacuLogix, Middletown, PA) dark adaptometer—that can be used for testing the time to dark-adapt in patients. Its standard protocol bleaches an area of 2 degrees superior to the central fovea (from now on denoted as DA testing spot) and measures time to dark-adapt with very high sensitivity and specificity.¹²

Most of the published literature about DA in AMD characterized the disease using color fundus photographs (CFP),^{5,11,12} as these remain the gold standard for diagnosis and staging.¹³ CFPs predominantly use drusen as an index for AMD and have well-recognized limitations.¹⁴ As a noninvasive imaging method capable of resolving cross-sectional anatomy, optical coherence tomography (OCT) offers several important advantages in the assessment of AMD,^{15–17} and is currently widely used in daily clinical practice. Importantly, OCT has enabled clinicians and researchers to better identify some lesions, such as subretinal drusenoid deposits,¹⁸ which may have important independent prognostic value.¹⁹

Little has been published about the relationship between time to dark-adapt and structural OCT changes in AMD.^{20–22} Given the growing role of functional measures in AMD, like DA, and the foundational role of OCT in clinical practice, we set out to better define this structure–function relationship of OCT and DA in AMD. In this study, we used spectral-domain OCT (SD OCT) to assess macular morphology in a cohort of AMD and healthy eyes, and evaluated the time to dark-adapt, measured as rod-intercept time (RIT). We then assessed the relationship between DA and type of abnormalities seen in the DA testing spot, as well as within the entire macula.

Methods

This study was developed by the Massachusetts Eye and Ear, Harvard Medical School, Boston, Massachusetts, and is part of a prospective, cross-sectional, observational project on AMD biomarkers. It was conducted in accordance with Health Insurance Portability and Accountability Act requirements and the tenets of the Declaration of Helsinki, and was approved by the Massachusetts Eye and Ear Institutional Review Board. All included participants provided written informed consent.

Study Protocol and Procedures

We recruited and consented consecutive patients with a diagnosis of AMD (assessed by a retina specialist) when they came to their regular appointments at our Retina Service. We excluded subjects with any other vitreoretinal disease, active uveitis or ocular infection, significant media opacities that precluded the observation of the ocular fundus, refractive error equal to or greater than 6 diopters of spherical equivalent, formal diagnosis of glaucoma with a cup-to-disc ratio superior to 0.7, history of retinal surgery, history of any ocular surgery or intraocular procedure (such as laser and intraocular injections) within the 90 days before enrollment, and diagnosis of diabetes mellitus, with or without concomitant diabetic retinopathy. Additionally, a comparison group of subjects aged 50 years or older, without any evidence of AMD in both eyes, was included and the same exclusion criteria were applied.

All participants underwent a comprehensive eye examination, including best-corrected VA (for analysis, converted to logMAR), current refraction, intraocular pressure, slit-lamp biomicroscopy, and dilated fundus examination. A standardized questionnaire was designed specifically for this study (including data on demographics, past medical history, and current medications) and applied to all study participants.

The eyes of subjects were also imaged with nonstereoscopic 7-field CFP (Topcon TRC-50DX; Topcon Corporation, Tokyo, Japan) for AMD diagnosis and grading (detailed below), as well as with SD OCT (Spectralis; Heidelberg Engineering, Heidelberg, Germany). The initial SD OCT imaging protocol was an enhanced-depth imaging (EDI) high-resolution volume centered in the fovea, with 61 lines, 30×25 degrees, 30 frames automatic real time (ART). Due to the burden on patients, this was modified in the course of the study to an EDI high-resolution volume, 97 lines, 20×20 degrees, 15 frames ART. If the referring retina specialist deemed it necessary, fluorescein angiography was performed as part of the regular clinical assessment of patients with CNV.

Finally, subjects underwent DA testing, according to the protocol below. To avoid prior light exposure, DA was performed on a separate day, within a maximum time limit of 1 month after study inclusion.

Dark-Adaptation Testing

A trained optometrist confirmed the current refraction of all participants and optimized it when required. After dilation to ≥6 mm, DA was performed using the AdaptDx dark adaptometer (MacuLogix, Middletown, PA). Corrective lenses were introduced to account for the 30-cm viewing distance. Before the beginning of the actual testing, a 2-minute demonstration test (available in the commercialized software) was performed to familiarize the patient with the AdaptDx procedures. This test is performed in the dark, and it uses a 5 scotopic cd/m² bleaching flash, which is the same intensity as the maximum stimulus intensity. When the demonstration test was over, the patients were asked about any questions. If they were clear on the task, the optometrist proceeded to the actual testing—between transitions (from the demonstrating test to the actual test) the room lights were kept off. Both eyes were tested separately (the right eye always first), with a minimum resting period of 15 minutes between them (during testing, the fellow eye was occluded with an eye patch). The extended protocol (20 minutes) was followed.¹² Eyes were bleached by exposure to a 505-nm photoflash (0.8-ms duration, 1.8×10⁴ scot cd/m² intensity), equivalent to 76% bleaching level for rods. The flash of light passed through a square aperture sized to bleach a 6° area of the retina centered at 5° on the inferior visual meridian. Sensitivity measurements began immediately after bleaching. The subject focused on the fixation light and indicated when a stimulus light was visible by pushing a hand-held button. The stimulus light was a 505-nm, 2° circular test spot, located at 5° on the inferior visual meridian (anatomically, 5° superior to the central fovea) (Fig 1).

Sensitivity was estimated by using a 3-down/1-up modified staircase threshold estimate procedure. The initial stimulus intensity was 5 scot cd/m². The stimulus light was presented every 2 or 3 seconds for a 200-ms duration. If the stimulus was detected, the patient was given 2 seconds to respond by pushing a response button. If the subject indicated that the stimulus was visible, the intensity was decreased for each successive presentation in steps of 0.3 log units until the subject stopped responding that the stimulus was visible. If the subject indicated that the stimulus light was not visible, the intensity of the target was increased for each successive presentation in 0.1-log-unit steps until the subject responded that the stimulus light was once again visible. This intensity was defined as a threshold. Successive threshold measurements started with the

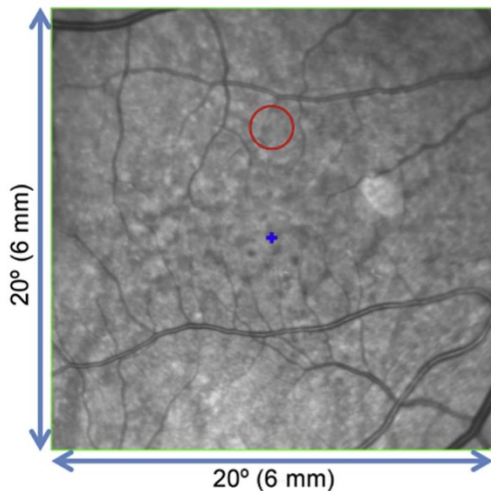


Figure 1. Infrared fundus image (HRA Spectralis, Heidelberg Engineering, Heidelberg, Germany) with the area evaluated by dark-adaptation (DA) testing marked by a red circle. This circle represents the 2° circular DA testing spot located 5° superior to the fovea (which is represented as a blue cross and not on scale). The field of view is 20°×20°, corresponding to an area of approximately 6 mm × 6 mm on the retina.

stimulus intensity 0.2 log units brighter than the previous threshold measurement. The subject had a 15-second rest period between threshold measurements. However, if a threshold had a large deviation from prior thresholds, the measurement was considered unreliable and a fixation error was recorded, and an additional threshold was measured immediately. Threshold measurements were made approximately once a minute for the duration of the DA test. The test ended when the subject's sensitivity was twice consecutively measured to be greater than 5×10^{-3} scot cd/m^2 or the test duration reached 20 minutes, whichever was shorter. The AdaptDx estimates the slope of the second component of rod-mediated dark adaptation and extrapolates the amount of time required to achieve a sensitivity of 5×10^{-3} scot cd/m^2 . This value is named the rod-intercept time (RIT). Subjects failing to reach the RIT within the 20 minutes of testing were assigned a value of 20. For analysis purposes, eyes with fixation errors $\geq 30\%$ were excluded ($n = 3$).

AMD Diagnosis and Staging

Considering that CFP remain the gold standard for AMD diagnosis and staging,¹³ 2 independent graders, masked to any clinical and demographical data, analyzed all field 2 CFP on IMAGENet 2000 software (version 2.56; Topcon Medical Systems) and graded them according to the Age-related Eye Disease Study (AREDS) classification system.^{13,25} In cases of disagreement, the senior author (DH) established the final categorization. We adopted the most recent AREDS2 definitions,¹³ namely that the standard disc diameter equals 1800 μm , which affects the size of the Early Treatment Diabetic Retinopathy Study grid and of the standard drusen circles; and that GA is present if the lesion has a diameter equal to or greater than 433 μm (AREDS circle I-2) and at least 2 of the following features are present: absence of retinal pigment epithelium (RPE) pigment, circular shape, or

sharp margins (involvement of the central fovea was not required). Therefore, we established the following groups,^{13,23} which were used for statistical analysis: comparison group (AREDS level 1)—presence of drusen maximum size < circle C0 and total area < C1; early AMD (AREDS level 2)—drusen maximum size \geq C0 but < C1 or presence of AMD characteristic pigment abnormalities in the inner or central subfields; intermediate AMD (AREDS level 3)—presence of drusen maximum size \geq C1 or drusen maximum size \geq C0 if the total area occupied is > I2 for soft indistinct drusen and > O2 for soft distinct drusen; late AMD (AREDS level 4)—presence of GA according to the criteria described above or evidence of neovascular AMD.

OCT B-scans within the DA Testing Spot

An experienced grader (I.L.) confirmed the automatic segmentation of the inner limiting membrane (ILM) and Bruch membrane (BM) by the Heidelberg software (version 1.9.10), in all the obtained OCT volumes, for each B-scan separately. When these boundaries were not properly delineated by the automatic software, the grader manually corrected them based on the international consensus definitions.²⁴ The "Thickness Profile" mode was selected, and then the function "Edit Layer Segmentations." After this, we exported the OCT B-scans, with the ILM and BM delineated (red line), as PNG files (Fig 2). These scans were then imported to a software program that we developed (E.T., T.C.C.) (OpenCV image processing library of C++, v2.4.3, Intel Corporation, Willow Garage. Graphical user interface developed with Qt application programming framework - v4.8, Qt Company), which reads the OCT image sequence and allows the investigators to precisely identify and set the position of the fovea. For each eye, 2 of 3 independent graders (I.L., S.D., S.R.) determined the location of the fovea (Fig 2) using the infrared photograph combined with the OCT B-scans, based on thickness and the identification of the hyperreflective outer plexiform band's inward bend, which forms a singular promontory at the foveal center.²⁵

For each B-scan located within the DA testing spot, the program automatically delineated the lateral extent of the stimulus (how wide the stimulus is in terms of A-lines) using blue lines (Fig 3). Additionally, in these frames, the mean retinal thickness in the DA spot was automatically obtained (summing the distances between the ILM and BM for all A-lines and dividing the sum by the number of A-lines covered by the stimulus).

Currently, there is no automatic segmentation available for the choroid with the Spectralis SD OCT. After identifying the B-scans located within the DA testing spot for each eye, 2 of 3 independent investigators (I.L., S.R., S.D.) used the Heidelberg software to manually determine choroidal boundaries by moving the ILM curve to delineate the external choroid limit (scleral/choroidal interface) using the functions described above ("Thickness Profile" mode, "Edit Layer Segmentations" function). The BM segmentation was reutilized. This was necessary only for frames covered by the stimulus (in the initial EDI protocol, 3 B-scans; in the second EDI protocol, 9 B-scans). The images marked with the modified layer delineations were then exported. The adjusted frames were processed by the same program to yield the choroidal thickness, similarly to what has been described for retinal thickness.

Evaluation of OCT Images

Two of 4 independent investigators (I.L., D.H.P., S.R., S.D.), masked to clinical and DA data, analyzed the B-scans included in the DA testing spot for the presence or absence (dichotomous variable) of the following: ellipsoid zone disruption; classic drusen, defined as sub-RPE deposits; presence of ≥ 1 druse was graded as

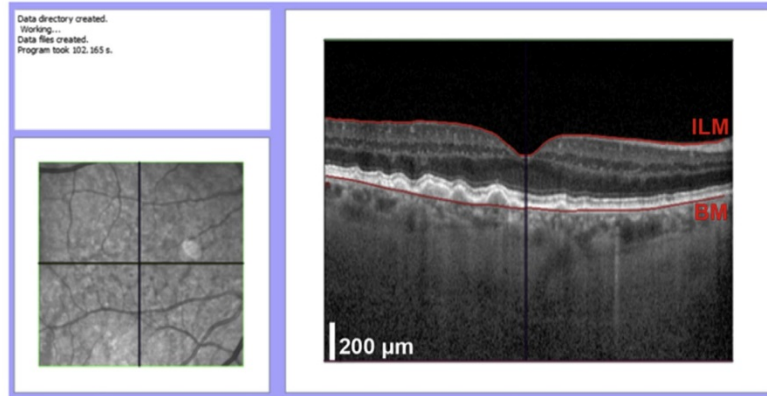


Figure 2. Graphical interface of the software program used to locate the dark-adaptation testing area in the optical coherence tomography (OCT) volumetric scans. In the left corner, an infrared (IR) image is displayed, with the position of the fovea marked by the intersecting lines. In the right window, a cross-sectional OCT scan (B-scan) is displayed to enable the investigator to precisely locate the fovea. Commands in the interface allow simultaneous location of the fovea in the IR image and B-scan. Red lines delineate the inner limiting membrane (ILM) and Bruch membrane (BM). Scale bar = 200 μm .

“yes”; subretinal drusenoid deposits²⁶ (presence of ≥ 1 was graded as “yes”); hyperreflective foci (presence of ≥ 1 was graded as “yes”); retinal atrophy (defined as increased signal transmission to the choroid and loss of external retinal layers,²⁷ i.e., not AREDS definition of GA); fibrosis; subretinal and intraretinal fluid; choroidal neovascularization (i.e., subretinal or intraretinal fluid with concomitant hyperreflectivity below the RPE); and serous pigment epithelium detachment (PED). The graders also described any abnormalities observed within the DA testing spot (presence vs. absence, among the listed). Similarly, the volume scans of the entire macula imaged were also independently evaluated by 2 of 4 investigators (LL., D.H.P., S.R., S.D.) for the presence or absence of the same abnormalities. Importantly, the presence of these abnormalities was not considered mutually exclusive (i.e., 1 eye could present several of the detailed abnormalities), in the assessment of both the DA testing spot and the macula in general. The senior author of the manuscript (DH) resolved any cases of disagreement.

Statistical Analysis

The demographics and clinical characteristics of our study cohort were evaluated using traditional descriptive methods. According to our aims, we defined RIT—a continuous variable—as our outcome. For subjects who did not reach RIT within the 20 minutes of testing, the value of 20 was assigned.²² Considering the inclusion of both eyes of the same patients, we used multilevel mixed-effects linear models. By definition, these models are appropriate for research designs where data for participants are organized at more than 1 level (i.e., nested data). In this study, the units of analysis were considered the eyes (at a lower level), which are nested within patients—contextual/aggregate units (at a higher level).²⁸ Univariable multilevel mixed-model linear regression analyses (i.e., with a single predictor variable) were performed for all clinical and OCT parameters studied, as detailed below. Additionally, we performed multiple regression assessments (i.e., with more than 1 predictor variable) accounting for AMD stage and age, as these

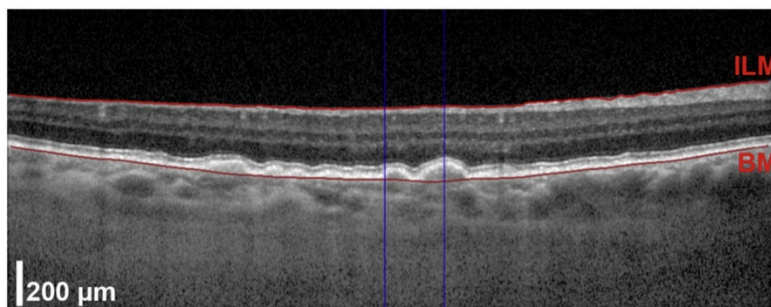


Figure 3. Optical coherence tomography B-scan image (HRA Spectralis) processed with the described software. The lateral extent of the dark-adaptation testing spot in this scan is marked with blue lines. Within and outside this area, we can see the presence of classic drusen. The retinal segmentation is delineated with red lines (BM = Bruch membrane; ILM = inner limiting membrane) and obtained automatically with the software. Scale bar = 200 μm .

covariates are clinically and statistically associated with abnormalities in DA. For all multilevel assessments we report *P* values and beta coefficients. The beta coefficients represent the change in the outcome variable—RIT—for 1 unit of change in the predictor variable (while holding other predictors in the model constant, in the case of multivariable analyses).²⁹ This means, for example, that for a continuous variable such as age, beta coefficients represent the change in RIT per each year of increase in age. For binomial outcomes, such as the OCT parameters evaluated, their absence was considered the reference term, so beta coefficients refer to the change in RIT in the presence of each specific lesion.

We also performed a subanalysis of eyes that reached RIT within the 20 minutes of testing compared with those that did not present an RIT within the 20-minute testing period. This was defined as a binomial outcome, and logistic univariable and multivariable multilevel mixed models were performed, following the same approach described above.

All statistics were performed using Stata version 14.1 (StataCorp LP, College Station, TX) and *P* values < 0.05 were considered statistically significant.

Results

Study Population

We included and tested 72 subjects (*n* = 144 eyes). Three eyes were excluded due to poor fixation and 4 additional eyes due to lack of adequate imaging quality for appropriate assessments on at least 1 of the OCT B-scans (as defined by the investigators that evaluated these images). Therefore, we considered data of 137 eyes (*n* = 72 subjects) for analysis. Based on CFP, 72.3% of the eyes (*n* = 99) presented AMD and the remaining were graded as belonging to the comparison group (27.7% of the eyes, *n* = 38). Table 1 presents the demographic and clinical characteristics of the included study cohort. Table 2 details the AMD staging and the corresponding median RITs. Among eyes with late AMD, 6 (46.2%) presented GA and the remaining (*n* = 7, 53.4%) neovascular AMD.

Our univariable assessments showed that AMD stage was significantly associated with impaired RITs (as compared with the comparison group, early $\beta = -0.48$, *P* = 0.698; intermediate $\beta = 8.96$, *P* < 0.001; late $\beta = 9.98$, *P* < 0.001). This means, for example, that eyes with intermediate AMD present an RIT 8.96 minutes longer than eyes from the comparison group; and that eyes with late AMD present an RIT 9.98 minutes longer than eyes belonging to the comparison group. The same was observed for age ($\beta = 0.33$, *P* = 0.001—for each 1 year age increase there was a 0.33-minute increase in RIT). Lens status (phakic vs. pseudophakic) did not show a significant association with RIT. Therefore, the presented data for multivariate assessments always account for age and AMD stage as covariates.

As detailed in the Methods section, we included eyes imaged with 2 distinct OCT protocols. Most of them (*n* = 109, 79.6%) were imaged with an EDI protocol using 97 lines, which provided 9 B-scans within the DA testing spot. The remaining eyes were imaged with an EDI protocol using 61 lines, including only 3 B-scans within the same region. Importantly, there was no difference in the rates of detection of abnormalities within the testing spot (*P* = 0.619) or the macula (*P* = 0.503) between the 2 groups that had the different imaging procedures (97 lines vs. 61 lines).

Presence of Structural Abnormalities in OCT

Among all analyzed AMD eyes, 44.5% (*n* = 61) presented OCT structural abnormalities within the DA testing spot, all of them with intermediate (*n* = 50, 82.0%) or late AMD (*n* = 11, 18.0%), according to CFP. The mean retinal and choroidal thicknesses in this region were 335.9 ± 23.8 μm and 261.9 ± 83.5 μm , respectively. In the entire macula imaged, lesions were seen in 71.5% of the eyes (*n* = 98), with a discrepancy between CFP and OCT observed in 3 cases. One case graded as “comparison group” in CFP presented abnormalities on the OCT images evaluated; and 2 cases graded as “early AMD” had no lesions reported on OCT grading. Table 3 presents the distribution of the evaluated structural abnormalities within the testing spot and the entire macula in our study population.

Table 1. Characterization of the Eyes Included in the Study

	AMD Eyes	Control Eyes	Total
Demographic and clinical characteristics			
Number (%) of eyes	99 (72.3)	38 (27.7)	137 (100)
Included eye, <i>n</i> (%)			
OD	49 (49.5)	18 (47.4)	67 (48.9)
OS	50 (50.5)	20 (52.6)	70 (51.1)
Age, mean \pm SD	68.8 \pm 6.4	66.1 \pm 7.7	68.0 \pm 6.9
Gender, <i>n</i> (%)			
Male	39 (39.4)	22 (57.9)	61 (44.5)
Female	60 (60.6)	16 (42.1)	76 (55.5)
Race/ethnicity, <i>n</i> (%)			
White	98 (99.9)	36 (94.7)	134 (97.8)
Asian	1 (0.1)	0 (0)	1 (0.7)
Black	0 (0)	2 (5.3)	2 (1.5)
Eye examination and past history			
BCVA (logMAR), mean \pm SD (range)	0.10 \pm 0.2 (−0.1; 0.5)	0.04 \pm 0.1 (−0.1; 0.3)	0.1 \pm 0.2 (−0.1; 0.5)
Spherical equivalent (diopters), mean \pm SD	0.4 \pm 1.5	−0.4 \pm 2.5	0.2 \pm 1.9
IOP (mm Hg), mean \pm SD	15.1 \pm 2.9	14.3 \pm 2.7	14.9 \pm 2.9
Pseudophakic, <i>n</i> (%)	21 (21.2)	1 (2.6)	22 (16.1)
Previous PDT, <i>n</i> (%)	1 (1.0)	0 (0)	1 (0.7)
Previous intravitreal injections, <i>n</i> (%)	6 (6.1)	0 (0)	6 (4.4)

AMD = age-related macular degeneration; BCVA = best-corrected visual acuity; IOP = intraocular pressure; logMAR = logarithm of the minimal angle of resolution; OD = right eye; OS = left eye; PDT = photodynamic therapy; SD = standard deviation.

Table 2. Age-Related Macular Degeneration Staging and Rod Intercept Time for the Study Eyes

	Number (%) of Eyes	RIT Median (IQR)
AMD stage		
Control	38 (27.7)	4.4 (3.5–5.6)
Early AMD	22 (16.1)	5.0 (4.1–7.2)
Intermediate AMD	64 (46.7)	17.1 (10.0–20)
Late AMD	13 (9.5)	20 (12.5–20)

AMD = age-related macular degeneration; IQR = interquartile range (in minutes); RIT = rod intercept time (in minutes). Twenty-six percent of the AMD eyes did not reach RIT within the 20-minute testing period.

DA and Structural Changes within the DA Testing Spot

In our univariable analysis, we observed that the presence of any OCT abnormality within the DA testing spot was associated with impaired RITs ($\beta = 6.70, P < 0.001$). Among the specific OCT parameters assessed, the presence of ellipsoid disruption ($P < 0.001$), subretinal drusenoid deposits ($P = 0.002$), classic drusen ($P < 0.001$), atrophy ($P = 0.013$), and serous PED ($P = 0.007$) were significantly associated with impaired DA. A reduced mean retinal thickness also showed a statistically significant association ($P = 0.006$; Table 4).

When accounting for age and AMD stage, multivariable assessments revealed that the presence of any abnormality within the DA testing spot remained significantly associated with delayed RIT ($\beta = 4.8, P < 0.001$). The same was observed for the presence of ellipsoid disruption ($P = 0.001$), subretinal drusenoid deposits ($P = 0.001$), classic drusen ($P = 0.006$), and serous PED ($P = 0.018$). Figure 4 presents an example of an eye with subretinal drusenoid deposits within the DA testing spot.

DA and Structural Changes within the Imaged Macula

We then evaluated the association of RIT with the structural abnormalities observed in the entire macular region, as imaged with SD OCT. The presence of abnormalities on OCT in this area was also associated with impairments in RIT ($\beta = 5.03,$

Table 3. Presence of Optical Coherence Tomography Structural Abnormalities in the Study Population

Presence of Observed Abnormalities	DA Testing Spot, N (%)	All Macula, N (%)
Ellipsoid disruption	30 (21.9)	71 (51.8)
Subretinal drusenoid deposits	22 (16.1)	72 (52.3)
Classic drusen	46 (33.6)	87 (63.5)
Hyperreflective foci	6 (4.4)	36 (26.3)
Subretinal fluid	1 (0.7)	7 (5.1)
Intraretinal fluid	0 (0)	2 (1.5)
Atrophy	9 (6.6)	27 (19.7)
Choroidal neovascularization	0 (0)	5 (3.7)
Fibrosis	1 (0.7)	2 (1.5)
Serous pigment epithelium detachment	2 (1.5)	14 (10.2)
Outer retinal tubulations	0 (0)	3 (2.2)

DA = dark adaptation. The presented percentages refer to the total number of included eyes (N = 137).

$P < 0.001$). Table 5 presents our univariable analyses, which revealed that the presence of ellipsoid disruption, subretinal drusenoid deposits, classic drusen, hyperreflective foci, or atrophy ($P \leq 0.009$) were significant predictors of impaired RIT.

Multivariable analysis revealed that, controlling for age and AMD stage, the presence of any abnormalities within the macula was significantly associated with prolonged RITs ($\beta = 2.43, P = 0.047$). Among the OCT structural parameters evaluated, the presence of subretinal drusenoid deposits and ellipsoid disruption ($P < 0.001$ for both) remained statistically significant after accounting for age and AMD stage.

Eyes without OCT Abnormalities within the DA Testing Spot

We analyzed eyes without OCT abnormalities within the testing spot (n = 76, 55.5%) to assess whether the presence of structural abnormalities in the remaining macula was associated with time to dark-adapt. The mean RIT for these eyes was 7.11 ± 4.76 minutes. Among them, 48.7% (n = 37) had structural lesions in the remaining macula. The presence of structural abnormalities within this remaining area was significantly associated with impaired RIT, both on univariable assessments ($\beta = 2.72, P = 0.002$) and after correcting for age and AMD stage ($\beta = 2.00, P = 0.046$). Regarding the specific lesions seen, multivariable analysis revealed that the presence of subretinal drusenoid deposits ($\beta = 4.07, P < 0.001$) and ellipsoid disruption ($\beta = 3.72, P = 0.002$) were significant predictors. We also evaluated eyes with AMD in isolation, and found that the association between presenting subretinal drusenoid deposits in the remaining macula and prolonged RITs was present ($\beta = 4.55, P < 0.001$). Figure 5 shows an example of an eye without any structural lesion within the DA testing spot, but with abnormalities seen in the remaining macula.

Inability to Reach RIT within the Testing Time

As described (Methods section), in our study we included eyes (n = 36) unable to reach RIT within the 20 minutes of testing. In all but 4 (88.9%), OCT abnormalities were observed within the DA testing spot; and all presented abnormalities in the entire macula. Table 6 presents a description of the OCT structural lesions seen in this subgroup.

We performed an analysis considering a dichotomous outcome (able to reach RIT within 20-minute testing period vs. unable to reach RIT within 20-minute testing period) to assess if the results described were also valid to predict inability to reach RIT within the 20 minutes of testing. Our results revealed that the presence of OCT abnormalities within the DA testing spot was significantly associated with an inability to reach RIT within the 20-minute testing time, even after accounting for age and AMD stage ($\beta = 0.31, P < 0.001$). With multivariable analysis, we found that the presence of ellipsoid disruption ($\beta = 0.36, P < 0.001$), subretinal drusenoid deposits ($\beta = 0.31, P < 0.001$), and serous PED ($\beta = 0.53, P = 0.020$), as well as a reduced mean choroidal thickness ($\beta = -0.001, P = 0.044$), significantly impaired the ability to reach RIT. When looking at the entire macular region, the presence of any abnormalities on OCT was not a significant predictor of the inability to reach RIT within 20 minutes, after controlling for age and AMD stage ($P = 0.181$). However, multivariable analysis revealed that ellipsoid disruption ($\beta = 0.20, P = 0.034$) and subretinal drusenoid deposits ($\beta = 0.17, P = 0.021$) were significant predictors of this outcome.

Table 4. Multilevel Mixed Linear Regression Analyses of Structural Parameters within the Dark Adaptation Testing Spot

Variable*	Univariable Analyses		Multivariable Analyses (Controlling for Age and AMD Stage)	
	β Coefficient	P Value	β Coefficient	P Value
Ellipsoid disruption	5.20	<0.001 [†]	3.71	0.001 [†]
Subretinal drusenoid deposits	3.52	0.002 [†]	3.51	0.001 [†]
Classic drusen	4.32	<0.001 [†]	2.69	0.006 [†]
Hyperreflective foci	0.91	0.537	0.40	0.794
Atrophy	4.95	0.013 [†]	2.32	0.209
Serous PED	6.54	0.007 [†]	5.93	0.018 [†]
Mean retinal thickness	-0.06	0.006 [†]	-0.011	0.589
Mean choroidal thickness	-0.01	0.133	-0.007	0.242

AMD = age-related macular degeneration; PED = pigment epithelium detachment.

*For all parameters, the reference term is absence of their visualization. No eyes presented intraretinal fluid, choroidal neovascularization, or outer retinal tubulations within the spot; thus these parameters were not assessed. Fibrosis, subretinal fluid, and tubulations were only observed in 1 eye, so these parameters were also not included in the analysis.

[†]P value < 0.05.

Discussion

We correlated structural morphology by OCT with visual function, using rod-mediated DA, in a cohort of eyes with AMD as compared with a comparison group, including eyes with apparent normal macular health. Unlike previous work, we evaluated OCT abnormalities in the DA testing area (DA testing spot), in addition to the entire macula. Our results revealed that, even accounting for age and AMD stage, the presence of any abnormalities on OCT within the DA testing spot and in the macula overall was significantly associated with impairments in DA. Interestingly, in eyes with no structural changes within the DA testing spot, the presence of abnormalities on OCT in the remaining macula was also associated with delayed RITs. This finding supports the notion that DA is a good test for detecting abnormalities in the entire macula and not just within the DA testing spot. When looking at the specific structural lesions, multivariable analyses revealed that the presence of subretinal drusenoid deposits and ellipsoid disruption, whether within the DA testing spot or in the macula overall, were consistent predictors of

impaired DA. Within the DA testing spot, the presence of classic drusen and serous PED were also significantly associated with impairment in time to dark-adapt.

Our results suggest a strong structural–functional association between pathology seen on OCT and functional loss, assessed as time to dark-adapt. To our knowledge, no other group has performed such a comprehensive evaluation. Clark et al²⁰ used OCT solely to assess retinal thickness and its relationship with DA. Sevilla et al²¹ mapped with high detail the OCT regions located within the DA testing spot. However, the authors only described the association between time to dark-adapt and pathologic features seen in the entire macula, thus not performing a specific evaluation of the area stimulated during testing. Flamendorf et al²² analyzed OCT volumes of AMD patients and a comparison group, but this comparison group was defined by the presence of no large drusen, therefore not excluding eyes with small or intermediate drusen. Furthermore, the authors focused on the presence of structural changes throughout the entire macula, only briefly describing the findings of 1 horizontal and 1

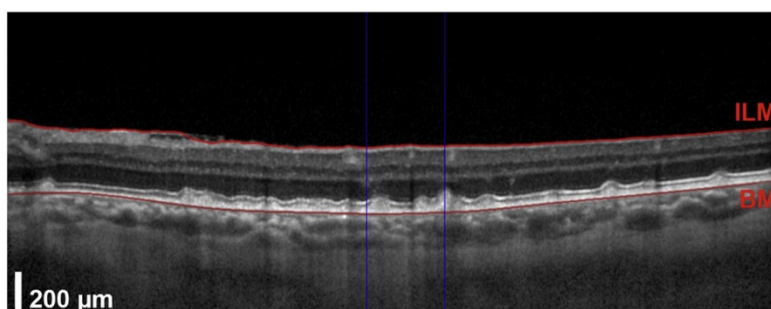


Figure 4. Example of an eye with subretinal drusenoid deposits within and outside the dark-adaptation testing spot (HRA Spectralis). This image was processed with the developed software. The lateral extent of the dark-adaptation testing spot is marked with blue lines. The retinal segmentation is delineated with red lines (BM = Bruch membrane; ILM = inner limiting membrane) and obtained automatically with the software. Scale bar = 200 μ m.

Table 5. Multilevel Mixed Regression Analysis of Structural Parameters in the Entire Macula

Variable*	Univariable Analyses		Multivariable Analyses (Controlling for Age and AMD Stage)	
	β Coefficient	P Value	β Coefficient	P Value
Ellipsoid disruption	5.20	<0.001 [†]	3.74	<0.001 [†]
Subretinal drusenoid deposits	4.19	<0.001 [†]	3.19	<0.001 [†]
Classic drusen	5.94	<0.001 [†]	2.39	0.095
Hyperreflective foci	2.53	0.030 [†]	0.57	0.613
Subretinal fluid	0.80	0.552	-0.79	0.579
Intraretinal fluid	-1.08	0.669	-0.63	0.810
Atrophy	3.45	0.009 [†]	1.08	0.392
Fibrosis	3.02	0.647	-2.90	0.542
Choroidal neovascularization	2.82	0.321	1.19	0.636
Serous PED	2.67	0.086	1.90	0.192
Outer retinal tubulations	3.64	0.120	1.53	0.512

AMD = age-related macular degeneration; PED = pigment epithelium detachment.

*For all parameters, the reference term is absence of their visualization.

[†]P value < 0.05.

vertical scan through the DA testing spot. Interestingly, they only observed a longer mean RIT and focal abnormalities in the testing spot in subjects with large drusen and without late AMD in both eyes, but without a similar finding in those with large drusen in 1 eye and late AMD in the other eye.

Altogether, our results suggest that impaired dark adaptation cannot be solely explained by focal structural changes within the DA testing spot. This is consistent with recent work showing that, in the normal aging retina, rod sensitivity recovery seems to measure the integrity of the entire retina.³⁰ In our cohort, even in eyes with no structural

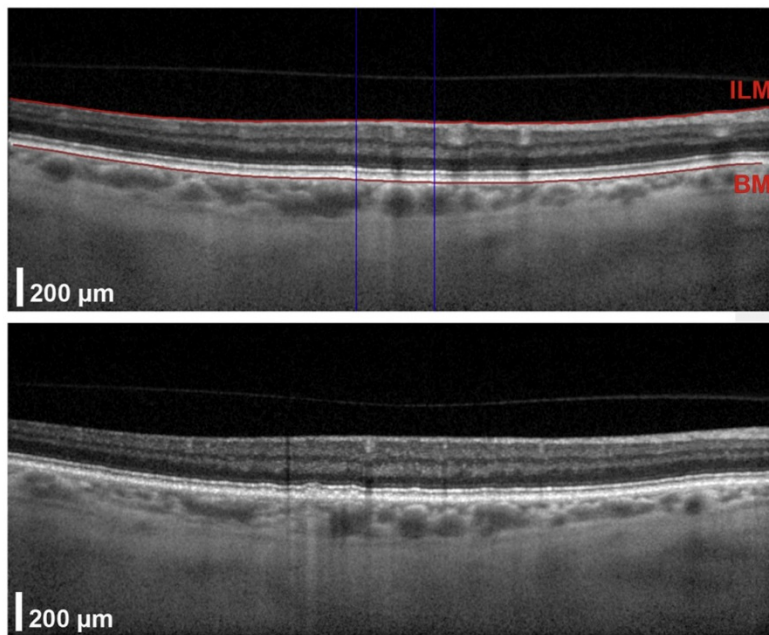


Figure 5. The top image shows the fifth B-scan located within the dark-adaptation testing spot (9 lines) of an eye without any abnormalities seen within this area. In the remaining macula of the same eye, subretinal drusenoid deposits were noted, as shown in the bottom B-scan. (The image on the top was processed with the developed software. The lateral extent of the dark-adaptation testing spot is marked with blue lines. The retinal segmentation is delineated with red lines—BM = Bruch membrane; ILM = inner limiting membrane—and obtained automatically with the software). Scale bar = 200 µm.

Table 6. Presence of Optical Coherence Tomography Structural Abnormalities in Eyes Unable to Reach Rod-Intercept Time within the 20 Minutes of Testing (N = 36)

Presence of Observed Abnormalities	DA Testing Spot, N (%)	All Macula, N (%)
Ellipsoid disruption	21 (58.3)	33 (91.7)
Subretinal drusenoid deposits	15 (41.7)	32 (88.9)
Classic drusen	22 (61.1)	35 (97.2)
Hyperreflective foci	4 (11.1)	18 (50.0)
Subretinal fluid	1 (2.8)	2 (5.6)
Intraretinal fluid	0 (0)	1 (1.8)
Atrophy	7 (19.4)	16 (44.4)
Choroidal neovascularization	0 (0)	3 (8.3)
Fibrosis	1 (2.8)	1 (2.8)
Serous pigment epithelium detachment	2 (5.6)	8 (22.2)
Outer retinal tubulations	0 (0)	1 (2.8)

DA = dark adaptation.

lesions within the testing region, the presence of structural abnormalities in the remaining macula led to a statistically significant reduction in RIT. This impaired dark adaptation in eyes with structural changes in the macula, both within and outside the testing spot, suggests that dark adaptation can be an appropriate functional measure of the structural status of the macula overall, and a useful measure for the assessment of AMD.

Among the different OCT features assessed, the presence of subretinal drusenoid deposits showed a particularly consistent association with impairments in time to dark-adapt. This confirms previous findings of impaired dark adaptation²² and builds on prior literature suggesting a link between subretinal drusenoid deposits and rod topography^{31–33} and dysfunction.¹⁹ It also highlights the limitations of currently available AMD grading schemes, all solely based on color fundus photographs, which have a very limited ability to recognize these lesions.³⁴

The advent of OCT substantially increased the interest in and knowledge of these lesions.³⁵ It is currently established that subretinal drusenoid deposits are more commonly located in the parafoveal area and superior macula.^{31,33} This area has more rods than cones,³⁶ and the photoreceptors' morphology seems to be disturbed above subretinal drusenoid deposits (photoreceptors deflected and shortened).³⁵ In contrast, classic drusen are more prevalent and thicker in the fovea, where there is a high density of cones. Therefore, Curcio et al³⁵ suggested that subretinal drusenoid deposits and classic drusen probably reflect differential aspects of rod and cone physiology, respectively. In this way, the change in photoreceptor morphology associated with the presence of subretinal drusenoid deposits^{35,37} is likely a cause of impairment in time to dark-adapt. Steinberg et al also observed a more pronounced reduction of scotopic³⁸ and mesopic³⁹ sensitivity in areas with subretinal drusenoid deposits. Cone function may also be affected by these lesions.^{19,40}

Despite the evidence that subretinal drusenoid deposits cause abnormalities in DA, the exact molecular mechanism has not been established. One possibility, as suggested by

previous authors,⁴¹ is that these deposits create a diffusion barrier between the choroid and photoreceptors. This mechanism has been described for Sorsby's fundus dystrophy⁴² and has also been proposed for the observed prolonged RITs with aging and AMD in general, with the associated BM thickening and formation of basal laminar deposits.^{43,44} In AMD, besides these changes, there is also drusen formation,²² thus likely further compromising transport of several molecules and nutrients to photoreceptors, such as vitamin A. Vitamin A deficiency can cause dysfunction and photoreceptor death, as well as slowing in the regeneration rate of rhodopsin.^{36,45,46} The normal recycling process for rhodopsin requires that a sufficient quantity of 11-cis-retinal (a metabolite of vitamin A) be available to the photoreceptors' outer segments, or rhodopsin regeneration is slowed.^{45,47} Whereas cones have alternative sources through Müller cells, rods primarily depend on vitamin A from the RPE/BM complex,⁴⁸ as supported by clinical studies including subjects with vitamin A deficiency.⁴⁹

Interestingly, within the DA testing spot, the presence of classic drusen and serous PED were also significantly associated with delayed DA. This is in agreement with the proposed influence of a diffusion barrier. In this region, as well as in the remaining macula, having ellipsoid disruption was also associated with impairments in time to dark-adapt. The ellipsoid zone observed on SD OCT has a hyperreflective region and there are different thoughts about its anatomic–pathologic correlation. Some authors have argued that it represents the interface between inner and outer photoreceptor segments. However, recent consensus²⁴ proposed that it represents the ellipsoid component of the photoreceptors, which are packed with mitochondria.²⁶ Disruption of this zone of the photoreceptors could certainly correlate with cell function. Ellipsoid disruption has been proposed as a biomarker for retinal function, as assessed by visual acuity,⁵⁰ microperimetry,⁵¹ and multifocal electroretinography.⁵² However, this remains controversial,⁵³ as the literature has shown that relying on this feature can also lead to misinterpretation of photoreceptor anatomy in a variety of diseases.^{54,55} We are not aware of previous studies associating ellipsoid disruption and DA impairment in AMD. In Stargardt disease, it has been associated with dark-adapted fundus-related perimetry.⁵⁶ In this study, however, we did not quantify the extent of ellipsoid disruption on B-scans or using *en face* images, which could potentially provide more details.⁵⁷

Retinal thickness has been shown to relate to DA in nonexudative AMD.²⁰ However, in this study, we did not observe a similar association, agreeing with previous work.²¹ We also systematically evaluated mean choroidal thickness within the DA testing spot and it does not seem to be a relevant predictor of time to dark-adapt. Similar results were described for young subjects with healthy macula.⁵⁸ Flamendorf et al²² reported a correlation between subfoveal choroidal thickness and mean RIT. However, these authors acknowledged that this was likely linked with the presence of subretinal drusenoid deposits and their focus on a single location. Using the software that

we developed, we were able to determine mean choroidal thickness in the multiple points included in the B-scans within the DA testing spot. Although mean choroidal thickness within the DA testing spot did not appear to be a good predictor of overall time to dark-adapt, in this cohort it seemed to be relevant for those eyes that were unable to reach RIT within the 20-minute testing period. This suggests that choroidal thickness may be more relevant for eyes with severe impairments in DA. Further studies are needed to clarify these findings. Of note, in this subpopulation (inability to reach RIT within the testing time), all the remaining findings (such as presence of ellipsoid disruption and subretinal drusenoid deposits) were consistent with those observed for the entire study population. The observation that all these eyes (with severe impairments in DA) presented OCT lesions in the macula further enhances the existence of a strong association between morphology and function as assessed by DA.

This study has several limitations, including its relatively small sample size. This might have affected our results, especially in the group with late AMD, where almost half of the included eyes ($n = 6$; 46.2%) had received prior intraocular treatments with photodynamic therapy (PDT) and/or antiangiogenic injections. Despite our exclusion criteria (none of them with treatment in the 90 days prior to inclusion), it is possible that these interventions affect dark adaptation. This sample size limitation also precluded our doing statistical analyses for some of the OCT parameters considered, due to their low frequency in our study population (for example, subretinal fluid and outer retinal tubulations). In evaluating these associations, multiple tests were completed that could have led to false-positive results. We relied on OCT to characterize subretinal drusenoid deposits, and a multimodal approach utilizing OCT and fundus autofluorescence might offer some advantages.^{59,60} However, previous studies⁶¹ demonstrated that SD OCT alone has the highest sensitivity (95%) and specificity (98%), among all imaging modalities, to identify subretinal drusenoid deposits, thus supporting our choice of methods. We also did not account for eye length, corneal curvature, and refractive error to map the DA testing spot, which could affect its localization.⁶² Despite this, according to our exclusion criteria, all eyes had a spherical equivalent less than 6 diopters and no corneal diseases. Also of note is that the current commercially available device (AdaptDx) does not provide an image of the fundus of the eye. We based our mapping of the DA testing spot on the provided settings (as detailed in the Methods section), but this might not represent the exact location of bleaching in eyes with eccentric fixation.

Another limitation is that in this study we only assessed the presence or absence of different OCT lesions associated with AMD, but did not account for their extent. For example, we did not assess areas of atrophy, as well as drusen number and volume, which seem to have an important prognostic value.^{21,63} We also did not look at thickness of the different retinal layers and we did not evaluate the interdigitation zone. Despite the experience of the optometrist who performed all DA testing,¹² we did not

assess reliability in this cohort. Additionally, we did not assess how different degrees of cataract could interfere with the observed results. An important percentage of our study cohort (26.3%, $n = 36$) was not able to reach RIT within the testing time. According to the prior literature,²² for these cases we assumed the value of 20 for statistical assessments. This assumption likely highly underestimates the real time to dark-adapt of these eyes and might have affected our results. In the future, studies including subjects with intermediate or late AMD should ideally refine the current available protocol.

Finally, it would be interesting to evaluate other factors, such as dietary patterns, vitamin A serum levels, and AMD genetic risk profiles, which might affect DA. Nevertheless, to our knowledge, the current study is the first with a comprehensive analysis of the influence of OCT-based structural parameters in the DA testing spot and the entire macula on DA in AMD. Longitudinal studies are needed to confirm our findings and assess how different pathologic abnormalities and their evolution with time affect DA.

In conclusion, our results suggest a strong association between AMD macular anatomy evaluated by OCT and time to dark-adapt. Dark adaptation correlates with morphologic abnormalities throughout the macula and within the DA testing spot, and appears to be a useful outcome measure for AMD studies. This is particularly relevant as, with the current available commercial device (AdaptDx), dark adaptation can be tested in a practical and less time-consuming manner than what was previously possible.^{64,65} Our data also support the important association between subretinal drusenoid deposits and ellipsoid zone changes and impaired dark adaptation, highlighting the relevance of considering multimodal imaging in future AMD grading schemes. Finally, this work also suggests that further research into the molecular mechanisms has the potential to lead to insights into disease mechanism and novel treatment for AMD. OCT and DA appear to provide important structure–function correlation in AMD pathogenesis, and support the need for further research in AMD to establish other structure–function connections.

Acknowledgments. The authors thank Russell L. Woods, PhD (Schepens Eye Research Institute, Massachusetts Eye and Ear, Department of Ophthalmology, Harvard Medical School, Boston, MA), for his scientific support and advice on the statistical analyses of this manuscript. The authors also thank Gregory Jackson, PhD (MacuLogix, Middletown, PA), for his critical review of this paper.

References

1. Miller JW. Age-related macular degeneration revisited—Piecing the puzzle: The LXIX Edward Jackson Memorial Lecture. *Am J Ophthalmol.* 2013;155(1):1-35.e13.
2. Wong WL, Su X, Li X, et al. Global prevalence of age-related macular degeneration and disease burden projection for 2020 and 2040: a systematic review and meta-analysis. *Lancet Glob Health.* 2014;2(2):e106-e116.
3. Yonekawa Y, Miller JW, Kim IK. Age-related macular degeneration: advances in management and diagnosis. *J Clin Med.* 2015;4(2):343-359.

4. Sobrin L, Seddon JM. Nature and nurture—genes and environment—predict onset and progression of macular degeneration. *Prog Retin Eye Res.* 2014;40:1-15.
5. Owsley C, Huisingsh C, Clark ME, et al. Comparison of visual function in older eyes in the earliest stages of age-related macular degeneration to those in normal macular health. *Curr Eye Res.* 2015;1-7.
6. Owsley C, Clark ME, Huisingsh CE, et al. Visual function in older eyes in normal macular health: association with incident early age-related macular degeneration 3 years later. *Invest Ophthalmol Vis Sci.* 2016;57(4):1782.
7. Haymes SA, Roberts KF, Cruess AF, et al. The letter contrast sensitivity test: clinical evaluation of a new design. *Invest Ophthalmol Vis Sci.* 2006;47(6):2739-2745.
8. Hogg RE, Chakravarthy U. Visual function and dysfunction in early and late age-related maculopathy. *Prog Retin Eye Res.* 2006;25(3):249-276.
9. Vujosevic S, Smolek MK, Lebow KA, et al. Detection of macular function changes in early (AREDS 2) and intermediate (AREDS 3) age-related macular degeneration. *Ophthalmologica.* 2011;225(3):155-160.
10. Ying G-S, Maguire MG, Liu C, Antoszyk AN, Complications of Age-related Macular Degeneration Prevention Trial Research Group. Night vision symptoms and progression of age-related macular degeneration in the Complications of Age-related Macular Degeneration Prevention Trial. *Ophthalmology.* 2008;115(11):1876-1882.
11. Owsley C, McGwin G, Jackson GR, et al. Cone- and rod-mediated dark adaptation impairment in age-related maculopathy. *Ophthalmology.* 2007;114(9):1728-1735.
12. Jackson GR, Scott IU, Kim IK, et al. Diagnostic sensitivity and specificity of dark adaptometry for detection of age-related macular degeneration. *Invest Ophthalmol Vis Sci.* 2014;55(3):1427-1431.
13. Danis RP, Domalpally A, Chew EY, et al. Methods and reproducibility of grading optimized digital color fundus photographs in the Age-Related Eye Disease Study 2 (AREDS2 Report Number 2). *Invest Ophthalmol Vis Sci.* 2013;54(7):4548-4554.
14. Yehoshua Z, Gregori G, Sadda SR, et al. Comparison of drusen area detected by spectral domain optical coherence tomography and color fundus imaging. *Invest Ophthalmol Vis Sci.* 2013;54(4):2429.
15. de Sisternes L, Simon N, Tibshirani R, et al. Quantitative SD-OCT imaging biomarkers as indicators of age-related macular degeneration progression. *Invest Ophthalmol Vis Sci.* 2014;55(11):7093.
16. Schmidt-Erfurth U, Waldstein SM. A paradigm shift in imaging biomarkers in neovascular age-related macular degeneration. *Prog Retin Eye Res.* 2016;50:1-24.
17. Leuschen JN, Schuman SG, Winter KP, et al. Spectral-domain optical coherence tomography characteristics of intermediate age-related macular degeneration. *Ophthalmology.* 2013;120(1):140-150.
18. Zweifel SA, Spaide RF, Curcio CA, et al. Reticular pseudodrusen are subretinal drusenoid deposits. *Ophthalmology.* 2010;117(2):303-312.e1.
19. Sivaprasad S, Bird A, Nitiapapand R, et al. Perspectives on reticular pseudodrusen in age-related macular degeneration. *Surv Ophthalmol.* 2016;61(5):521-537.
20. Clark ME, McGwin G, Neely D, et al. Association between retinal thickness measured by spectral-domain optical coherence tomography (OCT) and rod-mediated dark adaptation in non-exudative age-related maculopathy. *Br J Ophthalmol.* 2011;95(10):1427-1432.
21. Sevilla MB, McGwin G, Lad EM, et al. Relating retinal morphology and function in aging and early to intermediate age-related macular degeneration subjects. *Am J Ophthalmol.* 2016;165:65-77.
22. Flamendorf J, Agrón E, Wong WT, et al. Impairments in dark adaptation are associated with age-related macular degeneration severity and reticular pseudodrusen. *Ophthalmology.* 2015;122(10):2053-2062.
23. The Age-Related Eye Disease Study system for classifying age-related macular degeneration from stereoscopic color fundus photographs: the Age-Related Eye Disease Study Report Number 6. *Am J Ophthalmol.* 2001;132(5):668-681.
24. Staurengi G, Sadda S, Chakravarthy U, Spaide RF. Proposed lexicon for anatomic landmarks in normal posterior segment spectral-domain optical coherence tomography: the IN•OCT consensus. *Ophthalmology.* 2014;121(8):1572-1578.
25. Curcio CA, Messinger JD, Sloan KR, et al. Human chorioretinal layer thicknesses measured in macula-wide, high-resolution histologic sections. *Invest Ophthalmol Vis Sci.* 2011;52(7):3943.
26. Spaide RF, Curcio CA. Anatomical correlates to the bands seen in the outer retina by optical coherence tomography: literature review and model. *Retina.* 2011;31(8):1609-1619.
27. Pilotto E, Guidolin F, Convento E, et al. En face optical coherence tomography to detect and measure geographic atrophy. *Invest Ophthalmol Vis Sci.* 2015;56(13):8120.
28. Burton P, Gurrin L, Sly P. Extending the simple linear regression model to account for correlated responses: an introduction to generalized estimating equations and multi-level mixed modelling. *Stat Med.* 1998;17(11):1261-1291.
29. Fitzmaurice GM, Laird NM, Ware JH. Linear mixed effect models. In: *Applied Longitudinal Analysis*. 2nd ed. Hoboken, NJ: Wiley; 2011:189-240.
30. Tahir HJ, Rodrigo-Diaz E, Parry NRA, et al. Slowed dark adaptation in older eyes; effect of location. *Exp Eye Res.* 2016;155:47-53.
31. Zarubina AV, Neely DC, Clark ME, et al. Prevalence of subretinal drusenoid deposits in older persons with and without age-related macular degeneration, by multimodal imaging. *Ophthalmology.* 2016;123(5):1090-1100.
32. Curcio CA, Sloan KR, Kalina RE, Hendrickson AE. Human photoreceptor topography. *J Comp Neurol.* 1990;292(4):497-523.
33. Schmitz-Valckenberg S, Alten F, Steinberg JS, et al. Reticular drusen associated with geographic atrophy in age-related macular degeneration. *Invest Ophthalmol Vis Sci.* 2011;52(9):5009-5015.
34. Chan H, Cougnard-Grégoire A, Delyfer M-N, et al. Multimodal imaging of reticular pseudodrusen in a population-based setting: The Alienor Study. *Invest Ophthalmol Vis Sci.* 2016;57(7):3058.
35. Curcio CA, Messinger JD, Sloan KR, et al. Subretinal drusenoid deposits in non-neovascular age-related macular degeneration: morphology, prevalence, topography, and biogenesis model. *Retina.* 2013;33(2):265-276.
36. Curcio CA. Photoreceptor topography in ageing and age-related maculopathy. *Eye (Lond).* 2001;15(Pt 3):376-383.
37. Rudolf M, Malek G, Messinger JD, et al. Sub-retinal drusenoid deposits in human retina: organization and composition. *Exp Eye Res.* 2008;87(5):402-408.
38. Steinberg JS, Fitzke FW, Fimmers R, et al. Scotopic and photopic microperimetry in patients with reticular drusen and age-related macular degeneration. *JAMA Ophthalmol.* 2015;133(6):690.

39. Steinberg JS, Saßmannshausen M, Fleckenstein M, et al. Correlation of partial outer retinal thickness with scotopic and mesopic fundus-controlled perimetry in patients with reticular drusen. *Am J Ophthalmol*. 2016;168:52-61.
40. Mrejen S, Sato T, Curcio CA, Spaide RF. Assessing the cone photoreceptor mosaic in eyes with pseudodrusen and soft drusen in vivo using adaptive optics imaging. *Ophthalmology*. 2014;121(2):545-551.
41. Zhang Y, Wang X, Rivero EB, et al. Photoreceptor perturbation around subretinal drusenoid deposits as revealed by adaptive optics scanning laser ophthalmoscopy. *Am J Ophthalmol*. 2014;158(3):584-596.e1.
42. Jacobson SG, Cideciyan AV, Regunath G, et al. Night blindness in Sorsby's fundus dystrophy reversed by vitamin A. *Nat Genet*. 1995;11(1):27-32.
43. Pauleikhoff D, Harper CA, Marshall J, Bird AC. Aging changes in Bruch's membrane. A histochemical and morphologic study. *Ophthalmology*. 1990;97(2):171-178.
44. Curcio CA, Johnson M, Rudolf M, Huang J-D. The oil spill in ageing Bruch membrane. *Br J Ophthalmol*. 2011;95(12):1638-1645.
45. Jackson GR, Owsley C, McGwin G. Aging and dark adaptation. *Vision Res*. 1999;39(23):3975-3982.
46. Lamb TD, Pugh EN. Dark adaptation and the retinoid cycle of vision. *Prog Retin Eye Res*. 2004;23(3):307-380.
47. Curcio CA, Owsley C, Jackson GR. Spare the rods, save the cones in aging and age-related maculopathy. *Invest Ophthalmol Vis Sci*. 2000;41(8):2015-2018.
48. Garlipp MA, Gonzalez-Fernandez F. Cone outer segment and Müller microvilli pericellular matrices provide binding domains for interphotoreceptor retinoid-binding protein (IRBP). *Exp Eye Res*. 2013;113:192-202.
49. McBain VA, Egan CA, Pieris SJ, et al. Functional observations in vitamin A deficiency: diagnosis and time course of recovery. *Eye (Lond)*. 2007;21(3):367-376.
50. Casalino G, Bandello F, Chakravarthy U. Changes in neovascular lesion hyperreflectivity after anti-VEGF treatment in age-related macular degeneration: an integrated multimodal imaging analysis. *Invest Ophthalmol Vis Sci*. 2016;57(9):OCT288.
51. Takahashi A, Ooto S, Yamashiro K, et al. Photoreceptor damage and reduction of retinal sensitivity surrounding geographic atrophy in age-related macular degeneration. *Am J Ophthalmol*. 2016;168:260-268.
52. Wu Z, Ayton LN, Guymer RH, Luu CD. Relationship between the second reflective band on optical coherence tomography and multifocal electroretinography in age-related macular degeneration. *Invest Ophthalmol Vis Sci*. 2013;54(4):2800-2806.
53. Coscas F, Coscas G, Lupidi M, et al. Restoration of outer retinal layers after aflibercept therapy in exudative AMD: prognostic value. *Invest Ophthalmol Vis Sci*. 2015;56(6):4129.
54. Scoles D, Flatter JA, Cooper RF, et al. Assessing photoreceptor structure associated with ellipsoid zone disruptions visualized with optical coherence tomography. *Retina*. 2015;36(1):1-13.
55. Sumaroka A, Matsui R, Cideciyan AV, et al. Outer retinal changes including the ellipsoid zone band in Usher syndrome 1B due to *MYO7A* mutations. *Invest Ophthalmol Vis Sci*. 2016;57(9):OCT253.
56. Salvatore S, Fishman GA, McAnany JJ, Genead MA. Association of dark-adapted visual function with retinal structural changes in patients with Stargardt disease. *Retina*. 2014;34(5):989-995.
57. Chew EY, Clemons TE, Peto T, et al. Ciliary neurotrophic factor for macular telangiectasia type 2: results from a phase 1 safety trial. *Am J Ophthalmol*. 2015;159(4):659-666.e1.
58. Munch IC, Altuntas C, Li XQ, et al. Dark adaptation in relation to choroidal thickness in healthy young subjects: a cross-sectional, observational study. *BMC Ophthalmol*. 2016;16(1):105.
59. Sohrab MA, Smith RT, Salehi-Had H, et al. Image registration and multimodal imaging of reticular pseudodrusen. *Invest Ophthalmol Vis Sci*. 2011;52(8):5743-5748.
60. Smith RT, Sohrab MA, Busuioc M, Barile G. Reticular macular disease. *Am J Ophthalmol*. 2009;148(5):733-743.e2.
61. Ueda-Arakawa N, Ooto S, Tsujikawa A, et al. Sensitivity and specificity of detecting reticular pseudodrusen in multimodal imaging in Japanese patients. *Retina*. 2013;33(3):490-497.
62. Delori F, Greenberg JP, Woods RL, et al. Quantitative measurements of autofluorescence with the scanning laser ophthalmoscope. *Invest Ophthalmol Vis Sci*. 2011;52(13):9379-9390.
63. Abdelfattah NS, Zhang H, Boyer DS, et al. Drusen volume as a predictor of disease progression in patients with late age-related macular degeneration in the fellow eye. *Invest Ophthalmol Vis Sci*. 2016;57(4):1839.
64. Dimitrov PN, Robman LD, Varsamidis M, et al. Relationship between clinical macular changes and retinal function in age-related macular degeneration. *Invest Ophthalmol Vis Sci*. 2012;53(9):5213-5220.
65. Dimitrov PN, Robman LD, Varsamidis M, et al. Visual function tests as potential biomarkers in age-related macular degeneration. *Invest Ophthalmol Vis Sci*. 2011;52(13):9457-9469.

Footnotes and Financial Disclosures

Originally received: December 15, 2016.

Final revision: March 27, 2017.

Accepted: March 31, 2017.

Available online: May 10, 2017.

Manuscript no. 2016-1037.

¹ Retina Service, Massachusetts Eye and Ear, Harvard Ophthalmology AMD Center of Excellence, Department of Ophthalmology, Harvard Medical School, Boston, Massachusetts.

² Faculty of Medicine, University of Coimbra, Coimbra, Portugal.

³ Association for Innovation and Biomedical Research on Light, AIBILI, Coimbra, Portugal.

⁴ Centro Hospitalar e Universitário de Coimbra, Coimbra, Portugal.

⁵ Department of Ophthalmology, School of Medicine, Kyungpook National University, South Korea.

⁶ Glaucoma Service, Massachusetts Eye and Ear, Department of Ophthalmology, Harvard Medical School, Boston, Massachusetts.

Presented in part as at the Association for Research in Vision and Ophthalmology (ARVO) Annual Meeting, May 1-5, 2016, Seattle, WA; and as an oral presentation at the ARVO Annual Meeting, May 7-11, 2017, Baltimore, Maryland.

Financial Disclosure(s):

The authors made the following disclosures: J.W.M.: Scientific Advisory Board — MacuLogix, but receives no compensation; Financial support — Miller Retina Research Fund (Massachusetts Eye and Ear Infirmary); Champalimaud Vision Award; Unrestricted departmental grant — Research to Prevent Blindness, Inc, New York; Portuguese Foundation for Science and Technology/Harvard Medical School Portugal Program (HMSP-ICJ/006/2013).

D.H.P.: Financial support — Basic Science Research Program of the National Research Foundation of Korea (NRF); Funding — Ministry of Education (NRF-2014R1A1A2055007); Korea Health Technology R&D Project of the Korea Health Industry Development Institute (KHIDI); Ministry of Health & Welfare, Republic of Korea (H116C1501). All of the above-mentioned funding organizations had no role in the design or conduct of this research. Massachusetts Eye and Ear Infirmary received donation of an AdaptDx dark adaptometer.

Author Contributions:

Conception and design: Laíns, Silva, Kim, Vavvas, Joan W. Miller, Husain
Analysis and interpretation: Laíns, John B. Miller, Park, Tsikata, Davoudi, Rahmani, Pierce, Silva, Chen, Kim, Vavvas, Joan W. Miller, Husain

Data collection: Laíns, John B. Miller, Park, Tsikata, Davoudi, Rahmani, Pierce, Silva, Chen, Kim, Vavvas, Joan W. Miller, Husain

Obtained funding: Not applicable

Overall responsibility: Laíns, John B. Miller, Park, Tsikata, Davoudi, Rahmani, Pierce, Silva, Chen, Kim, Vavvas, Joan W. Miller, Husain

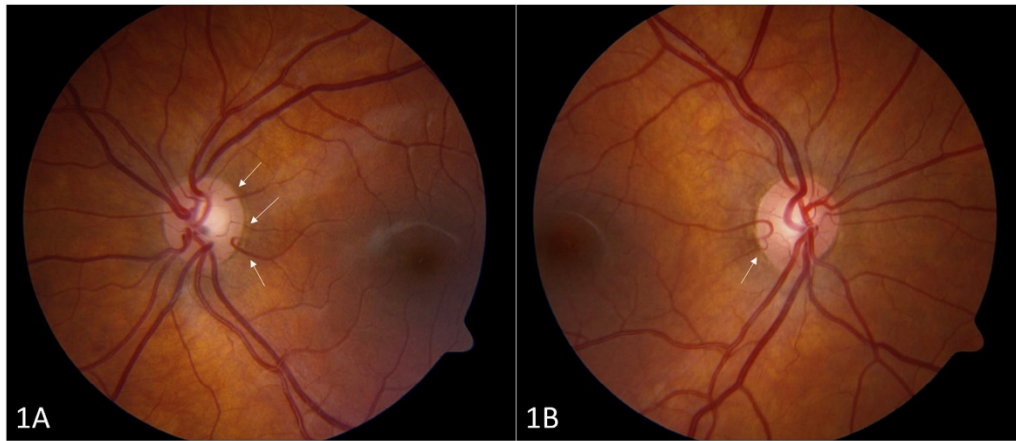
Abbreviations and Acronyms:

AMD = age-related macular degeneration; **AREDS** = Age-Related Eye Disease Study; **BM** = Bruch membrane; **CFP** = color fundus photographs; **CNV** = choroidal neovascularization; **DA** = dark adaptation; **EDI** = enhanced depth imaging; **GA** = geographic atrophy; **ILM** = inner limiting membrane; **OCT** = optical coherence tomography; **PED** = pigment epithelium detachment; **PDT** = photodynamic therapy; **RIT** = rod intercept time; **RPE** = retinal pigment epithelium; **SD OCT** = spectral-domain optical coherence tomography; **VA** = visual acuity.

Correspondence:

Deeba Husain, MD, Retina Service, Massachusetts Eye and Ear, Harvard Medical School, 243 Charles Street, Boston, MA 02114. E-mail: Deeba_Husain@meei.harvard.edu.

Pictures & Perspectives



Multiple and Bilateral Cilioretinal Arteries with Shwachman-Diamond Syndrome

An 11-year-old boy with Shwachman-Diamond syndrome confirmed by *SBDS* gene mutation, manifesting with myelodysplastic syndrome and exocrine pancreatic insufficiency, presented to pediatric ophthalmology clinic after temporary visual disturbance during hospitalization for bone marrow biopsy. Vision, motility, and anterior segment examinations were normal. Left fundus revealed at least 3 cilioretinal arteries involving macula (Fig 1A, arrows), and right fundus showed larger, branching, cilioretinal artery (Fig 1B, arrow). Shwachman-Diamond syndrome is an autosomal recessive disorder of *SBDS* gene (7q11, critical for ribosome function), characterized by ineffective hematopoiesis, leukemia risk, and exocrine pancreatic dysfunction, although it has not been previously associated with ocular anomalies (Magnified version of Figure 1A-B available online at www.aaojournal.org).

MARK P. BREAZZANO, MD

NANCY M. BENEGAS, MD

Vanderbilt Eye Institute, Department of Ophthalmology & Visual Sciences, Vanderbilt University Medical Center, Nashville, Tennessee

HEALTH CONDITIONS LINKED TO AGE-RELATED MACULAR DEGENERATION ASSOCIATED WITH DARK ADAPTATION

INÊS LAÍNS, MD, MSc,*† JOHN B. MILLER, MD,* RYO MUKAI, MD, PhD,* STEVEN MACH, BSc,* DEMETRIOS VAVVAS, MD, PhD,* IVANA K. KIM, MD,* JOAN W. MILLER, MD,* DEEBA HUSAIN, MD*

Purpose: To determine the association between dark adaptation (DA) and different health conditions linked with age-related macular degeneration (AMD).

Methods: Cross-sectional study, including patients with AMD and a control group. Age-related macular degeneration was graded according to the Age-Related Eye Disease Study (AREDS) classification. We obtained data on medical history, medications, and lifestyle. Dark adaptation was assessed with the extended protocol (20 minutes) of AdaptDx (MacuLogix). For analyses, the right eye or the eye with more advanced AMD was selected. Multivariate linear and logistic regressions were performed, accounting for age and AMD stage.

Results: Seventy-eight subjects (75.6% AMD; 24.4% controls) were included. Multivariate assessments revealed that body mass index (BMI; $\beta = 0.30$, $P = 0.045$), taking AREDS vitamins ($\beta = 5.51$, $P < 0.001$), and family history of AMD ($\beta = 2.68$, $P = 0.039$) were significantly associated with worse rod intercept times. Abnormal DA (rod intercept time ≥ 6.5 minutes) was significantly associated with family history of AMD ($\beta = 1.84$, $P = 0.006$), taking AREDS supplements ($\beta = 1.67$, $P = 0.021$) and alcohol intake ($\beta = 0.07$, $P = 0.017$).

Conclusion: Besides age and AMD stage, a higher body mass index, higher alcohol intake, and a family history of AMD seem to impair DA. In this cohort, the use of AREDS vitamins was also statistically linked with impaired DA, most likely because of an increased severity of disease in subjects taking them.

RETINA 0:1–11, 2017

Age-related macular degeneration (AMD) is the leading cause of adult blindness in developed countries and ranks third worldwide.¹ Severe vision loss typically occurs late in the disease course, when

chorioretinal atrophy (geographic atrophy) or choroidal neovascularization develops. It is widely recognized that visual acuity, the most common functional outcome in ophthalmology, remains preserved in the early and intermediate AMD stages, and thus have important limitations for the assessment of this disease.²

Several researchers have tried to establish other functional outcome measurements, including contrast sensitivity,³ dark adaptation (DA),² low luminance visual acuity, and photopic or scotopic light sensitivity.^{4,5} There is increasing evidence that DA appears to provide one of the best functional assessments for the earliest phases of the disease.² This is in agreement with reports of patients with early AMD that described vision problems under dim lighting or at night,^{6,7} as well as with histopathologic data showing that rods degenerate earlier and more severely than cones,^{8,9} and that AMD initially affects the parafoveal region (that has more rods than cones). Progressive loss of

From the *Retina Service, Massachusetts Eye and Ear, Department of Ophthalmology, Harvard Medical School, Boston, Massachusetts; and †Department of Ophthalmology, Faculty of Medicine, University of Coimbra, Coimbra, Portugal.

Supported by Miller Retina Research Found (Mass. Eye and Ear), Miller Champalimaud Award (Mass. Eye and Ear), unrestricted departmental Grant from Research to Prevent Blindness, Inc, New York, and Portuguese Foundation for Science and Technology/Harvard Medical School Portugal Program (HMSP-ICJ/006/2013).

The authors disclose that J. W. Miller is on the Scientific Advisory Board for MacuLogix, but receives no compensation. In kind, Massachusetts Eye and Ear received donation of an AdaptRx dark adaptometer. The remaining authors have no conflicting interests to disclose.

Reprint requests: Deeba Husain, MD, Retina Service, Massachusetts Eye and Ear, Harvard Medical School, 243 Charles Street, Boston, MA 02114; e-mail: Deeba_Husain@meei.harvard.edu

rods is associated with normal aging, but it seems to be more pronounced in subjects with AMD.^{8,9} Until recently, the use of DA in the clinical setting was difficult because of its long test duration and lack of standardized devices. The AdaptDx (MacuLogix, Hummelstown, PA) dark adaptometer recently became commercially available and helps to differentiate patients with AMD from controls with high sensitivity and specificity within less than 10 minutes.¹⁰ Moreover, with a 20-minute assessment, rod intercept time (RIT) appears to differ among subjects with early, intermediate, and late stage AMD.¹⁰

Despite acceptance of the association of AMD with a prolonged time to dark-adapt, the interaction with other health parameters that are known to affect AMD incidence and progression remains only partially understood. Owsley et al¹¹ studied the association between DA time and several health parameters known to increase AMD risk, such as smoking and body mass index (BMI), on a cohort of older adults with normal maculae. Their main focus was on how these conditions might lead to a transition from normal aging to disease; however, these same parameters also affect AMD severity and progression. Before adopting DA as a useful measure of retinal dysfunction in AMD, the effect of other conditions on the time to dark-adapt should be studied.¹²

This study aimed to evaluate the influence of various health conditions, as well as known AMD risk factors, on DA in a clinic-based sample of patients with AMD in different stages of disease and a group of controls without any retinal pathology.

Methods

Study Design

This study was part of a cross-sectional observational study on AMD biomarkers at Massachusetts Eye and Ear, Harvard Medical School, Boston, United States. The research protocol was conducted in accordance with Health Insurance Portability and Accountability Act (HIPAA) requirements and the tenets of the Declaration of Helsinki and was approved by the Mass. Eye and Ear Institutional Review Board (IRB).

Study Protocol

From January 2015 to July 2016, we prospectively recruited and consented consecutive subjects with a diagnosis of AMD at the time of their regular appointments at the Mass. Eye and Ear Retina Service. Exclusion criteria included diagnosis of any other

vitreoretinal disease, active uveitis or ocular infection, significant media opacities that precluded the observation of the ocular fundus, refractive error equal or greater than 6 diopters of spherical equivalent, history of retinal surgery, history of any ocular surgery, or intraocular procedure (such as laser and intraocular injections) within the 90 days before enrollment, and diagnosis of diabetes mellitus, with or without concomitant diabetic retinopathy (due to the remaining study purposes). In addition, a control group of subjects aged 50 years or older, without any evidence of AMD in both eyes, was identified and consented at the Mass. Eye and Ear Comprehensive Ophthalmology and Optometry Services. The same exclusion criteria were applied. All included participants provided written informed consent.

All participants underwent a comprehensive eye examination, including best-corrected visual acuity (BCVA) (converted to logMAR for analysis), current refraction, intraocular pressure, slit-lamp biomicroscopy, and dilated fundus examination. Nonstereoscopic, seven fields, color fundus photographs (Topcon TRC-50DX; Topcon Corporation, Tokyo, Japan) were also obtained. A standardized medical history questionnaire was designed specifically for this study, based on the current knowledge of AMD pathogenesis and the input of five Retina specialists. Data collected on this questionnaire included: age; sex; smoking habits (smokers were considered those who reported current smoking and ex-smokers those who have ever smoked, regardless of when they stopped. Data on the mean number of cigarettes smoked per day, as well as the age when subjects started and stopped smoking, were also collected if applicable); history of known diagnosis, and time of diagnosis of several medical conditions, including hypertension, dyslipidemia, congestive heart failure, coronary artery disease, myocardial infarction, stroke, or any cardiovascular surgery, blood or clotting disorders, kidney or liver disease, neurologic diseases, cancer (including type of cancer, year of diagnosis, year of remission/cure, and current treatment, if applicable), autoimmune diseases (specifically including rheumatoid arthritis, systemic lupus erythematosus, and multiple sclerosis) and thyroid disease. Women were asked about menstrual status (including age of menopause and current or past treatment with hormonal therapy). The same questionnaire also included queries regarding known family history of AMD (first-degree relatives). The current height and weight were recorded to calculate BMI, which was used as a continuous variable for analysis. If the study participants did not know their current height and/or weight, these were obtained by a study investigator. History of any other ocular

conditions was also obtained, and current ocular or systemic medications were registered. For data analysis, the medications were organized in the following categories: vitamins with the Age-Related Eye Disease Study (AREDS) formula (including both AREDS and AREDS2), other multivitamins, statins, aspirin, other nonsteroidal anti-inflammatory drugs, anticoagulants, and steroids.

In addition, all subjects completed a validated food frequency questionnaire¹³ and a questionnaire on their usual levels of physical activity—the Rapid Assessment of Physical Activity test.¹⁴ For the purposes of this analysis, data on alcohol consumption (average in the last year) was obtained from the food frequency questionnaire, processed by the Harvard School of Public Health, and used as a continuous variable for statistical assessments in grams/day. The physical activity Rapid Assessment of Physical Activity test is an easy to use nine-question (yes/no) questionnaire, which has been specifically built and validated for subjects older than 50 years. Scoring was performed according to the protocol,¹⁴ namely, subjects were categorized as active if they reported the practice of moderate physical activities at least 30 minutes per day, 5 or more days a week; or vigorous activities 20 minutes or more a day, 3 or more days a week.

All the study participants underwent DA testing, according to the protocol below. To avoid previous light exposure, DA was performed on a separate day from the ophthalmologic examination and fundus imaging, within a maximum interval of 1 month after study entry.

Dark Adaptation Testing

An experienced and trained Mass. Eye and Ear optometrist confirmed the current refraction of all participants and optimized it when required. After dilation to ≥ 6 mm (using 1% tropicamide and 2.5% phenylephrine hydrochloride), DA was performed using the AdaptDx dark adaptometer (MacuLogix). Corrective lenses were used to correct for the 30-cm viewing distance. Both eyes were tested separately (the right eye always first), with a minimum resting period of 15 minutes between them. During testing, the fellow eye was occluded with an eye patch.

The extended protocol (20 minutes) was followed, as previously described.¹⁰ Briefly, the operator centered the subject's eye to a red fixation light, and with the eye focused on this light, the eye was bleached by exposure to a 505-nm photoflash (0.8-ms duration, 1.8×10^4 scot cd/m² second intensity), equivalent to 76% bleaching level for rods. The flash of light passed through a square aperture sized to bleach a 4° area

of the retina centered at 5° on the inferior visual meridian. Sensitivity measurements began immediately after bleaching. The subject focused on the fixation light and indicated when a stimulus light was visible by pushing a hand-held button. The stimulus light was a 505-nm, 2° circular test spot located at 5° on the inferior visual meridian. Sensitivity was estimated using a three-down/one-up modified staircase threshold estimate procedure. The initial stimulus intensity was 5 scot cd/m². The stimulus light was presented every 2 or 3 seconds for a 200-ms duration. The patient was given 2 seconds to respond if the stimulus was detected by pushing a response button. If the subject indicated that the stimulus was visible, the intensity was decreased for each successive presentation in steps of 0.3 log units until the subject could not see the stimulus. If the subject indicated that the stimulus light was not visible, the intensity of the target was increased for each successive presentation in 0.1-log-unit steps until the subject stopped seeing the stimulus. This intensity was defined as a threshold. Successive threshold measurements started with the stimulus intensity 0.2 log units brighter than the previous threshold measurement. The subject had a 15-second rest period between threshold measurements. However, if a threshold had a large deviation from previous thresholds in the DA function, the point was considered unreliable; a fixation error was recorded and an additional threshold was measured immediately. Threshold measurements were made approximately once a minute for the duration of the DA test. The test ended when the subject's sensitivity was measured to be greater than 5×10^{-3} scot cd/m² twice consecutively or the test duration reached 20 minutes, whichever was shorter. The time to reach this point was designated the RIT. When subjects did not reach the RIT within the 20 minutes of testing, this was registered.

Age-Related Macular Degeneration Diagnosis and Grading

Two independent experienced graders (I.L., R.M.) analyzed all field 2 color fundus photograph on IMAGENet 2000 software (version 2.56; Topcon Medical Systems, Oakland, NJ) to establish an AMD diagnosis and grade, according to the AREDS classification system.^{15,16} In cases of disagreement, a senior author (DH) established the final categorization. All graders were masked to the patients' clinical and demographic characteristics during this process.

We adopted the most recent AREDS2 definitions,¹⁶ namely that the standard disc diameter equals 1,800 μ m (rather than 1,500 μ m), which affects the size of the Early Treatment Diabetic Retinopathy Study grid

and of the standard drusen circles; and that geographic atrophy is present if the lesion has a diameter equal or greater than 433 μm (AREDS circle I-2) and has at least 2 of the following features—absence of RPE pigment, circular shape, or sharp margins (foveal involvement not a requirement). With these criteria, we established the following groups,^{15,16} which were then used for statistical assessments: controls—presence of drusen maximum size <circle C0 and total area <C1; early AMD—drusen maximum size \geq C0 but <C1 or presence of AMD characteristic pigment abnormalities in the inner or central subfields; intermediate AMD—presence drusen maximum size \geq C1 or of drusen maximum size \geq C0 if the total area occupied was >I2 for soft indistinct drusen and >O2 for soft distinct drusen and; late AMD—presence of geographic atrophy according to the criteria described above or evidence of neovascular AMD.

Selection of Dark Adaptation Data for Analysis

All patients who met the eligibility criteria were considered for analysis, and as described, all of them had DA performed on both eyes. For the purposes of this study, we considered DA data from one eye only, which was selected based on the following criteria: 1) The eye graded with the most advanced AMD severity stage was selected. In cases where this eye had a fixation error equal to or greater than 30%, the patient was excluded ($n = 3$). 2) If both eyes presented with the same stage of AMD, the right eye was selected, except if it had a fixation error of more than 30%. If this was the case, the left eye parameters were used ($n = 3$).

Statistical Analysis

The demographics, clinical, and medical history characteristics of the included subjects were summarized with mean and standard deviation for continuous variables, and percentages for dichotomous and categorical variables. Time to dark-adapt (RIT, a continuous variable) was the first outcome considered. For subjects who did not reach the RIT within the 20 minutes of testing, the value of 20 was assumed.¹⁷ Univariate linear regression analyses were performed for all parameters studied, as detailed below (Table 1). Those that presented a P value ≤ 0.250 (Table 2) were considered for multivariate assessments, which accounted for AMD staging and age, considering the clinical and statistical relevance of these covariates for DA. In addition, we performed logistic regression analyses considering two other outcomes: abnormal DA (defined as a RIT ≥ 6.5 minutes¹⁰); and inability to reach RIT within the testing time (>20 minutes).

Similarly, univariate assessments were performed for all studied parameters and those with a P -value ≤ 0.250 were considered for multivariate analysis. Age and AMD stage was always accounted for in multivariate analyses. Beta-coefficients, 95% confidence intervals, and odds ratios are presented. All statistics were performed using Stata version 14.1 (StataCorp LP, College Station, TX) and P values < 0.05 were considered statistically significant.

Results

Study Population

We included 78 eyes of 78 subjects, 75.6% ($n = 59$) with AMD and the remaining controls (24.4%, $n = 19$). Their mean RIT was 12.5 ± 6.6 minutes and 5.6 ± 3.2 minutes for subjects with AMD and for controls, respectively. An abnormal RIT (defined as ≥ 6.5 minutes¹⁰) was registered for 4 (21.1%) control subjects and 72.9% ($n = 43$) of the patients with AMD. All controls had RIT value within the 20 minutes of testing. Nineteen (32.2%) of the AMD subjects had RIT of more than 20 minutes, all of them with intermediate or late AMD. Table 1 presents the demographic and clinical characteristics of the included study group. As shown, most participants were taking vitamins according to the AREDS composition or other multivitamins.

Univariate and Multivariate Analyses—Rod Intercept Time

We started our statistical approach by considering RIT as a continuous variable. All parameters detailed in Table 1 were considered for our univariate assessments, which showed that AMD stage was highly associated ($P < 0.001$) with an increased RIT (Table 2). While subjects with early AMD did not present a significant increase in RIT as compared to controls ($P = 0.837$), a statistically significant association was observed for those with intermediate ($\beta = 8.74$, $P < 0.001$; i.e., subjects with intermediate AMD presented a RIT 8.74 minutes higher than controls) and late ($\beta = 9.78$, $P < 0.001$; i.e., subjects with intermediate AMD presented a RIT 8.74 minutes higher than controls) stage AMD. Figure 1 presents examples of DA curves of patients with AMD and a control.

Older age ($P = 0.001$), worst BCVA ($P = 0.004$), pseudophakia ($P = 0.009$), diagnosis of heart failure ($P = 0.046$), and family history of AMD ($P = 0.001$) were also significantly associated with a prolonged RIT on the univariate analyses. The same was observed for taking AREDS ($P < 0.001$) or other multivitamins ($P = 0.002$), as presented in Table 2.

Table 1. Study Population Characterization

	Controls	AMD Patients	Total
Demographic and clinical characteristics			
Subjects, n (%)	19 (24.4)	59 (75.6)	78 (100)
Included eye, n (%)			
OD	19 (26.4)	53 (73.6)	72 (92.3)
OS	0 (0)	6 (100)	6 (7.7)
Age, mean \pm SD	66.1 \pm 7.7	68.9 \pm 6.5	68.3 \pm 6.9
Sex, n (%)			
Male	11 (34.4)	21 (66.6)	32 (41.0)
Female	8 (17.4)	38 (83.6)	46 (59)
Race/ethnicity, n (%)			
White	17 (23.9)	54 (76.1)	71 (91.0)
Asian	0 (0)	1 (100)	1 (1.2)
Black	1 (100)	0 (0)	1 (1.2)
Hispanic	1 (20)	4 (80)	5 (6.4)
AMD stage, n (%)			
Controls	19 (100)	0 (0)	19 (24.4)
Early AMD	0 (0)	14 (100)	14 (17.9)
Intermediate AMD	0 (0)	34 (100)	34 (43.6)
Late AMD	0 (0)	11 (100)	11 (14.1)
BMI, kg/m ² , mean \pm SD	26.1 \pm 3.7	27.5 \pm 4.4	27.2 \pm 4.2
Eye exam			
BCVA, logMAR, mean \pm SD (Snellen)	0.10 \pm 0.13 (20/25)	0.11 \pm 0.15 (20/25)	0.10 \pm 0.15 (20/25)
Spherical equivalent diopters, mean \pm SD	-0.5 \pm 2.6	0.5 \pm 1.4	0.3 \pm 1.8
IOP, mmHg, mean \pm SD	14 \pm 2.6	15.1 \pm 2.8	14.8 \pm 2.8
Pseudophakic, n (%)	0.05 \pm 0.2	0.2 \pm 0.4	12 (16.7)
Medical history			
Smoking habits, n (%)			
Non-smoker	8 (22.2)	28 (77.8)	36 (46.1)
Ex-smoker	10 (25)	30 (75)	40 (51.3)
Smoker	1 (50)	1 (50)	2 (2.56)
Alcohol consumption, g/day, mean \pm SD*	9.7 \pm 13.3	10.9 \pm 13.6	10.7 \pm 13.5
Hypertension, n (%)	5 (20.8)	19 (79.2)	24 (30.8)
Dyslipidemia, n (%)	9 (26.5)	25 (73.5)	34 (43.6)
Heart failure, n (%)	0 (0)	2 (100)	2 (2.56)
Coronary disease	0 (0)	8 (100)	8 (10.3)
Previous heart or vascular surgery, n (%)	0 (0)	10 (100)	10 (12.8)
Blood or clotting disorders, n (%)	1 (20)	4 (80)	5 (6.49)
Previous stroke or transient ischemic heart attack, n (%)	3 (42.8)	4 (57.2)	7 (9.0)
Kidney disease, n (%)	2 (33.3)	4 (66.7)	6 (7.7)
Liver disease, n (%)	1 (50)	1 (50)	2 (2.6)
Neurologic disease, n (%)	1 (25)	3 (75)	4 (5.1)
Cancer, n (%)	8 (26.7)	22 (73.3)	30 (38.5)
Autoimmune diseases, n (%)	1 (7.7)	12 (92.3)	13 (16.7)
Thyroid disease, n (%)	3 (42.8)	4 (57.2)	7 (9.0)
Reached menopause, n (%)†	7 (15.5)	38 (85.5)	45 (97.8)
Current medication, n (%)			
AREDS vitamins	1 (2.7)	36 (96.3)	37 (47.4)
Other multivitamins	12 (18.5)	53 (82.5)	65 (83.3)
Vitamin A	0 (0)	2 (100)	2 (2.6)
Aspirin	4 (12.5)	28 (87.5)	32 (41.6)
Other NSAIDs	2 (33.3)	4 (66.7)	6 (7.8)
Statins	10 (35.7)	28 (64.3)	38 (49.4)
Anticoagulants	2 (33.3)	4 (66.7)	6 (7.8)

(continued on next page)

Table 1. (Continued)

	Controls	AMD Patients	Total
Steroids	1 (33.3)	2 (66.7)	3 (3.9)
Family history			
Any relatives with AMD n (%)	4 (12.5)	28 (87.5)	32 (43.2)
RAPA physical activity questionnaire			
Physically active, n (%)	10 (35.7)	33 (64.3)	43 (55.1)
Aerobic score, mean ± SD	5.3 ± 1.8	5.3 ± 1.6	5.2 ± 1.6
Strength and flexibility, mean ± SD	1.6 ± 1.3	1.4 ± 1.3	1.4 ± 1.3

*Data missing for two patients.

†Percentage calculated only considering the total number of women (n = 46).
n, number; IOP, intraocular pressure; NSAIDs, nonsteroidal anti-inflammatory drugs; OD, right eye; OS, left eye; RAPA, Rapid Assessment of Physical Activity; SD, standard deviation; BCVA, best corrected visual acuity; BMI, body mass index.

As detailed in the Methods section, variables presenting a P value ≤ 0.250 (Table 2) were considered for further multivariate assessments. All these variables were evaluated controlling for AMD stage and patient age, because of their clinical and statistical relevance (described above). After accounting for these covariates, higher BMI (considered as a continuous variable, $\beta = 0.30$, $P = 0.045$), taking AREDS vitamins ($\beta = 5.51$, $P < 0.001$), and a family history of AMD ($\beta = 2.68$, $P = 0.039$) demonstrated a statistically significant relationship with RIT.

Univariate and Multivariate Analyses—Abnormal Rod Intercept Time

We then compared abnormal RIT (≥ 6.5 minutes) with normal RIT as a dichotomous outcome for logistic regression assessments. Similar to what was observed for RIT as a continuous variable, older age ($P = 0.008$), AMD stage ($P < 0.001$), worst BCVA ($P = 0.004$), taking AREDS or other multivitamins ($P < 0.001$ and $P = 0.006$), and having a family history of AMD ($P < 0.001$) had a statistically significant association with an abnormal time to dark-adapt on the univariate analyses

Table 2. Univariate and Multivariate Linear Regression Analyses of RIT

Variable	Univariate Analysis			Multivariate Analysis (Controlling for Age and AMD Stage)		
	β Coefficient	95% CI	P	β Coefficient	95% CI	P
Eye (reference term OD)	4.18	−1.38 to 9.73	0.139	2.31	−2.03 to 6.65	0.292
Age	0.34	0.14 to 0.55	0.001	NA	NA	NA
AMD stage (reference term controls)	4.00	2.83 to 5.18	<0.001	NA	NA	NA
BMI	0.30	−0.05 to 0.65	0.088	0.29	0.006 to 0.58	0.045
BCVA	14.79	5.01 to 24.58	0.004	6.93	−1.33 to 15.19	0.099
Pseudophakic (reference term phakic)	5.17	1.31 to 9.02	0.009	1.95	−1.43 to 5.33	0.255
Alcohol consumption	0.08	−0.03 to 0.20	0.143	0.05	−0.04 to 0.14	0.269
Heart failure*	9.41	0.16 to 18.67	0.046	4.79	−2.56 to 12.14	0.198
Autoimmune diseases*	3.81	−0.13 to 7.75	0.058	2.06	−1.08 to 5.20	0.195
AREDS vitamins*	8.16	5.80 to 10.52	<0.001	5.51	2.82 to 8.19	<0.001
Other multivitamins*	6.04	2.25 to 9.83	0.002	1.49	−1.91 to 4.89	0.385
Other NSAIDs*	−3.40	−8.96 to 2.15	0.226	−1.73	−6.15 to 2.69	0.438
Statins*	2.11	−0.85 to 5.08	0.160	0.78	−1.58 to 3.14	0.512
Anticoagulants*	5.20	−0.28 to 10.68	0.062	3.41	−0.94 to 7.76	0.123
Relatives with AMD*	5.06	2.12 to 7.99	0.001	2.68	0.14 to 5.21	0.039
Physically active*	2.45	−0.52 to 5.41	0.105	0.88	−1.47 to 3.24	0.457

Only parameters with P values ≤ 0.250 are shown.

For variables with "*" (binomial, yes versus no) the reference term is "no," which means that their presence was associated with an increase in RIT correspondent to the β coefficient (i.e., for multivariate analysis, subjects taking AREDS vitamins presented an increase of 5.51 minutes in RIT as compared to those not taking them, holding age and AMD stage as constant). For the remaining variables (continuous) the β coefficient corresponds to the increase in RIT per unit of that variable (i.e., per year of increase in age, there is an increase in 4.00 minutes in RIT—univariate analysis). P values < 0.05 are highlighted as bold.

BCVA, best-corrected visual acuity (considered as a continuous variable in LogMAR); NSAIDs, nonsteroidal anti-inflammatory drugs; NA, nonapplicable; CI, confidence interval RIT, rod intercept time.

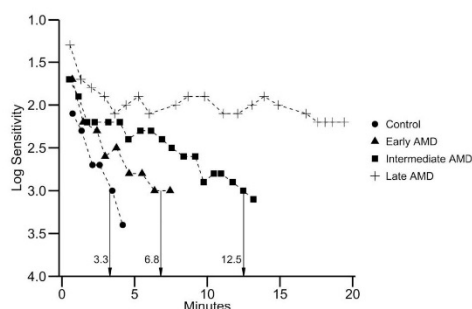


Fig. 1. Example of dark adaptation data of four study participants: a control, subjects with early AMD, intermediate AMD and late AMD. The y axis corresponds to sensitivity (log units) and x axis corresponds to the rod intercept time (RIT) in minutes. The patient with late AMD was not able to reach RIT within the 20 minutes of testing.

(Table 3). The same was observed for a higher consumption of alcohol per day ($P = 0.023$); alcohol intake was assessed as a continuous variable.

Controlling for AMD stage ($\beta = 0.74$, $P = 0.037$) and age ($\beta = 0.10$, $P = 0.037$), taking AREDS vitamins ($\beta = 1.67$, $P = 0.021$) was statistically significantly associated with an abnormal RIT. The odds of having an abnormal RIT was 5.29 higher for subjects taking AREDS vitamins than for those who were not taking them, when holding age and AMD stage as a fixed value. Controlling for the same covariates (AMD stage and age), similar results were observed for having a family history of AMD

($\beta = 1.84$, $P = 0.006$); subjects with direct relatives with a diagnosis of this disease presented a 6.32 increased odds of having an abnormal time to dark-adapt. The same was verified for higher alcohol intake per day ($\beta = 0.07$, $P = 0.017$), also controlling for age and AMD stage. For the last model, considering the potential differences in alcohol intake among men and women, sex was also considered as a covariate, but it was not significant and did not change any parameters in the model.

Univariate and Multivariate Analyses—Inability to Reach RIT (>20 Minutes)

Around 24% ($n = 19$) of our study group was not able to reach the RIT within the 20 minutes of testing; covariates that could potentially be related to this were explored. Similar to what was observed in our previous analysis, AMD stage ($\beta = 1.45$, $P = 0.001$), age ($\beta = 0.10$, $P = 0.022$), taking AREDS vitamins ($\beta = 3.63$, $P = 0.001$), having direct relatives with AMD ($\beta = 1.10$, $P = 0.047$), and being pseudophakic ($\beta = 1.64$, $P = 0.011$) were statistically significantly associated with a RIT > 20 minutes on the univariate assessments. The multivariate analysis revealed that after controlling for age and AMD stage, only taking AREDS vitamins remained statistically significant ($\beta = 4.22$, odds ratio = 68.3, $P = 0.006$).

Subanalysis of Patients With Intermediate AMD

To understand the intriguing results indicating higher RITs in subjects taking AREDS vitamins, we

Table 3. Univariate and Multivariate Logistic Regression Analysis Considering Abnormal RIT as the Outcome

Variable	Univariate Analysis			Multivariate Analysis (Controlling for Age and AMD Stage)		
	β Coefficient	95% CI	P	β Coefficient	95% CI	P
Age	0.11	0.03 to 0.19	0.008	NA	NA	NA
AMD stage (reference term controls)	1.32	-0.003 to 0.18	<0.001	NA	NA	NA
BCVA	4.13	0.19 to 8.07	0.004	2.21	-2.10 to 6.53	0.315
Pseudophakic (reference term phakic)	1.49	-0.10 to 3.07	0.066	0.503	-1.43 to 2.44	0.610
Alcohol consumption	0.05	0.007 to 0.97	0.023	0.07	0.01 to 0.13	0.017
Hypertension*	0.66	-0.37 to 1.70	0.207	0.51	-0.76 to 1.77	0.432
Stroke*	1.48	-0.69 to 3.65	0.181	2.23	-0.38 to 4.83	0.094
Autoimmune diseases*	0.93	-0.46 to 2.31	0.189	0.62	-0.95 to 2.20	0.439
AREDS vitamins*	2.41	1.27 to 3.54	<0.001	1.66	0.25 to 3.08	0.021
Other multivitamins*	1.94	0.55 to 3.33	0.006	0.84	-0.85 to 2.52	0.330
Aspirin*	0.65	-0.29 to 1.60	0.176	0.04	-1.12 to 1.21	0.943
Other NSAIDs*	-1.18	-2.95 to 0.58	0.189	-1.03	-3.20 to 1.13	0.350
Relatives with AMD*	2.07	0.94 to 3.21	<0.001	1.84	0.52 to 3.17	0.006
Physically active*	0.67	-0.25 to 1.59	0.153	0.34	-0.78 to 1.46	0.553

Only parameters with P values ≤ 0.250 are shown.

Logistic regression analyses considering abnormal RIT (≥ 6.5 minutes) compared with normal RIT (< 6.5 minutes, reference term) as the outcome. For categorical variables ("*"), β coefficients represent the difference in the log of having abnormal dark adaptation in subjects that have that parameter present (vs. those who do not have). The same applies for the continuous variables, per unit of change (e.g., per year of increase in age). P values < 0.05 are highlighted as bold.

BCVA, best-corrected visual acuity (considered as a continuous variable in LogMAR); NSAIDs, nonsteroidal anti-inflammatory drugs; NA, nonapplicable; RIT, rod intercept time; CI, confidence interval.

further analyzed our patients with intermediate AMD. This analysis was performed as the intermediate stage of AMD has a wide spectrum of drusen, it represents the largest group in our study, and subjects with intermediate AMD are recommended the AREDS vitamins. Of the 34 participants with intermediate AMD, 7 did not report taking AREDS vitamins. Their mean RIT was 8.5 ± 4.2 minutes; those who reported taking AREDS medication had a mean RIT of 15.8 ± 5.4 minutes.

Two experienced graders (I.L., R.M.) independently reviewed the color fundus photographs of these subjects (IMAGeNet 2000) and evaluated the presence of drusen larger than C2, which was predefined by the investigators as an arbitrary proxy for more severe intermediate AMD. Among subjects who were on AREDS vitamins, 88.9% ($n = 24$) had C2 drusen visible on color photographs, and their mean number within the Early Treatment Diabetic Retinopathy Study grid was 24.8 (range 0–103). Conversely, of the 7 subjects not taking AREDS vitamins, only 42.9% ($n = 3$) presented drusen larger than C2, with a mean number of 6.7 (range 0–32) C2 drusen within the grid. This indicates that patients taking AREDS vitamins had a higher number of large drusen.

Discussion

We present a cross-sectional assessment of the influence of several medical conditions and established AMD risk factors on time to dark-adapt in a cohort of patients with AMD with early, intermediate, and late disease, as well as a control group without any retinal pathology. A valid, reliable, and clinically available DA protocol was used. Our results support previous research showing that a prolonged RIT is highly associated with increased age^{11,17,18} and AMD stage.^{10,17,19} After accounting for these two covariates, our study showed that having a higher BMI and presenting a family history of AMD were also significantly associated with a prolonged time to dark-adapt. Similar results were observed when abnormal DA (≥ 6.5 minutes) was considered as the outcome. Even after controlling for age and AMD stage, a higher daily alcohol intake was also significantly associated with increased odds of presenting abnormal DA. Surprisingly, statistically significant associations between taking AREDS vitamins and worse DA were also observed, even after controlling for confounding factors.

The definitive biological explanation for the strong association between impaired DA with age and more advanced AMD stage remains to be established.

However, one possibility may be related to the diffusion barriers that develop due to Bruch membrane thickening²⁰ and drusen formation.¹⁷ This impairs transport to photoreceptors, of substances such as oxygen and vitamin A. Increased drusen height has been shown to be related to photoreceptor hypoxia and subsequent retinal degeneration (personal communication, “A Patient-Specific Model of Retinal Oxygenation in Age-Related Macular Degeneration,” Leo Kim et al, ASRS 2014). Vitamin A deficiency can also cause dysfunction and photoreceptor death, as well as slowing in the regeneration rate of rhodopsin.^{9,18,21} The normal recycling process for rhodopsin requires that a sufficient quantity of 11-cis-retinal (a metabolite of vitamin A) is available to the photoreceptors’ outer segments. Otherwise, rhodopsin regeneration is slowed.¹⁸ While cones have alternative sources through the retinal vasculature, rods primarily depend on vitamin A from the RPE/Bruch membrane complex.²² Owsley et al²³ showed that the rate of rod-mediated DA in older adults with normal retinal health or AMD improved after a 30-day course of high-dose retinol, whereas cone-mediated DA parameters remained unaffected. Unlike other groups,^{2,10} we did not observe a statistical significant difference in RIT between subjects with early AMD and controls. Although this was not the goal of our study, the difference in the results might be linked to our relatively small sample size (19 control subjects and 14 early patients with AMD).

We also found an association between a higher alcohol intake per day and abnormal DA. The first report about a potential association between DA and alcohol dates back to the 1950s.²⁴ Since then, controversial findings were described both for acute²⁵ and chronic^{26,27} alcohol consumption.²⁸ The rationale for a potential effect of alcohol on DA is based on the fact that ethanol might be a competitive inhibitor with retinol (vitamin A) in the retina.^{24,29} Retinol dehydrogenases (RDHs) are the oxidoreductase enzymes that convert retinol to retinal, which is the chromophore of the photoreceptors. Many RDHs have been identified, including class IV alcohol dehydrogenases (ADH4). RDH12 is the primary enzyme that reduces all-*trans* retinal (released from bleached photopigments) to retinol during the visual cycle recovery phase, and it is part of the superfamily of alcohol dehydrogenases and reductases.^{30,31} In addition, it has been suggested that alcohol consumption might result in retinal thinning³² and that this may also be linked with impairments in rod recovery.³³ Interestingly, when we repeated the statistical analyses only with subjects with AMD (i.e., not including subjects with normal macular health on color fundus photographs),

all the reported results were reproducible, except for the association between higher alcohol intake and abnormal DA (data not shown). This might be due to a reduced power when decreasing the number of subjects in the analysis or due to a true lack of association between alcohol consumption and DA in the specific context of an AMD-only analysis. A previous study¹¹ only including subjects with normal macular health also verified that those who reported consuming more than 14 drinks per week were more likely to display abnormal DA. Despite the limitations of our study, including the lack of data on the time since last alcohol intake prior to DA testing, we used a well-validated questionnaire and our findings support that alcohol use by itself might affect DA and is valuable because it is potentially modifiable.

Our results showing an association between higher BMI and impaired DA are challenging to explain. To our knowledge, no previous clinical studies have reported similar findings. Obesity is associated with problems in lipid metabolism and considered a chronic inflammatory condition.³⁴ Importantly, it is currently recognized that there is an association between inflammatory conditions and impaired nutritional status of vitamin A, inflammation seems to lead to an increased need for vitamin A, which leads to the depletion of its stores.³⁵ Vitamin A is a fat-soluble vitamin. Besides the liver, which is its main reserve, the adipose tissue also contains substantial amounts of retinol and the adipocytes seem not only to store but also to metabolize and mobilize their retinol stores to meet body demands.³⁶ Indeed, Trasino et al³⁷ showed that obesity reduces vitamin A levels and signaling in multiple major organs. Studies in children also reported that reduced levels of vitamin A can be linked with an increased risk of class III obesity.³⁵ The current evidence suggests that this might actually represent a vicious cycle: the highest BMI, the lowest vitamin A levels, which then contribute further to obesity.

The observed association between the intake of vitamins with AREDS composition and worst DA outcomes (RIT as a continuous outcome, normal versus abnormal RIT, and inability to reach the RIT within the 20 minutes time of testing) is difficult to interpret. We believe that this is most likely a statistical finding because of our relatively small sample size and not a real association. As described, further analysis of the patients with intermediate AMD showed that those who were on AREDS supplements had more drusen that were larger in size (C2 or greater) compared with those who were not on AREDS supplements, likely contributing to their worse DA outcomes, even after accounting for AMD stage and other covariates. We also speculate that a retina physician may be more

likely to strongly encourage AREDS vitamins with greater drusen burden, even within the intermediate AMD subgroup. One limitation of our assessment of medication and supplements is that the data were self-reported, although confirmed through the medical record. It is possible that there may be a differential effect on DA between supplementation with vitamin A (original AREDS) versus lutein/zeaxanthin (AREDS2),³⁸ which we were not able to evaluate. In addition, because our cohort was not genotyped, we also could not detect any potential interaction between genetic background, AREDS³⁹ supplementation, and DA. Further research in this field is necessary to investigate our observations. Indeed, the observed positive association between a family history of AMD and abnormalities in DA might also point to a potential influence of genetic risk factors on this functional outcome. Previous studies suggest¹² that family history and genetic testing incorporate overlapping information and are partly complementary for determining familial risk.

Of note, in our study, some of the associations found in univariate assessments did not hold when accounting for confounding factors (such as age and AMD stage). This was observed, for example, for BCVA. Flamendorf et al¹⁷ described that worst BCVA values were associated with an increasing RIT in eyes without any large drusen or advanced AMD, but the authors did not perform multivariate assessments. We also did not observe an association between pseudophakic status and prolonged DA after accounting for confounding factors. This is in agreement with the previous literature⁴⁰ that also suggested that this relationship was only present on univariate assessments and was not observed after accounting for age.

Limitations and Future Directions

This study has a relatively small sample size and subjects were recruited from a tertiary care hospital, which might affect the observed results. Despite the limitation of our sample size, to our knowledge, this is the first time that a comprehensive analysis of the influence of several clinical parameters and risk factors on DA has been evaluated for AMD. Importantly, the questionnaire used to assess demographics and medical history was not validated. In addition, all data were collected through self-reported questionnaires; thus, response bias needs to be considered. This might have particularly affected answers related to well-established risk factors for AMD (such as smoking, physical activity, and medication with AREDS or other multivitamins), because patients might be aware of how they can impact their disease; and to BMI.⁴¹ Despite being currently the best accepted

anthropometric measure, BMI has relevant limitations as an assessment of obesity, and its correlation with body fat is nonlinear.⁴²

An important percentage of our study subjects (24%, n = 19 eyes) were not able to reach RIT within the testing time. According to the previous literature,¹⁷ for these cases, we assumed the value of 20 for statistical assessments. This assumption likely highly underestimates the real-time to dark-adapt of these eyes and might have affected our results. In the future, studies including subjects with intermediate or late AMD should ideally refine the current available protocol.

Other important limitations of this study relate to its cross-sectional design. Despite the assessment with multivariate analyses and accounting for confounding factors, data from prospective studies are needed to definitively establish how different clinical parameters affect DA. In addition, we did not evaluate how other relevant factors for AMD natural history, namely dietary patterns and genetic profiles, might affect DA. There is also absence of data such as vitamin A serum levels. For the subanalysis of patients with intermediate AMD, we established an arbitrary proxy for more severe disease (presence of drusen larger than C2). Future work should assess the impact of more refined anatomical details (such as drusen parameters and other retinal abnormalities) on time to dark-adapt, as some correlation with DA has been suggested.^{17,43}

Conclusions

In addition to age and AMD stage, other health parameters seem to affect DA, including a higher BMI, higher alcohol intake, and possibly taking AREDS supplements. Family history of AMD also seem to play a role, but the influence of genetic profiles, as well as of dietary patterns, remains to be established. There is increasing evidence that DA is a valuable functional outcome for AMD. Therefore, it is crucial to understand what risk factors affect it and how these might influence its interpretation.

Key words: age-related macular degeneration, dark adaptation, medical history.

Acknowledgments

The authors thank Gregory Jackson, PhD (MacuLogix, Middletown, PA) for his critical review of this paper.

References

1. Wong WL, Su X, Li X, et al. Global prevalence of age-related macular degeneration and disease burden projection for 2020 and 2040: a systematic review and meta-analysis. *Lancet Glob Health* 2014;2:e106–e116.
2. Owsley C, Huisingh C, Clark ME, et al. Comparison of visual function in older eyes in the earliest stages of age-related macular degeneration to those in normal macular health. *Curr Eye Res* 2016;41:266–272.
3. Haymes SA, Roberts KF, Cruess AF, et al. The letter contrast sensitivity test: clinical evaluation of a new design. *Invest Ophthalmol Vis Sci* 2006;47:2739–2745.
4. Hogg RE, Chakravarthy U. Visual function and dysfunction in early and late age-related maculopathy. *Prog Retin Eye Res* 2006;25:249–276.
5. Vujosevic S, Smolek MK, Lebow KA, et al. Detection of macular function changes in early (AREDS 2) and intermediate (AREDS 3) age-related macular degeneration. *Ophthalmologica* 2011;225:155–160.
6. Mangione CM, Gutierrez PR, Lowe G, et al. Influence of age-related maculopathy on visual functioning and health-related quality of life. *Am J Ophthalmol* 1999;128:45–53.
7. Owsley C, McGwin G, Scilley K, Kallies K. Development of a questionnaire to assess vision problems under low luminance in age-related maculopathy. *Invest Ophthalmol Vis Sci* 2006;47:528–535.
8. Curcio CA, Medeiros NE, Millican CL. Photoreceptor loss in age-related macular degeneration. *Invest Ophthalmol Vis Sci* 1996;37:1236–1249.
9. Curcio CA. Photoreceptor topography in ageing and age-related maculopathy. *Eye (Lond)* 2001;15:376–383.
10. Jackson GR, Scott IU, Kim IK, et al. Diagnostic sensitivity and specificity of dark adaptometry for detection of age-related macular degeneration. *Invest Ophthalmol Vis Sci* 2014;55:1427–1431.
11. Owsley C, Huisingh C, Jackson GR, et al. Associations between abnormal rod-mediated dark adaptation and health and functioning in older adults with normal macular health. *Invest Ophthalmol Vis Sci* 2014;55:4776–4789.
12. Gorin MB, Weeks DE, Baron RV, et al. Endophenotypes for age-related macular degeneration: extending our reach into the preclinical stages of disease. *J Clin Med* 2014;3:1335–1356.
13. Willett WC, Sampson L, Stampfer MJ, et al. Reproducibility and validity of a semiquantitative food frequency questionnaire. *Am J Epidemiol* 1985;122:51–65.
14. Topolski TD, LoGerfo J, Patrick DL, et al. The Rapid assessment of physical activity (RAPA) among older adults. *Prev Chronic Dis* 2006;3:A118.
15. Age-Related Eye Disease Study Research Group. The age-related eye disease study system for classifying age-related macular degeneration from stereoscopic color fundus photographs: the age-related eye disease study report number 6. *Am J Ophthalmol* 2001;132:668–681.
16. Danis RP, Domalpally A, Chew EY, et al. Methods and reproducibility of grading optimized digital color fundus photographs in the Age-Related Eye Disease Study 2 (AREDS2 Report Number 2). *Invest Ophthalmol Vis Sci* 2013;54:4548–4554.
17. Flamendorf J, Agrón E, Wong WT, et al. Impairments in dark adaptation are associated with age-related macular degeneration severity and reticular pseudodrusen. *Ophthalmology* 2015;122:2053–2062.
18. Jackson GR, Owsley C, McGwin G. Aging and dark adaptation. *Vision Res* 1999;39:3975–3982.
19. Jackson GR, Clark ME, Scott IU, et al. Twelve-month natural history of dark adaptation in patients with AMD. *Optom Vis Sci* 2014;91:925–931.
20. Curcio CA, Johnson M, Rudolf M, Huang J-D. The oil spill in ageing Bruch membrane. *Br J Ophthalmol* 2011;95:1638–1645.

21. Lamb TD, Pugh EN. Dark adaptation and the retinoid cycle of vision. *Prog Retin Eye Res* 2004;23:307–380.
22. Garlipp MA, Gonzalez-Fernandez F. Cone outer segment and Müller microvilli pericellular matrices provide binding domains for interphotoreceptor retinoid-binding protein (IRBP). *Exp Eye Res* 2013;113:192–202.
23. Owsley C, McGwin G, Jackson GR, et al. Effect of short-term, high-dose retinol on dark adaptation in aging and early age-related maculopathy. *Invest Ophthalmol Vis Sci* 2006;47:1310–1318.
24. Blomberg LH, Wassen A. Preliminary report on the effect of alcohol on dark adaptation, determined by an objective method. *Acta Ophthalmol* 1959;37:274–278.
25. Adams AJ, Brown B. Alcohol prolongs time course of glare recovery. *Nature* 1975;257:481–483.
26. Khan SA, Timney B. Alcohol does not affect dark adaptation or luminance increment thresholds. *J Stud Alcohol Drugs* 2007;68:493–502.
27. Campbell TD, Sampliner RE, Russell RM, Garrett MS. Night driving (mesopic) visual acuity in sober male alcoholics with and without liver disease. *Alcohol Clin Exp Res* 1981;5:34–37.
28. Russell RM, Morrison SA, Smith FR, et al. Vitamin-A reversal of abnormal dark adaptation in cirrhosis. Study of effects on the plasma retinol transport system. *Ann Intern Med* 1978;88:622–626.
29. Russell RM. Vitamin A and zinc metabolism in alcoholism. *Am J Clin Nutr* 1980;33:2741–2749.
30. Thompson DA, Janecke AR, Lange J, et al. Retinal degeneration associated with RDH12 mutations results from decreased 11-cis retinal synthesis due to disruption of the visual cycle. *Hum Mol Genet* 2005;14:3865–3875.
31. Maeda A, Maeda T, Imanishi Y, et al. Role of photoreceptor-specific retinol dehydrogenase in the retinoid cycle in vivo. *J Biol Chem* 2005;280:18822–18832.
32. Myers CE, Klein BEK, Meuer SM, et al. Retinal thickness measured by spectral-domain optical coherence tomography in eyes without retinal abnormalities: the Beaver Dam Eye Study. *Am J Ophthalmol* 2015;159:445–456.e1.
33. Bavinger JC, Dunbar GE, Stem MS, et al. The effects of diabetic retinopathy and pan-retinal photocoagulation on photoreceptor cell function as assessed by dark adaptometry. *Invest Ophthalmol Vis Sci* 2016;57:208–217.
34. Andersen CJ, Murphy KE, Fernandez ML. Impact of obesity and metabolic syndrome on immunity. *Adv Nutr* 2016;7:66–75.
35. Pereira SE, Saboya CJ, Saunders C, Ramalho A. Serum levels and liver store of retinol and their association with night blindness in individuals with class III obesity. *Obes Surg* 2012;22:602–608.
36. Jeyakumar SM, Vajreswari A. Vitamin A as a key regulator of obesity & its associated disorders: evidences from an obese rat model. *Indian J Med Res* 2015;141:275–284.
37. Trasino SE, Tang XH, Jessurun J, et al. Obesity leads to tissue, but not serum vitamin A deficiency. *Sci Rep* 2015;5:15893.
38. AREDS2 Research Group, Chew EY, Clemons T, SanGiovanni JP, et al. The Age-Related Eye Disease Study 2 (AREDS2): study design and baseline characteristics (AREDS2 report number 1). *Ophthalmology* 2012;119:2282–2289.
39. Seddon JM, Silver RE, Rosner B. Response to AREDS supplements according to genetic factors: survival analysis approach using the eye as the unit of analysis. *Br J Ophthalmol* 2016;100:1731–1737.
40. Owsley C, McGwin G, Clark ME, et al. Delayed rod-mediated dark adaptation is a functional biomarker for incident early age-related macular degeneration. *Ophthalmology* 2016;123:344–351.
41. Vuksanović M, Safer A, Palm F, et al. Validity of self-reported BMI in older adults and an adjustment model. *J Public Health (Bangkok)* 2014;22:257–263.
42. Rothman KJ. BMI-related errors in the measurement of obesity. *Int J Obes (Lond)* 2008;32:S56–S59.
43. Sevilla MB, McGwin G, Lad EM, et al. Relating retinal morphology and function in aging and early to intermediate age-related macular degeneration subjects. *Am J Ophthalmol* 2016;165:65–77.

Chapter IV – Discussion and Future Directions

In any study design, one of the most important features is the classification of the phenotype. Otherwise, a classification bias is introduced and dramatically can affect the assessment of any outcomes of interest.¹⁰¹ Indeed, if one thinks that, by definition, metabolomics represents the interaction between the genetic transcription process and environmental exposures, and therefore it is the closest representation to the phenotype,¹⁰² it becomes even more evident how it is crucial to properly assess it.

To follow the current validated AMD classification systems, we assessed CFP. We observed that the images obtained presented a wide-range of brightness and contrast, even those taken with the same camera in the same study location. It is well-recognized in the literature that suboptimal images can impede the diagnosis or correct staging of AMD,¹⁰³ however we verified that all the available strategies to standardize CFP relied on manual procedures that need to be individually performed for each image.^{74,104} This is extremely time-consuming and introduces some extent of variation. Therefore, we developed a software to automatically standardized CFP to conform to a color model optimized for AMD grading, and that proved to improve the rate of gradable images.¹⁰⁵ All CFP were processed with this software before the grading that was then used in our remaining analysis.

Indeed, our work on the application of metabolomics to the study of AMD has relied so far on phenotype classifications based on CFP. Using NMR metabolomics, we observed, for the first time, small differences in the plasma levels of some circulating metabolites (some amino acids and organic acids, dimethyl sulfone, lipid and protein moieties) between multiple AMD stages, in both study cohorts (Coimbra and Boston).¹⁰⁶ Interestingly, the metabolomic fingerprints of AMD suggested for the two cohorts presented both similarities and differences. The observed similarities suggest that such variations may be a universal reflection of the disease. On the other hand, cohort differences may reflect the potential importance of local diet and lifestyle effects on the suggested AMD metabolic fingerprints. We also observed a number of small metabolite variations potentially differentiating controls from early AMD. This is particularly relevant as these might represent specific signals to distinguish disease from non-disease status. This study was the first assessment of AMD using NMR metabolomics, and the first time that the different stages of the disease (early, intermediate and late) were characterized.

These results supported our hypothesis that metabolomics could identify fingerprints of AMD and its severity stages, so we decided to pursue our work by performing MS metabolomics. As mentioned, MS metabolomics has a higher sensitivity and, particularly ultra-high-performance liquid chromatography (UPLC), is becoming increasingly popular and it is probably the most widely used technology nowadays to perform metabolomics in health

sciences.¹⁰² This is primarily due to the ability of LC to separate and detect a wide range of metabolites,^{107,18} and also to the large number of accessible instruments and open-source data processing software available for this technique.¹⁰⁷ Using UPLC-MS to characterize the plasma metabolomic profile of AMD patients as compared to controls, and the different severity stages, we observed that most changes were related to lipid metabolites, and in particular, there was a significant dysregulation of the glycerophospholipids pathway. Glycerophospholipids are a major component of cell membranes and are especially enriched in neural membranes. Among other functions, they provide structural stability and membrane fluidity. They also participate in the formation of ion channels and receptors, generation of second messengers in signal transduction, and in regulating neurotransmitter release.^{108,109} Our findings of reduced key glycerophospholipids metabolites lowered in subjects with AMD suggest that an impaired cell membrane structure and function may be an important component of AMD pathogenesis. We also observed significant changes in some amino acids, in particular altered levels of alanine were observed in both our study cohorts. Alanine is a non-essential amino acid involved in central nervous system and retina glycolytic processes,¹¹⁰ thus suggesting that in AMD energy production pathways may also be affected. Interestingly, polymorphisms associated with alanine have also been linked to AMD.¹¹¹

These findings raise multiple important questions that we aim to pursue with our future research. First of all, considering that OCT provides a near-histologic detail of retinal structure, and that some of the most important AMD features, such as classic drusen and subretinal drusenoid deposits, have lipids as a central component,^{112,113} it is crucial to analyze if plasma metabolomic profiles vary with AMD structural abnormalities. For example, do patients with classic drusen have a different metabolomic profile as compared to those who have subretinal drusenoid deposits? Is drusen volume associated with changes in plasma metabolome? Choroidal parameters (such as thickness and density) seem to be an important component of dry AMD expression,⁴⁹ do they also have any association with changes in plasma metabolomic profiles? We aim to address these questions in our future work, namely by using the complete phenotypic characterization that we have been performing.

Additionally, the photoreceptors and the RPE are rich in phospholipids, and these are important for the transduction of visual stimuli.^{114,115} Therefore, our goal is also to move from structure-function association studies, to integrative analysis to understand how both (structure and function) are associated with the metabolomic signals of AMD. For example, based on our results, the presence of macular subretinal drusenoid deposits and ellipsoid zone changes (i.e. a marker of photoreceptors damage) is associated with impaired dark adaptation. It will be interesting to analyze how these parameters have or not a characteristic metabolomic feature, which can eventually provide new insights on the visual impairments observed in patients with AMD. Our work on functional assessments in AMD has been so far

primarily focused on DA. However, we also have work in progress in microperimetry, which we aim to analyze in a similar fashion.

As described, our results with MS metabolomics are still limited to a Boston cohort of 120 subjects. However, we have already data available for our entire study population, which we are currently analyzing. These data were recently accepted as an abstract for the ARVO 2018 Annual Meeting (Supplement 7). The results of our two independent cohorts, confirm that AMD patients presented a distinct plasma MS metabolomic profile as compared to subjects with a normal macula. Some of the identified metabolites are common to both cohorts, thus further supporting the development of plasma-based metabolomics biomarkers of AMD. The use of independent cohorts is the most powerful strategy to validate biomarkers' discover.¹¹⁶ Following this, targeted metabolomics and studies to assess the biological mechanisms are also recommended, which we are already planning. Namely, we aim to study how the observed findings in the circulating plasma mirror AMD changes in the eye. Therefore, we are planning to perform tissue metabolomics and mass spectroscopy imaging on donor eyes with AMD and controls, and analyze its association with plasma metabolites in the same donor.

Of note, in this study, we also collected urine samples from all study participants. These samples have been analyzed with NMR metabolomics, and we are currently in the process of manuscript preparation. While most work applying metabolomics to derive biofluid biomarkers has relied on blood samples,^{18,117–120} urine has been increasingly employed due to its non-invasiveness.¹²¹ Compared to blood, urine composition is not regulated by homeostatic mechanisms, and greater varieties of endogenous metabolites can occur.¹²² Although this adds an additional challenge, it also means that urine may better reflect changes in human metabolism, and thus better mirror diseases states. If this is observed in our study cohort, we will certainly also aim to pursue our work in urine metabolomics of AMD. This includes an attempt to integrate the metabolomic signatures between tissue, plasma and urine. An organism's biochemical pool comprises complex transboundary relationships, which can only be understood by investigating metabolic interactions and physiological processes spanning multiple parts of the human body.⁹

Additionally, as described, we also performed genetic profiling of our study population, by using an Illumina HumanOmniExpress-24 BeadChip, which allows the study of more than >715,000 single nucleotide polymorphisms (SNPs). We are analyzing these data, as well as the data collected with the lifestyle questionnaires, in the collaboration with the Harvard School of Public Health and the Channing Division of Network Medicine of the Brigham and Women Hospital. Currently, we are performing quality control procedures, but we will initiate our statistical assessments in the very near future. We will follow two complementary approaches to explore metabolomic-genomic associations in AMD: 1) looking at SNPs with

well-established relations to AMD, and 2) following a GWAS approach. Moreover, we will build AMD risk scores including metabolomics data, in addition to genetic and environmental profiling. Despite the current lack of treatments for early AMD, the benefits of risk score models are clear: targeting modifiable risk factors¹²³ and more careful follow-up in high-risk individuals; assisting differential diagnosis of AMD and its subtypes; improving homogeneity of study populations in clinical trials; and ultimately selecting appropriate therapies.^{124,9}

Finally, even though our results point to the identification of plasma metabolomic signatures of early, intermediate and late AMD, so far, we have not studied AMD progression *per se*. For now, we only obtained a single snapshot of the metabolome for the study participants. For the Portuguese cohort, we have phenotypic data (i.e. classification based on CFP from five years before inclusion in this study), which we are analyzing to obtain pilot results on eventual metabolomic signals of AMD progression. Additionally, we are now initiating a longitudinal study to assess the evolution of the metabolome with the progression of AMD. Our hypothesis is that we will identify signatures that can represent potential biomarkers of subjects at increased risk for AMD progression.

In conclusion, we believe that our collaborative project has already made considerable impact on the assessment and understanding of AMD, and it is laying the path to several investigations that have the potential to further consolidate our work and revolutionize this field.

For the first time, we performed a comprehensive overview of AMD metabolomics, and described that plasma metabolomic profiling is a powerful tool to identify biomarkers of AMD. Indeed, by exploring the advantages of studying two distinct cohorts, our results are pointing to the existence of metabolomic signatures specific to AMD and to its severity stages. These have the great potential, with further research, of being translated to the development of reliable and accessible AMD biomarkers. This will fulfill a great unmet need all over the world. Our findings also contribute to the current knowledge on AMD pathophysiology, namely by pointing to the relevance of lipids and amino acids, and the need for further research on their role in AMD. The identification of metabolomic signs that are distinct in two geographic locations also has the potential to further contribute to the understanding of gene-environmental interactions on the development and progression of AMD, especially if integrated with genomic and lifestyle profiling, which we are now pursuing. These integrative analyses will introduce a paradigm shift, and the outcomes will be further expanded by systematic structural and functional characterization of AMD phenotypes. Indeed, we have also been performing pioneering work in the study of structural-functional associations on AMD, which are crucial to identify biomarkers able to mirror both anatomical changes and visual function.

This project is laying the path and is the basis of several investigations in the field of biofluid and tissue metabolomics, pathogenesis of AMD, and identification of novel targets for AMD treatment. We believe that our work is going to offer novel tools, applicable to clinical practice, for early diagnosis and screening, and for providing prognostic information. This work will also aid in better understanding AMD mechanisms, and may lead to identifying druggable targets for the treatment of this condition. This has the potential to lead us to an era of precision medicine in AMD, and can lead to novel interventions based on preventive strategies to reduce progression to blindness stages and ultimately to reduce the burden of AMD.

We are looking forward to continuing our work on this project, and to keep opening novel avenues for the assessment and study of age-related macular degeneration.

References

1. Wong WL, Su X, Li X, et al. Global prevalence of age-related macular degeneration and disease burden projection for 2020 and 2040: a systematic review and meta-analysis. *Lancet Glob Heal*. 2014;2(2):e106-16. doi:10.1016/S2214-109X(13)70145-1.
2. Handa JT. How does the macula protect itself from oxidative stress? *Mol Aspects Med*. 2012;33(4):418-435.
3. Sobrin L, Seddon JM. Nature and nurture- genes and environment- predict onset and progression of macular degeneration. *Prog Retin Eye Res*. December 2013. doi:10.1016/j.preteyeres.2013.12.004.
4. Yonekawa Y, Miller JW, Kim IK. Age-Related Macular Degeneration: Advances in Management and Diagnosis. *J Clin Med*. 2015;4(2):343-359.
5. Cachulo L, Silva R, Fonseca P, et al. Early markers of choroidal neovascularization in the fellow eye of patients with unilateral exudative age-related macular degeneration. *Ophthalmologica*. 2011;225(3):144-149.
6. Swaroop A, Chew EY, Rickman CB, Abecasis GR. Unraveling a multifactorial late-onset disease: from genetic susceptibility to disease mechanisms for age-related macular degeneration. *Annu Rev Genomics Hum Genet*. 2009;10:19-43.
7. Ratnapriya R, Chew EY. Age-related macular degeneration-clinical review and genetics update. *Clin Genet*. 2013;84(2):160-166.
8. Fritsche LG, Igl W, Bailey JNC, et al. A large genome-wide association study of age-related macular degeneration highlights contributions of rare and common variants. *Nat Genet*. 2016;48(2):134-143. doi:10.1038/ng.3448.
9. Seddon JM. Macular Degeneration Epidemiology: Nature-Nurture, Lifestyle Factors, Genetic Risk, and Gene-Environment Interactions – The Weisenfeld Award Lecture. *Investig Ophthalmology Vis Sci*. 2017;58(14):6513. doi:10.1167/iovs.17-23544.
10. Mitta VP, Christen WG, Glynn RJ, et al. C-reactive protein and the incidence of macular degeneration: pooled analysis of 5 cohorts. *JAMA Ophthalmol*. 2013;131(4):507-513.
11. Hong T, Tan AG, Mitchell P, Wang JJ. A review and meta-analysis of the association between C-reactive protein and age-related macular degeneration. *Surv Ophthalmol*. 56(3):184-194.
12. Klein R, Myers CE, Cruickshanks KJ, et al. Markers of inflammation, oxidative stress, and endothelial dysfunction and the 20-year cumulative incidence of early age-related macular degeneration: the Beaver Dam Eye Study. *JAMA Ophthalmol*. 2014;132(4):446-455. doi:10.1001/jamaophthalmol.2013.7671.
13. Uğurlu N, Aşık MD, Yülek F, Neselioglu S, Cagil N. Oxidative stress and anti-oxidative

- defence in patients with age-related macular degeneration. *Curr Eye Res.* 2013;38(4):497-502.
14. Chakravarthy U, Wong TY, Fletcher A, et al. Clinical risk factors for age-related macular degeneration: a systematic review and meta-analysis. *BMC Ophthalmol.* 2010;10:31.
 15. Klein R, Myers CE, Buitendijk GHS, et al. Lipids, Lipid Genes, and Incident Age-Related Macular Degeneration: The Three Continent Age-Related Macular Degeneration Consortium. *Am J Ophthalmol.* 2014;158(3):513-524.e3. doi:10.1016/j.ajo.2014.05.027.
 16. Fiehn O. Metabolomics--the link between genotypes and phenotypes. *Plant Mol Biol.* 2002;48(1-2):155-171.
 17. Fritsche LG, Igl W, Bailey JNC, et al. A large genome-wide association study of age-related macular degeneration highlights contributions of rare and common variants. *Nat Genet.* 2016;48(2):134-143. doi:10.1038/ng.3448.
 18. Nicholson JK, Holmes E, Kinross JM, Darzi AW, Takats Z, Lindon JC. Metabolic phenotyping in clinical and surgical environments. *Nature.* 2012;491(7424):384-392.
 19. Nicholson J.K., Lindon J.C. HE. "Metabonomics": understanding the metabolic responses of living systems to pathophysiological stimuli via multivariate statistical analysis of biological NMR spectroscopic data. *Xenobiotica.* 1999:1181-1189.
 20. Dessi A, Marincola FC, Fanos V. Metabolomics and the great obstetrical syndromes – GDM, PET, and IUGR. *Best Pract Res Clin Obstet Gynaecol.* 2015;29(2):156-164. doi:10.1016/j.bpobgyn.2014.04.023.
 21. Kelly RS, Virkud Y, Giorgio R, Celedón JC, Weiss ST, Lasky-Su J. Metabolomic profiling of lung function in Costa-Rican children with asthma. *Biochim Biophys Acta - Mol Basis Dis.* February 2017. doi:10.1016/j.bbadis.2017.02.006.
 22. Wishart DS. Emerging applications of metabolomics in drug discovery and precision medicine. *Nat Rev Drug Discov.* 2016;15(7):473-484. doi:10.1038/nrd.2016.32.
 23. Lima AR, Bastos M de L, Carvalho M, Guedes de Pinho P. Biomarker Discovery in Human Prostate Cancer: an Update in Metabolomics Studies. *Transl Oncol.* 2016;9(4):357-370. doi:10.1016/j.tranon.2016.05.004.
 24. Kalita-de Croft P, Al-Ejeh F, McCart Reed AE, Saunus JM, Lakhani SR. 'Omics Approaches in Breast Cancer Research and Clinical Practice. *Adv Anat Pathol.* 2016;23(6):356-367. doi:10.1097/PAP.000000000000128.
 25. Mapstone M, Lin F, Nalls MA, et al. What success can teach us about failure: the plasma metabolome of older adults with superior memory and lessons for Alzheimer's disease. *Neurobiol Aging.* 2017;51:148-155. doi:10.1016/j.neurobiolaging.2016.11.007.

26. Whiley L, Sen A, Heaton J, et al. Evidence of altered phosphatidylcholine metabolism in Alzheimer's disease. *Neurobiol Aging*. 2014;35(2):271-278. doi:10.1016/j.neurobiolaging.2013.08.001.
27. Proitsi P, Kim M, Whiley L, et al. Association of blood lipids with Alzheimer's disease: A comprehensive lipidomics analysis. *Alzheimer's Dement*. 2017;13(2):140-151. doi:10.1016/j.jalz.2016.08.003.
28. Junot C, Fenaille F, Colsch B, Bécher F. High resolution mass spectrometry based techniques at the crossroads of metabolic pathways. *Mass Spectrom Rev*. 33(6):471-500. doi:10.1002/mas.21401.
29. Beckonert O, Keun HC, Ebbels TMD, et al. Metabolic profiling, metabolomic and metabonomic procedures for NMR spectroscopy of urine, plasma, serum and tissue extracts. *Nat Protoc*. 2007;2(11):2692-2703. doi:10.1038/nprot.2007.376.
30. Psychogios N, Hau DD, Peng J, et al. The human serum metabolome. *PLoS One*. 2011;6(2):e16957. doi:10.1371/journal.pone.0016957.
31. Osborn MP, Park Y, Parks MB, et al. Metabolome-wide association study of neovascular age-related macular degeneration. *PLoS One*. 2013;8(8):e72737.
32. Suhre K, Gieger C. Genetic variation in metabolic phenotypes: study designs and applications. *Nat Rev Genet*. 2012;13(11):759-769.
33. Wang JJ, Rochtchina E, Smith W, et al. Combined effects of complement factor H genotypes, fish consumption, and inflammatory markers on long-term risk for age-related macular degeneration in a cohort. *Am J Epidemiol*. 2009;169(5):633-641.
34. Adamski J, Suhre K. Metabolomics platforms for genome wide association studies--linking the genome to the metabolome. *Curr Opin Biotechnol*. 2013;24(1):39-47.
35. Adamski J. Genome-wide association studies with metabolomics. *Genome Med*. 2012;4(4):34.
36. Robinette SL, Holmes E, Nicholson JK, Dumas ME. Genetic determinants of metabolism in health and disease: from biochemical genetics to genome-wide associations. *Genome Med*. 2012;4(4):30.
37. Dharuri H, Demirkan A, van Klinken JB, et al. Genetics of the human metabolome, what is next? *Biochim Biophys Acta*. June 2014.
38. Gottesman II, Gould TD. The endophenotype concept in psychiatry: etymology and strategic intentions. *Am J Psychiatry*. 2003;160(4):636-645. doi:10.1176/appi.ajp.160.4.636.
39. Wojczynski MK, Tiwari HK. Definition of Phenotype. In: *Advances in Genetics*. Vol 60. ; 2008:75-105. doi:10.1016/S0065-2660(07)00404-X.
40. Manchia M, Cullis J, Turecki G, Rouleau GA, Uher R, Alda M. The impact of phenotypic and genetic heterogeneity on results of genome wide association studies

- of complex diseases. Reif A, ed. *PLoS One*. 2013;8(10):e76295.
doi:10.1371/journal.pone.0076295.
41. Age-Related Eye Disease Study Research Group. The Age-Related Eye Disease Study system for classifying age-related macular degeneration from stereoscopic color fundus photographs: the Age-Related Eye Disease Study Report Number 6. *Am J Ophthalmol*. 2001;132(5):668-681.
 42. AREDS2 Research Group, Chew EY, Clemons T, et al. The Age-Related Eye Disease Study 2 (AREDS2): study design and baseline characteristics (AREDS2 report number 1). *Ophthalmology*. 2012;119(11):2282-2289.
doi:10.1016/j.ophtha.2012.05.027.
 43. Miller JW, Bagheri S, Vavvas DG. Advances in Age-related Macular Degeneration Understanding and Therapy. *US Ophthalmic Rev*. 2017;10(2):119.
doi:10.17925/USOR.2017.10.02.119.
 44. Cohen SY, Dubois L, Tadayoni R, Delahaye-Mazza C, Debibie C, Quentel G. Prevalence of reticular pseudodrusen in age-related macular degeneration with newly diagnosed choroidal neovascularisation. *Br J Ophthalmol*. 2007;91(3):354-359.
doi:10.1136/bjo.2006.101022.
 45. Marsiglia M, Boddu S, Bearely S, et al. Association between geographic atrophy progression and reticular pseudodrusen in eyes with dry age-related macular degeneration. *Investig Ophthalmol Vis Sci*. 2013;54(12):7362-7369.
doi:10.1167/iovs.12-11073.
 46. Lewis H, Straatsma BR, Foos RY, Lightfoot DO. Reticular degeneration of the pigment epithelium. *Ophthalmology*. 1985;92(11):1485-1495.
 47. Kanski JJ. Peripheral retinal degenerations. *Trans Ophthalmol Soc U K*. 1975;95(1):173-179.
 48. Domalpally A, Clemons TE, Danis RP, et al. Peripheral Retinal Changes Associated with Age-Related Macular Degeneration in the Age-Related Eye Disease Study 2. *Ophthalmology*. 2017;124(4):479-487. doi:10.1016/j.ophtha.2016.12.004.
 49. Spaide RF. Disease Expression in Nonexudative Age-related Macular Degeneration Varies with Choroidal Thickness. *Retina*. May 2017:1.
doi:10.1097/IAE.0000000000001689.
 50. Spaide RF. Improving the Age-related Macular Degeneration Construct. *Retina*. May 2017:1. doi:10.1097/IAE.0000000000001732.
 51. Owsley C, Huisinigh C, Clark ME, Jackson GR, McGwin G. Comparison of Visual Function in Older Eyes in the Earliest Stages of Age-related Macular Degeneration to Those in Normal Macular Health. *Curr Eye Res*. March 2015:1-7.
 52. Csaky KG, Richman EA, Ferris FL. Report from the NEI/FDA Ophthalmic Clinical Trial

- Design and Endpoints Symposium. *Invest Ophthalmol Vis Sci.* 2008;49(2):479-489. doi:10.1167/iovs.07-1132.
53. Mangione CM, Gutierrez PR, Lowe G, Orav EJ, Seddon JM. Influence of age-related maculopathy on visual functioning and health-related quality of life. *Am J Ophthalmol.* 1999;128(1):45-53.
 54. Owsley C, McGwin G, Scilley K, Kallies K. Development of a questionnaire to assess vision problems under low luminance in age-related maculopathy. *Invest Ophthalmol Vis Sci.* 2006;47(2):528-535. doi:10.1167/iovs.05-1222.
 55. Curcio CA, Medeiros NE, Millican CL. Photoreceptor loss in age-related macular degeneration. *Invest Ophthalmol Vis Sci.* 1996;37(7):1236-1249.
 56. Curcio CA. Photoreceptor topography in ageing and age-related maculopathy. *Eye (Lond).* 2001;15(Pt 3):376-383.
 57. Cassels NK, Wild JM, Margrain TH, Chong V, Acton JH. The use of microperimetry in assessing visual function in age-related macular degeneration. *Surv Ophthalmol.* 2018;63(1):40-55. doi:10.1016/j.survophthal.2017.05.007.
 58. Acton JH, Greenstein VC. Fundus-driven perimetry (microperimetry) compared to conventional static automated perimetry: similarities, differences, and clinical applications. *Can J Ophthalmol.* 2013;48(5):358-363. doi:10.1016/j.jcjo.2013.03.021.
 59. Cachulo MDL, Laíns I, Lobo C, et al. Age-related macular degeneration in Portugal: prevalence and risk factors in a coastal and an inland town. The Coimbra Eye Study – Report 2. *Acta Ophthalmol.* 2016;94(6). doi:10.1111/aos.12950.
 60. Cachulo MDL, Lobo C, Figueira J, et al. Prevalence of age-related macular degeneration in Portugal: The Coimbra eye study - Report 1. *Ophthalmologica.* 2015;233. doi:10.1159/000371584.
 61. Topolski TD, LoGerfo J, Patrick DL, Williams B, Walwick J, Patrick MB. The Rapid Assessment of Physical Activity (RAPA) among older adults. *Prev Chronic Dis.* 2006;3(4):A118.
 62. Santos R, Nunes A, Ribeiro JC, Santos P, Duarte JAR, Mota J. Obesidade, Síndrome Metabólica e Atividade Física: Estudo exploratório realizado com adultos de ambos os sexos, da Ilha de S. Miguel, Região Autónoma dos Açores, Portugal. *Rev Bras Educ Fís Esp.* 2005;19(4):317-328.
 63. Craig CL, Marshall AL, Sjöström M, et al. International physical activity questionnaire: 12-Country reliability and validity. *Med Sci Sports Exerc.* 2003;35(8):1381-1395. doi:10.1249/01.MSS.0000078924.61453.FB.
 64. Laíns I, Miller JB, Park DH, et al. Structural Changes Associated with Delayed Dark Adaptation in Age-Related Macular Degeneration. *Ophthalmology.* May 2017. doi:10.1016/j.ophtha.2017.03.061.

65. Lains I, Miller JB, Mukai R, et al. Health Conditions linked to Age-related Macular Degeneration Associated with Dark Adaptation. *Retina*. April 2017:1. doi:10.1097/IAE.0000000000001659.
66. Emwas A-HM. The Strengths and Weaknesses of NMR Spectroscopy and Mass Spectrometry with Particular Focus on Metabolomics Research. In: *Methods in Molecular Biology (Clifton, N.J.)*. Vol 1277. ; 2015:161-193. doi:10.1007/978-1-4939-2377-9_13.
67. Barnes S, Benton HP, Casazza K, et al. Training in metabolomics research. I. Designing the experiment, collecting and extracting samples and generating metabolomics data. *J Mass Spectrom*. 2016;51(7):461-475. doi:10.1002/jms.3782.
68. Gika HG, Theodoridis GA, Plumb RS, Wilson ID. Current practice of liquid chromatography-mass spectrometry in metabolomics and metabonomics. *J Pharm Biomed Anal*. 2014;87:12-25. doi:10.1016/j.jpba.2013.06.032.
69. Marshall DD, Powers R. Beyond the paradigm: Combining mass spectrometry and nuclear magnetic resonance for metabolomics. *Prog Nucl Magn Reson Spectrosc*. 2017;100:1-16. doi:10.1016/j.pnmrs.2017.01.001.
70. Dunn WB, Broadhurst D, Begley P, et al. Procedures for large-scale metabolic profiling of serum and plasma using gas chromatography and liquid chromatography coupled to mass spectrometry. *Nat Protoc*. 2011;6(7):1060-1083. doi:10.1038/nprot.2011.335.
71. A randomized, placebo-controlled, clinical trial of high-dose supplementation with vitamins C and E, beta carotene, and zinc for age-related macular degeneration and vision loss: AREDS report no. 8. *Arch Ophthalmol*. 2001;119(10):1417-1436.
72. SEDDON J, SHARMA S, ADELMAN R. Evaluation of the Clinical Age-Related Maculopathy Staging System. *Ophthalmology*. 2006;113(2):260-266. doi:10.1016/j.ophtha.2005.11.001.
73. Klein R, Meuer SM, Moss SE, Klein BEK, Neider MW, Reinke J. Detection of age-related macular degeneration using a nonmydriatic digital camera and a standard film fundus camera. *Arch Ophthalmol (Chicago, Ill 1960)*. 2004;122(11):1642-1646. doi:10.1001/archopht.122.11.1642.
74. Hubbard LD, Danis RP, Neider MW, et al. Brightness, contrast, and color balance of digital versus film retinal images in the age-related eye disease study 2. *Invest Ophthalmol Vis Sci*. 2008;49(8):3269-3282. doi:10.1167/iovs.07-1267.
75. Yun C, Oh J, Ahn S-E, Hwang S-Y, Kim S-W, Huh K. Peripapillary choroidal thickness in patients with early age-related macular degeneration and reticular pseudodrusen. *Graefes Arch Clin Exp Ophthalmol*. 2016;254(3):427-435. doi:10.1007/s00417-015-3054-7.

76. Garg A, Oll M, Yzer S, et al. Reticular pseudodrusen in early age-related macular degeneration are associated with choroidal thinning. *Invest Ophthalmol Vis Sci*. 2013;54(10):7075-7081. doi:10.1167/iovs.13-12474.
77. Hogg RE, Silva R, Staurengi G, et al. Clinical characteristics of reticular pseudodrusen in the fellow eye of patients with unilateral neovascular age-related macular degeneration. *Ophthalmology*. 2014;121(9):1748-1755.
78. Alten F, Clemens CR, Heiduschka P, Eter N. Localized reticular pseudodrusen and their topographic relation to choroidal watershed zones and changes in choroidal volumes. *Investig Ophthalmol Vis Sci*. 2013;54(5):3250-3257. doi:10.1167/iovs.13-11923.
79. Humphrey WT, Carlson RE, Valone JA. Senile reticular pigmentary degeneration. *Am J Ophthalmol*. 1984;98(6):717-722.
80. Gass JD. Drusen and disciform macular detachment and degeneration. *Trans Am Ophthalmol Soc*. 1972;70:409-436.
81. Humphrey WT, Carlson RE, Valone JA. Senile reticular pigmentary degeneration. *Am J Ophthalmol*. 1984;98(6):717-722.
82. Nagiel A, Lalane RA, Sadda SR, Schwartz SD. Ultra-widefield Fundus Imaging: A Review of Clinical Applications and Future Trends. *Retina*. 2016;36(4):660-678. doi:10.1097/IAE.0000000000000937.
83. Lengyel I, Csutak A, Florea D, et al. A Population-Based Ultra-Widefield Digital Image Grading Study for Age-Related Macular Degeneration-Like Lesions at the Peripheral Retina. *Ophthalmology*. 2015;122(7):1340-1347. doi:10.1016/j.ophtha.2015.03.005.
84. Shuler RK, Schmidt S, Gallins P, et al. Peripheral reticular pigmentary change is associated with complement factor H polymorphism (Y402H) in age-related macular degeneration. *Ophthalmology*. 2008;115(3):520-524. doi:10.1016/j.ophtha.2007.06.021.
85. Seddon JM, Reynolds R, Rosner B. Peripheral Retinal Drusen and Reticular Pigment: Association with *CFHY402H* and *CFHrs1410996* Genotypes in Family and Twin Studies. *Investig Ophthalmology Vis Sci*. 2009;50(2):586. doi:10.1167/iovs.08-2514.
86. Munch IC, Ek J, Kessel L, et al. Small, Hard Macular Drusen and Peripheral Drusen: Associations with AMD Genotypes in the Inter99 Eye Study. *Investig Ophthalmology Vis Sci*. 2010;51(5):2317. doi:10.1167/iovs.09-4482.
87. Ooto S, Suzuki M, Vongkulsiri S, Sato T, Spaide RF. Multimodal Visual Function Testing in Eyes with Nonexudative Age-related Macular Degeneration. *Retina*. 2015;35(9):1726-1734. doi:10.1097/IAE.0000000000000608.
88. Owsley C, Clark ME, Huisinigh CE, Curcio CA, McGwin G. Visual Function in Older Eyes in Normal Macular Health: Association with Incident Early Age-Related Macular

- Degeneration 3 Years Later. *Investig Ophthalmology Vis Sci.* 2016;57(4):1782. doi:10.1167/iovs.15-18962.
89. Jackson GR, Scott IU, Kim IK, Quillen DA, Iannaccone A, Edwards JG. Diagnostic Sensitivity and Specificity of Dark Adaptometry for Detection of Age-Related Macular Degeneration. *Investig Ophthalmology Vis Sci.* 2014;55(3):1427. doi:10.1167/iovs.13-13745.
 90. Owsley C, McGwin G, Jackson GR, Kallies K, Clark M. Cone- and Rod-Mediated Dark Adaptation Impairment in Age-Related Maculopathy. *Ophthalmology.* 2007;114(9):1728-1735. doi:10.1016/j.ophtha.2006.12.023.
 91. Owsley C, McGwin G, Jackson GR, Kallies K, Clark M. Cone- and rod-mediated dark adaptation impairment in age-related maculopathy. *Ophthalmology.* 2007;114(9):1728-1735.
 92. Jackson GR, Scott IU, Kim IK, Quillen DA, Iannaccone A, Edwards JG. Diagnostic sensitivity and specificity of dark adaptometry for detection of age-related macular degeneration. *Invest Ophthalmol Vis Sci.* 2014;55(3):1427-1431. doi:10.1167/iovs.13-13745.
 93. de Sisternes L, Simon N, Tibshirani R, Leng T, Rubin DL. Quantitative SD-OCT Imaging Biomarkers as Indicators of Age-Related Macular Degeneration Progression. *Investig Ophthalmology Vis Sci.* 2014;55(11):7093. doi:10.1167/iovs.14-14918.
 94. Schmidt-Erfurth U, Waldstein SM. A paradigm shift in imaging biomarkers in neovascular age-related macular degeneration. *Prog Retin Eye Res.* 2016;50:1-24. doi:10.1016/j.preteyeres.2015.07.007.
 95. Leuschen JN, Schuman SG, Winter KP, et al. Spectral-Domain Optical Coherence Tomography Characteristics of Intermediate Age-related Macular Degeneration. *Ophthalmology.* 2013;120(1):140-150. doi:10.1016/j.ophtha.2012.07.004.
 96. Clark ME, McGwin G, Neely D, et al. Association between retinal thickness measured by spectral-domain optical coherence tomography (OCT) and rod-mediated dark adaptation in non-exudative age-related maculopathy. *Br J Ophthalmol.* 2011;95(10):1427-1432. doi:10.1136/bjo.2010.190355.
 97. Sevilla MB, McGwin G, Lad EM, et al. Relating Retinal Morphology and Function in Aging and Early to Intermediate Age-related Macular Degeneration Subjects. *Am J Ophthalmol.* 2016;165:65-77. doi:10.1016/j.ajo.2016.02.021.
 98. Flamendorf J, Agrón E, Wong WT, et al. Impairments in Dark Adaptation Are Associated with Age-Related Macular Degeneration Severity and Reticular Pseudodrusen. *Ophthalmology.* 2015;122(10):2053-2062.
 99. Owsley C, Huisingh C, Jackson GR, et al. Associations between abnormal rod-mediated dark adaptation and health and functioning in older adults with normal

- macular health. *Invest Ophthalmol Vis Sci*. 2014;55(8):4776-4789.
100. Gorin MB, Weeks DE, Baron R V, Conley YP, Ortube MC, Nusinowitz S. Endophenotypes for Age-Related Macular Degeneration: Extending Our Reach into the Preclinical Stages of Disease. *J Clin Med*. 2014;3(4):1335-1356. doi:10.3390/jcm3041335.
 101. Wojczynski MK, Tiwari HK. Definition of phenotype. *Adv Genet*. 2008;60:75-105. doi:10.1016/S0065-2660(07)00404-X.
 102. Patti GJ, Yanes O, Siuzdak G. Innovation: Metabolomics: the apogee of the omics trilogy. *Nat Rev Mol Cell Biol*. 2012;13(4):263-269. doi:10.1038/nrm3314.
 103. Neelam K, Muldrew A, Hogg R, Stack J, Chakravarthy U, Beatty S. Grading of age-related maculopathy: slit-lamp biomicroscopy versus an accredited grading center. *Retina*. 2009;29(2):192-198. doi:10.1097/IAE.0b013e31818c178f.
 104. van Leeuwen R, Chakravarthy U, Vingerling JR, et al. Grading of age-related maculopathy for epidemiological studies: is digital imaging as good as 35-mm film? *Ophthalmology*. 2003;110(8):1540-1544.
 105. Tsikata E, Laíns I, Gil J, et al. Automated Brightness and Contrast Adjustment of Color Fundus Photographs for the Grading of Age-Related Macular Degeneration. *Transl Vis Sci Technol*. 2017;6(2):3. doi:10.1167/tvst.6.2.3.
 106. Laíns I, Duarte D, Barros AS, et al. Human plasma metabolomics in age-related macular degeneration (AMD) using nuclear magnetic resonance spectroscopy. *PLoS One*. 2017;12(5). doi:10.1371/journal.pone.0177749.
 107. Jové M, Portero-Otín M, Naudí A, Ferrer I, Pamplona R. Metabolomics of human brain aging and age-related neurodegenerative diseases. *J Neuropathol Exp Neurol*. 2014;73(7):640-657. doi:10.1097/NEN.0000000000000091.
 108. Farooqui AA, Horrocks LA, Farooqui T. Glycerophospholipids in brain: their metabolism, incorporation into membranes, functions, and involvement in neurological disorders. *Chem Phys Lipids*. 2000;106(1):1-29.
 109. Hopiavuori BR, Agbaga M-P, Brush RS, Sullivan MT, Sonntag WE, Anderson RE. Regional changes in CNS and retinal glycerophospholipid profiles with age: a molecular blueprint. *J Lipid Res*. 2017;58(4):668-680. doi:10.1194/jlr.M070714.
 110. Levin LA, Adler FH. *Adler's Physiology of the Eye*.
 111. Kowalski M, Bielecka-Kowalska A, Oszańca K, et al. Manganese superoxide dismutase (MnSOD) gene (Ala-9Val, Ile58Thr) polymorphism in patients with age-related macular degeneration (AMD). *Med Sci Monit*. 2010;16(4):CR190-196.
 112. Oak ASW, Messinger JD, Curcio CA. Subretinal Drusenoid Deposits. *Retina*. 2014;34(4):825-826. doi:10.1097/IAE.0000000000000121.
 113. Zweifel SA, Spaide RF, Curcio CA, Malek G, Imamura Y. Reticular pseudodrusen are

- subretinal drusenoid deposits. *Ophthalmology*. 2010;117(2):303-12.e1.
doi:10.1016/j.ophtha.2009.07.014.
114. Giusto NM, Pasquaré SJ, Salvador GA, Ilincheta de Boschero MG. Lipid second messengers and related enzymes in vertebrate rod outer segments. *J Lipid Res*. 2010;51(4):685-700. doi:10.1194/jlr.R001891.
 115. Delgado R, Muñoz Y, Peña-Cortés H, Giavalisco P, Bacigalupo J. Diacylglycerol activates the light-dependent channel TRP in the photosensitive microvilli of *Drosophila melanogaster* photoreceptors. *J Neurosci*. 2014;34(19):6679-6686. doi:10.1523/JNEUROSCI.0513-14.2014.
 116. Xia J, Broadhurst DI, Wilson M, Wishart DS. Translational biomarker discovery in clinical metabolomics: an introductory tutorial. *Metabolomics*. 2013;9(2):280-299. doi:10.1007/s11306-012-0482-9.
 117. Senn T, Hazen SL, Tang WHW. Translating metabolomics to cardiovascular biomarkers. *Prog Cardiovasc Dis*. 55(1):70-76.
 118. Duarte IF, Gil AM. Metabolic signatures of cancer unveiled by NMR spectroscopy of human biofluids. *Prog Nucl Magn Reson Spectrosc*. 2012;62:51-74.
 119. Duarte IF, Rocha CM, Barros AS, et al. Can nuclear magnetic resonance (NMR) spectroscopy reveal different metabolic signatures for lung tumours? *Virchows Arch*. 2010;457(6):715-725.
 120. Rocha CM, Carrola J, Barros AS, et al. Metabolic signatures of lung cancer in biofluids: NMR-based metabolomics of blood plasma. *J Proteome Res*. 2011;10(9):4314-4324. doi:10.1021/pr200550p.
 121. Emwas A-H, Roy R, McKay RT, et al. Recommendations and Standardization of Biomarker Quantification Using NMR-Based Metabolomics with Particular Focus on Urinary Analysis. *J Proteome Res*. 2016;15(2):360-373. doi:10.1021/acs.jproteome.5b00885.
 122. Mal M. Noninvasive metabolic profiling for painless diagnosis of human diseases and disorders. *Futur Sci OA*. 2016;2(2):fsoa-2015-0014. doi:10.4155/fsoa-2015-0014.
 123. Swaroop A, Chew EY, Rickman CB, Abecasis GR. Unraveling a multifactorial late-onset disease: from genetic susceptibility to disease mechanisms for age-related macular degeneration. *Annu Rev Genomics Hum Genet*. 2009;10:19-43. doi:10.1146/annurev.genom.9.081307.164350.
 124. Buitendijk GHS, Ročtchina E, Myers C, et al. Prediction of age-related macular degeneration in the general population: the Three Continent AMD Consortium. *Ophthalmology*. 2013;120(12):2644-2655. doi:10.1016/j.ophtha.2013.07.053.

Supplements

Supplement 1

Ethics Committee Approval, Faculty of Medicine, University of Coimbra



FMUC FACULDADE DE MEDICINA
UNIVERSIDADE DE COIMBRA

COMISSÃO DE ÉTICA DA FMUC

Of. Ref^a 037-CE-2015

Data 18/05/2015

Exmo Senhor

Prof. Doutor Joaquim Neto Murta

Presidente do Conselho Científico

C/C à aluna de doutoramento

Assunto: Projecto de Investigação no âmbito do Programa Doutoral em Ciências da Saúde (ref^a CE-097/2014). Introdução de emendas e de uma versão actualizada do consentimento informado.

Candidato(a): Inês Maria de Carvalho Laíns

Título do Projecto: "Metabolómica, genética e ambiente: uma nova abordagem integradora na degenerescência macular relacionada com a idade".

A Comissão de Ética da Faculdade de Medicina, após análise do projecto de investigação supra identificado, decidiu emitir o parecer que a seguir se transcreve: "**Parecer favorável à introdução das alterações propostas e à nova versão de consentimento informado**".

Queira aceitar os meus melhores cumprimentos,

O Presidente,

Prof. Doutor João Manuel Pedroso de Lima

GC

SERVIÇOS TÉCNICOS DE APOIO À GESTÃO - STAG - COMISSÃO DE ÉTICA

Pólo das Ciências da Saúde - Unidade Central

Azinhaga de Santa Comba, Colas, 3000-354 COIMBRA - PORTUGAL

Tel.: +351 239 857 707 (Ext. 542707) | Fax: +351 239 823 236

E-mail: comissaoetica@fmed.ucp | www.fmed.ucp

Supplement 2

Ethics Committee Approval, Association for Innovation and Biomedical Research on Light and Image



Comissão de Ética para a Saúde

Exma. Senhora
Dra. Inês Láins
AIBILI – CEC
Azinhaga de Santa Comba, Celas
3000-548 Coimbra

Nossa Referência *Coimbra,*
006/2015/AIBILI/CE 2015-02-11

Assunto: Comissão de Ética – 126ª Reunião de 2015/02/09

CE 207 - “Metabolomics, genetics and environment: a novel integrative approach to age-related macular degeneration.” - Protocol IN0654


Comunicação do Promotor a enviar a Versão 3 do “Documento de informação para o participante e formulário de Consentimento Informado”, de 26/12/2014

Exma. Senhora,

Na sequência da 126ª Reunião da Comissão de Ética de 2015/02/09, e após aprovadas as alterações ao “Documento de informação para o participante e formulário de Consentimento Informado”, como anteriormente solicitado, junto envio parecer favorável relativo ao seguinte estudo observacional:

CE 207 – “Metabolomics, genetics and environment: a novel integrative approach to age-related macular degeneration.” - Protocol IN0654

Mais se recorda que, para além das obrigações decorrentes das Boas Práticas Clínicas e Diretivas Europeias, no âmbito do nº 4 do artº 19 da Lei 21/2014 de 16 de Abril, deve submeter a esta Comissão todas comunicações e publicações relativas ao estudo clínico, no prazo de 30 dias após a sua divulgação.

Com os melhores cumprimentos, 

O Presidente da Comissão de Ética


(Francisco Corte-Real Gonçalves)

Anexo:

1 Parecer

Exma. Senhora
Dra. Inês Láins
AIBILI – CEC
Azinhaga de Santa Comba, Celas
3000-548 Coimbra

COMISSÃO DE ÉTICA – 2015/02/09

S/ referência: Ofício 039/2014/AIBILI/CEC, datado de 2014-12-26

Assunto: CE 207 - “Metabolomics, genetics and environment: a novel integrative approach to age-related macular degeneration.” - Protocol IN0654

Parecer favorável

Exma. Senhora,

Tenho a honra de comunicar a V. Exa. que, na sua 126ª Reunião de 2015/02/09, a Comissão de Ética, após analisada a seguinte documentação: “Modelo Específico da Comissão de Ética” - Mod.CEv8, de 2014/12/03; Nome e Morada do Promotor; Nome e Morada do Investigador Principal e Sub-Investigadores; Curriculum Vitae do Investigador Principal; “Study Protocol nº IN0654”, Versão 1 de 2014/12/03; CRF, Versão 1, de 2014/12/03; “Documento de Informação para o Participante e Formulário de Consentimento Informado”, Versão 2, de 2014/09/30, Inquérito sobre Estilos de Vida e Hábitos Alimentares, Questionário de Atividade Física, Parecer da Comissão de Ética para a Saúde da FMUC, de 2014/10/27, Protocolo de Colaboração entre a Universidade de Coimbra, a AIBILI e a Universidade de Aveiro, de 2014/04/08, Termo de Aceitação e Acordo Financeiro com a FCT, de 2014/05/08 e Candidatura submetida à FCT, de 2013/09/25, submetida através do v/ ofício 038/2014/AIBILI/CEC, datado de 2014-12-04 e “Documento de informação para o participante e formulário de Consentimento Informado” – Versão 3 (26/12/2014) - Protocolo IN0654, submetida através do v/ ofício mencionado em epígrafe, emitiu parecer favorável ao estudo observacional em questão, estando salvaguardados os princípios do consentimento informado e da confidencialidade.

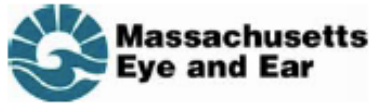
Com os melhores cumprimentos, 

O Presidente da Comissão de Ética

(Francisco Corte-Real Gonçalves)

Supplement 3

Institutional Review Board Approval, Massachusetts Eye and Ear



Human Studies Committee
HSC@meei.harvard.edu

PROTOCOL APPROVAL

DATE: December 26, 2014
TO: Deeba Husain
FROM: HUMAN STUDIES COMMITTEE
TITLE: [635373-2] Age Related Macular Degeneration: a new integrative approach to identify biomarkers
PROTOCOL #: 14-111H
SPONSOR: Departmental
SUBMISSION TYPE: Response/Follow-Up
SUBMISSION DATE: November 14, 2014
ACTION: APPROVED
RISK LEVEL: MINIMAL RISK
REVIEW TYPE: FULL INITIAL REVIEW
EFFECTIVE DATE: DECEMBER 26, 2014
EXPIRATION DATE: DECEMBER 25, 2015
IND/IDE #: N/A
ClinicalTrials.gov: N/A

Dear Dr. Husain,

Thank you for your submission of Response/Follow-Up materials for this research study.

This protocol has been reviewed and approved by the HSC. During the review of this protocol, the HSC specifically considered (i) the minimization of risks to subjects (ii) the risks and anticipated benefits, if any, to subjects; (iii) the equitable selection of subjects; (iv) the procedures for obtaining and documenting informed consent; (v) the monitoring of data related to subject safety; and (vi) subject privacy and confidentiality of data in accordance with 45 CFR 46.111 and 21 CFR 56.111, criteria for IRB approval of research.

Notes, Determinations, Findings:

Minimal Risk/Expedite: The HSC determined that this study is minimal risk and eligible for expedited review in the future per Expedited Category 9.

NSR device: As used in this study, both the TopCon Swept Source and Cannon's Adaptive Optics have been determined by the HSC to be non-significant risk device in accordance with 21 CFR 812.3 (m). Please note that the abbreviated IDE requirements at 21 CFR 812.2 (b) apply to the conduct of this investigation.

Waiver of Consent/Authorization: A waiver of Consent/Authorization has been approved in accordance with the Common Rule and Privacy Rule regulations (for the screening or recruitment part of the study only).

Short Form: The HSC approved use of the short form consent process. Please note that only the HSC approved short forms found on the HRPP SharePoint site can be used when obtaining consent from non-English speakers. The consent process for enrolling subjects using the 'short form' consent document is outlined in the HSC Guidance on Obtaining and Documenting Consent of non-English Speaking Subjects (available on the HRPP SharePoint site).

Pregnant Women: The HSC has approved the inclusion of pregnant women in this study in accordance with 45 CFR 46.204.

Illiterate Subjects: An impartial witness must be present during the informed consent process and sign as a witness on the consent form.

TERMS OF APPROVAL

As Principal Investigator you are responsible for the following:

1. Submission in writing of any changes to this project (e.g., personnel, protocol, recruitment materials, consent form, etc.) to the HSC for review and approval prior to initiation of the change(s), except where necessary to eliminate apparent immediate hazards to the subject(s). Changes made to eliminate apparent immediate hazards to subjects must be reported to the HSC within 24 hours.
2. So long as this project continues to involve human subjects, filing for continuing review and re-approval of this study (at least 6-8 weeks) prior to the expiration date noted above. Once the study is complete or no longer involves human subjects, filing a closure report with the HSC.
3. For FDA-regulated studies, compliance with IND and/or IDE requirements, including applicable sponsor and/or investigator responsibilities and adherence to Good Clinical Practice standards. Please contact the HSC for detailed information, guidance, and resources to assist you in fulfillment of these responsibilities.
4. Submission, in writing, of any reportable events as required by HSC policy. Please ensure you are familiar with HSC reporting policies. Should you have questions about whether or not an event is reportable or how to report an event, you are strongly encouraged to seek guidance by contacting the HSC. You are also responsible for any reporting requirements imposed by the FDA, OHRP, sponsor, funding agency or others.
5. Use of only current and HSC validated copies of the consent/authorization form(s), in your research. Do not use expired consent/authorization forms.
6. Informing all personnel listed on the protocol of changes, adverse events, and unanticipated problems.
7. FDA-regulated research: Maintaining study documentation in accordance with FDA requirements and Good Clinical Practice standards. Please use the Harvard Catalyst Regulatory Binder template (available on the SharePoint site) if a binder has not been provided by the sponsor. MEE template logs are available on the HRPP SharePoint site for use and should be adapted to meet the needs of

your study. If you have any questions about the applicability of record requirements please [contact the HRPP staff](#) for assistance. Please note that all study-related records must be accessible for inspection by authorized individuals including the FDA, HSC, and study monitors (as applicable).

8. For all research: Maintaining up-to-date and comprehensive study files, you are encouraged to review the Harvard Catalyst Regulatory Binder template as a helpful resource in organizing study documents related to the conduct of this study.
9. For retaining all records associated with the conduct of this study for at least 6 years following the completion of the study (unless otherwise required by the HSC to destroy them sooner (e.g., master key, identifiable data)). This is the minimum institutional requirement however, you should ensure you are aware of any record retention requirements imposed by the FDA, funding agency, or sponsor.

ENCLOSED DOCUMENTS: Validated consent/HIPAA form version 635373-2.

Please do not hesitate to [contact the HSC](#) with questions or for assistance or guidance. You may also contact the sender of this communication, name and contact information is provided below.

Sincerely,

Fariba Houman
617-573-3448
fariba_houman@meei.harvard.edu

The HSC acknowledges your submission which includes the following item (s):

- Application Form - SUPP N - RESEARCH SUMMARY (UPDATED: 11/14/2014)
- Application Form - SUPP I - DEVICES (UPDATED: 11/14/2014)
- Application Form - FORM I - INITIAL APPLICATION (UPDATED: 11/14/2014)
- Consent Form - Portuguese ICF_translation (UPDATED: 11/14/2014)
- Consent Form - Portuguese ICF (UPDATED: 11/14/2014)
- Consent Form - INFORMED CONSENT FORM (UPDATED: 11/14/2014)
- Cover Sheet - COVER SHEET (UPDATED: 11/14/2014)
- Cover Sheet - POINT BY POINT RESPONSE (UPDATED: 11/14/2014)
- Data Collection - DATA COLLECTION SHEET (UPDATED: 11/14/2014)
- Letter - Portuguese IRB approval_translation (UPDATED: 11/14/2014)
- Letter - Portuguese IRB approval (UPDATED: 11/14/2014)
- Other - Product information (swept source) (UPDATED: 11/14/2014)
- Other - Product information (swept source) (UPDATED: 11/14/2014)
- Other - Product information (AOSLO) (UPDATED: 11/14/2014)
- Other - Product information (AOSLO) (UPDATED: 11/14/2014)
- Other - Product information (AOSLO) (UPDATED: 11/14/2014)
- Questionnaire/Survey - Food frequency questionnaire (UPDATED: 11/14/2014)
- Study Plan - Material and data transfer agreement (UPDATED: 11/14/2014)

Supplement 4

Approval of the Portuguese National Data Protection Committee (CNPd)

Processo N.º 16875/2014 | 1



AUTORIZAÇÃO N.º 1019 /2015

I. Pedido

A Faculdade de Medicina da Universidade de Coimbra notificou à Comissão Nacional de Protecção de Dados (CNPd) um tratamento de dados pessoais com a finalidade de elaborar um estudo intitulado "Metabólica, Genética e Ambiente: uma Nova Abordagem Integradora na Degenerescência Macular Relacionada com a Idade."

O objetivo principal do estudo consiste em avaliar os vários fatores que contribuem para a evolução da degenerescência macular relacionada com a idade (DMI) e a forma como eles se relacionam entre si.

Este estudo prevê a participação de aproximadamente 309 doentes adultos do Centro de Saúde de Mira que entre 2009 e 2011 foram incluídos num estudo epidemiológico levado a cabo pela mesma equipa de investigação e que na altura apresentavam sinais ligeiros ou moderados de DMI. Serão também incluídos 50 participantes sem quaisquer lesões na mácula, para controlo.

A participação no estudo consistirá numa consulta de oftalmologia por um médico investigador no estudo, que incluirá fotografias do fundo do olho, tomografia de coerência óptica, colheita de sangue e recolha de urina, bem como resposta a um questionário de estilo de vida e alimentação.

Os dados serão recolhidos num "caderno de recolha de dados" no qual não há identificação nominal do titular, sendo aposto um código de doente. A chave desta codificação só pode ser conhecida da equipa de investigação.

Os destinatários são ainda informados sobre a natureza facultativa da sua participação e garantida confidencialidade no tratamento, caso decidam participar, recolhendo o médico assistente/investigador o seu consentimento informado para o efeito.

Rua de São Bento, 148-3º • 1200-821 LISBOA
Tel: 213 928 400 Fax: 213 976 832
www.cnpd.pt

21 393 00 39
LINHA PRIVACIDADE
Dias úteis das 10 às 13 h
duvidas@cnpd.pt



II. Análise

A CNPD já se pronunciou na sua Deliberação n.º 227/2007 sobre o enquadramento legal, os fundamentos de legitimidade, os princípios orientadores para o correto cumprimento da LPD, bem como as condições gerais aplicáveis ao tratamento de dados pessoais para a finalidade de estudos de investigação na área da saúde.

Porque em grande parte referentes à vida privada e também à saúde, os dados recolhidos pela requerente têm a natureza de sensíveis, nos termos do disposto no n.º 1 do artigo 7.º da LPD.

Em regra, o tratamento de dados sensíveis é proibido, de acordo com o disposto no n.º 1 do artigo 7.º da LPD. Todavia, nos termos do n.º 2 do mesmo artigo, o tratamento de dados da vida privada e de saúde é permitido, quando haja uma disposição legal que consagre esse tratamento de dados, quando por motivos de interesse público importante o tratamento for indispensável ao exercício das atribuições legais ou estatutárias do seu responsável ou quando o titular dos dados tiver prestado o seu consentimento.

Não estando preenchidas as duas primeiras condições de legitimidade, o fundamento de legitimidade só pode basear-se no consentimento dos titulares dos dados ou dos representantes legais, quando os titulares dos dados sejam incapazes.

Assim, é necessário o «consentimento expresso do titular», entendendo-se por consentimento qualquer manifestação de vontade, livre, específica e informada, nos termos da qual o titular aceita que os seus dados sejam objeto de tratamento (cf. artigo 3.º, alínea *h*), da LPD), o qual deve ser obtido através de uma “declaração de consentimento informado” onde seja utilizada uma linguagem clara e acessível.

Nos termos do artigo 10.º da LPD, a declaração de consentimento tem de conter a identificação do responsável pelo tratamento e a finalidade do tratamento, devendo ainda conter informação sobre a existência e as condições do direito de acesso e de retificação por parte do respetivo titular.



Os titulares dos dados, de acordo com a declaração de consentimento informado junta aos autos, apõem as suas assinaturas na mesma, deste modo satisfazendo as exigências legais.

No que concerne à recolha do dado raça, o responsável pelo tratamento justifica a sua necessidade do seguinte modo:

"O tratamento do dado "raça" tem por intuito a avaliação da influência da mesma no perfil genético, nos metabolitos e na sua interação, que vai ser efetuada neste estudo. De acordo com a literatura, os polimorfismos genéticos de risco (conhecidos como SNP's - single nucleotide polymorphisms) para DMI apresentam variações entre diferentes raças (por exemplo: Klein et al, Am J Ophthalmology, 2013, <http://www.ncbi.nlm.nih.gov/pubmed/23938121>). Considerando que se trata de uma área totalmente nova de investigação não existem ainda dados sobre potenciais variações do perfil de metabolitos na DMI de acordo com a raça. No entanto, esta está comprovada para outras patologias, nomeadamente para o cancro, onde a metabolómica tem tido uma aplicação exponencial (Shen et al, Transl Oncol 2013, <http://www.ncbi.nlm.nih.gov/pubmed/24466379>).

Deste modo, a análise dos dados que iremos obter quer de genética quer de metabolómica, implicam uma avaliação da potencial influência da raça nos perfis obtidos. Trata-se de um potencial fator confundidor na avaliação dos restantes resultados, pelo que a correta análise requer a sua avaliação.

Apesar de em Portugal não existir uma grande variedade racial, este estudo terá lugar também nos Estados Unidos (como mencionado na Sinopse do Estudo enviada, uma vez que foi financiado pela FCT/Programa Harvard Medical School Portugal) pelo que este dado será imprescindível para a avaliação global dos resultados. Trata-se portanto do tratamento de um dado sensível em virtude do interesse público, estando sempre salvaguardada a não discriminação de indivíduos."

Tendo em conta o teor da justificação e a pertinência das razões nele invocadas para o estudo ora em causa, entende a CNPD que é legítima a recolha e tratamento do dado raça.



**COMISSÃO NACIONAL
DE PROTECÇÃO DE DADOS**

Cabe ao Investigador assegurar a confidencialidade dos dados pessoais e da informação tratada, conforme o estatuído na alínea *g*) do artigo 10.º da Lei n.º 21/2014, de 16 de abril (Lei da investigação clínica).

Assim, apenas poderão ter acesso aos registos médicos originais o médico assistente e um monitor, (nos termos do artigo 11.º da Lei da investigação clínica), e apenas na medida do estritamente necessário, também recaindo sobre este a obrigação de confidencialidade.

O responsável declarou a existência de comunicação de dados para uma outra entidade nacional, bem como para uma entidade situada fora da União Europeia, mas apenas são transmitidos dados anonimizados, pelo que não se verificam comunicação ou fluxos transfronteiriços de dados pessoais.

A informação tratada é recolhida de forma lícita (artigo 5.º, n.º1 alínea *a*) da Lei n.º 67/98), para finalidades determinadas, explícitas e legítimas (cf. alínea *b*) do mesmo artigo) e não é excessiva.

O fundamento de legitimidade é o consentimento expresso do titular dos dados.

III. Conclusão

Assim, nos termos das disposições conjugadas do n.º 2 do artigo 7.º, n.º 1 do artigo 27.º, alínea *a*) do n.º 1 do artigo 28.º e artigo 30.º da Lei de Protecção de Dados, com as condições e limites fixados na referida Deliberação n.º 227/2007, que se dão aqui por reproduzidos e que fundamentam esta decisão, autoriza-se o tratamento de dados *supra* referido, consignando-se o seguinte:

Responsável pelo tratamento: Faculdade de Medicina da Universidade de Coimbra;
Finalidade: estudo intitulado “Metabólica, Genética e Ambiente: uma Nova Abordagem Integradora na Degenerescência Macular Relacionada com a Idade.”;
Categoria de Dados pessoais tratados: código do participante; género; data de nascimento; raça; profissão desempenhada a maior parte da vida; grau de



COMISSÃO NACIONAL
DE PROTECÇÃO DE DADOS

escolaridade; estado civil; História clínica médica geral (tabagismo, hipertensão, diabetes, dislipidémia, insuficiência cardíaca, outros problemas cardíacos, distúrbios do sangue ou da coagulação, doença renal, doenças neurológicas, cancro, traumatismo craniano, acidente vascular isquémico, psoríase, artrite reumatóide, lúpus eritematoso sistémico, patologia tiroideia, menopausa); Medicação habitual; História clínica oftalmológica (outras patologias oculares, cirurgias intra-oculares, história de laser ocular, injeções intra-vitreas); Questionário de frequência alimentar e de atividade física; História familiar de degenerescência macular relacionada com a idade; História familiar de doença neurológica ou psiquiátrica; peso; altura; perímetro abdominal; pressão arterial; acuidade visual não corrigida; melhor acuidade visual corrigida; refração atual; biomicroscopia; pressão intra-ocular; exame do fundo do olho, Exames de imagem (fotografias do fundo do olho (cor, *infra-red*, *red-free* e autofluorescência); tomografia de coerência óptica (OCT) *spectral domain* e *swept-source*; sangue; urina.

Entidades a quem podem ser comunicados: Não há.

Formas de exercício do direito de acesso e retificação: Junto do médico assistente/investigador.

Interconexões de tratamentos: Não há.

Transferências de dados para países terceiros: Não há.

Prazo de conservação: A chave de codificação dos dados do titular deve ser destruída um mês após o fim do estudo.

Dos termos e condições fixados na Deliberação n.º 227/ 2007 e na presente Autorização decorrem obrigações que o responsável deve cumprir. Deve, igualmente, dar conhecimento dessas condições a todos os intervenientes no circuito de informação.

Lisboa, 03 de fevereiro de 2015

Luís Barroso (o Vogal, em substituição da Presidente)

Supplement 5

Medical history questionnaire created for this project

STUDY ID: _____

Date: _____

1. DEMOGRAPHICS - For questions with boxes please fill just one box.

1.1 Gender Male Female

1.2 Race White Black Asian Hispanic Other

1.3 Occupation held most of life _____

1.4 Number of years working in this occupation _____

1.5 Are you currently Working Retired

1.6 Highest scholar degree Up to 4 years 5 to 9 years 10 to 12 years More than 12 years

1.7 Are you currently Married/Unmarried couple Divorce/ Separate Single Widower

2. HABITS

2.1 Regarding smoking, are you currently a

Non-smoker (i.e: never been a smoker)

Smoker

Ex-smoker (i.e: used to be a smoker, but not smoking anymore)

2.1.1 If your answer was smoker:

At what age did you start smoking: _____ (years)

How many cigarettes per day do you smoke? ____

2.2.2 If your answer was ex-smoker:

At what age did you start smoking: _____ (years)

At what age did you stop smoking: _____ (years)

How many cigarettes per day do you used to smoke? ____

3. MEDICAL HISTORY

3.1 Please fill the table below about your current or past medical conditions:

Condition	Has a doctor ever told you that you have any of the following conditions?	When was it diagnosed?	Other
Diabetes	<input type="checkbox"/> No <input type="checkbox"/> Yes <input type="checkbox"/> I don't know	(year of diagnosis)	Which medication are you currently taking for diabetes? <input type="checkbox"/> Pills <input type="checkbox"/> Insulin <input type="checkbox"/> None <input type="checkbox"/> I don't know
Hypertension	<input type="checkbox"/> No <input type="checkbox"/> Yes <input type="checkbox"/> I don't know	(year of diagnosis)	
High cholesterol	<input type="checkbox"/> No <input type="checkbox"/> Yes <input type="checkbox"/> I don't know	(year of diagnosis)	
High triglycerides	<input type="checkbox"/> No <input type="checkbox"/> Yes <input type="checkbox"/> I don't know	(year of diagnosis)	
Congestive heart failure	<input type="checkbox"/> No <input type="checkbox"/> Yes <input type="checkbox"/> I don't know	(year of diagnosis)	
NYHA functional class	<input type="checkbox"/> I <input type="checkbox"/> II <input type="checkbox"/> III <input type="checkbox"/> IV		*I – Ordinary physical activity <u>does not cause</u> undue dyspnea or fatigue II – <u>Ordinary physical activity</u> results in dyspnea or fatigue III – <u>Less than ordinary activity</u> causes dyspnea or fatigue, but comfortable at rest IV – Dyspnea or fatigue present <u>even at rest</u> , increasing if any physical activity is undertaken
Angina pectoris*	<input type="checkbox"/> No <input type="checkbox"/> Yes <input type="checkbox"/> I don't know	(year of diagnosis)	*Pain, heaviness or pressure in chest or upper body when walking quickly or uphill, which subdues when at rest
Heart attack (myocardial infarction)	<input type="checkbox"/> No <input type="checkbox"/> Yes <input type="checkbox"/> I don't know	(year of diagnosis)	
Heart surgery, bypass or vascular surgery	<input type="checkbox"/> No <input type="checkbox"/> Yes <input type="checkbox"/> I don't know	(year of diagnosis)	Type of surgery: _____
Blood or clotting disorders	<input type="checkbox"/> No <input type="checkbox"/> Yes <input type="checkbox"/> I don't know	(year of diagnosis)	Type of blood or clotting disorder: _____
Stroke or transient ischemic attack	<input type="checkbox"/> No <input type="checkbox"/> Yes <input type="checkbox"/> I don't know	(year of diagnosis)	
Kidney disease	<input type="checkbox"/> No <input type="checkbox"/> Yes <input type="checkbox"/> I don't know	(year of diagnosis)	What type of kidney disease do you have? _____ Have you been submitted to a kidney transplant? <input type="checkbox"/> No <input type="checkbox"/> Yes Are you currently doing dialysis? <input type="checkbox"/> No <input type="checkbox"/> Yes
Liver disease	<input type="checkbox"/> No <input type="checkbox"/> Yes <input type="checkbox"/> I don't know	(year of diagnosis)	What type of liver disease do you have? _____

Migraine	<input type="checkbox"/> No <input type="checkbox"/> Yes <input type="checkbox"/> I don't know	(year of diagnosis)	
Brain trauma	<input type="checkbox"/> No <input type="checkbox"/> Yes <input type="checkbox"/> I don't know	(year of diagnosis)	
Epilepsy	<input type="checkbox"/> No <input type="checkbox"/> Yes <input type="checkbox"/> I don't know	(year of diagnosis)	
Parkinson disease	<input type="checkbox"/> No <input type="checkbox"/> Yes <input type="checkbox"/> I don't know	(year of diagnosis)	
Any form of dementia	<input type="checkbox"/> No <input type="checkbox"/> Yes <input type="checkbox"/> I don't know	(year of diagnosis)	
Other neurologic diseases	<input type="checkbox"/> No <input type="checkbox"/> Yes <input type="checkbox"/> I don't know	(year of diagnosis)	If yes, which type of neurologic disease? _____
Cancer	Have you ever had a diagnosis of cancer? <input type="checkbox"/> No <input type="checkbox"/> Yes <input type="checkbox"/> I don't know	(year of diagnosis)	If yes, which type of cancer do you have diagnosed? _____ Are you currently undergoing treatment for the cancer? <input type="checkbox"/> No <input type="checkbox"/> Yes <input type="checkbox"/> I don't know If yes, which type of treatment? <input type="checkbox"/> Chemotherapy <input type="checkbox"/> Radiotherapy <input type="checkbox"/> Hormonal therapy <input type="checkbox"/> I don't know <input type="checkbox"/> None of this When (year) was your cancer considered in remission? _____
Psoriasis/eczema	<input type="checkbox"/> No <input type="checkbox"/> Yes <input type="checkbox"/> I don't know	(year of diagnosis)	
Rheumatoid arthritis	<input type="checkbox"/> No <input type="checkbox"/> Yes <input type="checkbox"/> I don't know	(year of diagnosis)	

Systemic lupus erythematosus	<input type="checkbox"/> No <input type="checkbox"/> Yes <input type="checkbox"/> I don't know	(year of diagnosis)	
Multiple sclerosis	<input type="checkbox"/> No <input type="checkbox"/> Yes <input type="checkbox"/> I don't know	(year of diagnosis)	
Thyroid disease	<input type="checkbox"/> No <input type="checkbox"/> Yes <input type="checkbox"/> I don't know	(year of diagnosis)	

3.2 If you are a woman, please answer to the following questions. If you are a man, please skip to question 4.

3.2.1 Did you already reach the menopause? No Yes I don't know

If you already reach the menopause, please reply also to these questions:

At what age did you reach the menopause? _____

Are you currently doing hormonal therapy? No Yes

If yes, when did you start it? _____ (mm/dd/yy)

Have you done hormonal therapy in the past? No Yes

If yes, when did you start it? _____ (mm/dd/yy)

If yes, when did you stop it? _____ (mm/dd/yy)

4. OPHTHALMOLOGICAL HISTORY

4.1 Do you currently use glasses or contact lens? No Yes I don't know

4.1.1 If yes, do you know your current refraction? If yes, please write it down below:

Right eye _____ Left eye _____

4.2 Do you have any known ocular diseases? No Yes I don't know

If yes, please fill the table below

Which type of ocular disease do you have, e.g., glaucoma, cataracts, dry eye?	Which eye is affected?	When was it diagnosed?
	<input type="checkbox"/> Right <input type="checkbox"/> Left <input type="checkbox"/> Both <input type="checkbox"/> I don't know	(year)
	<input type="checkbox"/> Right <input type="checkbox"/> Left <input type="checkbox"/> Both <input type="checkbox"/> I don't know	(year)

	<input type="checkbox"/> Right <input type="checkbox"/> Left <input type="checkbox"/> Both <input type="checkbox"/> I don't know	(year)
	<input type="checkbox"/> Right <input type="checkbox"/> Left <input type="checkbox"/> Both <input type="checkbox"/> I don't know	(year)
	<input type="checkbox"/> Right <input type="checkbox"/> Left <input type="checkbox"/> Both <input type="checkbox"/> I don't know	(year)
	<input type="checkbox"/> Right <input type="checkbox"/> Left <input type="checkbox"/> Both <input type="checkbox"/> I don't know	(year)

4.3 Are you currently using any eye drops? No Yes I don't know

If yes, please fill the table below with the names and details about all the eye drops that you are currently using.

Name of the eye drop	In which eye are you using the eye drop?	For how long have you been using the eye drop?	How many times per day are you applying this eye drop?
	<input type="checkbox"/> Right <input type="checkbox"/> Left <input type="checkbox"/> Both <input type="checkbox"/> I don't know	(number of months)	
	<input type="checkbox"/> Right <input type="checkbox"/> Left <input type="checkbox"/> Both <input type="checkbox"/> I don't know	(number of months)	
	<input type="checkbox"/> Right <input type="checkbox"/> Left <input type="checkbox"/> Both <input type="checkbox"/> I don't know	(number of months)	
	<input type="checkbox"/> Right <input type="checkbox"/> Left <input type="checkbox"/> Both <input type="checkbox"/> I don't know	(number of months)	

4.4 Have you had any eye surgeries? No Yes I don't know

If yes, please fill the table below

Which type of eye surgery have you had?	Which was the operated eye?	When was the surgery performed?
	<input type="checkbox"/> Right <input type="checkbox"/> Left <input type="checkbox"/> Both <input type="checkbox"/> I don't know	(mm/dd/yy)
	<input type="checkbox"/> Right <input type="checkbox"/> Left <input type="checkbox"/> Both <input type="checkbox"/> I don't know	(mm/dd/yy)
	<input type="checkbox"/> Right <input type="checkbox"/> Left <input type="checkbox"/> Both <input type="checkbox"/> I don't know	(mm/dd/yy)

4.5 Have you had any laser treatments in the eye? No Yes I don't know

If yes, please fill the table below

Type of laser	Did you receive this laser treatment in the past?	Which was the treated eye?	When was the laser performed?
Refractive laser (ie: PRK, LASIK)	<input type="checkbox"/> No <input type="checkbox"/> Yes <input type="checkbox"/> I don't know	<input type="checkbox"/> Right <input type="checkbox"/> Left <input type="checkbox"/> Both <input type="checkbox"/> I don't know	(year) (!) If both eyes please introduce the most recent date

Photodynamic therapy (“PDT” or “Visudyne”)	<input type="checkbox"/> No <input type="checkbox"/> Yes <input type="checkbox"/> I don’t know	<input type="checkbox"/> Right <input type="checkbox"/> Left <input type="checkbox"/> Both <input type="checkbox"/> I don’t know	(year) (!) If both eyes please introduce the most recent date
Retinal laser (photocoagulation) therapy	<input type="checkbox"/> No <input type="checkbox"/> Yes <input type="checkbox"/> I don’t know	<input type="checkbox"/> Right <input type="checkbox"/> Left <input type="checkbox"/> Both <input type="checkbox"/> I don’t know	(mm/dd/yy) (!) If several sessions, please introduce the
YAG capsulotomy (ie: laser to “clean” the lens after cataract surgery)	<input type="checkbox"/> No <input type="checkbox"/> Yes <input type="checkbox"/> I don’t know	<input type="checkbox"/> Right <input type="checkbox"/> Left <input type="checkbox"/> Both <input type="checkbox"/> I don’t know	(year) (!) If both eyes please introduce the most recent date

4.6 Have you had injections in the eye? No Yes I don’t know

If yes:

4.6.1 Which type of injections did you receive?

Lucentis (Ranibizumab) Avastin (Bevacizumab) Eylea (Aflibercept) I don’t know

4.6.2 Which eye received the injections? Right Left Both I don’t know

4.6.3 How many injections did you already received?

Right eye: _____ Left eye: _____ I don’t know

4.6.4 When was the day of your last injection?

Right eye: _____ (mm/dd/yy) Left eye: _____ (mm/dd/yy) I don’t know

5. CURRENT SYSTEMIC MEDICATION

5.1 Vitamins

5.1.1 Are you currently taking vitamin supplements? Yes No I don’t know

If yes, please fill this table

Name of vitamin supplement	Dose	Frequency	How many months ago did you start?

If you replied yes to the two previous questions, please skip to question 5.1.2

5.1.2 Have you taken vitamin supplements in the past? Yes No I don't know

If yes, please fill this table

Name of vitamin supplement	Dose	Frequency	Year start	Year end

5.2 Other medications

Please fill this table with all the remaining medication that you are currently taking?

Name of medication	Dose	Frequency	Date start (mm/dd/yy)	Reason for taking the medication

6. Other

6.1 Do you have any direct relatives with Age-Related Macular Degeneration? No
 Yes I don't know

If yes, please fill the boxes to all that apply:

Father Mother Aunt or uncle Brother or sister Son or daughter

Do you know which type of AMD these relatives have (wet/dry)?
 _____ (please specify for each relative)

6.2 Do you have any direct relatives with neurologic or psychiatric diseases? No Yes
 I don't know

If yes, please fill the boxes to all that apply:

Father Mother Aunt or uncle Brother or sister Son or daughter

Please specify which type of neurological or psychiatric disease for each of the above mentioned relatives:

Supplement 6
Study Imaging Protocols

Exam	Required	Protocol specifications	Performed?	Date execution (mm/dd/yy)	Name of the photographer
Color fundus photographs * please export using TIFF (*.tif)	YES	7 Fields (non-stereoscopic) + single fundus reflex photo (35° Topcon; 30° MSRP)	<input type="checkbox"/> Yes <input type="checkbox"/> No		
Infra-red, red-free and autofluorescence * please export using .E2E	YES	50°, Field 2 High-speed (HS) ART ≥ 15 Setting “Normalized” activated	<input type="checkbox"/> Yes <input type="checkbox"/> No		
Spectral-domain (Spectralis) OCT * please export using .E2E	YES	1. Volume scan IR + OCT, 20 x 20 degrees (49 section/lines, 16 frames ART), high speed, macula centred 2. Raster line scan 30 x 5 degrees (7 section/lines, 25 frames ART), high resolution, horizontal + vertical (90 and 180 degrees), macula centred 3. Enhanced depth imaging protocol – high-resolution volume, 30 x 25 degrees, 61 lines, 30 frames ART, macula centered	<input type="checkbox"/> Yes <input type="checkbox"/> No		
Optos widefield photos: color and autofluorescence (!) On MEEI main building all subjects should do this exam. Only for Stoneham patients it is optional. * please export using TIFF (*.tif)	<input type="checkbox"/> Yes <input type="checkbox"/> No	1. Color photo , centered on the fovea + 2 color images after steering the field of view superiorly and inferiorly to the greatest extent possible 2. FAF, green-light (532 nm), centered on the fovea + 2 FAF images after steering the field of view superiorly and inferiorly to the greatest extent possible	<input type="checkbox"/> Yes <input type="checkbox"/> No		
Swept-source OCT	<input type="checkbox"/> Yes <input type="checkbox"/> No	1. 3 D horizontal 12 x 9 mm 2. 5 line macular cross 12 mm 3. Horizontal sub-foveal line 96 overlapping, 12 mm	<input type="checkbox"/> Yes <input type="checkbox"/> No		

Supplement 7

Abstract accepted for oral presentation at the ARVO (Association for Research in Vision and Ophthalmology) Annual Meeting

CONTROL ID: 2915455

SUBMISSION ROLE: Abstract Submission

AUTHORS

AUTHORS (LAST NAME, FIRST NAME): Lains, Ines^{1, 2}; Kelly, Rachel S.³; Miller, John B.¹; Gil, João^{2, 4}; Marques, Marco^{4, 5}; Silverman, Rebecca¹; Vavvas, Demetrios¹; Kim, Ivana¹; Murta, Joaquim N.^{2, 4}; Lasky-Su, Jessica³; Silva, Rufino M.^{2, 5}; Miller, Joan W.¹; Husain, Deeba¹

INSTITUTIONS (ALL):

1. Massachusetts Eye and Ear, Boston, MA, United States.
2. Faculty of Medicine, University of Coimbra, Coimbra, Portugal.
3. Systems Genetics and Genomics Unit, Channing Division of Network Medicine Brigham and Women's Hospital and Harvard Medical School, Boston, MA, United States, Boston, MA, United States.
4. Ophthalmology Department, Centro Hospitalar e Universitário de Coimbra, Coimbra, Coimbra, Portugal.
5. Association for Innovation and Biomedical Research on Light and Image, Coimbra, Portugal.

Commercial Relationships Disclosure (Abstract): Ines Lains: Commercial Relationship(s);Allergan:Code R (Recipient) | Rachel Kelly: Commercial Relationship: Code N (No Commercial Relationship) | John Miller: Commercial Relationship(s);Allergan:Code R (Recipient) | João Gil: Commercial Relationship: Code N (No Commercial Relationship) | Marco Marques: Commercial Relationship: Code N (No Commercial Relationship) | Rebecca Silverman: Commercial Relationship: Code N (No Commercial Relationship) | Demetrios Vavvas: Commercial Relationship: Code N (No Commercial Relationship) | Ivana Kim: Commercial Relationship(s);Alcon:Code C (Consultant) ;Biophytis:Code C (Consultant) | Joaquim Murta: Commercial Relationship(s);Alcon:Code C (Consultant) | Jessica Lasky-Su: Commercial Relationship(s);Metabolon, Inc:Code C (Consultant) | Rufino Silva: Commercial Relationship(s);Alimera:Code C (Consultant) ;Bayer:Code C (Consultant) ;Novartis:Code C (Consultant) ;Allergan:Code C (Consultant) ;Alcon:Code C (Consultant) ;Thea:Code C (Consultant) | Joan Miller: Commercial Relationship(s);Valeant Pharmaceuticals:Code R (Recipient) ;ONL Therapeutics, LLC:Code C (Consultant) ;KalVista Pharmaceuticals:Code C (Consultant) ;KalVista Pharmaceuticals:Code R (Recipient) ;Genetech/ Roche:Code C (Consultant) ;Genetech/ Roche:Code R (Recipient) ;Valeant Pharmaceuticals:Code P (Patent) ;ONL Therapeutics, LLC:Code P (Patent) ;ONL Therapeutics, LLC:Code R (Recipient) ;Alcon Research Institute:Code C (Consultant) ;Alcon Research Institute:Code R (Recipient) ;Lowy Medical Research Institute, Ltd:Code F (Financial Support) | Deeba Husain: Commercial Relationship: Code N (No Commercial Relationship)

Study Group: (none)

ABSTRACT

TITLE: Human Plasma Metabolomics in Age-related Macular Degeneration – Results of Two Distinct Cohorts

ABSTRACT BODY:

Purpose: Biomarkers of age-related macular degeneration (AMD) are still lacking and, considering AMD's multifactorial nature, their identification is challenging. Metabolomics, the study of all metabolites (<1 kDa) in a biological sample, is well suited to address this challenge. Metabolites are the downstream products of the genome, but also reflect environmental interactions, thus closely mirroring phenotype. This study aimed to compare the plasma metabolomic profiles of AMD patients and controls in two distinct cohorts, and to identify new potential biomarker targets.

Methods: Prospective, cross-sectional study. In two sites (Boston, US and Coimbra, Portugal), we included subjects with AMD and controls without any vitreoretinal disease (> 50 years). All participants were imaged with color fundus photographs, used for AMD staging according to the AREDS classification scheme. Fasting blood samples were collected and analyzed by Metabolon Inc., using ultra-performance liquid chromatography (UPLC) and high-resolution mass spectrometry (MS). Metabolon's software was used for peak identification and quality control. Multivariate analysis, including partial-least square discriminant analysis (PLS-DA), was performed to assess clustering between AMD and controls. The discriminatory ability of the identified significantly different metabolites was assessed using receiver operator curve analysis.

Results: We included 505 subjects: 207 in Boston, 77% with AMD (n= 160) and 23% (n= 47) controls; and 298 in Coimbra, 82% with AMD (n= 244) and 18% (n= 54) controls. Using UPLC-MS, 411 named endogenous plasma metabolites were identified. In both cohorts, PLS-DA revealed a clear separation between AMD patients and controls, with the top 15 metabolites (mostly lipids and amino acids) presenting a variable importance in projection (VIP) score ≥ 2.5 . Three of these metabolites were common to both cohorts. The top 15 metabolites presented a discriminatory ability (Area Under the Curve) of 82% (95% CI: 0.7-0.9) and 73% (95% CI: 0.6-0.8) in Boston and Coimbra, respectively.

Conclusions: In two independent cohorts, AMD patients presented a distinct plasma metabolomic profile as compared to subjects with a normal macula. Some of the identified metabolites are common to both cohorts, thus supporting the development of plasma-based metabolomics biomarkers of AMD.

(No Image Selected)

Layman Abstract (optional): Provide a 50-200 word description of your work that non-scientists can understand.

Describe the big picture and the implications of your findings, not the study itself and the associated details.: Age-related Macular Degeneration (AMD) is the leading cause of blindness in people over than 50 years in developed countries. While it is acknowledged that the disease is associated with genetic and lifestyle risk factors, we currently lack reliable and useable means to identify subjects at risk of developing AMD and of progressing to the late blinding forms of the disease.

In this study, we demonstrate that "metabolomics" (the study of small molecules in biofluids, the "metabolites") enables the identification of blood profiles associated with AMD. This was assessed by studying two independent cohorts, and offers the great promise for future development of reliable biomarkers for AMD.

DETAILS

PRESENTATION TYPE: #1 Paper, #2 Poster

CURRENT REVIEWING CODE: 1310 AMD: clinical research - RE

CURRENT SECTION: Retina

Clinical Trial Registration (Abstract): No

Other Registry Site (Abstract): (none)

Registration Number (Abstract): (none)

Date Trial was Registered (MM/DD/YYYY) (Abstract): (none)

Date Trial Began (MM/DD/YYYY) (Abstract): (none)

Grant Support (Abstract): Yes

Support Detail (Abstract): Harvard Portugal Program/ Portuguese Foundation for Science and Technology: HMSP-ICJ/0006/2013

TRAVEL GRANTS and AWARDS APPLICATIONS

AWARDS: ARVO Members-in-Training Outstanding Poster Award

AFFIRMATIONS

Affirmations: Affirmation of compliance with ARVO's Statement for Use of Human Subjects and/or Declaration of Helsinki.

Affirmations: Affirmation of compliance with ARVO policy on registering clinical trials.

Affirmations: Affirmation of compliance with ARVO's Statement for Use of Animals.

Affirmations: Affirmation to pay Annual Meeting's full registration fee.

Affirmations: Affirmation that submission of this abstract has been approved by the Principal Investigator.

Affirmations: Affirmation that abstract data/conclusions have not been published; not redundant with other submissions from same investigators.

Affirmations: Affirmation to reveal essential structure, novel compound elements, or identify new gene compounds.

